AD-A095 612 OKLAHOMA UNIV NORMAN SCHOOL OF AEROSPACE MECHANICAL --ETC F/G 21/2
COMBUSTION OF DROPS AND SPRAYS OF HEAVY FUEL OILS AND THEIR EMU--ETC(U)
DEC 80 S R GOLLAHALLI, M L RASMUSSEN DOT-CG-93621-A

UNCLASSIFIED OU-AMNE-80-19 USCG-D-64-80 NL

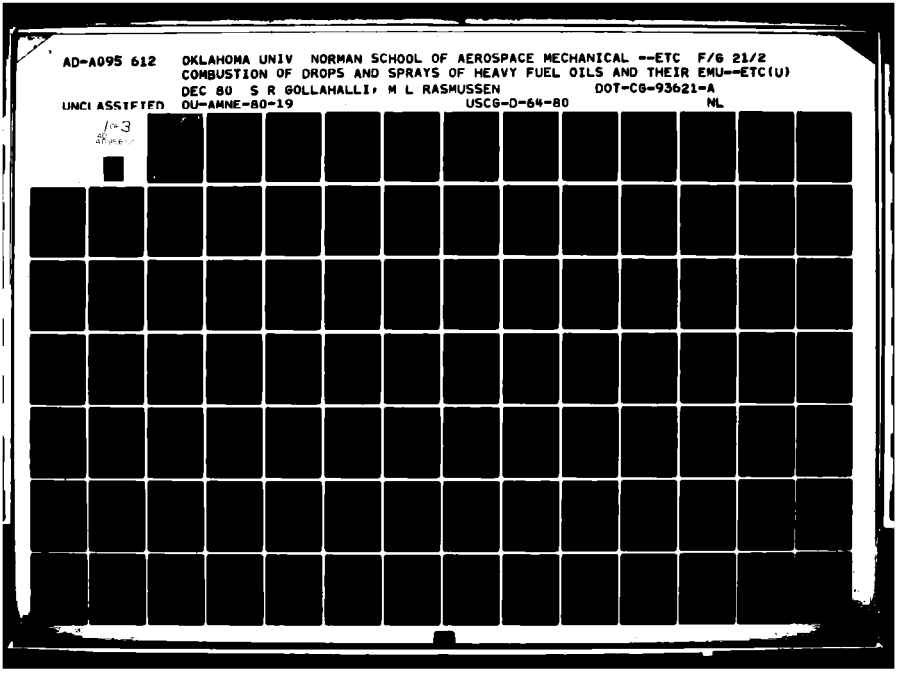

COMBUSTION OF DROPS AND SPRAYS OF HEAVY FUEL OILS AND THEIR EMISSIONS

S.R. Gollahalli, M.L. Rasmussen, and S.M. Salek
School of Aerospace, Mechanical and Nuclear Engineering
The University of Oklahoma
Norman, OK 73019

DECEMBER 1980
FINAL REPORT

Prepared for

U.S. DEPARTMENT OF TRANSPORTATION
U.S. COAST GUARD
Office of Research and Development
Washington, DC 20593

Technical Report Documentation Page

1. Report No.	2. Government Accession No.	3. Recipient's Catalog No.
USCG D-64-80	AD-A095 612	

4. Title and Subtitle	5. Report Date	6. Performing Organization Code
Combustion of Drops and Sprays of Heavy Fuel Oils and Their Emulsions.		

7. Author(s)	8. Performing Organization Report No.
S.R. Gollahalli, M.L. Rasmussen, S.M. Salek	OU-AMNE-80-19

9. Performing Organization Name and Address	10. Work Unit No. (TRAIS)	11. Contract or Grant No.	13. Type of Report and Period Covered
University of Oklahoma School of Aerospace, Mechanical and Nuclear Engineering Norman, Okalhoma 73019		DOT-CG-93621-A	Final Report. Sept. 79 - Dec 80

12. Sponsoring Agency Name and Address	14. Sponsoring Agency Code
United States Coast Guard 2100 Second Street, S.W. Washington, D.C. 20593	

15. Supplementary Notes

F. Weidner (Technical Monitor)
U.S. Coast Guard Headquarters (G-DMT-3/54)

16. Abstract

An investigation directed to understand the combustion behavior of heavy fuels (No. 4 and No. 6 oils) and their emulsions forms the subject of this report. This study is an extension of an earlier study on a distillate fuel (No. 2) and its emulsion, and has been carried out in four parts: (i) study of emulsion characteristics; (ii) single drop combustion experiments of No. 4 oil and its emulsions; (iii) spray experiments of No. 4 and No. 6 oils and their emulsions; and (iv) theoretical studies of single drop combustion. The effects of water content and the coupling influences of injection temperature, chamber temperature, chamber pressure, chamber oxygen content, and injector opening pressure are examined.

The results show that unsupported drops of emulsions of heavy fuels with water also undergo fragmentation. Disruption time of emulsion drop increases with gravity of the fuel and decreases with the increases of injection temperature, chamber oxygen concentration, and chamber temperature. It is also seen to attain a minimum value at a water content of about 8 percent (by volume) under the conditions of this study. The completeness of combustion, soot and nitrogen oxide emissions of the heavy fuel sprays are affected by emulsification.

The first year's effort was presented in Report Nos. DOT/RSPA/DPB-50/80/1 and 80/2, dated January 1980, NTIS Nos. PB-80-178213 and PB-80-178221, respectively.

17. Key Words	18. Distribution Statement
Combustion of Emulsions, Heavy Oils, Sprays, Droplets, Emissions.	Document is available to the U.S. Public through the National Technical Information Service, Springfield, Virginia 22161

19. Security Classif. (of this report)	20. Security Classif. (of this page)	21. No. of Pages	22. Price
Unclassified	Unclassified		

Form DOT F 1700.7 (8-72) Reproduction of completed page authorized

METRIC CONVERSION FACTORS

Approximate Conversions to Metric Measures

Symbol	When You Know	Multiply by	To Find	Symbol
		LENGTH		
in	inches	*2.5	centimeters	cm
ft	feet	30	centimeters	cm
yd	yards	0.9	meters	m
mi	miles	1.6	kilometers	km
		AREA		
in^2	square inches	6.5	square centimeters	cm^2
ft^2	square feet	0.09	square meters	m^2
yd^2	square yards	0.8	square meters	m^2
mi^2	square miles	2.6	square kilometers	km^2
	acres	0.4	hectares	ha
		MASS (weight)		
oz	ounces	28	grams	g
lb	pounds	0.45	kilograms	kg
	short tons (2000 lb)	0.9	tonnes	t
		VOLUME		
tsp	teaspoons	5	milliliters	ml
Tbsp	tablespoons	15	milliliters	ml
fl oz	fluid ounces	30	milliliters	ml
c	cups	0.24	liters	l
pt	pints	0.47	liters	l
qt	quarts	0.95	liters	l
gal	gallons	3.8	liters	l
ft^3	cubic feet	0.03	cubic meters	m^3
yd^3	cubic yards	0.76	cubic meters	m^3
		TEMPERATURE (exact)		
°F	Fahrenheit temperature	5/9 (after subtracting 32)	Celsius temperature	°C

*1 in = 2.54 (exactly). For other exact conversions and more detailed tables, see NBS Misc. Publ. 286, Units of Weights and Measures. Price $2.25. SD Catalog No. C13.10:286

Approximate Conversions from Metric Measures

Symbol	When You Know	Multiply by	To Find	Symbol
		LENGTH		
mm	millimeters	0.04	inches	in
cm	centimeters	0.4	inches	in
m	meters	3.3	feet	ft
m	meters	1.1	yards	yd
km	kilometers	0.6	miles	mi
		AREA		
cm^2	square centimeters	0.16	square inches	in^2
m^2	square meters	1.2	square yards	yd^2
km^2	square kilometers	0.4	square miles	mi^2
ha	hectares (10,000 m^2)	2.5	acres	
		MASS (weight)		
g	grams	0.035	ounces	oz
kg	kilograms	2.2	pounds	lb
t	tonnes (1000 kg)	1.1	short tons	
		VOLUME		
ml	milliliters	0.03	fluid ounces	fl oz
l	liters	2.1	pints	pt
l	liters	1.06	quarts	qt
l	liters	0.26	gallons	gal
m^3	cubic meters	35	cubic feet	ft^3
m^3	cubic meters	1.3	cubic yards	yd^3
		TEMPERATURE (exact)		
°C	Celsius temperature	9/5 (then add 32)	Fahrenheit temperature	°F

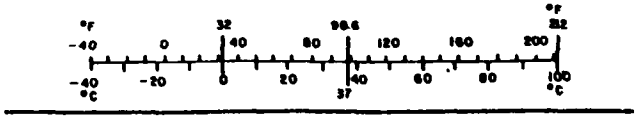

EXECUTIVE SUMMARY

The rapidly depleting petroleum resources and the increasing demand for energy have initiated many efforts to improve the burning characteristics and reduce the emission of pollutants from combustion systems. Among the several methods under study which are aimed towards providing solutions to these problems, emulsification of liquid fuels with other immiscible liquids having lower boiling points is promising. Hence, this program with objectives to investigate the fundamental combustion and emission characteristics of emulsified petroleum fuels was initiated under the sponsorship of the U.S. Department of Transportation (The Office of University Research) in 1978. The first phase of the program dealt with basic experimental and theoretical studies of single emulsion drops and an experimental study of sprays of a distillate fuel (No. 2 Diesel Oil). The second phase of the study funded by the United States Coast Guard, which is presented in this report, deals with similar studies on the combustion and pollutant emission characteristics of heavy fuels (No. 4 and No. 6 oils) and their emulsions.

The following is a summary of the main observations and conclusions of this study.

2.1 Emulsions Characteristics

(a) The emulsions of No. 4 and No. 6 oils with water prepared without additional surfactant remain stable for periods of several weeks. The emulsions of these oils with methanol, however, separate fast.

(b) With increase in water content, clustering of droplets occur.

(c) The mean droplet size of water is 2.5 μm and 4 μm in the emulsions of No. 4 and No. 6 oils with water prepared with mechanical blending.

(d) The addition of an external surfactant makes the water droplet size more uniform and prevents their clustering.

2.2 Single Drop Combustion Studies

(a) Pure No. 4 oil drops burn with smooth laminar flames similar to No. 2 oil drops and do not exhibit signs of fragmentation. They also burn with optically denser flames and produce more smoke than No. 2 oil drops. Pure No. 4 oil cokes the injector needle much faster than No. 2 oil.

(b) The emulsification of No. 4 oil with water decreases the injector coking tendency indicating that the liquid-phase pyrolysis reactions are curtailed by emulsification.

(c) No. 4 oil drops when emulsified with water exhibit fragmentation, similar to No. 2 and No. 6 oils reported earlier.

(d) The ignition characteristics of No. 4 oils are changed by emulsification to a lesser degree than those of No. 2 oil.

(e) Emulsification of No. 4 oil with water decreases soot liberation by a much larger extent than the emulsification of No. 2 oil with water.

(f) With very low volume fraction of water (W = 0.01), the disruption of drops is not intense and occurs late. With water content (by volume) of 3-8 percent, the disruption time is minimum. With further increase of water content, disruption time increases and again at very large water contents ($W \geq 0.20$), it starts decreasing.

(g) Disruption time of No. 4 oil-water drops also decreases with increase in chamber temperature, chamber oxygen concentration, and injection temperature and does not vary significantly with pressure.

2.3 Spray Combustion Studies

2.3.1 No. 4 Oil

(a) Flames of No. 4 oil sprays are more yellowish than No. 2 oil flames. They turn (i) brighter with emulsification with water ($W \leq 0.20$) and increase in chamber oxygen concentration and (ii) do not change considerably with increases in preheat temperature, additions of methanol and external surfactant, and changes in injection pressure.

(b) The soot liberation of No. 4 oil sprays is markedly curtailed by the emulsification with water and to a much smaller extent by emulsification with methanol. Increasing chamber oxygen concentration decreases soot liberation from both pure oil and emulsion flames and increases of chamber pressure enhances it. Changes in preheat injection temperature and injection pressure affect soot liberation weakly.

(c) Increase of water content up to W = 0.03 does not change oxygen utilization significantly and increases it when $0.03 < W < 0.12$. The oxides of nitrogen increase slightly when $0 < W \leq 0.04$ and beyond W = 0.04 decrease considerably.

(d) Increase of injection temperature decreases the extent of the benefits of emulsification with water (W = 0.08). It increases the emission of NO_x and curtails the oxygen utilization.

(e) The emulsion flames burn better than pure fuel flames in oxygen enriched atmospheres. In vitiated atmospheres, emulsification of No. 4 oil worsens combustion efficiency. The emission of oxides of nitrogen of both pure oil and emulsion (W = 0.08) are affected similarly by the changes in oxygen content of the atmosphere.

(f) Addition of methanol (8 percent by volume) improves the combustion efficiency and decreases NO and NO_x. However, these benefits do not increase at higher contents of methanol.

(g) Although an external surfactant is not needed to keep the No. 4 oil-water emulsions stable, small additions of it help to improve the combustion and decrease NO slightly.

(h) The changes in chamber pressure and injector opening pressure do not affect the changes caused by emulsification considerably.

2.3.2 *No. 6 Oil*

(a) The characteristics of No. 6 oil spray flames are qualitatively similar to those of No. 2 and No. 4 oils except for some differences which are attributable to its higher viscosity, boiling point, carbon to hydrogen ratio, and fuel-bound nitrogen than the latter. Emulsification of fuel improves combustion efficiency, reduces soot emission, and emission of nitric oxide. A water content of 5 percent (by volume) was seen to be the optimum under the present experimental conditions. When methanol was used as internal phase (3 percent by volume) slight reductions in NO_x and NO occur, but further additions of methanol do not change them further.

(b) The effects of emulsification are not altered significantly by the increase in chamber pressure, injector opening pressure, and chamber oxygen concentration. However, in atmospheres with lower oxygen concentration, emulsification of No. 6 oil seems to improve its combustion.

(c) Addition of external surfactant although not necessary to keep the emulsion visibly stable affects the combustion behavior of No. 6 oil-water emulsion sprays also. It seems to improve combustion efficiency and also the emissions of NO_x.

2.4 Theoretical Modelling of Single Drop Combustion

In this part of the study, a detailed differential model and an approximate integral model developed previously were used to analyze the combustion behavior of isolated single emulsion droplets. The composite droplet was assumed to consist of a water core surrounded by an oil shell. The variations of the water temperature within the droplet and drop fragmentation time with several ambient and emulsion parameters were examined. It is seen that the predicted variations of drop disruption time with the parameters examined are in good qualitative agreement with measurements. However, the differential model, which does not account for convective heating, is seen to predict much higher disruption times than the measured values. The agreement between the predicted values of the integral model and experiments is satisfactory.

In summary, this study has shown that unsupported drops of the emulsions of heavy fuels (No. 4 and No. 6) with water undergo fragmentation. The effects of emulsification on fuels depend upon the fuel properties such as viscosity, carbon content, and nitrogen content. Some improvements in combustion efficiency and oxygen utilization are possible with both No. 4 and No. 6 oils. Under the conditions of this study, the optimum water contents for improving the completeness of combustion are seen to be 8 and 5 percent for No. 4 and No. 6 oils. The degree of reduction of NO_x that can be achieved by emulsification is smaller in No. 4 oil than in No. 6 oil. The major benefit of emulsification with both fuels seems to be the reduction of soot liberation. Similar to the case of No. 2 fuel oil, the other ambient and emulsion variables affect the changes derived by emulsification to some extent, but do not seem to nullify them. Hence, emulsification of heavy-fuels is beneficial and those benefits can be enhanced by optimally choosing other emulsion parameters.

PREFACE

This work was performed for the United States Coast Guard under the contract DOT-CG-932621-A during 1979-80. This project was an extension of the research on the combustion of distillate petroleum fuel-water emulsions carried out during 1978-79 for the contract DOT-RC-82011.

The authors gratefully acknowledge the helpful discussions they had with Mr. Fred Weidner of the United States Coast Guard, the technical monitor of the project, and Mr. Robert Walter of the Transportation Systems Center, Cambridge, MA.

TABLE OF CONTENTS

LIST OF TABLES

LIST OF PHOTOGRAPHS

LIST OF FIGURES

NOMENCLATURE

a	Radius of inner core or fuel shell
b	Ratio of the inner core radius to the fuel shell radius
C_p	Heat capacity
D	Diffusion coefficient
d_{di}	Initial diameter of the dispersed internal phase droplet
d_{fi}	Initial diameter of the droplet
F	Fuel
G	Functions defined in Chapter 6
H	Heat of reaction
h	Specific enthalpy, convective heat transfer coefficient
$\vec{j}$	Diffusion flux vector
k	Thermal conductivity
L	Normalized heat of vaporization
Le	Lewis number
L_f	Length of the single drop flames
L_{ign}	Ignition distance (distance from the injector nozzle at which the spray ignites)
L_{pen}	Penetration distance (maximum distance from the injector to the leading edge of the spray flame)
M	Volume fraction of methanol in emulsion
m	Dimensionless parameter defined in equation 6.22
N	Neutral species
P_{ch}	Chamber pressure
P_N	Nozzle opening pressure

pps	Picture per second
Q_R	Cumulative fractions of heat release
$\vec{q}$	Heat flux vector
R	Gas constant
R_{CO_2}	Ratio of carbon dioxide mole fraction to nitrogen mole fraction in the exhaust
R_{O_2}	Ratio of oxygen mole fraction to nitrogen mole fraction in the exhaust
r	Radius
S	Volume fraction of surfactant
s	Laplace transform variable
T	Temperature
T_{ch}	Chamber temperature
T_{di}	Initial temperature of the drop
T_{ia}	Inlet air temperature
T_{inj}	Injection temperature
t	Time
t_{bl}	Blending time
t_{st}	Storage time
$\vec{V}$	Velocity vector
$\vec{V}_{fp}$	Velocity of flame propagation
W	Volume fraction of water in emulsion
W_f	Width of the single drop flame
X	Oxidizer species
X_f	Distance of the leading edge of the single drop flame from the injector
Y	Mass traction

Greek Symbols:

α	Thermal diffusivity
β	Volumetric expansivity
ϵ	$(\rho_2/\rho_\infty)^{-1}$
λ	Variable in series expansion
ν	Stoichiometric coefficient
ρ	Density
τ	$(\epsilon D_\infty t)/a_0^2$
τ_{fs}	Duration of spray combustion with flame sheath
τ_{id}	Duration of spray combustion with individual drop flames
Ω	Chemical reaction rate

Subscripts:

1	Inner core of internal phase
2	Fuel shell
3	Gas phase
∞	Ambient conditions
b	Breakup conditions
ch	Chamber conditions
d	Dispersant or drop
e	Emulsion
F	Fuel
f	Fuel
i	Initial conditions
N	Neutral species
o	Initial conditions
P	Product species
sh	Superheat conditions
x	Oxidizer

CHAPTER 1

INTRODUCTION

In recent years, the emphasis to curtail the national dependence on imported oil has resulted in several efforts to conserve the high-grade petroleum derived fuels. The application of heavy residual fuels, development of mixed fuels and synthetic fuels from coal and other sources are among the several measures that are drawing increased attention. Fuels emulsified with water or alcohols have shown the potentials of decreasing pollutant emissions, and under some conditions, of even increasing the thermal efficiency of spray combustion systems. In order to understand the effects of emulsion and ambient parameters on the burning behavior of emulsified fuels, particularly under the conditions of diesel-engine combustion chambers, this research on the combustion of isolated free droplets and transient sprays was initiated. In the first phase of the program, the effects of internal phase content, surfactant content, initial emulsion temperature, ambient pressure, ambient temperature, and ambient oxygen concentration on the combustion of drops and sprays of No. 2 diesel distillate oil and its emulsions with water and methanol were studied. References 1 and 2 contain the results of experimental and theoretical parts of that study. The extension of that project to the heavy fuels (No. 4 and No. 6) and its emulsions was carried out in the second phase of the program and forms the subject of this report.

The experimental portion of the investigation performed for this report includes microstructure of emulsions, photographically documented

disruption and burning behavior of isolated-single drops of pure fuels and emulsions, and flame characteristics and exhaust emission of sprays. Single drop studies were carried out for No. 4 oil only,whereas microstructure and spray studies were performed for both No. 4 and No. 6 oils.

The theoretical part of the study deals with the development and application of two models for analyzing the combustion behavior of composite emulsion drops. The first model is a differential model which accounts for the temperature variation in the interior of the drop and considers both diffusional and heat capacity effects. The second model is an approximate integral model that assumes a uniform temperature over the entire drop. The variations of disruption time of a composite drop with ambient and emulsion variables predicted by these models are presented.

CHAPTER 2

CONCLUSIONS AND RECOMMENDATIONS

This study has demonstrated that combustion characteristics of the drops and sprays of heavy fuels (No. 4 and No. 6 oils) can be considerably altered by emulsifying them with water. External surfactants are not necessary for keeping the emulsions stable.

Droplets of the emulsions of No. 4 and No. 6 oils undergo fragmentation and thus enhance mixing in the flames. Disruption time of emulsion drops increases with the increase of gravity of the fuel and decreases with the increases of injection temperature, chamber oxygen concentration, and chamber temperature. But, it is not significantly affected by the chamber pressure and attains minimum values at certain volume fraction of water, which at the base conditions of this experiment is in the vicinity of 8 percent. The differential model developed for theoretically analyzing the disruption behavior of drops predicts qualitative variations in good agreement with measurements. The predicted values of disruption times, however, are very high and the approximate integral model yields better results.

Spray experiments have shown that emulsification of No. 4 and No. 6 oils with water decreases soot liberation markedly. However, the reductions of the emission of the oxides of nitrogen that can be achieved by emulsification is marginal and depends upon the water content and the amount of fuel-bound nitrogen. Combustion efficiency measured in terms of the completeness of combustion of fuel can be increased slightly

(up to 6 percent) and the degree of improvement depends upon water content and the gravity and carbon/hydrogen ratio of the fuel. Under the conditions of the present experiments, a water content of 5-8 percent appears to be optimum which is in qualitative agreement with engine studies [55]. Furthermore, other variables such as injection temperature, chamber oxygen content, and pressure have strong coupling influences on the effects of emulsification.

It is recommended that detailed diagnostic probing of emulsion spray flames at various axial and radial locations be carried out to determine the dominant processes in the near- and far-nozzle regions. Such a study will yield information to determine the mechanisms by which the effects of emulsification are caused and how those are coupled to the influence of other variables.

CHAPTER 3

LITERATURE REVIEW

The existing literature on the combustion of heavy fuels and their emulsions has been reviewed in this chapter. While there have been a large number of investigations of the combustion of pure (single-component) fuel droplets over the past twenty-five years, the number of investigations on the combustion of multicomponent fuels (residual fuels) has been very limited, in spite of the fact that the common fuels used in spray combustion devices such as diesel engines, gas turbines, and industrial and domestic furnaces are all multicomponent fuels. The combustion behavior of pure fuel drops can be said to be fairly well understood at the present time, although the behavior at elevated pressures and in the midst of an actual spray in a combustor are still matters of controversy.

Multicomponent distillate fuel drops, in general, burn very much like pure fuel drops and have similar mass burning rates. Residual oils, however, show marked differences in burning behavior. Most of the information obtained about residual fuel burning has been qualitative, and realistic physical models which should serve as the basis for quantitative analyses are lacking.

3.1 Combustion of Heavy Oils

The following survey of the literature existing on the combustion of residual fuels and their emulsions has been categorized into three different sub-sections: single drop combustion, spray combustion, and combustion in practical combustors.

2.1.1 *Single Droplet Combustion*

In their suspended drop experiments with fuels of grades 5 and 6, Michael and El-Wakil (4) observed two distinct burning phases, viz. liquid-phase burning and residue burning. Similar behavior has been noticed by almost all researchers [5-12]. During liquid-phase burning, the volatile components diffuse through the drop and evaporate from it, forming a diffusion flame on the downstream side of the drop in the presence of the convective field. In addition to the initial thermal expansion of the liquid as a result of droplet heating, the drops swell [10] because of the formation of volatiles inside the drop, which evolve at a rate faster than they diffuse outwards. This volatile material, while diffusing out, gives rise to the customary envelope flame. Combustion proceeds with the drop alternately swelling and contracting and so maintaining the drop diameter at approximately the initial value [9]. This points out the unreliability of using the variation in drop diameter to characterize the degree of combustion in the case of heavy fuel drops.

In spite of the non-uniformity of the process, Masdin and Thring [9] found a correlation between D_o^2 and the burning time of volatiles. This was confirmed by Kobayasi [6]. This was to be expected if the swelling behavior of the different sized drops was similar. The value of the burning constant for the volatiles was of the same order as that for kerosene, which meant that under similar conditions it took about the same time to burn the volatiles from a residual fuel drop as it would to burn completely a kerosene drop of the same initial size.

It was noted that the extent of swelling increased [4] with temperature and time because of the greater accumulation of vapor and greater vapor

pressure. In a parallel study with nitrogen instead of air, Michael and El-Wakil [4] noticed similar swellings, thus indicating that they were caused by thermal decomposition rather than by peroxidation.

In order to understand the phenomenon of splashing accompanying the combustion of heavy oil drops, Kobayasi [6] did a similar study. He allowed the heavy oil drops to vaporize in a hot nitrogen atmosphere. He, too, observed the same results as Michael and El-Wakil [4] and came to the same conclusion.

References [6] and [14] noticed vapor bubbles formed by internal vaporization and by liquid-phase cracking in the droplet burst, producing large splashes of viscous residue which were seen to fly through the flame front, and these in turn produced secondary splashes at the droplet surface, "like sparks formed by grinding carbon steel".

A characteristic feature observed in the case of heavy oil droplets was that they vanished suddenly after a final expansion. This was explained as being caused by the combustion of the final splashes which had solidified to carbon. However, this explanation does not appear to be satisfactory. Hottel et al. [7] noted a sharp reduction in the slope at around 10% of the initial mass in their curves of degree of combustion vs. residence time. This shows that the solid residue burns much more slowly than the rest of the constituents.

In several of the investigations [7-9] of the combustion of residual fuel drops, towards the end of the volatile combustion period, the outer droplet became more viscous and got inflated and finally ruptured by internal phase gas pressure. Almost simultaneously solidification occurred, presumably caused by cracking of the non-volatile residue. The resulting carbonaceous residue, termed as cenosphere, burned heterogeneously by a

surface reaction. It was found [7-9] that the cenospheres formed by evaporation at low temperatures were large, fragile, and thin-walled while those formed from droplets burning in higher temperatures were smaller and more compact and more similar to particles of coke than to hollow spheres. It was to be expected that fuels giving rise to cenospheres should contain components which could not be volatilized, that is, residual components from coal, tar, and petroleum. These residual fuels appear to be intermediate between a vaporizing oil such as kerosene and pulverized coal in their combustion behavior.

It has been found [5], that drops of heavy fuels when contacted on a hot surface vaporized and burned differently from pure and distillate fuels. First, the volatile part in the fuel evaporated and ignited, and at the end left tarry matter on the hot surface, which also burned at air temperatures of about 1000°C, and left various kinds of carbon skeletons, deposits and ashes after completion of the combustion.

In an attempt to ascertain the components of residual fuels which contributed to their irregular burning behavior, Michael and El-Wakil [4] undertook a study of four combinations of their fractions: (i) grade 6 fuel, (ii) same fuel with asphaltenes extracted, (iii) asphaltenes only, and (iv) bottoms of grade 6 fuel only, consisting of one-third asphaltenes and the rest residues and other heavy oils. It was concluded from studies made over 100 drops that most of the irregularity in the residual fuel burning could be attributed to asphaltenes, and to a lesser extent to the heavy unstable resin components, but not to any peroxidation.

Shyu and co-workers [12] did concurrent analytical and experimental studies of temperature and mass histories during the vaporization, combustion, and thermal decomposition of a multicomponent liquid fuel drop

in a high temperature flow field. Their prediction of drop mass and temperature histories was based on the traditional quasi-steady theory and the spherico-symmetric droplet burning model. Their conclusions show that analytical predictions of drop history are improved by the use of temperature-dependent properties; that the drop temperature rise is fairly rapid in the pre-ignition stage, but slows down as thermal decomposition becomes significant; that the rate of the thermal decomposition, as heat absorbed per unit time, is insignificant at the beginning of drop lifetime, but reaches a maximum value at about 800°F drop temperature.

Various methods have been adopted for evaluating the degree of combustion of residual fuel drops. Gerald [15] and Chang [16] burned droplets of Bunker C fuel oil by dropping them through a vertical tubular furnace, and catching and extinguishing them at the bottom. By measuring the difference in mass of the droplets, their degree of combustion was quantitatively established for different residence times. Hottel et al. [7] employed a similar method. They also recognized that measurement of variation of drop diameter would not provide a reliable indication of the mass consumption rate because the density of the droplets of residual fuels changed markedly during combustion. The mass consumption rate, $\dot{m}$ is related to the evaporation constant, $\lambda = - dD^2/dt$ by $\dot{m} = \rho_l \Pi \lambda D/4$ where ρ_l is the density of the liquid, and hence would be strictly applicable only when ρ_l is constant, or at least does not vary too much to permit a mean value to be assumed. Hence, Peterson [17] correlated the mass burning rates of residual oil droplets with an equation of the form $(M/M_o) = \exp(- 3/2\ (K\tau/D_o^2))$, where M is the mass of the droplet, τ is the time, D is the diameter of the droplet, and subscript 'o' refers to the initial

condition. The experiments performed by Jacques et al. [18] on suspended heavy fuel (viscosity 950 Redwood seconds) droplets also showed that the droplets undergo some swelling before ignition and swell further after ignition before completely burning. Jacques et al. also noticed disruption of oil drops after ignition, which probably was triggered by the suspending wire.

2.1.2 *Spray Combustion*

Very little effort has been devoted to study the structure and physico-chemical process of burning residual oil sprays, although some recent studies have been directed to probe burning distillate fuel sprays [19,20]. Goodger and Najjar [24] made some preliminary tests with a combustion chamber burning fuels of different carbon content, ranging from kerosene to a 25% blend of residual fuel oil in gas oil, at a chamber pressure of 10 atm. The presence of the residual fuel oil in the gas oil was found to promote significant increases in the mean levels of radiation, emissivity, and smoke density, with a modest increase in liner temperature. Onuma et al. [21] studied the flame structure (spatial profiles of the number density of droplets, concentration of species, and temperature) of a heavy oil (kinematic viscosity 11.8 cs at 50°C) flame over an air-blast atomizer. By comparing those results with the measurements in a distillate oil flame, they concluded that there was no significant difference between the structure of the flames over distillate and residual fuels, and both behave similarly to turbulent gas diffusion flames. However, their comparisons may not be valid in general, since preheating temperatures of fuels were not the same. Nasrullah [22] performed a detailed study of the effects of preheating the fuel, atomizing air-flow rate, and fuel flow

rate on flame properties such as flame length, radiation, stability and temperature profiles in a No. 6 fuel oil flame, and has found the flame structure of heavy fuels is a strong function of the operating parameters. Hajzargarbhashi [23] investigated the composition profiles of O_2, N_2, CO_2 in the same flame. The studies of both [22] and [23] employed an air-blast atomizer. Also, unlike the investigation of [21], they did not use a pilot flame to anchor the spray flame. All these studies were carried out on steady flames.

3.1.3 Combustion in Practical Combustors

Most of the work that has been done on practical combustors has been towards studying the nature and causes of solid residues formed during the combustion of residual fuel oil. Sakai and Sugiyama [25] investigated the distribution and mean diameter of residual carbon particles (coke) discharged from a furnace by combustion of atomized heavy fuel oil droplet size distribution. They distinguished between two types of solids produced during combustion of heavy oil droplets, soot particles, which, because of their smaller diameter (10 to 100°A) completely burned away in the time and space available, and coke particles (1 to 100 μm) which did not. This has been reported by other researchers [8,10,11,14, 26] too. Sakai et al. used a theoretical model which assumed a two-staged combustion process, no amalgamation or disruption of droplet and coke particles, and the d^2-law for both the combustion of volatiles and the cenosphere, to derive an expression for the "critical coke generating droplet diameter" i.e., residual carbon particles were generated from droplets larger than this diameter, and smaller droplets could burn out completely before emission from the combustor. It was found that the distribution

and mean diameter of the coke particles discharged from the furnace were determined mainly by the distribution of the initial heavy oil spray and the properties of the fuel oil, but not by the overall fuel/air ratio.

The most important factors controlling coke formation are (i) the fineness of atomization [11], (ii) the flame temperature and the fuel/air ratio [25]. In general, the higher the distillation range of the oil, the higher would be its coking tendency.

Godridge and Hammond have collected data from the flame of a full size steam atomized burner operating with a residual fuel oil throughput of 6100 kg/h. The results they reported were the first obtained for a steam atomized oil burner of that throughput. They measured flame temperatures, flame radiation, gas velocities and total heat fluxes. They studied three flame conditions; one with 0.5% excess O_2, the other with 1.5% excess O_2 and the third with 0.5% excess O_2 but with vitiated air at the burner inlet. They showed that a maximum flame temperature of 1725 $\pm$ 20°C occurs in the first two flames, but the vitiated flame has a maximum temperature of only 1680°C $\pm$ 20°C. The maximum emissivity of 0.95 $\pm$ 0.05 occurs in the second flame although the largest local absorption coefficient of $2.4m^{-1} \pm 0.7m^{-1}$ was reported in the third flame.

Studies carried out on the effects of using residual fuels in gas turbines [24,28] and boilers [26] have concluded that the increased viscosity could cause larger droplet size and consequently larger flame lengths. It would seem that if the heavy oils were atomized into a fine mist, the heavier components would be blasted into a good vapor mixture with the lighter components and would be ignited before they had a chance to deteriorate into the more difficult-to-burn components.

Higher liner temepratures in gas turbines, increases in the mean level of radiation and smoke density, and an increase in combustor carbon deposits have been reported [24,28] by the use of residual fuel oils. Higher levels of radiation and smoke density could be explained by the higher C:H ratio inherent in these residual fuel oils and the increase in the carbon deposits could be attributed to the increased residual carbon.

Residual fuel oils are known to contain polynuclear aromatic and naphthenic hydrocarbons with long paraffinic side chains, the number of rings per molecule ranging from 2 or 3 up to more than 10 in the resinous and asphaltic constituents, with as high as 16 carbon atoms in the side chains [9]. Sulzer [29] pointed out that primary cause of oil-ash deposits and corrosion during the operation of gas turbine plants on heavy oil was the considerable organic and inorganic metal-compound content of these fuels.

The combustion of residual fuel in spray furnaces [10] and boilers [26] can lead to excessive deposition, to corrosion, to excessive loss of combustibles, or pollutant emission in the exhaust gas unless special precautions are taken. One method of dealing with this phenomena is combustion control. Moderate levels of staged combustion or flue gas recirculation will not produce major changes in particulate emissions. Severe staging as well as interstage heat transfer to cool the gases between stages will produce significantly more particulate emissions [26]. Similarly, high levels of flue gas recirculation will produce substantially more particulates. But when steam was used [9], the effect was to lower the soot formation. This was due to the increase in the OH concentration and the residence time and decrease in temperature and drop size.

3.2 Combustion of Heavy Oil-Water Emulsions

In recent years, there seem to have been some attempts to understand the combustion behavior of fuel blends (especially binary mixtures) in terms of the combustion behavior of the individual constituents. There has been considerable interest in the use of emulsions of residual oils as fuels in spray combustion devices. Recently, Glassman et al. [30] suggested emulsifying the liquid fuel with water prior to injection as a viable means of achieving cleaner and more efficient combustion of the fuel spray in practical combustors. The possibility of achieving reductions in emissions of pollutants without any serious adverse effect on thermal efficiency has been the principal factor causing this interest. The various potential benefits can be roughly classified, as those arising from dilution effects in both the gas and liquid phase reactions and those from the "secondary atomization" effects caused by violent rupturing of the emulsion droplet as the interior water micro-droplets become superheated.

3.2.1 Single Drop Combustion

Some systematic research has been conducted recently on emulsified fuel combustion. Ivanov and Nefedov [31], Dryer et al. [32], and Dryer et al. [33], did observe explosive combustion of oil/water emulsion droplets suspended on thin fibers. However, as indicated in the recent survey article by Dryer [34], most investigators have focussed their attention on the measurements of overall effects, on factors such as the overall thermal efficiency, rate of emission of particulate and gaseous pollutants and heat transfer rates. Although there are some basic studies directed to determine the nature of combustion of the isolated drops of emulsions [34-38], still considerable uncertainty exists about the exact

mechanism causing the effects observed in the combustion devices. These investigators [31,34,35,37] employed the suspended drop method and documented the burning process of drops of water-fuel emulsions supported on solid materials such as quartz fibers, thermocouple beads and syringe needles. All these studies showed the evidence for the occurrence of a phenomenon termed "micro-explosion" resulting from preferential vaporization of small internal dispersed phase droplets. Since micro-explosions lead to secondary atomization and an increase in the extent of fuel air mixing, they are believed to be the primary reasons for the effects observed in spray combustion devices. Jacques [37] in his theoretical study has shown that the reduction in the heat abstraction by endothermic liquid-phase reactions of the fuels, caused by the thermal sink effects of internal phase water drops could also be a factor responsible for the decrease in particulate emissions.

Dryer [34] raised some doubts about the validity of the suspended drop method for studying the burning of emulsion drops. He pointed out that the presence of suspending wire affects the coalescence of internal phase drops and could considerably decrease the temperature required for the formation of vapor bubbles, by providing artificial nucleating sites. The occurrence of such disruption during the combustion of suspended drops [27] but not free-drops [34,39] lends some support to Dryer's argument.

Because of the intrinsically unsteady nature of droplet combustion, attempts to correlate the overall behavior in terms of individual burning constants or some average characteristic would be an over-simplification of the problem. The composition changes during combustion of a multicomponent mixture could be described as simple batch distillation.

In his investigation of the combustion of residual oil-water emulsions, Gollahalli [39] noted that the drops exhibit intensely luminous yellow flames similar to those of neat oil. The droplets disrupted violently with an audible characteristic sputtering noise after ignition. Droplet disruption of emulsions before ignition was not noticed in his investigation as was observed by Jacques et al. [35]. Both his theoretical and experimental results show that the drops of emulsions disrupt in the early part of their life time and this break-up time can be controlled by varying the internal phase weight fraction, size of internal phase drops, preheating the emulsion, and degree of primary atomization.

Recently, Lasheras et al. [40] have shown that free droplets of emulsions of water and distillate oils can undergo combustion. Spadaccini and Pelmas [41] have reported similar observations on residual oil-water emulsion drop combustion. Reference [40] has confirmed the notion that for micro-explosion to occur, the saturation temperature of the fuels must be at least greater than the nucleate temperature of the fuel. Similar experimental results on occurrence of micro-explosions during the combustion of No. 2 diesel oil-water emulsions have been reported in Reference [1]. Law and his associates [42] have shown that the existence of internal circulation inhibits micro-explosion.

3.2.2 *Combustion of Heavy Oil-Water Emulsion Sprays and Their Application in Practical Devices*

The studies on the flame structure of heavy oil-water emulsion sprays are very few in the literature. Nasrullah [22] investigated the effects of water content (without any additional surfactant) on flame length,

radiation level, temperature profiles, and particulate concentrations in the steady burning sprays of No. 6 oil-water emulsions over air-blast atomized sprays. Hajzargarbhashi [23] studied the composition structure of (CO_2,O_2,N_2,NO,NO_x) the same burning sprays. Their results indicated that the emulsification of heavy oils with water would (a) increase the temperature levels, (b) decrease the radiation emitted, (c) decrease particulate concentration, and (d) decrease peak concentrations of NO and NO_x by about 10% only.

Several studies [41,43-53] have been reported on the use of oil-water emulsions in practical combustors. Many of these studies have concluded that smoke emission can be decreased and fireside cleanliness can be increased when the heavy fuels are emulsified with water. Reference [41] has also indicated that the SAE smoke number attains a minimum at a volumetric water content of 5%. Volkmar and Carruette have noted that decreases of the order of 60-80% in particulate emission can be achieved in the case of No. 6 fuel oil through a pressure jet atomizer. They have also reported slightly smaller decreases (50-60%) with lighter fuel oils (No. 4 and No. 5). However, Moon et al. [48] report reductions of particulates in the order of only 10-13%, which they attribute to the lower preheat temperature in their study.

The results of the effects of emulsification of heavy fuels on the emission of NO_x do not seem to show a clear trend. Hall [43] and Koval et al. [44] have reported no significant change in the NO_x emission of boilers when No. 6 oil was emulsified with water. Spadaccini and Pelmas [41] observed actually an increase of NO emissions when residual fuel oil they had used was emulsified with water, and the NO emission reached

a peak value around water content of 5%. However, Reference [45] indicates that NO_x emission can be reduced, and the degree of reduction depends upon the specific installations.

All studies agree that excess air needed for combustion can be decreased by emulsification of residual fuels. A consequent benefit of that would be the reduction in the emissions of sulfur oxides [45]. However, Hall did not find any significant change in SO_2 emission, the residual fuel was emulsified with water. Moon et al. [48] also report that by dissolving soda ash in the water prior to emulsification, SO_2 emission could be curtailed considerably because sulfur forms sodium sulfate which goes through fly ash.

Further, there appears to be no consensus among various investigations on the improvement of combustion efficiency. Reference [41] indicates that combustion efficiency can be improved by as much as 15% at water contents of about 5% in the emulsion. However, Bouquet and Delatronche [47] did not find a significant change in combustion efficiency although they found some improvement in thermal efficiency of the boiler which they attributed to the reduction of excess air. It appears that some gains in the improvement of fuel economy can be made with residual-oil emulsification because of reductions in excess air and improvements in fireside cleanliness.

Most of the above discussed studies on the combustion of residual oils and their emulsions were performed in the steady flow combustion systems and very few investigations have been done in the transient combustion systems. Winkler [54] recently reported his studies on the use of residual oil-water emulsions in two large diesel engines (500 and 5100 hp). Fuel was a blend of 85% Bunker C and 15% distillate oil. He

noticed that fuel consumption could be decreased by emulsification of oil with water and the minimum fuel consumption occurred at a volumetric water content of 8%. However, the variation of exhaust temperature with water content was somewhat dependent on the engine. He also noticed an increase of HC emission with water which peaked at a water content of 6% and the smoke opacity of exhaust reached a minimum at the same water content.

In summary, there is ample evidence that particulate emission from residual oil combustors can be decreased significantly by the emulsification of the fuel with water. However, the effects of emulsification of oils on the emissions of NO_x, SO_x, and combustion efficiency are still matters of controversy and seem to depend on the operating conditions of the combustors.

CHAPTER 4

EXPERIMENTAL DETAILS

4.1 Description of the Set-Up

The experiments performed for this project were essentially similar to those carried out for the study on the combustion of No. 2 distillate oil and its emulsions except for the fuels. Hence, the design requirements of the test chamber and associated equipment were the same except for the fuel handling systems. Thus, the apparatus fabricated for the previous study, after effecting some modifications, was used in this investigation also. A brief description of the set-up and the modifications is presented in this chapter. For the detailed description of the experimental facility, the readers are referred to References [1] and [3].

The schematic diagrams of the arrangement of the facility and the cross-sectional diagrams of the combustion test chamber and injector mount are shown in Figures 1 to 4. Essentially, the apparatus consists of the following subsystems: (1) high pressure air supply system, (2) air heating system, (3) combustion test chamber, (4) fuel drop and spray injection system, (5) instrumentation, and (6) safety features. Photograph 1 also shows a view of the experimental set-up.

The heart of the facility is a cylindrical shell (ID = 180 mm, OD = 230 mm, and height - 610 mm) flanged at both ends. This chamber is provided with two rectangular viewing windows (fused quartz disks, length = 178 mm, width = 38 mm, and thickness = 19 mm) on one side and a circular window (fused quartz disk, diameter = 89 mm and thickness 25 mm) diametrically opposite to them. The air inlet pipe connected through the

bottom flange can be fitted with different caps to produce swirling air flow or plug flow in the chamber. The top flange consists of several holes drilled radially outwards and leading to an exhaust manifold, by means of which the chamber gases can be exhausted without introducing any directional asymmetry of flow in the chamber. The test chamber is surrounded by a sheet metal jacket through which hot gases from the air-heating system are passed to minimize the heat losses from the chamber.

The high-pressure air supply system consists of two large (60 m^3) capacity tanks which can be charged to 24 MPa (3500 psi) by mears of a two-stage reciprocating compressor. Air required for both the air-heating system and test chamber is piped from this facility through a network of pressure regulators, filters, and solenoid valves. The air-heating system consists of a double-walled cylindrical shell (ID - 200 mm, thickness = 12 mm, length = 1.22 m) and is connected to a gas burner head at one end and the test chamber at the other. The burner head consists of a plenum chamber and circular steel plate which contains several holes (0.33 mm dia.) through which propane gas supplied from commercial cylinders and air emerge. A 25 kV aircraft type igniter is used to start the combustion of propane which forms a multiple-jet turbulent diffusion flame. The product gases of this flame are used to heat air required for the test chamber and to keep the test chamber walls hot by passing them through a heating jacket surrounding the test chamber. Air required for the test chamber is heated by passing it through a stainless steel (Grade 316) coil (*ID = 7.75 mm and overall length 6 m*).

The fuel injection system is designed to facilitate (a) injection of single drops, (b) injection of sprays from different diesel-engine injectors, (c) control of injection temperature, and (d) the movement of

injectors relative to the viewing windows to allow the observation of different parts of the sprays. The main component of this system is a thick-walled stainless steel pipe (OD = 89 mm, ID = 64 mm) to the bottom end of which interchangeable plugs with different injectors can be attached. The tubing for inlet and outlet of cooling water, the fuel supply and return lines to the injector, and the lines to supply propane gas to a ring of pilot flames near the injector tip are all installed inside this pipe. This pipe can be moved in the vertical direction, and thus the entire injection system can be positioned at different locations. A series of isolated drops can be generated by supplying the fuel from a pressurized fuel tank through a fine needle shaped hypodermic tube. For spray experiments, the fuel is supplied from an actual diesel engine injection pump. By means of an electronic control operating the fuel rack of the pump, it was possible to obtain single spray injections into the chamber.

The instrumentation essentially consists of a 16 mm high-speed photographic system (Hycam Camera - Red Lake Labs. CA) and gas analyzers to determine the composition of exhaust gases (a gas chromatograph and on-line analyzers for determining CO, NO, and NO_x). A suitable arrangement of plane mirrors was used to bring the images through both circular and rectangular windows on to the same focal plane of the camera. Kodak 4X reversal films were used to photograph the burning single drops and sprays (framing rate 100-1000 pps), which were analyzed frame by frame by means of 16 mm film editor. The temperatures and pressures at various locations of the set-up were recorded by means of chromel-alumel thermocouples and bourdon-gages. Photographs 2 and 5 show views of the control panel and gas analysis instrumentation.

4.2 Modifications

In view of the higher viscosity, lower volatility, and higher carbon/hydrogen ratio of the residual oils that were studied in this phase of the project than those of distillate fuels studied earlier, several modifications to the fuel-handling system had to be made to the experimental facility outlined above which are described below.

(i) The fuel passages and ports on the fuel storage tank and the piping from the tank to the injector system were enlarged to prevent their blockages and decrease pressure drop in the line.

(ii) Since carbon to hydrogen ratio and asphaltene content of residual fuels are higher than in distillate fuels, the major problem that confronted us was the production of very large amounts of smoke in the test chamber, particularly while burning pure No. 4 oil. During the first few series of experiments, it was noticed by the time the injection of a steady stream of droplets was established and we were ready to switch on the camera, the quartz-windows were completely coated with black soot so that further photography would be of little use. Increasing the air flow through the chamber, although reducing this problem a certain extent, was not deemed to be a solution. Hence, we decided to install facilities for pneumatically cleaning the interior surfaces of the windows while the test is being conducted. After several designs and trials, a device to blow high pressure gases on the interior surfaces of rectangular windows was constructed, which is shown in Fig. 5. This device consists of a 6 mm ID copper tubing coiled around the test chamber and located within the heating jacket surrounding the test chamber. One end of this tube is connected to a high pressure gas supply (main air line or a nitrogen gas bottle) and

the other end is connected to another copper tube installed inside the test chamber. The stainless-steel tube branches into two parts and each part is located such that it delivers a high velocity gas jet flowing tangential to each of the windows. After several trials, it was found that main-air line supply was not satisfactory and nitrogen jets at pressures in excess of 800 psi have to be used to clear the soot blocking the windows. It was also necessary to heat the nitrogen gas before the jets impinge on the hot quartz windows, to avoid sudden thermal quenching and the consequent breakage of quartz windows.

(iii) Another severe problem that arose during these tests was clogging of the hypodermic needle through which single drops were injected. This was thought to be caused essentially by the liquid phase cracking of the fuel inside the hypodermic needle. Therefore, we decided to use a slightly larger inside diameter tubing which would decrease the surface/volume ratio of the liquid inside the tubing. However, the outside diameter of the tube was kept the same as before in order to maintain the size of the droplets released as small as possible, since the drop diameter is governed essentially by the outside diameter of the tube and surface tension of the liquid.

Further, to allow frequent changes of the injection needles, the existing set-up needed complete dismantling of the injector mount assembly which was very time-consuming. Since with No. 2 fuel oil tests the injection needles seldom needed to be changed, the design was simple and did not have the provision to replace the needles quickly. No. 4 oil tests, however, needed frequent change of needles, and hence the plug of the injector mount was modified as shown in Fig. 6. Since the screw-

mount fabricated for the injection needles resulted in a much longer uncooled length of hypodermic needle, the fuel still coked inside the needle, and thus the problem remained in another form. To overcome this, a series of asbestos plate rings were installed around the exposed part of the tubing to minimize heat transfer from hot gases to the tubing and thus prevent coking of the fuel inside. This arrangement works satisfactorily for about 3-4 runs. Then the windows have to be dismantled and cleaned to remove the fine soot which clings to the windows and cannot be blown away by the jets.

(iv) For spray combustion tests, as the nozzles used in the previous study were meant for No. 2 diesel oil only, a new injection pump and nozzle assembly used on Fairbank Morse diesel engine [Model 38T D8-1/8] were acquired from Transportation Systems Center at Cambridge, MA. Since the high pressure injection tubing associated with the equipment was not received, it was decided to make adaptations to the system to be used in conjunction with the existing piping. Some problems were encountered in accomplishing the same and the following summarizes the modification work carried out on this system.

Photograph 4 shows the nozzle as received. This nozzle could not be accommodated in the injector-mount assembly of the set-up because of the large size of the nozzle holder. However, we found that the oval shaped nozzle-holder could be machined to a smaller diameter circular shape without causing any changes to the injector assembly. Hence, the nozzle holder was machined so that it can be incorporated in the stainless steel pipe of the injector mount (Ref. Vol. I of the Report DOT/RSPA/DPB/80/1-1). Photograph 4 also shows the modified version.

Figure 7 shows the sketch of the pump mount and drive. Photograph 3 shows a view of the mounted pump. Since the torque needed to drive this pump was larger than that needed to drive the pump in the previous study on No. 2 fuel oil, the speed ratio of the motor to the cam shaft was increased by a factor of 3.

4.3 Procedure

The sequence of operations, precautions, and adjustments followed in this study were essentially the same as that detailed in Appendices 1 and 2 of Reference [1] except for the following differences.

(1) After filling the fuel tank with the test fuel or emulsions of No. 6 oil, the electrical heaters wrapped around the tank and the fuel lines leading to the pump and to the injector were switched on and about 15 minutes were allowed for the fuel to get heated up to about 130°F.

(ii) At the end of each day's experiments during both single drop and spray studies, the entire fuel supply train was washed with No. 2 oil to prevent coking of the heavy fuels and thus to avoid injector and line blockage.

4.3.1 Test Conditions

Material Used: The heavy fuels used in this study were No. 4 and No. 6 oils meeting the ASTM specifications. Number 6 oil was procured from CONOCO (Lake Charles, LA). Number 4 oil was prepared by blending No. 6 oil and No. 2 oils in proportions of 45:55 (Ref. 56). The typical properties of these fuels are listed in Tables 1 and 2. Ordinary tap water and 99.9% pure technical grade methanol were used as internal phases of the emulsions. For most of the runs, no additional surfactants were used.

In a few runs where the additional surfactant was used to study its effect, the surfactant was prepared by mixing SPAN 80 and TWEEN 85 (ICI-America, Delaware)(see Table 3 for properties) to yield an HLB of 6. The emulsions of No. 4 oil and water were prepared using a high-speed domestic blender. The emulsions of No. 6 oil and water were prepared using a counter-rotating mixer since the blender increased the temperature of No. 6 oil considerably because of the high viscosity of the fuel. The NO calibration gas for the chemiluminescent analyzer was supplied by LINDE, a special gases company. The calibration gas for the CO analyzer was supplied by HORIBA Instruments Co., IL. Oxygen and nitrogen used to vary the composition of the test chamber environment were of technical grade 99.9% pure. Propane used in the air heating system was procured locally and was of commercial grade.

4.3.2 Test Matrices

The matrices of test conditions at which single drop and spray experiments were performed are listed in Tables 4 and 5. Many experiments were repeated about 3-5 times at the same conditions to obtain a measure of repeatability.

4.4 Data Analysis

The internal-phase droplet size and the variation in microstructure of emulsions were studied by printing the micrographs to yield overall magnifications of about 1000. The movie films were analyzed frame by frame with a 16 mm movie editor. The following information was recorded from films of the single drop tests: (a) framing rate, (b) the initial size of the flame and liquid drop (if visible), (c) the length of the flame,

(d) the width of the flame at the leading front, (e) the distance of the leading edge of the flame from the injector, and (f) the qualitative information about splitting of flames, sudden expansion of flame width, and sudden changes in flame length.

From the films of spray flames, the following information was recorded: (a) framing rate, (b) the distance from the injector at which the spray first ignites, (c) the rate of which flame propagates upstream from the location of ignition, (d) flame stand-off distance, and (e) maximum flame length (in cases where the spray flame does not reach the bottom of the chamber).

The concentrations of NO and NO_x were directly read from the meter on the chemiluminescent analyzer. The concentrations of CO_2, N_2, and O_2 were obtained from the areas under chromatograms using thermal response factors given by Dietz [57]. The qualitative information on smoke formation was obtained by visual observation.

CHAPTER 5

EXPERIMENTAL RESULTS

This chapter presents the experimental observations and discussion of results of the studies on (a) emulsion characteristics, (b) single drop combustion, and (c) spray combustion of No. 4 oil and its emulsions. Also, it contains the studies on emulsion characteristics and spray studies of No. 6 oil and its emulsions.

5.1 Emulsion Characteristics

As in the previous program on No. 2 oil-water emulsions, at first we tried to prepare emulsions using a high-speed blender (HSB) (General Electric - 3 blade, 8 speed). We noticed that blending times of over 15 minutes were necessary to prepare one quart of No. 6 oil-water emulsion with an acceptable homogeneity. In fact, blending times of about 30 minutes were necessary to obtain the spherical shapes for all internal phase drops. But, because of large viscous shear in the No. 6 oil, the temperature of the liquid increased considerably (100°F) during blending which appeared to (1) decrease the viscosity of the liquid considerably and (2) result in the loss of some volatile fractions of No. 6 oil. Also, when attempts were made to keep the oil cool and blend it, excessive power needed to blend the No. 6 oil resulted in the burning of electric motor wiring of the blender. Hence, to prepare the emulsions of No. 6 oil, we adapted a counter-rotating mixer (CRM). Because of the counter rotating motion, the fluid shearing action was better and we could obtain satisfactory emulsions with reasonable blending times (5 min).

However, for No. 4 fuel oil-water emulsions, the high-speed blender adapted for No. 2 oil emulsions proved satisfactory. It was noticed that emulsions could be prepared with blending times of the order 5 minutes and practically no increase of liquid temperature. In fact, the emulsions were prepared with the counter-rotating mixer for comparison and the internal-phase drops were very large when compared to those of emulsions prepared with the high-speed blender. Thus, it was clear that the high-speed blender would yield better emulsions with low-viscosity liquids (No. 2 & No. 4 oils), whereas the counter-rotating mixer would be preferable for high-viscosity (No. 6 oil). Hence, it was decided to use the high-speed blender for preparing emulsions of No. 4 oil and the counter-rotating mixer for emulsions of No. 6 oil.

5.1.1 *Stability of Emulsions by Visual Examination*

The emulsions of No. 4 and No. 6 oils with 8% water and no-surfactant addition were prepared as described above and stored in transparent bottles. They were visually examined periodically for separation of phases. It was noticed that the water and oil did not separate and form different layers even after a month of the preparation of the emulsion.

5.1.2 *Micrographs of No. 6 Oil-Water Emulsions*

Photographs 6 and 7 show the effect of blending time on No. 6 oil emulsions with water contents of 8 and 15%, respectively. It is seen that for blending times over 5 minutes, no significant change in the microstructure occurs. The diameter of water droplets varies in the range of 1.5 μm to 6 μm. Also, droplets seem to cluster together in groups, but not coalesce with one another, which is in contrast to the microstructure of No. 2 oil-

water emulsions stabilized with surfactant studied earlier.

The effect of water content on unstabilized emulsions (S=0) of No. 6 oil and water are shown in photograph 8. It is seen from this set of micrographs that (i) at low water content the droplets in the range of 1.5 to 6 μm appear and remain separate from one another, (ii) as the water content is increased both small and large droplets increase in number, and (iii) clustering of droplets increases with increase in water contents. Small droplets are also seen to move rapidly as evidenced by some streaks on these photographs with exposure time of 0.5 second.

Photograph 9 shows the effect of adding surfactant (2% by volume of the mixture of 75% SPAN 80 and 25% TWEEN 85) while preparing the No. 6 oil-water emulsion. It is clear from these micrographs that (i) the water droplets have more uniform distribution when surfactant is added, and (ii) the droplets remain separate and do not cluster together in the presence of surfactant. Hence, the additional surfactant, even though it is not needed to prevent visible separation of phases in emulsions of No. 6 oil and water, is seen to improve the homogeneity of the microstructure.

Photograph 10 compares the microstructure of emulsions of No. 6 oil and water prepared using the counter-rotating mixer (t_{bl} = 5 min) and the high-speed blender (t_{bl} = 15 min). It is seen that although the high-speed blender yielded more uniform size distribution, it needed almost thrice the blending period required by the counter-rotating mixer. Further, at large water contents (pictures c and d) there is no marked difference between the microstructure of emulsions obtained with the high-speed blender (t_{bl} = 15 min) and the counter-rotating mixer (t_{bl} = 5 min), and hence, it was decided to use the counter rotating mixer, which would not cause significant temperature changes during blending.

3.1.3 Micrographs of No. 4 Oil-Water Emulsions

The effects of blending time on the microstructure of No. 4 oil-water emulsions with 8% water and 15% water (by volume) are shown in photographs 11 and 12. Micrographs a,b,c on photograph 11 and c and d on photograph 12 pertain to the emulsions prepared using the blender at high speed, whereas micrographs a and b pertain to the emulsions prepared with the blender running at low speed. It is seen that the speed of the blender has a strong effect on the size distribution of the droplets, but at a given speed, the blending time influences the size distribution very weakly. Also, at high speed, the droplets are seen to be very uniform ($\simeq$3 μm) in size and smaller than those of corresponding No. 6 oil-water emulsions. However, clustering of droplets is evident in these emulsions also, similar to the No. 6 oil-water emulsions prepared without surfactant.

The effects of water content on the microstructure of emulsions of No. 4 oil and water are shown in photograph 13. It is clear from these micrographs that the droplet size distribution continues to be uniform with a mean diameter about 2.5 μm and only the number density of these droplets increases with water content.

Photograph 14 compares the microstructure of emulsions prepared with the counter-rotating mixer at two different speeds, and the emulsion prepared with the high-speed blender with and without the additional surfactant. It is noticed that the counter-rotating mixer yields large droplets even at the high speed (pictures a and b), whereas the high-speed blender yields small droplets (picture c) for the same blending time. Also, the clustering of the droplets that occur in unstabilized emulsions is completely eliminated by the addition of surfactant.

Although the addition of external surfactant seems to increase the homogeneity of the microstructure of emulsions of both No. 6 and No. 4 oils with water, it is not found to be necessary to prevent the separation of phases (at least visible separation). Since the heavy oils are supposed to contain natural surfactants, additional surfactants are perhaps not necessary and the probability of their use in practice is low in view of the extra cost. Further, the recent evidence [Dryer 58], that a critical minimum size of internal phase drops would be necessary for the occurrence of microexplosions, seems to favor the existence of clusters of droplets. Hence, it was decided not to use external surfactant for preparing emulsions during this project, except during the runs in which its effect itself was studied.

Photographs 15 and 16 show the effects of passing the emulsions of No. 4 and No. 6 oil - with water through injection hardware. It is seen that internal phase droplet size distribution becomes more uniform after the emulsion exits through the injection system. Photograph 16 also shows the effect of preheating (370 K) No. 6 oil-water emulsion. It is seen that microstructure of emulsion is not significantly affected by preheating. Photograph 17 shows the micrographs of emulsions of No. 4 and No. 6 oil with methanol. It is noticed that microstructure of these emulsions changes rapidly as evidenced by the presence of coalesced large droplets.

5.2 Single Drop Combustion Studies (No. 4 Oil and its Emulsions)

5.2.1 Observations

After a few preliminary tests, it was found that preheating of the flow lines was not necessary to handle No. 4 oil. The drop generator functioned quite well to produce droplets with a frequency which was satisfactory to maintain the isolated nature of burning drops. The modifications carried out on the single drop injector system described in Chapter 4, although minimizing undesired preheating of drops in the injection lines before they were released, generated droplets of fairly large size (2-3 mm). The high viscosity of the fuel and the large hypodermic needle used in order to avoid blockage of the passages were the main reasons for it.

From the movie films, it was noticed that drops of both pure oil and emulsions stayed attached to the tip of the needle for 10 or 20 ms. before they were released. During that period, drops underwent some preheating and when the viscosity and interfacial tension between the liquid and tube material decreased, they were released. Further, ignition of drops occurred mostly just prior to the release of the drops. Contrary to the case of No. 2 oil experiments, the continuous presence of a flame anchored at the needle tip was not necessary to ignite the drops. Burning drops after getting released from the needle travelled vertically downwards and could be observed in both bottom and top windows. The total fall time of drops in the test chamber was about 250 ms. In no case was a complete burn out of a drop noticed during its fall.

The following conspicuously evident qualitative observations were

noteworthy: (i) Pure No. 4 oil drops also burned with smooth edges and laminarish wakes similar to those of No. 2 oil, but produced more soot than No. 2 oil drops. As a consequence, their flames were optically denser and more yellowish than the flames of No. 2 oil drops. During some experiments, smoke trails being released from the wakes of the drops could be seen which was in contrast to the experiments on No. 2 oil drops. The higher carbon/hydrogen ratio and lower volatility of the fuel are the prime causes for this difference between the two fuels. In a few instances, the drop generating needle also got clogged because of coking of the fuel inside the needle which never occurred with No. 2 oil. That indicates liquid-phase pyrolysis is more likely with heavier fuels; (ii) When No. 4 oil-water emulsions were used, the nozzle clogging problem disappeared indicating the liquid-phase cracking reactions are suppressed by emulsification. This observation similar to the findings of Ref. 39 in the case of No. 6 oil emulsions lends a substantial support to the hypothesis of Jacques et al. [35] at least in the case of heavy fuels; (iii) The problem of soot deposition on the chamber windows decreased considerably when emulsions were burnt, which extended the number of runs between window cleaning. This observation thus supports the premise that vapor-phase soot formation is also decreased by emulsification; (iv) No. 4 oil-water emulsion drops seemed to disrupt at lower water contents than No. 2 oil-water emulsion drops. Significant disruptions of No. 2 oil-water emulsion drops were noticed for only $W \geq 0.08$. The disruptions of No. 4 oil-water emulsion drops, however, were marked at $W \geq 0.03$ and were noticeable even at $W = 0.01$; (v) Experiments were successfully carried out with No. 4 oil-water emulsions even up to $W = 0.40$ without the

additional pilot gas flame. This was in contrast to the experiments on No. 2 oil-water emulsion drops, the ignition of which could not be achieved under similar chamber conditions without the aid of an additional pilot gas flame. This observation suggests that ignition characteristics of heavy-fuels are altered to a lesser degree than distillate fuels, by emulsification with water. This behavior can be traced to the lower diffusivity of higher molecular weight vapors of heavy fuels than the diffusivity of distillate fuel vapors.

Photograph 18 shows the cinematography sequence of a typical burning pure No. 4 oil drop, whereas photographs 19 to 26 are the film sequences of burning No. 4 oil-water emulsion drops of different water contents. In all these sequences, time increases from right to left as the drops continue to travel downwards. As the flames were yellow and optically dense in this case also, the liquid core cannot be seen in the films. Also, as the photographic prints are made from the positively developed reversal films, the flames are seen black in the photographs. Photographs 27 to 31 show the film sequences of the burning drops of emulsions with constant internal phase content when other parameters (chamber temperature, chamber oxygen concentration, initial temperature of the drop, changing the internal phase to methanol, and adding an external surfactant) were changed one at a time. In all these photographs, except for the variables mentioned in the caption, other parameters were held at the base values shown in Table 4.

A total of 30 rolls of 100 feet long were exposed to document the combustion behavior of single drops of pure No. 4 oil and its emulsions in this study. For each condition about 3-6 sequences of burning drops

were photographed. All the film sequences were examined for flame length, flame width near the drop, disruption tendencies (sudden appearance of rough edges, satellite drops and sudden expansion near the drop described in Ref. 1). The results of the qualitative observations are summarized below. (a) The effects of preheat temperature (T_{di}) on the combustion of No. 4 oil-water emulsions are similar to those of No. 2 oil-water emulsions. The increase of T_{di} in the present experiments also led to an increase of drop fragmentation, (b) The effect of increasing T_{ch} is to increase fragmentation, decrease smoke, and make the drop flames more luminous, (c) The increase of chamber oxygen concentration also results in the enhancement of disruption activity, makes the flames more luminous and decreases smoke liberation, (d) The No. 4 oil-methanol emulsion drop flames also are bright, exhibit long wakes particularly during the final phases of droplet travel in the chamber. Furthermore, emulsion seems to sputter many times near the droplet generating needle itself, which is caused probably by the lower boiling point of methanol. Also, the violent sputtering activity of No. 4 oil-methanol droplets occurs only in the early periods (i.e., seen only in the top half of the upper window), and the flames in the later parts of the droplet travel appear to have the characteristics of pure No. 4 oil flames (such as laminar type, smooth edged wakes and absence of satellite drops). This behavior is probably caused by the dissolution of methanol, in oils at higher droplet temperatures attained towards the end of the droplet travel, which curtails the microexplosions, (e) The droplet flames of No. 4 oil-water (12% by volume) emulsions to which 2% (by volume) of surfactant (75% SPAN 80 - 25% TWEEN 85 with HLB of 6.0 - same as that used in the studies of

No. 2 oil emulsions) also exhibited much less disruption intensity than the droplets of the same emulsion prepared without the additional surfactant. The decrease of intensity is probably caused by the decrease of the internal phase droplet size noticed in the micrographs. This observation thus supports the notion that very fine internal-phase droplet structure is not favorable for microexplosions. However, the disruptions are seen to occur earlier.

Figures 8-10, 11-13, and 14-16 show the variations of the distance of the leading edge of the flame from the injector (X_f), the maximum flame width (W_f), and the flame length (L_f), respectively, of the burning drops of No. 4 oil and its emulsions with water (W = 0.08 and W = 0.15). Similar to No. 2 oil-water emulsion drops, No. 4 oil-water emulsion drops also exhibit jittery motion, sudden changes in flame width, and decreasing flame length which are considered as the confirming signs of fragmentation.

5.3 Spray Combustion Studies

This section deals with the observations and results of the experiments on transient burning sprays of No. 4 oil, No. 6 oil and their emulsions with water and methanol.

5.3.1 No. 4 Oil and Its Emulsions

As in the previous study on No. 2 oil and its emulsions [1], single injection was used for flame photography and steady intermittent injection (≈ 100 injections per minute) was used for exhaust gas analysis. Preheating of fuel lines upstream of the fuel pump was not necessary in these experiments.

5.3.1.1 Ignitability. Ignition of sprays of both No. 4 oil and its emulsions ($W \leq 0.20$) was achieved in the chamber without the aid of an additional ignition source at the base operating conditions. Compared to No. 2 oil, No. 4 oil sprays were more difficult to ignite. Hence, the chamber pressure for base conditions was raised to 0.65 MPa and the injector nozzle opening pressure was raised to 20.8 MPa. With increases in the water content, ignition of the sprays became more difficult and hence the maximum water content was limited to $W = 0.20$. Increasing of preheat temperature, oxygen concentration and chamber temperature, and chamber pressure, improved the ignitability of sprays of both pure oil and emulsions with water.

5.3.1.2 Flame Appearance. Flames of the sprays of No. 4 oil were more yellowish and optically denser than the burning sprays of No. 2 oil. The exhaust gases from the chamber were black in contrast to the grey

color of No. 2 oil sprays. These differences are caused primarily by the higher carbon/hydrogen ratio and viscosity of the No. 4 oil than that of No. 2 oil. Both factors favor the higher formation of soot in case of No. 4 oil. Although the emulsification of No. 4 oil with water turned the spray flames somewhat brighter, yellow was still the dominant color of the flames. The chamber exhaust also turned grey in color with emulsification and became lighter with increase in water content. The extent of changes in the colors of the flame and the exhaust were less apparent with methanol as the internal phase than water.

Flame brightness of both pure oil and its emulsion with water (W = 0.12) increased dramatically at higher ambient oxygen concentrations and decreased at higher nitrogen concentrations in the chamber. These observations can be attributed primarily to the enhancement of oxidation of soot caused by higher local oxygen concentration and temperatures in the flames. The changes in preheat temperatures and addition of external surfactant and methanol did not cause any appreciable changes in the flame appearance.

5.3.1.3 Soot Liberation Tendency. The soot liberation tendency was qualitatively measured by noting the sooting of quartz windows and the frequency of their cleaning needed. With pure No. 4 oil flames, at the air-fuel ratios corresponding to the tests on No. 2 fuel oil [1], the windows were getting blocked very quickly causing problems for photography. To some extent this problem was alleviated by increasing the air flow rate through the test chamber. Emulsification of No. 4 oil mitigated this problem considerably as evidenced by the very little deposition of soot on quartz windows.

5.3.1.4 Exhaust Gas Composition and Flame Temperature. To obtain a measure of combustion efficiency and production of nitrogen oxides at various operating conditions, the temperature inside the combustion chamber and the relative concentrations of CO_2, O_2, N_2, NO, and NO_x were determined under intermittent burning sprays. The first series of experiments was performed to determine the effects of water content. The subsequent experiments were directed to determine how the other variables affected the results of emulsification. Hence, all those experiments were performed at three levels of each variable for both pure oil and the emulsion (W = 0.12).

Figures 17 to 26 show the effects of chamber and ambient variables on the emissions of NO, NO_x, the relative concentrations of CO_2 and O_2 (viz, R_{CO_2} and R_{O_2}) and the steady temperature attained in the flame. As in the previous study [1], the relative concentration of CO_2 and O_2 are expressed as the ratios of CO_2 and O_2 concentrations to the concentrations of N_2. The magnitudes of CO_2 and O_2 are measures of the extent of fuel conversion to final products and the efficiency of utilization of oxygen. Thus, they provide the means of measuring the effects of different variables on combustion efficiency. When the water content in the emulsion was changed, the measured readings of CO_2 and O_2 were corrected to account for the reduction in the fuel content.

Effect of Water Content

The effects of water content on the average T_f, R_{CO_2}, R_{O_2}, NO, and NO_x are shown in Figs. 17 and 18. It is noticed that (i) T_f does not vary significantly up to W = 0.08 and then drops; (ii) both R_{CO_2} and R_{O_2} do not significantly change up to W = 0.03 and then R_{CO_2} increases and

R_{O_2} decreases; however, above W = 0.12 these changes vanish; and (iii) NO and NO_x increase slightly for small water contents and decrease considerably for $W \geq 0.04$.

These effects can be explained by considering the physico-chemical structure of burning pressure-jet atomized sprays. It is known that in the near-nozzle region, the droplets evaporate and the evaporated fuel burns mainly in a flame sheath enveloping the spray (mode 1). In this region fuel also pyrolyses and forms soot. The drops that survive in this region and the soot formed burn in the far-nozzle region (mode 2) essentially with individual flames. As the oxygen concentration is higher in this region than in the near-nozzle region, individual droplet flames can be supported. Since burning in the mode 1 is confined to a narrow flame surface region, NO and NO_x production will be smaller than that which can occur if combustion occurs in mode 2 where heat release occurs volumetrically. However, if all the soot formed in the near-nozzle region is burned subsequently, there should not be much change in R_{O_2} or R_{CO_2}. For some reason if combustion cannot be supported in both modes, for instance because of excessive dilution, R_{CO_2} should drop significantly and the unburnt products should leave the chamber.

From the results, it appears that small water contents (up to W = 0.08) change burning from mode 1 to mode 2 because of increase in ignition delay and larger droplet size from the spray as a consequence of higher viscosity of emulsions than pure oil. That would result in no significant change in R_{CO_2}, R_{O_2}, and T_f, and an increase of NO and NO_x as seen in Fig. 17. Further increases of water content would result in the increase of R_{CO_2} and decreases of R_{O_2} which suggests that mode 1 combustion becomes important

probably because the higher mixing rate and decreased formation of soot in the near-nozzle region become more important. Also, as the flame volume becomes smaller, the average T_f over the measurement region falls. Similarly, both NO and NO_x decrease at large water contents because of the decrease of the reaction zone volume over which they are produced and decrease of temperature levels.

Effect of Injection Temperature

Figures 19 and 20 show the effects of injection temperature on R_{CO_2}, R_{O_2}, T_f, NO, and NO_x of pure No. 4 oil and No. 4 oil-water (W = 0.08) emulsion flames. It is seen that (i) T_f slightly decreases for both pure oil and emulsions, (ii) R_{CO_2} decreases for emulsion and does not significantly vary for pure oil, (iii) R_{O_2} increases for both pure oil and emulsions, (iv) NO and NO_x decrease slightly for pure oil and increase for emulsion when T_{inj} is increased.

As T_{inj} is increased, the sensible heat requirement of the liquids decrease and atomization would be finer and consequently the oil evaporation rate in the near-nozzle region would increase. In pure oil sprays, this could increase the amount of fuel burning in the flame sheath (mode 1) and thus result in more CO_2. It could also increase the vapor-phase pyrolysis and thus lead to more soot formation which would result in incomplete combustion, emitting some of the carbon in the form of soot and CO, instead of CO_2. That could result in no significant change in R_{CO_2}, higher R_{O_2} in the exhaust, and lower T_f. However, in emulsion sprays, where combustion occurs primarily in mode 1, the incremental increase of CO_2 generated in the flame sheath does not seem to

keep up with the decrease of CO_2 caused by the higher pyrolysis at higher T_{inj}.

The increase of evaporation rate in the near-nozzle region would also decrease the amount of fuel that burns as individual drops (mode 2) and hence decrease NO and NO_x in pure oil flames. However, for emulsion flames, the increase of T_{inj} increases both NO and NO_x, which could be attributed to the increased mixing rate because of drop disruptions in the near-nozzle region itself.

Further, the differences in the values of R_{CO_2} and O_2 between pure fuel and emulsions show that energy release would be higher in the case of emulsions.

Effect of Oxygen Concentration in the Chamber

The effects of having the oxygen concentration in the chamber above and below atmospheric values by enriching the inlet air with oxygen and nitrogen are shown in Figs. 21 and 22. T_f increases with the increase of X_{O_2} primarily because of the increase of higher rate of heat release in both near- and far-nozzle regions and higher adiabatic flame temperatures. The increase of R_{O_2} at X_{O_2} = 0.25 in both pure oil and emulsion flames is primarily because of the additional oxygen supplied. The decrease of R_{CO_2} can be attributed to the higher pyrolysis rate because of higher O_2 concentration in the entrained air in the near-nozzle region. Small amounts of oxygen are known to catalyze and increase soot formation in diffusion flames [59,60]. Although this soot burns in the far-nozzle region, their heterogeneous combustion rate is slower than the homogeneous gas phase combustion in the flame sheath of the near-nozzle region and consequently CO_2 prouction rate falls. As the inlet air flow rate was

maintained almost invariant in the experiments, R_{CO_2} falls at higher X_{O_2}. At subatmospheric oxygen concentrations, the gas temperature levels are low and thus soot production and burning fall. The effects of diluents on the soot production of spray flames have been studied in the past [60,61,62] and all have shown soot formation can be curtailed by the introduction of small amounts of diluents. However, with emulsions where near-nozzle dilution is already high because of water, further dilution makes the combustion poor in the near-nozzle region and thus R_{CO_2} falls. It is interesting to note that emulsion has higher R_{CO_2} and lower O_2 relative to pure oil at and above atmospheric X_{O_2} and is thus expected to perform better.

NO and NO_x increase sharply with increased X_{O_2} both for pure oil and emulsion. That is primarily because of the increased temperature-sensitive thermal NO_x and availability of oxygen. However, at $X_{O_2} = 0.11$, NO_x does not seem to change significantly. It suggests that formation of NO_x through routes such as HCN mechanism is probably compensating the decrease of thermal NO_x caused by the dilution effect of the excess N_2.

Effect of Using Methanol as Internal Phase

Figures 23 and 24 show the effects of using methanol instead of water as internal phase. It is seen that 8% (by volume) of methanol addition decreases R_{O_2}, increases CO_2, and decreases both NO and NO_x. However, further increase of methanol does not result in significant changes. Flame temperature decreases considerably with increases in methanol. Although it is not clear whether methanol goes into solution in No. 4 oil or remains as separate phase, it is likely that in both cases drop

fragmentation would occur [40] although the intensity of disruption would be lower in the former case. In any case, the addition of methanol would enhance evaporation rate in the near-nozzle region and thus increase the combustion in mode 1. Further, it also probably reduces vapor-phase soot formation because the pyrolysis of methanol itself can release active species such as OH radicals which oxidize the soot precursor species from the oil. This would result in higher oxygen consumption and higher R_{CO_2}. Also, because of reduction in the extent of individual drop burning (mode 2), NO and NO_x also decrease. However, higher additions of methanol do not seem to enhance these effects. The average flame temperature falls primarily because of the decrease in the flame volume and rapid dilution in the far-nozzle region.

Effects of External Surfactant Addition

Table 7 presents the results of the effects of adding external surfactant (SPAN 80 75% - TWEEN 85 25%, volume fraction 2%) on the combustion parameters of No. 4 oil-water emulsions. It is noticed from the micrographs that the emulsion internal phase droplet diameter decreases significantly when the external surfactant was added although it was not necessary to keep the emulsion stable. That effect appears to manifest in the decrease of R_{O_2}, increase of R_{CO_2}, decrease of NO, and decrease of T_f. All of the effects are possible when combustion dominance starts shifting from volumetrically distributed individual droplet burning in the far-nozzle region (mode 2) to the flame sheath burning (mode 1) in the near-nozzle region. That change can occur because of the earlier disruption of drops in the near-nozzle region itself because of the smaller internal phase droplets.

Effects of Chamber Pressure

The effects of increasing chamber pressure are shown in Figures 25 and 26. It is noticed that R_{CO_2} decreases; R_{O_2} and T_f increase for both pure oil and emulsion flames. NO and NO_x seem to have small peaks at P_{ch} = 1 MPa. The increase of T_f can be attributed to increased reaction rates and larger flame volumes at higher pressures. The decrease of R_{CO_2}, however, is caused by the increase of N_2 concentration that is used to normalize the CO_2 concentration. N_2 increases because of larger air-mass flow rates needed to increase the chamber pressure. The increase of R_{O_2}, similarly, can be attributed to the higher air-mass flow rate. Thus, the increase of air-mass flow and increase of soot-coagulation tend to decrease R_{CO_2} at higher pressures. NO and NO_x both increase initially when P_{ch} is increased, probably because of the increase of reaction rates. The decrease of their concentrations at higher pressures suggest that the decrease of diffusion rates probably overshadow the effects of higher reaction rates. In any case, the changes caused by the emulsification do not seem to be affected either systematically or significantly by the chamber pressure.

Effect of Nozzle Opening Pressure

Table 8 shows the effects of reducing injector nozzle opening pressure on the combustion parameters of both No. 4 oil and its emulsion with water (W = 0.08). It is interesting to note that the relative effects of emulsification are not significantly altered by the change of nozzle opening pressure. This suggests that the effects of emulsification do not seem to be strongly dependent on the mean droplet size of the spray at least over the range examined.

4.3.2 No. 6 Oil and Its Emulsions

4.3.2.1 Observations. The experiments with No. 6 oil and its emulsions were similar to those of No. 4 oil and its emulsions. The major difference was that the fuel tank, the flow lines and the fuel pump were all heated with electrical heating tapes and maintained at about 330K. Further, the injection temperature for the base condition was raised to 370K. It was also found that when T_{inj} was varied to examine the effect of that variable, the spray characteristics were so poor that reliable ignition could not be achieved and hence that variable was removed from the test matrix. Carbon monoxide concentration was also determined in these experiments.

The appearances of No. 6 and No. 4 oil flames, and their corresponding emulsions were very similar. Both fuels exhibited yellow color flames, although No. 6 oil flames were optically more dense. Sooting problems were more severe with No. 6 oil as expected, which required more frequent cleaning of chamber windows. Emulsification of No. 6 oil also decreased soot production and deposition on windows.

4.3.2.2 Exhaust Gas Composition and Flame Temperature

Effect of Water Content

Figures 27 and 28 show the effects of water content on R_{CO_2}, R_{O_2}, NO, NO_x, CO, and T_f. From these figures it is apparent that (i) R_{CO_2} and T_f reach peak values at W = 0.05 and then start falling, (ii) R_{O_2} increases slightly, (iii) CO and NO increase slightly until W = 0.03 and then fall, and (iv) NO_x does not change significantly. The variation of T_f and R_{CO_2} are somewhat different from those of No. 4 and No. 2 oil flames. The

increase of R_{O_2} although is similar to that in those flames, is less dramatic. The peaking of NO is similar to, but occurs at a lower value of W than in those flames.

The differences in these exhaust emission characteristics can be attributed to the high viscosity and carbon content of No. 6 oil. Since the air flow rate was kept constant for the experiments on both No. 4 and No. 6 oils and the carbon content is higher in No. 6 oil, O_2 content in the exhaust of No. 6 oil is considerably lower. As the droplet size and boiling point of No. 6 oil are quite high, the burning in the mode 2 (individual drop burning) in the far-nozzle region is more dominant than the flame-sheath combustion in the near-nozzle region. The fact that R_{CO_2} increases when W is increased up to 0.05 shows that flame-sheath combustion in mode 1 probably becomes significant. That is caused by the decrease of fuel pyrolysis and soot formation in the near-nozzle region. Further increases in W above 0.06 probably increases dilution in the near-nozzle region and ignition delay such that unburnt fuel leaves the flame. Temperature and CO concentration profiles are in conformity with CO_2 profile. At low values of W, CO is higher and decreases significantly at the location where CO_2 is maximum. NO profile also shows a peak at W = 0.03. The peak is not so sharp as the corresponding peak in No. 4 oil-water emulsion flame, which is essentially due to the higher contribution of fuel-bound nitrogen, the conversion of which is not very strongly temperature sensitive to the formation of NO. Furthermore, the difference between NO and NO_x is also high in No. 6 oil-water emulsion flames indicating the significant proportion of NO_2 and other oxides of nitrogen. As the formation of these species and the conversion of fuel-bound nitrogen are supposed to

follow the HCN related mechanism rather than the strongly temperature sensitive Zeldovich route [63], the variation of NO_x with water content seems to be minimal.

Effect of Methanol Addition

The effects of adding methanol instead of water the internal phase are shown in Figs. 29,30. These effects are seen to be qualitatively similar to those in the case of No. 4 oil-methanol emulsions. With small additions of methanol, R_{CO_2} seems to increase and remain essentially constant thereafter. R_{O_2} also was seen to increase very slightly.

Also, NO, NO_x, and CO decreased when 3 percent (by volume) of methanol was added and remain invariant for further additions. It appears slight additions of methanol to No. 6 oil provide enough energy release, and oxygen atoms in the near-nozzle region seem to decrease soot nucleation and enhance burning in the mode 1 which results in the reductions of the emission of NO, NO_x, and CO and to enhance CO_2. Further additions of methanol probably result in sufficiently high energy release in the near-nozzle region so that temperatures in that region would increase and accentuate fuel pyrolysis which result in the dominance of energy release by mode 2 in the far-nozzle region and thus counteract the effects that occur at small methanol concentrations.

Effect of Chamber Pressure

Figures 33 and 34 show the effects of chamber pressure on the combustion parameters of No. 6 oil and its emulsion with water. Since the air mass flow rate through the chamber and the exhaust had to be varied, the concentrations of the species measured in the exhaust would be varying even if their production rates remained the same. Hence, this figure

is to be used to interpret the effects of pressure on the differences of parameters between pure oil and emulsion only. It is noticed that T_f increases because of the increase in flame length and volume at higher pressures. Since both soot production and coagulation increase and the diffusion coefficient decreases at high pressure, flame volume increases. The relative differences in the values of other parameters however, remain essentially same at all the three pressures tested, which is in conformity with the results obtained on No. 2 fuel oil-water emulsion experiments. That indicates no significant influence of pressure exits on the effectiveness of emulsification.

Effects of Oxygen Concentration in the Chamber

Figures 31 and 32 show the effects of changing chamber oxygen concentration, below and above the atmospheric value. It is noticed that increase of X_{O_2} increases T_f and does not significantly change R_{O_2}. However, CO_2 and CO seem to have minimum and maximum values at atmospheric X_{O_2}. These changes can be attributed to (i) the decrease of pyrolysis and soot formation primarily caused by the lower temperatures at $X_{O_2} < 0.21$ and (ii) the increase of oxidation of soot and CO at $X_{O_2} > 0.21$. The invariance of R_{O_2} with X_{O_2} indicates that the increase of oxidation reactions keep pace with its increase.

The relative differences in the measured parameters between pure oil and oil-water emulsion does not seem to be markedly changed by the increase in chamber oxygen concentration but seem to be affected by its decrease. That difference is noticeable in higher CO_2 and higher NO_x of emulsion than those of pure oil at $X_{O_2} < 0.21$. That suggests that the role of drop fragmentation occurring in emulsified fuels becomes more

important at low X_{O_2} when temperature and reaction rates are curtailed.

Effect of External Surfactant Addition

Table 7 also presents the effects of external surfactant addition to No. 6 oil-water emulsions. In this case, the effects of external surfactant appears to be slightly different from those with No. 4 oil-water emulsions. It is noticed that although R_{CO_2} increases and R_{O_2} decreases similar to that with No. 4 oil-water emulsion, NO and T_f increase. This suggests a possibility of enhancement of combustion in mode 2. As indicated earlier, because of higher viscosity and latent heat of No. 6 oil, individual droplet burning is dominant. Further, as micrographs indicated, the internal droplet size is also higher in the case of No. 6 oil and thus drop disruption also mainly occurs in the far-nozzle region. As external surfactant is added, internal-phase drop size is decreased and hence their number increases. The size of internal-phase droplets, even after external surfactant addition, appears to be large enough to generate enough force to cause disruption upon their evaporation. Thus, the disruption in the far-nozzle region is likely to be enhanced with the addition of the external surfactant. It leads to an increase of the mixing rate and consequently results in the enhancement of CO_2 and T_f and the decrease of CO.

Effect of Nozzle Opening Pressure

Table 8 presents the effects of changing the injector nozzle opening pressure on the changes caused by emulsifying No. 6 oil with water ($W = 0.08$). Similar to the case of No. 4 oil, here also no coupling effects of nozzle opening pressure on the changes caused by the emulsification are noticed.

5.3.3 Photographic Measurements

The cinematography sequences of burning sprays of pure No. 4 oil and No. 4 oil-water (W = 0.08) sprays are shown in photographs 32 and 33. The photographs of the sprays of No. 6 oil and its emulsions show essentially the same features and hence are not reproduced here. The following general features are apparent from these photographs: (i) The spray ignites generally away from the injector. As the water content is increased, the ignition point moves farther from the nozzle and at high water contents, particularly with No. 6 oil, ignition occurs when the spray tip touches the bottom of the chamber. This indicates that the ignition delay increases as the gravity of the fuel and water content of the emulsion increases, (ii) From the point of ignition, flame quickly spreads both upwards and downwards and the spray burns with a flame sheath surrounding it, and (iii) After a certain duration, the flame sheath starts receding from the injector side and moves towards the bottom of the chamber. During this period a number of droplets burn with individual flames. This burning period lasts for a considerable period.

These photographs provide a clear evidence for the existence of individual drop burning in the flames of heavy fuels. Thus, it should clear the controversy regarding the importance of individual drop burning [64] at least in the case of heavy oils and emulsions. The durations of the existence of flame sheath around the spray (τ_{fs}) and individual drop burning (τ_{id}) measured from photographs are shown in Table 12. Each measurement is an average of the readings taken from 3-4 burning sprays. The following points are noteworthy from this table: (i) The total burning time of spray increases with the increase in gravity and viscosity of

oil. That is caused primarily by the larger droplet size and higher latent heat requirements of heavier oils. (i) The total burning time slightly decreases as the fuel is emulsified and then again increases as the water-content of the emulsion becomes high. The slight decrease of τ_{total} is probably caused by the enhancement of faster homogeneous flame-sheath combustion relative to the combustion of individual soot particles because of reduction of soot and increased mixing. However, at high water contents, that effect appears to be partially offset by the increase of sensible and latent heat requirements caused by the additional water. The larger decrease of τ_{total} with emulsification of No. 6 oil than No. 4 oil is particularly noteworthy. (iii) With emlusification the ratio (τ_{fs}/τ_{id}) increases. That effect can be traced to the decrease of soot formation and the increase of mixing by droplet fragmentation.

CHAPTER 6

THEORETICAL ANALYSIS OF SINGLE DROP COMBUSTION

This chapter deals with a brief description of the formulation and results obtained from two theoretical models for analyzing the combustion behavior of single drops of oil having an internal phase core. These models were developed during the first phase of this program to analyze No. 2 oil-water emulsions, and hence for the detailed development of the models, the readers are referred to Reference [2].

6.1 Differential Model

The formulation of the problem for the combustion of an emulsified liquid droplet is the same as that of Birchley and Riley [38], which we summarize here. The idealized spherical droplet is illustrated in Figure 35. The inner core of radius $r = a_1$, is composed of the internal-phase liquid with properties designated by the subscript one. The internal phase is usually water, but it could be some combustible liquid. The outer shell, $a_1 < r < a(t)$, is composed of the liquid fuel, designated by the subscript two. The liquid fuel vaporizes at the moving surface $r = a(t)$. For $r > a(t)$, a gaseous state exists. At $r = r_*(t)$, a spherical diffusion flame surface is designated under the Burke-Schumann idealization of a flame discontinuity surface. In more general terms, $r = r_*(t)$ locates the localization of the combustion process. In the region $a(t) < r < r_*(t)$, a fuel-rich gaseous mixture of fuel, oxidant, product, and neutral species exists. The oxidant species exists by virtue of diffusion from outside the flame sphere. Under the Burke-Schumann idealization, the oxidant species

does not exist here because it has been consumed entirely by the flame surface at $r = r_*(t)$. Outside the flame surface, an oxidant-rich gaseous mixture of fuel, oxidant, product, and neutral species also exists. The fuel species exists by diffusion from inside the flame sphere, but it is nonexistent in the Burke-Schumann approximation since it has been consumed entirely by the flame. As $r \to \infty$, only the oxidant and neutral species exist. In the gaseous region, $r > a(t)$, the properties are denoted by the subscript three. The conditions at infinity are denoted by the subscript infinity.

6.1.1 Gaseous Region

The gaseous region exists in general in a quartic mixture with fuel (F), oxidant (X), product (P), and neutral (N) species. The mixture reacts according to the chemical equation

$$\nu_F F + \nu_X X \to \nu_P P \quad , \tag{6.1}$$

where ν_F, ν_X, and ν_P are the fuel, oxidant, and product stoichiometric coefficients.

We assume that the entire combustion process occurs at constant pressure, and thus the pressure, P, is a constant parameter of the problem. The thermal equation of state of the mixture is thus governed by

$$\rho_3 T_3 = \rho_\infty T_\infty \quad , \tag{6.2}$$

where ρ and T denote the mass density and temperature of the mixture. We assume that all species have the same temperature. If ρ_α denotes the density of species α, then we have

$$\rho_3 = \rho_F + \rho_X + \rho_P + \rho_N \quad . \tag{6.3}$$

Mass conservation of the mixture is governed by the equation

$$\frac{\partial \rho_3}{\partial t} + \text{div}\, \rho_3 \vec{V} = 0 \tag{6.4}$$

where $\vec{V}$ is the mass average velocity of the mixture. For spherical symmetry, we have $\vec{V} = v(r,t)\vec{e}_r$, and equation (6.4) can be written

$$\frac{\partial \rho_3}{\partial t} + \frac{1}{r^2}\frac{\partial}{\partial r}(\rho_3 v r^2) = 0 \tag{6.5}$$

Let $\bar{Y}_\alpha = \rho_\alpha/\rho_3$ denote the mass fraction of species α, such that

$$\bar{Y}_F + \bar{Y}_X + \bar{Y}_P + \bar{Y}_{N_2} = 1 \tag{6.6}$$

The equation of change for the species mass fractions can be written in the form

$$\rho_3 \frac{D\bar{Y}_F}{Dt} = -\text{div}\, \vec{j}_F - \rho_3 \nu_F W_F \omega^* \quad , \tag{6.7a}$$

$$\rho_3 \frac{D\bar{Y}_X}{Dt} = -\text{div}\, \vec{j}_X - \rho_3 \nu_X W_X \omega^* \quad , \tag{6.7b}$$

$$\rho_3 \frac{D\bar{Y}_P}{Dt} = -\text{div}\, \vec{j}_P + \rho_3 \nu_P W_P \omega^* \quad , \tag{6.7c}$$

$$\rho_3 \frac{D\bar{Y}_N}{Dt} = -\text{div}\, \vec{j}_N \quad , \tag{6.7d}$$

where $\vec{j}_\alpha$ is the diffusion flux vector of species α, W_α is the molecular weight of species α, ω^* is the chemical reaction rate, and

$$\frac{D}{Dt} = \frac{\partial}{\partial t} + \vec{V}\cdot\nabla = \frac{\partial}{\partial t} + v\frac{\partial}{\partial r} \tag{6.8}$$

is the material derivative of the mixture. Addition of equations (6.7) and accounting for equation (6.6) shows that the mass flux vectors are related by

$$\vec{j}_F + \vec{j}_X + \vec{j}_P + \vec{j}_N = 0 \tag{6.9}$$

and that the stoichiometric coefficients are related by

$$\nu_P W_P = \nu_F W_F + \nu_X W_X \quad . \tag{6.10}$$

We assume that thermal and pressure diffusion can be ignored along with multicomponent diffusion and utilize Fick's law of diffusion:

$$\vec{j}_\alpha = - \rho_3 D_\alpha \text{ grad } \bar{Y}_\alpha \quad , \quad \alpha = F,X,P,N \tag{6.11}$$

where D_α is the diffusion coefficient for species α. We further assume that $D_\alpha = D$ is the same for all species.

Let h_α denote the specific enthalpy of species α, and let the specific enthalpy of the mixture be denoted by

$$h_3 = \bar{Y}_F h_F + \bar{Y}_X h_X + \bar{Y}_P h_P + \bar{Y}_N h_N \quad . \tag{6.12}$$

With viscous dissipation ignored and the pressure a constant, the energy equation for the mixture can be written as

$$\rho_3 \frac{Dh_3}{Dt} = - \text{div } \vec{q} \quad , \tag{6.13}$$

where $\vec{q}$ is the heat-flux vector. The heat-flux vector is given by

$$\vec{q} = - k \text{ grad } T_3 + h_F \vec{j}_F + h_X \vec{j}_X + h_P \vec{j}_P + h_N j_N \quad , \tag{6.14}$$

where k is the thermal conductivity of the mixture. We now assume that each species is thermally perfect such that

$$\frac{Dh_\alpha}{Dt} = C_{P_\alpha} \frac{DT_3}{Dt} \tag{6.15}$$

wnere C_{P_α} is the specific heat at constant pressure for species α. The

energy equation can now be manipulated to yield the following equation of change for the temperature

$$\rho_3 C_p \frac{DT_3}{Dt} = \text{div}\,(k\nabla T_3) - \text{div}\,[\Sigma\, h_\alpha \vec{j}_\alpha] - \rho_3 \Sigma\, h_\alpha \frac{DY_\alpha}{Dt} \quad , \tag{6.16}$$

where the specific heat at constant pressure for the mixture is

$$C_p = \Sigma\, \bar{Y}_\alpha C_{p_\alpha} \tag{6.17}$$

and the indicated summations are over all the species. Making use of the equations of change, equation (6.7) now yields

$$\rho_3 C_p \frac{DT_3}{Dt} = \text{div}\,(k\nabla T_3) - (\Sigma\, C_{p_\alpha} \vec{j}_\alpha)\cdot\nabla T + \rho_3 H \nu_p W_p \Omega^* \quad , \tag{6.18}$$

where

$$H \equiv [\nu_F W_F h_F + \nu_X W_X h_X - \nu_p W_p h_p]/\nu_p W_p \tag{6.19}$$

is the heat of reaction. If C_{p_α} were the same for every species, then $\Sigma\, C_{p_\alpha} \vec{j}_\alpha$ would vanish identically by virtue of equation (6.9). We assume that the second term on the right side of equation (6.18) is thus small enough to neglect. The energy equation can thus be written

$$\rho_3 C_p \frac{DT_3}{Dt} = \text{div}\,(k\nabla T_3) + \rho_3 H \nu_p W_p \Omega^* \quad . \tag{6.20}$$

The chemical reactions thus contribute to an apparent temperature source.

6.1.2 Normalized Variables and Reduced Equations

We now assume that D, C_p, and H are constants. It is convenient to introduce new normalized variables. We define a nondimensional temperature T_3^* as

$$T_3^* = \frac{C_p T_3}{H} \quad . \tag{6.21}$$

We also introduce the parameters

$$m_F = \frac{\nu_P W_P}{\nu_F W_F} \quad \text{and} \quad m_X = \frac{\nu_P W_P}{\nu_X W_X} \tag{6.22}$$

such that

$$Y_F = m_F \bar{Y}_F \quad , \quad Y_X = m_X \bar{Y}_X \quad , \tag{6.23}$$

$$Y_P = \bar{Y}_P \quad , \quad Y_N = \bar{Y}_N \quad ,$$

and

$$\frac{Y_F}{m_F} + \frac{Y_X}{m_X} + Y_P + Y_N = 1 \quad . \tag{6.24}$$

A convenient new reaction rate is found to be

$$\Omega = \nu_P W_P \Omega^* \quad , \tag{6.25}$$

and a Lewis number, assumed constant, is defined as

$$L_e = \frac{k}{\rho C_P D} \quad . \tag{6.26}$$

To further simplify the equations, we assume that the thermal conductivity depends linearly on the temperature and the diffusion coefficient depends quadratically on the temperature such that

$$k = k_\infty \left(\frac{T}{T_\infty}\right) \quad ,$$

$$D = D_\infty \left(\frac{T}{T_\infty}\right)^2 \quad , \tag{6.27}$$

$$Le = \frac{k_\infty}{\rho_\infty C_P D_\infty} \quad .$$

The equations of change for species and temperature now take the forms

$$\frac{DY_F}{Dt} = \frac{D_\infty T_3^*}{T_\infty^{*2}} \operatorname{div} (T_3^* \nabla Y_F) - \Omega \quad , \tag{6.28a}$$

$$\frac{DY_X}{Dt} = \frac{D_\infty T_3^*}{T_\infty^{*2}} \operatorname{div} (T_3^* \nabla Y_X) - \Omega \quad , \tag{6.28b}$$

$$\frac{DY_N}{Dt} = \frac{D_\infty T_3^*}{T_\infty^{*2}} \text{ div } (T_3^* \nabla Y_N) \quad , \tag{6.28c}$$

$$\frac{DT_3^*}{Dt} = L_e \frac{D_\infty T_3^*}{T_\infty^{*2}} \text{ div } (T_3^* \nabla T_3) + \omega \quad . \tag{6.28d}$$

The product species mass fraction, Y_P, can be obtained from equation (6.24). The equations of change thus assume a similarity of form.

The reaction rate is given by the Arrhenius expression

$$\Omega = C\, Y_F^{\nu_F}\, Y_X^{\nu_X} \exp\left(-\frac{T_a}{T_3}\right) \quad , \tag{6.29}$$

where C is a constant relating to the frequency of molecular collisions and T_a is the activation temperature. In this analysis, the expression for ω will not be utilized since the Shvab-Zeldovich formulation will be adopted.

6.1.3 Liquid Drop

In both parts of the liquid drop, we ignore diffusion, chemical reactions, and fluid motion. The governing equations are thus the energy equations:

$$\frac{\partial T_1^*}{\partial t} = \alpha_1 \nabla^2 T_1^* \quad , \tag{6.30}$$

$$\frac{\partial T_2^*}{\partial t} = \alpha_2 \nabla^2 T_2^* \quad , \tag{6.31}$$

where

$$\alpha_1 \quad \frac{k_1}{\rho_1 C_{P_1}} \quad \text{and} \quad \alpha_2 \quad \frac{k_2}{\rho_2 C_{P_2}} \tag{6.32}$$

are the diffusivities of the internal-phase liquid and the liquid fuel. The thermal conductivities are denoted by k_1 and k_2. The physical properties of the liquids are assumed constant.

6.1.4 *Initial Conditions*

We imagine that the liquid drop is initially at a uniform temperature T_o when it is immersed into an infinite bath of oxidant and neutral species at temperature T_∞. Thus, the initial conditions are written

$$T_1^* = T_2^* = T_o^* \quad , \quad t = 0 \quad , \quad r < a(0) \equiv a_o \quad , \tag{6.33a}$$

$$T_3^* = T_\infty^* \quad , \quad t = 0 \quad , \quad r > a(0) \equiv a_o \quad . \tag{6.33b}$$

The initial temperature profile is illustrated in Figure 35 together with a typical temperature profile at a later time.

At time t = 0, the fuel is entirely in the liquid phase. Thus, we also have

$$\begin{aligned} Y_F &= Y_P = 0 \\ Y_X &= Y_{X_\infty} \\ Y_N &= 1 - \frac{Y_{X_\infty}}{m_X} \\ v &= 0 \end{aligned} \qquad \begin{aligned} &t = 0 \\ &r > a(0) \equiv a_o \end{aligned} \tag{6.34}$$

6.1.5 *Boundary Conditions*

At the center of the spherical drop, the heat-flux must vanish. Hence, we have

$$\frac{\partial T_1^*}{\partial r} = 0 \quad \text{at} \quad r = 0 \quad . \tag{6.35}$$

At the liquid-liquid interface, $r = a_1$, both the temperature and heat flux must be continuous:

$$\begin{aligned} &T_1^* = T_2^* \quad , \\ &k_1 \frac{\partial T_1^*}{\partial r} = k_2 \frac{\partial T_2^*}{\partial r} \quad , \end{aligned} \qquad r = a_1 \tag{6.36}$$

The fuel liquid-vapor interface is a moving discontinuity surface with the speed of the surface denoted by $\dot{a}$. The temperature at this interface is continuous; hence

$$T_2^* = T_3^* \quad , \quad r = a(t) \quad . \tag{6.37}$$

The jump condition for the mixture mass conservation is

$$\rho_3(v - \dot{a}) = \rho_2(-\dot{a}) \quad , \quad r = a(t) \quad . \tag{6.38a}$$

Solving for the velocity yields, after using equation (6.2),

$$v = -\left[\frac{\rho_2}{\rho_\infty}\frac{T_3^*}{T_\infty^*} - 1\right]\dot{a} \quad , \quad r = a(t) \quad . \tag{6.38b}$$

This gives the velocity of the mixture at the interface in terms of the velocity of the interface.

The jump condition for the species mass conservation is

$$\rho_{\alpha_3}(v_\alpha - \dot{a}) = -\rho_{\alpha_2}\dot{a} \quad . \tag{6.39}$$

The species velocity, v_α, however, is given in terms of diffusion-flux vector by

$$\vec{j}_\alpha = \rho_\alpha(\vec{v}_\alpha - \vec{v}) \quad . \tag{6.40}$$

Since $Y_{\alpha_2} = 0$ for $\alpha = X$, N, and P, we can obtain the interface conditions pertinent for the oxidant and neutral species

$$-Y_X\frac{\rho_2}{\rho_\infty}\dot{a}(t) = \frac{D_\infty T_3^*}{T_\infty^*}\frac{\partial Y_X}{\partial r} \qquad r = a(t) \tag{6.41a}$$

$$-Y_N\frac{\rho_2}{\rho_\infty}\dot{a}(t) = \frac{D_\infty T_3^*}{T_\infty^*}\frac{\partial Y_N}{\partial r} \tag{6.41b}$$

For the fuel species, $\bar{Y}_F = 1$, and hence we have

$$(m_F - Y_F)\frac{\rho_2}{\rho_\infty}\dot{a}(t) = \frac{D_\infty T_3^*}{T_\infty^*}\frac{\partial Y_1}{\partial r} \quad , \quad r = a(t) \quad . \tag{6.41c}$$

The jump condition for the energy flux across the interface discontinuity yields (neglecting the kinetic energy contributions)

$$-L\frac{\rho_2}{\rho_\infty}\dot{a}(t) = L_e\frac{D_\infty T_3^*}{T_\infty^*}\frac{\partial T_3^*}{\partial r} - \frac{\rho_2}{\rho_\infty}\frac{C_{p_2}}{C_p}\alpha_2\frac{\partial T_2^*}{\partial r} \quad , \quad r = a(t) \quad , \tag{6.42}$$

where $L = (h_{F_3} - h_2)/H$ is the normalized heat of vaporization of the fuel, assumed constant.

Finally, the Clausius-Clapeyron equation gives the fuel mass fraction at the vapor side of the interface as

$$Y_F(a(t),t) = m_F \exp\left[\chi\left(\frac{1}{T_B^*} - \frac{1}{T_3^*}\right)\right] \quad , \tag{6.43}$$

where T_B^* is the fuel boiling temperature and $\chi = L/R_F$, where R_F is the fuel-vapor gas constant.

The infinity conditions, $r \to \infty$, are the same as equations (6.33b) and (6.34).

6.1.2 *Solution Methodology*

The problem as formulated in the previous section contains four sources of nonlinearity in the differential equations.

(i) The convection nonlinearity, represented by the appearance of the velocity V in the material derivative D/Dt,

(ii) the variable density, manifested in the continuity equation (6.5) and the factor T_3^* multiplying the divergence terms in equations (6.38),

(iii) the variable transport properties, manifested by the appearance of T_3^* multiplying the gradient vectors in the divergence terms of

equation (6.28),

(iv) the nonlinear reaction rate ω.

The liquid-vapor interface boundary conditions are also nonlinear by virtue of (iii) and also because the Clausius-Clapeyron equation (6.43) is very nonlinear.

Some of these nonlinearities can be removed by recasting the equations in Lagrangian coordinates. Further, by invoking Schvab-Zeldovich formulation and using an approximate linear form of Clausius-Clapeyron equation, the problem can be turned amenable to analytical solution. Then the solution of this problem can be obtained by means of Laplace transform method. The details of the transformations and solution procedure are presented in Reference [2].

6.3.2 *Solutions*

Two important expressions, one for the instantaneous burning rate and the other for the instantaneous temperature within the composite drop are the primary outcomes of the solution of this analysis.

The instantaneous burning rate is cast in the form of the diameter^2-time variation which is customarily used in the droplet combustion literature.

$$\left(\frac{a}{a_o}\right)^2 = \left(1 - \frac{\tau}{\tau_\omega}\right) \frac{1 + \frac{2}{3}\frac{B_1}{m_o}\omega_o^{1/2} - \frac{1}{2}\left(\frac{B_2}{m_o} - \frac{1}{3}\frac{B_1^2}{m_o^2}\right)\omega_o - \frac{2}{5}\left(\frac{B_3}{m_o} + \frac{11}{12}\frac{B_1 B_2}{m_o^2} - \frac{1}{36}\frac{B_1^3}{m_o^3}\right)\omega_o^{3/2}}{1 + \frac{2}{3}\frac{B_1}{m_o}\omega_o^{1/2} - \frac{1}{2}\left(\frac{B_2}{m_o} - \frac{1}{3}\frac{B_1^2}{m_o^2}\right)\omega_o - \frac{2}{5}\left(\frac{B_3}{m_o} + \frac{11}{12}\frac{B_1 B_2}{m_o^2} - \frac{1}{36}\frac{B_1^3}{m_o^3}\right)\omega_o^{3/2}}, \tag{6.44}$$

where

$$\omega_o = \frac{2 m_o \left(1 - \frac{\tau}{\tau_\omega}\right)}{1 - \frac{3}{5}\left(1 - \frac{\tau}{\tau_\omega}\right)}, \tag{6.45}$$

and $\Omega_o \equiv 5\epsilon m_o$ and $\tau \equiv D_\infty t/a_o^2$.

Also, in the above expression,

$$B_1 \equiv \frac{BE_1}{\omega(1+B)} \tag{6.46}$$

$$B_2 = \frac{\omega B_1^2}{2} \tag{6.47}$$

$$B_3 \equiv \frac{BE_3}{(1+B)} - \frac{\omega^2 B_1^3}{3} \tag{6.48}$$

$$m_o \equiv \frac{\frac{\rho_2}{\rho_\infty} - 1}{\frac{\rho_2}{\rho_\infty} - \frac{T_\infty}{T_{3_s}}} \tilde{m} \tag{6.49}$$

$$\omega = \frac{\ell n(1+B)}{\tilde{m}} \frac{\frac{\rho_2}{\rho_\infty} - \frac{T_\infty}{T_{3_s}}}{\frac{\rho_2}{\rho_\infty} - 1} \tag{6.50}$$

$$\tilde{m} = \frac{1}{T^*}\left[T_\infty^* - Q_{T_s} + C_T\, \ell n\left(\frac{Q_{T_\infty} - C_T}{Q_{T_s} - C_T}\right) + C_F\, \ell n\left(\frac{Q_{T_\infty} - C_T}{Q_{T_f} - C_T}\right)\right] . \tag{6.51}$$

$$B = \left(1 - \frac{\rho_\infty}{\rho_2}\right)\left(\frac{Q_{T_\infty} - Q_{T_s}}{L}\right) \tag{6.52}$$

$$E_1 \equiv \frac{\Gamma(\frac{1}{2})}{\pi G_{oo}} \tag{6.53}$$

$$E_3 \equiv \frac{(Q_{F_s} - Q_{F_o})(Q_{T_s} - T_o^*)}{(m_F - Q_{F_s})(Q_{T_s} - Q_{T_o})} A_3^* \frac{\Gamma(\frac{3}{2})}{\pi} \left(\frac{D_\infty}{\alpha_1}\right)^{3/2} \tag{6.54}$$

$$G_{oo} = \frac{m_o}{e^{\omega m_o} - 1} \tag{6.55}$$

$$A_3^* = \frac{1}{3G_{oo}^2}\sqrt{\frac{\alpha_1}{D_\infty}}\frac{L_2}{L_1}\left[b^3\frac{k_1}{k_2} + \frac{\alpha_1}{\alpha_2}(1-b^3)\right] \tag{6.56}$$

$$b = \frac{a_1}{a} \tag{6.57}$$

$$Q_F = Y_F - Y_X \tag{6.58}$$

$$Q_T = T_3^* + Y_X \tag{6.59}$$

and α = thermal diffusivity, ρ = density, ω = chemical reaction rate, k = thermal conductivity, L = latent heat, D = diffusion coefficient, a = radius of the inner core of fuel shell, r = radial coordinate.

Further, the expression for the temperature within the drop as a function of location and time was derived to be

$$\bar{T}_1^*(r,t) = T_o^* + \frac{(T_{ss}^* - T_o^*)}{2R}\sum_{m=0}^{\infty} H_m F_m(R,\tau_1) \quad , \tag{6.60}$$

where the first eight terms of F_m are given by

$$F_o(R,\tau_1) \equiv 2\sqrt{\frac{\tau_1}{\pi}}(I_1 - I_2) \tag{6.61}$$

$$F_1(R,\tau_1) \equiv R\left[\operatorname{erfc}\left(\frac{1-R}{2\sqrt{\tau_1}}\right) + \operatorname{erfc}\left(\frac{1+R}{2\sqrt{\tau_1}}\right)\right] \tag{6.62}$$

$$F_2(R,\tau_1) \equiv \frac{1}{\sqrt{\pi\tau_1}}(I_1 - I_2) \tag{6.63}$$

$$F_3(R,\tau_1) \equiv \frac{1}{2\sqrt{\pi\tau_1^3}}\left[(1-R)\,I_1 - (1+R)\,I_2\right] \tag{6.64}$$

$$F_4(R,\tau_1) \equiv \frac{1}{2\sqrt{\pi\tau_1^3}}\left[I_1\left\{\frac{(1-R)^2}{2\tau_1} - 1\right\} - I_2\left\{\frac{(1+R)^2}{2\tau_1} - 1\right\}\right] \tag{6.65}$$

$$F_5(R,\tau_1) \equiv \frac{3}{4\sqrt{\pi\tau_1^5}}\left[I_1\left\{\frac{(1-R)^3}{6\tau_1} - (1-R)\right\} - I_2\left\{\frac{(1+R)^3}{6\tau_1} - (1-R)\right\}\right] \tag{6.66}$$

$$F_6(R,\tau_1) \equiv \frac{3}{4\sqrt{\pi\tau_1^5}}\left[I_1\left\{\frac{(1-R)}{12\tau_1^2} - \frac{(1-R)^2}{\tau_1} + 1\right\} - I_2\left\{\frac{(1+R)^4}{12\tau_1^2} - \frac{(1+R)^2}{\tau_1} + 1\right\}\right] , \tag{6.67}$$

$$F_7(R,\tau_1) \equiv \frac{15}{8\sqrt{\pi\tau_1^7}}\left[I_1\left\{\frac{(1-R)^5}{60\tau_1^2} - \frac{(1-R)^3}{3\tau_1} + (1-R)\right\} - I_2\left\{\frac{(1+R)}{60\tau_1^2} - \frac{(1+R)^3}{3\tau_1} + (1+R)\right\}\right] , \tag{6.68}$$

where

$$I_1 \equiv \exp\left\{-\frac{(1-R)^2}{4\tau_1}\right\} , \tag{6.69}$$

$$I_2 \equiv \exp\left\{-\frac{(1+R)^2}{4\tau_1}\right\} , \tag{6.70}$$

and

$$\tau_1 \equiv \frac{\alpha_1 t}{a^2} , \quad R = \frac{r}{a} . \tag{6.71}$$

$$H_m \equiv \sum_{n=0}^{m} \frac{A^*_{m-n}}{n!} \tag{6.72}$$

where $A^*_0 = 1$, $A^*_1 = 0$ and (6.73)

$$A^*_2 \equiv \frac{L_2}{L_1}\frac{G_{12} - G_{22}}{G_{oo}} - G_{12} , \tag{6.74}$$

$$A^*_3 \equiv \frac{L_2}{L_1}\sqrt{\frac{\alpha_1}{D_\infty}}\frac{G_{22} - G_{12}}{G^2_{oo}} \equiv \frac{1}{3G^2_{oo}}\sqrt{\frac{\alpha_1}{D_\infty}}\frac{L_2}{L_1}\left[b^3\frac{k_1}{k_2} + \frac{\alpha_1}{\alpha_2}(1-b^3)\right] , \tag{6.75}$$

$$A^*_4 = A^{*2}_2 - G_{14} + \frac{L_2}{L_1}\frac{D_2}{G_{oo}} , \tag{6.76}$$

$$A^*_5 = 2A^*_2A^*_3 - \frac{L_2}{L_1}\sqrt{\frac{\alpha_1}{D_\infty}}\frac{D_2}{G^2_{oo}} , \tag{6.77}$$

$$A^*_6 = A^{*2}_2 + A^{*2}_3 - G_{16} + \frac{L_2}{L_1}\frac{D_4}{G_{oo}} , \tag{6.78}$$

$$A^*_7 = 2A^*_2A^*_5 - A^{*2}_2A^*_3 - 2A^*_3\left[G_{14} - \frac{L_2}{L_1}\frac{D_2}{G_{oo}}\right] - \frac{L_2}{L_1}\sqrt{\frac{\alpha_1}{D_\infty}}\frac{D_4}{G^2_{oo}} \tag{6.79}$$

where

$$D_2 \equiv G_{14} - G_{24} + \frac{\alpha_1}{D_\infty} \frac{G_{12} - G_{22}}{G_{00}^2} \tag{6.80}$$

$$D_4 \equiv G_{16} - G_{26} + \frac{\alpha_1}{D_\infty} \frac{D_2}{G_{00}^2} \tag{6.81}$$

$$G_{00} \equiv \frac{m}{e^{\omega m} - 1} \tag{6.82}$$

where

$$G_{12} \equiv \frac{b^2}{6} \{1 + 2(1-b) \frac{k_1}{k_2}\} + \frac{\alpha_1}{\alpha_2} \frac{(1-b)^2}{6} (1+2b) \quad , \tag{6.83}$$

$$G_{14} \equiv \frac{b^4}{5!} \{1 + 4(1-b) \frac{k_1}{k_2}\} + \frac{(\frac{\alpha_1}{\alpha_2})^2 (1-b)^4 (1+4b)}{5!} \tag{6.84}$$

$$G_{16} = \frac{b^6}{7!} [(1 + 6 \frac{k_1}{k_2})(1-b) + b] + \frac{\alpha_1}{\alpha_2} \frac{b^4 (1-b)^2}{3!5!} [(1 + 4 \frac{k_1}{k_2})(1-b) + 3b]$$

$$+ (\frac{\alpha_1}{\alpha_2})^2 \frac{b^2 (1-b)^4}{3!5!} [(1 + 2 \frac{k_1}{k_2})(1-b) + 5b] + (\frac{\alpha_1}{\alpha_2})^3 \frac{(1-b)^6}{7!} [1 + 6b] \tag{6.85}$$

$$G_{22} \equiv \frac{b^2}{6} (1 + 2 \frac{k_1}{k_2}) + \frac{\alpha_1}{\alpha_2} \frac{1-b^2}{2} \tag{6.86}$$

$$G_{24} \equiv \frac{b^4}{5!} (1 + 4 \frac{k_1}{k_2}) + \frac{(\frac{\alpha_1}{\alpha_2})^2 (1-b)^3 (1+3b)}{4!}$$

$$+ \frac{1}{12} (\frac{\alpha_1}{\alpha_2}) b^2 (1-b) \{1 + b + 2(1-b) \frac{k_1}{k_2}\} \quad . \tag{6.87}$$

$$G_{26} = \frac{b^6}{7!}\left[1 + 6\,\frac{k_1}{k_2}\right] + \frac{\alpha_1}{\alpha_2}\,\frac{b^4(1-b)}{2!5!}\left[\left(1 + 4\,\frac{k_1}{k_2}\right)(1-b) + 2b\right]$$

$$+ \left(\frac{\alpha_1}{\alpha_2}\right)^2 \frac{b^2(1-b)^3}{3!4!}\left[\left(1 + 4\,\frac{k_1}{k_2}\right)(1-b) + 4b\right] + \left(\frac{\alpha_1}{\alpha_2}\right)^3 \frac{(1-b)^5}{6!}\left[1 + 5b\right] \qquad (6.88)$$

and

$$\lambda \equiv \sqrt{\frac{sa^2}{\alpha_1}} \qquad (6.89)$$

Whereas this series representation is valid for large time, a finite truncation does not diverge as $t \to 0$ (for $R \neq 1$) as happens for equation 8.2 in Ref. 2. Thus, a truncation of the series yields a better approximation than the corresponding asymptotic expansion.

6.2 Integral Thermal Model

This model is an approximate model where thermal energy balance equations are written in the integrated form. Although for a first look the equations appear to describe the problem only in terms of heat transfer, the mass transfer process is also accounted for through the terms involving evaporation rate and latent heat of vaporization of fuel. Empirical relations for the evaporation rate of fuel drops, the dependence of evaporation rate of fuel on pressure, temperature, and other ambient variables, and the rate of convective heat transfer to the drop are used in this approximate analysis.

A physical description of the processes assumed in this model is shown in Figure 36 and is outlined in the following. At t=0 an emulsion drop of initial radius a_0 is exposed to hot ambient gases flowing past the drop with a relative velocity V. The droplet temperature is assumed to be uniform throughout its volume. This assumption appears to be reasonable in view of the results of the more rigorous model of Birchley and Riley [38], which shows that the spatial variation of temperature in the drop is small, particularly at the instant of drop disruption. The internal phase of the drops is assumed to consist of monosized droplets uniformly distributed throughout the continuous phase. Heat transferred from the ambient gases to the drop is assumed to provide the sensible and latent heats of oil, sensible heat of the internal phase, and the heat of liquid phase pyrolysis of oil. When the droplet temperature reaches a certain value, the internal phase is assumed to begin evaporation, and hence the latent heat of evaporation is included as a heat sink term. Since it is not yet clear from the previous studies, whether this temperature corresponds to the saturation temperature

or super heat limit of the internal phase, both cases can be included here. The vapor formed by all the droplets is supposed to coalesce into a single vapor bubble which will be surrounded by a shell of oil. Further heating would cause an increase in the diameter of this bubble with a consequent increase in the outward force exerted on the oil film. During the same period, surface tension allowable in the oil film decreases because of increase in the temperature of the drop. The droplet is assumed to explode when the outward pressure exceeds the allowable internal pressure due to surface tension of the oil. Thermal properties of the liquid phase are assumed constant, but the variation of the properties needed to calculate the convective film heat transfer coefficient with temperature is considered. Also, the changes in volume of the internal phase and oil due to thermal expansion are taken into account.

This model is somewhat similar to the model of Jacques [37] with the following departures. In this model, for simplicity, the lumped system approach (Ozisik, [66]) has been taken for unsteady heat transfer analysis, which appears reasonable in the light of the results of the analysis of Birchley and Riley [38]. Secondly, evaporation of oil, which was neglected by Jacques [37] and was attributed as a possible reason for the unrealistically high droplet temperatures predicted by him, is included in the present analysis. Thirdly, Jacques considered a drop subjected to a radiant field, but the present analysis is carried out for a drop in a convective heat transfer field, in order to check the predictions with the experimental results of the present study.

Under the above assumptions the transient heat and mass balance equations are:

$$4\pi a_2^2 h(T_\infty - T_d) = m_2 c_{p2} \dot{T}_d + \dot{m}_2 L_2 + m_1 c_{p1} \dot{T}_d + m_2 \dot{H}_p$$

for $(T_d \cdot T_{sh})$ . . .

$$4\pi a_2^2 h(T_\infty - T_d) = \dot{m}_2 L_2 + \dot{m}_{1e} L_1 + m_2 \dot{H}_p$$

for $(T_d = T_{sh})$ . . .

$$4\pi a_2^2 h(T_\infty - T_d) = m_2 c_{p2} \dot{T} + \dot{m}_2 L_2 + m_1 c_{p1v} \dot{T}_d + m_2 \dot{H}_p$$

for $(T_d > T_{sh})$ . . .

$$a_2^3 = \frac{3}{4\pi} \left[\frac{m_2}{\rho_2} \{1 + \beta_2(T_d - T_{do})\} + v_1\right]$$

for $T_d \gtrless T_{sh}$ . . .

$$v_1 = \frac{m_1}{\rho_1} [1 + \beta_1(T_d - T_{do})] \qquad \text{for } (T_d < T_{sh}) \text{ . . .}$$

$$v_1 = m_1 \left[\frac{1}{\rho_1} + \frac{\int_o^t \dot{m}_{1e}\, dt}{m_1} \frac{1}{dv}\right] \qquad \text{for } (T_d = T_{sh}) \text{ . . .}$$

$$v_1 = m_1 \left[\frac{R_{1v} T_1}{P}\right] \qquad \text{for } T_d > T_{sh} \text{ . . .}$$

$$m_1 = W m_2$$

The force balance in the fuel film gives the following expression for tension induced in the oil film

$$\Gamma'_{2\infty} = a_{1e}^2 (P - P_\infty)/2(r_2 + r_{1e})$$

The instantaneous allowable surface tension in the oil film

$$\Gamma''_{2\infty} = \Gamma_{2\infty\, o}[(\rho_2 - \rho_{2v})/(\rho_{2o} - \rho_{2vo})]^4$$

from Perry and Chilton (1973) Ref. [67].

where, a = radius, T = temperature, t = time, m = instantaneous mass, V = instantaneous volume, c_p = specific heat, ρ = density, β = volumetric expansivity, H_p = heat of pyrolysis, k = coefficient in the burning rate equation $m_2 = m_{2o} \exp(-kt)$, w = ratio of internal phase to continuous phase masses, Γ = surface tension and the subscripts: 1 = internal phase, 2 = fuel phase, o = initial condition, b = break-up condition, and the dotted quantities refer to the time rate of change of variable.

6.2.1 *Approximate Solution*

As drop disruption is likely to occur when the drop temperature is close to the superheat limit temperature (T_{sh}) of the internal phase at which it flashes into vapor, the period when $T_d < T_{sh}$ is of interest. An approximate analytical solution for the time required for the drop temperature to reach T_{sh} and thus result in fragmentation has been derived in Ref. 2.

$$t_b = \frac{T_{sh} - T_{do}}{\Theta_1}$$

where t_b = disruption time and

$$\Theta_1 = k \frac{L_2 T_{do}}{c_{p_2} + wc_{p_1}} + \frac{4\pi a_o^2 h}{c_{p_2} + wc_{p_1}} \frac{T_\infty - T_{do}}{m_{2o}}$$

6.3 Results

6.3.1 *Calculation Procedure*

A computer program was developed to solve the equations 6.60 to 6.89. This program is general enough for predicting the temperature at any location of the interior of the droplet as a function of time for the emulsion

of any oil with water as internal phase if the properties of the continuous phase liquid are known. The input data needed for this program are: initial temperature of the drop, ambient temperature, boiling point, density, specific heat, thermal conductivity, latent heat of vaporization, ambient pressure, stoichiometric ratios m_F and m_X defined in equation 6.22, the heat of reaction per unit mass of products in the stoichiometric equation, and the ratio of the radius of the internal phase core to the drop radius at the initial conditions. The output of the computer program consists of the dimensionless temperature (C_pT/H) as a function of dimensionless time ($t\ D_\infty/a_0^2$), where t = time, T = temperature, H = heat of reaction per unit mass of products, D_∞ = diffusion coefficient, a_0 = initial radius of the drop. The program also allows for the variation of properties with temperature and pressure if the empirical relations for those variations are available. In the present study, this program was used to determine the droplet temperature-time curves for different values of water content, initial temperature of the drop, ambient temperature, ambient pressure, and ambient oxygen concentration. From these curves, the values of dimensionless time parameter ($D_\infty t/a_0^2$) required for the droplet center temperature to reach the vaporization temperature of the internal phase was determined. Droplet fragmentation was assumed to occur at that instant. The vaporization temperature was taken to be the arithmetic average of the normal boiling point and the superheat limit of the water, since the superheat limit for homogeneous nucleation is likely to be lowered in the drop because of dissolved gases. Further, the ratio of the volume of oil at the instant of disruption to its initial volume was also determined,

since that ratio would give a good indication of the effectiveness of the fragmentation in achieving better mixing in the combustion systems.

The computation of the variation of disruption time with water content was also performed with the approximate model.

7.3.2 No. 4 Oil-Water Emulsions

Figures 37 to 46 show the plots of dimensionless temperature at the center of the drop with dimensionless time for various parameters indicated on them. Figures 37 to 46 also show the variation of disruption time (time required for the drop center temperature to reach the vaporization temperature of the internal phase) with the ambient and emulsion parameters. Also, on these figures, the parameter (t_b/a_o^2) which can be used directly for predicting the disruption time if the initial radius of the drop is known is plotted. The values of the parameters used in the evaluation of the model for No. 4 oil-water emulsions are shown in Table 10.

The variation of disruption time with the initial radius ratio of the water core to the drop radius is in agreement with the results obtained earlier [2] for the conditions at which the model by Birchley and Riley [38] was analyzed. It shows that disruption time increases up to a certain value of B_o and then decreases. The initial increase with B_o is attributed to the dominance of the effects of increasing heat capacity of the composite drop because of the higher specific heat of water than oil. The decreasing part of the curve is believed to be caused by the dominance of the diffusional effects that increase the thermal diffusion as the water core comes closer to the drop surface.

The effects of ambient temperature on the dimensionless break-up time Fig. 42 is surprising at the first glance because the increase of ambient temperature seems to increase the disruption time. But this increase is essentially caused by the increase of D_∞ with T_∞ and hence the parameter (t_b/a_o^2) shows a decrease with ambient temperature. The increase of ambient temperature also increases the heat transfer rate to the drop and consequently accelerates its fragmentation.

The effects of ambient pressure on the variation of the drop temperature with time are shown in Fig. 45 and the variation of disruption time declines very rapidly with chamber pressure, the dimensional disruption time decreases much more slowly. This indicates that the decrease of diffusion coefficient offsets the decrease of disruption time considerably at higher pressures in this spherico-symmetric droplet model. However, the disruption time decreases slowly up to a pressure of 1.5 MPa and then remains essentially constant. There appear to be some effects of pressure on drop disruption time which counteract one another. Law [65] has pointed out these effects are (i) the faster heating up of droplet and relatively invariant superheat limits of homogeneous nucleation, which accelerate disruption at high pressures, (ii) the increased ambient density that increases convection and internal circulation of the droplet, and thus inhibit disruption, and (iii) the increased resistance for droplet breakup at higher pressures which further inhibit disruption. This model has not accounted for the second and third factors. However, the decrease of thermal and mass diffusivities at high pressures decrease heat transfer to the droplet and seem to counteract the effect of the decrease of the latent heat of vaporization of the fuel.

AD-A095 612 OKLAHOMA UNIV NORMAN SCHOOL OF AEROSPACE MECHANICAL --ETC F/G 21/2
COMBUSTION OF DROPS AND SPRAYS OF HEAVY FUEL OILS AND THEIR EMU--ETC(U)
DEC 80 S R GOLLAHALLI, M L RASMUSSEN DOT-CG-93621-A
UNCLASSIFIED OU-AMNE-80-19 USCG-D-64-80 NL

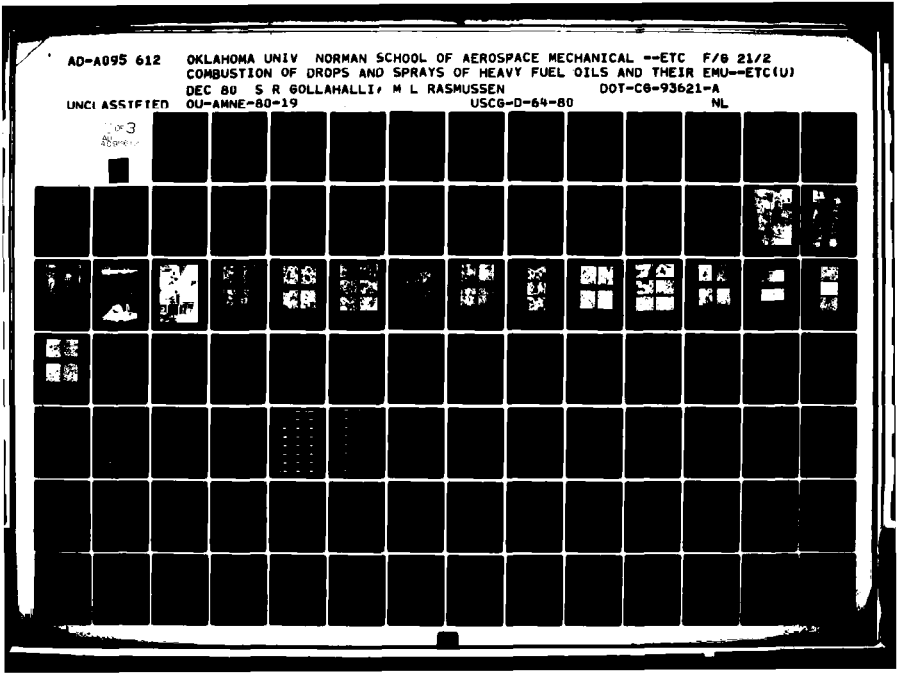

Figure 47 shows the comparison of (t_b/a_o^2) predicted by the differential model and the approximate integral model outlined in the Section 6.2. for various water contents of No. 4 oil-water emulsions. It is seen that integral model which does not account for the thermal diffusion in the interior of the composite droplet shows that disruption time increases weakly with water content. This increase of disruption time is primarily caused by the increase of thermal capacity of the composite drop because of the higher specific heat of water than that of oil. This trend predicted by the approximate model is in agreement with the prediction of the differential model for low water contents (in this case for $W \leq 0.03$). However, for larger contents, the disruption time decreases with water content as found in Ref. 2. Further, the values of disruption time predicted by the differential model is larger than those predicted by the integral model by factors of nearly 30. The reasons for this difference are (i) the differential model assumes a spherico-symmetric droplet where the heat and mass transfer in the gas phase are by molecular diffusion only, whereas the heat transfer in the gas phase by the much faster convection mode is considered in the approximate model and (ii) the evaporation of the oil film is accounted by the empirical relations in the integral model, whereas it is considered by the quasi-steady analysis in the differential model.

Figure 49 also shows the predicted ratio of the volume of oil at the instant of disruption to its initial volume plotted against water content. It is seen that this ratio decreases monotonically with water content indicating that disruption of drops at lower water contents would be better since a large part of the parent oil drop undergoes fragmentation.

The variation of disruption time with water content for No. 2, No. 4, and No. 6 oil-water emulsion drops predicted with the differential model is shown in Fig. 48. The trend of the variation is that, although similar for all three fuels, the water content at which disruption time peaks seems to be higher for lighter fuels. The probable reason for this behavior is the variation in the difference of the heat capacities of oil and water, $(\rho c_p)_{oil} - (\rho c_p)_{water}$. In the case of No. 2 oil-water emulsions, that difference is larger and hence the effect of water increasing disruption time is dominant.

6.3.3 Comparison of Predicted and Measured Disruption Times

In order to provide a check on the validity of the theoretical models, the variation of measured disruption times with some variables (W, T_{di}, X_{O_2}, P_{ch}) are plotted in Figs. 50 to 53. A comparison of these figures with Figs. 40, 44, 46, 47 reveal the following: (i) the values of the disruption times predicted by the differential model are nearly two orders of magnitude higher than the measured values, whereas the values predicted by the integral model, although slightly higher, compare reasonably well with the experimental values and (ii) the trends of variations of disruption times with variables shown predicted by the differential model, however, are in far better agreement with measured trends than the predictions of the integral model.

As discussed in Section 6.2.2, the prime reasons for the high values predicted by the differential model are: (i) the assumption of spherico-symmetric model and (ii) neglecting of radiative and convective heat transfer to the drop. Hence, the heat transfer rate to the drop

is grossly underpredicted by that model for drops in the present experiments, where they were subjected to convection and radiation from the chamber walls. Furthermore, although all attempts were made to ensure that the droplets remained at their injection temperature until they were released into the chamber, some additional preheating of the fuel could not be avoided because of the design considerations. That additional preheating would cause a shorter disruption time as noticed in Fig. 40 and thus lowers the measured disruption times.

The fact that the trends predicted by the differential model are in reasonable agreement with the measured values indicates that the basic analysis is satisfactory and the model needs refinements by way of accounting for convective and radiative heat input to the drops. The integral model which approximately accounts for the convective heat transfer to the drops predicts the disruption time values closer to the measured values. However, the trends predicted by it [2] agree qualitatively with experimentally recorded variations with T_{di} and X_{O_2} and only for small values of W. The reason for the lack of agreement over the entire range of W, is that the integral model accounts for only heat capacity effects of water in the composite drop which results in a linear increase of disruption time with water content.

REFERENCES

1. Gollahalli, S.R., Rasmussen, M.L., and Moussavi, S.J.: "Combustion of Drops and Sprays of No. 2 Diesel Oil and its Emulsions with Water and Methanol," Vol. I (Experimental), U.S. Department of Transportation Report No. DOT/RSPA/DPG-50/80/1 (1980), NTIS PB-80-178213.

2. Rasmussen, M.L. and Gollahalli, S.R.: "Combustion of Drops and Sprays of No. 2 Diesel Oil and its Emulsions with Water and Methanol," Vol. II (Theoretical), U.S. Department of Transportation Report No. DOT/RSPA/DPB-50/80/2 (1980), NTIS PB-80-178221.

3. Moussavi, S.J.: "Combustion of Drops and Sprays of No. 2 Diesel Oil and its Emulsions with Water and Methanol," M.S. Thesis, School of Aerospace, Mechanical and Nuclear Engineering, The University of Oklahoma, Norman, OK 73019 (1979).

4. Michael, M.I. and El-Wakil, M.M.: "On the Self-Ignition of Hydro-Carbon Mixtures," Eleventh Symposium (Int.) on Combustion, The Combustion Institute, pp. 1027-1035 (1967).

5. Tamura, Z. and Tanasawa, Y.: "Evaporation and Combustion of a Drop Contacting with a Hot Surface," Seventh Symposium (Int.) on Combustion, Butterworths, pp. 509-522 (1959).

6. Kobayasi, K.: "An Experimental Study on the Combustion of a Fuel Droplet," Fifth Symposium (Int.) on Combustion, Rienhold, pp. 141-144 (1955).

7. Hottel, H.C., Williams, G.C., and Simpson, H.C.: "Combustion of Droplets of Heavy Liquid Fuels," Fifth Symposium (Int.) on Combustion, Rienhold, pp. 101-129 (1955).

8. Masdin, E.G. and Foster, P.J.: "The Size and Structure of Cenospheres Formed from Residual Liquid Fuels," Fuel, 39, pp. 413-419 (1960).

9. Masdin, E.G. and Thring, M.W.: "Combustion of Single Droplets of Liquid Fuel," JIF, 35, pp. 251-260 (1962).

10. Archer, J.S. and Eisenklam, P.: "Multistage Combustion of Residual Fuel Oil. Parts 1 and 2," JIF, pp. 397-404, pp. 451-460 (1970).

11. Godridge, A.M.: "Carbon Formation in Large Residual Fuel Oil Fired Burners," JIF, 44, pp. 599-606 (1971).

12. Shyu, R.R., Chen, C.S., Goudie, G.O., and El-Wakil, M.M.: "Multi-component Heavy Fuel Drop Histories in a High Temperature Flow Field," Fuel, 51, p. 135 (1972).

13. Topps, J.E.C.: "An Experimental Study of the Evaporation and Combustion of Falling Droplets," JIF, 37, pp. 535-553 (1951).

14. Safford, D.: "Clean Burning of Residual Fuel Oil," ASHRAE Journal, pp. 41-43 (1969).

15. Gerald, C.F.: D.Sc. Thesis, (1940) Chemical Engineering, MIT, cited in Reference 7.

16. Chang. T.Y.: D.Sc. Thesis, (1941) Chemical Engineering, MIT, cited in Reference 7.

17. Peterson, F.: "The Mass of an Oil-Droplet During Combustion," Second European Symposium on Combustion, Academic Press, p. 366 (1974).

18. Jacques, M.T., Jordan, J.B., and Williams, A.: "The Combustion of Emulsions of Water and Fuel Oil," Second European Symposium on Combustion, Academic Press, p. 397 (1974).

19. McCreath, C. and Chigier, N.A.: "Liquid Spray Burning in the Wake of a Stabilizer Disc," Fourteenth Symposium (Int.) Combustion Instutute.

20. Onuma, Y. and Ogasawana, M.: "Studies on the Structure of a Spray Combustion Flame," Fifteenth Symposium (Int.) on Combustion, The Combustion Institute, Pittsburgh, PA, p. 453 (1975).

21. Onuma, Y., Ogasawana, M., and Inoue, T.: "Further Experiments on the Structure of a Spray Combustion Flame," Sixteenth Symposium (Int.) on Combustion, The Combustion Institute, Pittsburgh, PA, p. 561 (1977).

22. Nasrullah, M.K.: "Flame Structure of Burning Residual Oil and Residual Oil-Water Emulsion Sprays," M.S. Thesis, School of Aerospace, Mechanical and Nuclear Engineering, The University of Oklahoma (1979).

23. Hajzargarbhashi, J.: "Combustion of Heavy Oil-Water Emulsion and Oil-Water Emulsion and Oil-Coal-Water Slurries," M.S. Thesis, School of Aerospace, Mechanical and Nuclear Engineering, The University of Oklahoma (1980).

24. Goodger, E.M. and Najjar, S.H.: "Heavy Fuel Flame Radiation in Gas-Turbine Combustors - Exploratory Results," Fuel, 56, pp. 437-440 (1977).

25. Sakai, T. and Sugiyama, S.: "Residual Carbon Particles Yields by Combustion of Atomized Heavy Fuel-Oil Droplets," JIF, pp. 451-460 (1970).

26. Goldstein, H.L. and Siegmund, C.W.: "Particulate Emissions from Residual Fue Fired Burners: Influence of Combustion Modification," ASME, 76-WA/APC-3.

27. Godridge, A. and Hammond, E.: "Emissivity of a Large Residual Fuel Oil Flame," Twelfth Int. Combustion Symposium (Poiter)(1968), cited in Reference 8.

28. Schiefer, R.B.: "The Combustion of Heavy Distillate Fuels in Heavy Duty Gas Turbines," ASME, 71-GT-56.

29. Sulzer, P.T.: "The Influence of Some Chemicals and Physical Factors on the Formation of Deposits from Residual Fuels," Trans. ASME XI, pp. 995-1001 (1955).

30. Glassman, I., Dryer, F.L., and Naegeli, D.W.: "Fundamental Combustion Studies of Emulsified Fuels for Diesel Applications," Initiating Proposal to the NSF, Princeton University, Princeton, NJ (1975).

31. Ivanov, V.M. and Nefedov, P.I.: "Experimental Investigation of the Combustion Process of Natural and Emulsified Fuels," (1965), cited from Reference 24.

32. Dryer, F.L.: "Fundamental Concepts on the Use of Emulsions as Fuels," Paper presented at the Joint Meeting of the Central and Western States Sections of the Combustion Institute, San Antonio, TX (1975).

33. Dryer, F.L., Rambach, G.D., and Glassman, I.: "Some Preliminary Observations on the Combustion of Heavy Fuels and Water-in-Fuel Emulsions," Paper presented at the Spring Meeting of the Central State Section of the Combustion Institute, BMI, Columbus, OH (April 5,6, 1976).

34. Dryer, F.L.: "Water Addition to Practical Combustion Systems; Concepts and Applications," Sixteenth Symposium (Int.) on Combustion, The Combustion Institute, Pittsburg, PA, p. 279 (1977).

35. Jacques, M.T., Jordan, B., Williams, A., and Hadley-Coats, L.: "The Combustion of Water-in-Oil Emulsions and the Influence of Asphaltene Content," Sixteenth Symposium (Int.) on Combustion, p. 307 (1977).

36. Dooher, J., Gengberg, R., Lippman, R., Morronne, T., Moon, S., and Wright, D.: "Emulsions as Fuels," Mechanical Engineering, p. 36 (November, 1976).

37. Jacques, M.T.: "Transient Heating of an Emulsified Water-in-Oil Droplet," Combustion and Flame, 29, p. 77 (1977).

38. Birchley, J.C. and Riley, N.: "Transient Evaporation and Combustion of a Composite Water-Oil Droplet," Combustion and Flame, 29, p. 145 (1977).

39. Gollahalli, S.R.: "An Experimental Study of the Combustion of Unsupported Drops of Residual Oils and Emulsions," Combustion Science and Technology, 19, p. 245 (1979).

40. Lasheras, J.C., Fernandez-Pello, A.C., and Dryer, F.L.: "Initial Observations on the Free Droplet Combustion Characteristics of Water-in-Fuel Emulsions," Combustion Science and Technology, 21, pp. 1-14 (1979).

41. Spadaccini, L.J. and Pelmas, R.: "Evaluation of Oil/Water Emulsions for Application to Gas Turbine Engines," Paper presented in A.C.S. Meeting, San Francisco, Aug. 1976.

42. Law, C.K., Lee, C.H., and Srinivasan, N.: "Combustion Characteristics of Water-in-Oil Emulsions," Combustion and Flame, 37, p. 125 (1980).

43. Hall, R.E.: "The Effect of Water-Residual Oil Emulsions on Air Pollutant Emissions and Efficiency of Commerical Boilers," ASME paper 75-WA/APC-1 (1975).

44. Koval, A., Slupek, S., Kokkinos, A., Shaler, A., Miskovsky, N., and Essenhigh, R.H.: "Smoke Point and Heat Transfer Characteristics of Oil/Water/Air Emulsions without and with Coal Addition in a Hot Wall Furnace," Presented at the 1976 Spring Meeting of the Central States Section of the Combustion Institute.

45. Volkmar, D.S. and Carruette, B.: "Emulsion Production and Boiler Performance with the Total-Bertin Emulsified," First Symposium on Water-in-Fuel Emulsions in Combustion," Report No. CG-D-12-78, prepared for U.S. Department of Transportation, p. 62 (1978).

46. Kinney, R.R.: "Discussion of Test Results with Boilers and Gas Turbines," First Symposium on Water-in-Fuel Emulsion in Combustion, Report No. CG-D-12-78, prepared for U.S. Department of Transportation, p. 69 (1978), NTIS AD A061503.

47. Boquet, G. and Delatronche, C.: "New Development in Heavy Fuel-in-Water Emulsions," Second Symposium on Water-in-Fuel Emulsions in Combustion, Report No. CG-D-50-79, prepared for U.S. Department of Transportation, p. 56 (1979), NTIS AD A075837.

48. Moon, S. and Dooher, J.P.: "Emulsion Fuel Studies Using Low and High Sulfur Fuel Oil," Second Symposium on Water-in-Fuel Emulsions in Combustion, Report No. CG-D-50-79, prepared for U.S. Department of Transportation, p. 61 (1979), NTIS AD A075837.

49. Volkmar, D.S., Carruette, B., and Tranie, L.: "Total-Bertin Emulsifier," Second Symposium on Water-in-Fuel Emulsions in Combustion, Report No. CG-D-50-79, prepared for U.S. Department of Transportation, p. 65 (1979), NTIS AD A075837.

50. Kinney, R. and Lombard, P.: "Research Results on Emulsions in Boilers," Second Symposium on Water-in-Fuel Emulsions in Combustion, Report No. CG-D-50-79, prepared for U.S. Department of Transportation, p. 84, (1979), NTIS AD A075837.

51. Winkler, M.: "The Practical Effects of Burning Emulsions in Marine Gas Turbines and Boilers," Second Symposium on Water-in-Fuel Emulsions in Combustion, Report No. CG-D-50-79, prepared for U.S. Department of Transportation, p. 91 (1979), NTIS AD A075837.

52. Thompson, R.V.: "Application of Emulsified Fuels to Diesel and Boiler Plants," Second Symposium on Water-in-Fuel Emulsion in Combustion, Report No. CG-D-50-79, prepared for U.S. Department of Transportation, p. 96 (1979), NTIS AD A075837.

53. Walter, R.: "U.S. Coast Guard Emulsion Boiler Studies," Paper presented at the III Symposium on Emulsified Fuels in Combustion, Transportation Systems Center, Cambridge, MA (May 1980).

54. Winkler, M.: "MARAD Evaluation of Emulsion Fueled Diesel Engines," Paper presented at the III Symposium on Emulsified Fuels in Combustion, Transportation Systems Center, Cambridge, MA (May 1980).

55. Horner, J.E. and Nunez, C.A.: "Evalulation of Techniques for Improving Combustion Aboard Ships - Part II Medium Speed Diesel Engines, (Intermediate Grade Fuels)," Report prepared by Seaworthy Engine Systems, Inc., Essex, CT, U.S. Department of Commerce, NTIS PB80-126535, Nov. 1979.

56. Fogler, H.S.: Personal communication. November 1979.

57. Dietz, W.A.: "Response Factors for Gas Chromatographic Analysis," J. Gas Chrom., 5, p. 68 (1967).

58. Dryer, F.L., Kennedy, I.M., and Lasheras, J.C.: "Some Comparative Observations on the Vaporization and Combustion of Properties of Isolated Fuel Droplets Containing Water, Methanol or Ethanol," III Symposium on Emulsions, Transportation Systems Center, Boston, MA, May 1980.

59. Wright, F.J.: "Effect of Oxygen on the Carbon Forming Tendencies of Diffusion Flames," Fuel, 53, p. 232 (1974).

60. Gollahalli, S.R.: "Effects of Dilutents on the Flame Structure and Radiation of Propane Jet Flames in a Concentric Flame," Combustion Science and Technology, 15, p. 147 (1977).

61. Sjogren, A.: "Soot Formation by Combustion of an Atomized Liquid Fuel," Fourtheenth Symposium (International) on Combustion, The Combustion Institute, Pittsburgh, PA, p. 919 (1973).

62. Dunn, Jr., F.R.: "Improved Oil Burner Performance with Recirculation of Combustion Gases," Amer. Petrol. Inst. Conference Paper 61-8 (1961).

63. Glassman, I.: Combustion, Academic Press, 1977.

64. Chigier, N.: Discussion, Fifteenth Symposium (International) on Combustion, The Combustion Institute, Pittsburgh, PA, p. 319 (1973).

65. Law, C.K.: Discussion, Eighteenth Symposium (International) on Combustion, The Combustion Institute, Pittsburgh, PA (In press).

66. Ozisik, M.N.: Basic Heat Transfer, McGraw-Hill Book Co., 1976.

67. Perry, R.H. and Chilton, C.H.: Chemical Engineers Handbook, Fifth Edition, McGraw-Hill Book Co., pp. 3-240, 1973.

TABLES

TABLE 1

Properties of No. 6 Fuel Oil

Fuel Type: A.S.T.M. No. 6

Chemical Analysis % by Weight

Hydrogen	10.70
Carbon	86.00
Nitrogen	2.00
Sulfur	0.92
Ash	0.12
Water and Sediment	0.26

Pour Point °F	60
Flash Point °F (PM)	169
Gravity °API	17.8
Heating Value (Higher) Btu/lbm	18300

Viscosity at 100°F CS	1300
122°F CS	500
150°F CS	130
200°F CS	33
250°F CS	12

Distillation (wt) %	°F
IBP	250
10	430
20	550
30	660
40	750
50	900
60	950
90	1100

TABLE 2

Properties of No. 4 Fuel Oil

Fuel Type: A.S.T.M. No. 4

Chemical Analysis: % by weight

Hydrogen	12.00
Carbon	85.80
Nitrogen + oxygen	1.54
Sulfur	0.52
Ash	0.06
Water and sediment	0.08

Pour point, °F	20
Flash point, °F	150
Gravity °API	26
Heating value (higher) Btu/lbm	18860

Viscosity at

100°F CS	20.0
122°F CS	15.0
150°F CS	10.5
200°F CS	5.4
210°F CS	4.0

Distillation

wt %	°F
IBP	250
10	420
20	470
30	500
40	520
50	550
60	580
70	620
80	900
90	1050

TABLE 3

Surfactant Properties*

TWEEN 85

Description

Polysorbate 85
(Polyoxyethylene 20 sorbitan trioleate)

General Characteristics

Classification	Nonionic surfactant
Form @ 25°C	Amber liquid (may gel)
Specific gravity @ 25°C/25°C	Approx. 1.0
Viscosity @ 25°C	Approx. 300 cps
Flash point	Above 300°F
Fire point	Above 300°F
HLB number	11.0

Solubilities

(a) Soluble in most vegetable oils, cellosolve, lower alcohols, aromatic solvents, ethyl acetate, most mineral oils, mineral spirits, acetone, dioxane, carbon tetrachloride and ethylene glycol.

(b) Dispersible in water

Standard Specifications

Acid number	2.0 max
Saponification number	80-95
Hydroxyl number	39-52
Water, %	4.8-5.2

* Provided by ICI Americas Inc.

Table 3 - Cont'd

SPAN 80

Description

Sorbitan monooleate, NF

General Characteristics

Classification	Nonionic emulsifier
Form @ 25°C	Yellow liquid
Specific gravity @ 25°C/25°C	Approx. 1
Viscosity @ 25°C	Approx. 1000 cps
Flash point	Above 300°F
Fire point	Above 300°F
HLB number†	4.3

† Hydrophile-lipophile balance rating.

Solubilities

(a) Soluble in most mineral oils and vegetable oils, ethyl acetate and cellosolve.

(b) Slightly soluble in toluene, diethyl ether, dioxane, carbon tetrachloride, aniline and lower alcohols.

(c) Insoluble in water, acetone, propylene and ethylene glycols.

Standard Specifications

Acid number	8.0 max
Saponification number	145-160
Hydroxyl number	193-210
Water, %	1.0 max

Conforms to NF Specifications.

TABLE 4

Test Matrix for No. 4 Fuel Oil Single Drop Studies

Base Conditions	T_{ch} = 700 K, P_{ch} = 0.44 MPa, X_{O_2} = 0.21, W = 0.12 d_{di} = 2.5 μm, Internal Phase = Water, T_{di} = 295 K					
	W (Water)	M (Methanol)	T_{di}(K)	T_{ch}(K)	P_{ch}(MPa)	X_{O_2}
	0	0	300	672	1.13	0.280
Variation of	0.01	0.02	311	644	1.82	0.182
Parameters from	0.03	0.08	322	617	2.45	0.175
Base Conditions	0.08	0.15	333	589		
	0.15	0.20	344	561		
	0.20		356	533		
	0.30		361	506		
	0.40		367	477.8		

TABLE 5

Test Matrix for No. 4 Fuel Oil Spray Studies

Base Conditions	T_{ia} = 700 K, P_{ch} = .65 MPA, X_{O_2} = 0.21, W = 0.08, Internal Phase = Water, T_{inj} = 308 K, P_N = 20.8 MPa, Pintle Type Injector, d_{di} = 2.5 μm										
	W	T_{inj}(K)		X_{O_2}		P_{ch}(MPa)		P_N(MPa)		S	M
	Water	W=0	W=0.08	W=0	W=0.08	W=0	W=0.08	W=0	W=0.08	W=0.08	
	0	359	333	.25	.25	1.1	1.1	15.3	15.3	0.02	0.08
Variation of	0.01	379	379	.10	.10	1.8	1.8				0.20
Parameters from	0.03										
Base Conditions	0.12										
	0.20										

TABLE 6

Test Matrix for No. 6 Fuel Oil Spray Studies

Base Conditions	T_{ia} = 700 K, P_{ch} = .65 MPa, X_{O_2} = 0.21, W = 0.08 Internal Phase = Water, T_{inj} = 370 K, P_N = 20.8 MPa, Injector Type = Pintle, d_{di} = 2.5 μm								
	W	X_{O_2}		P_{ch}(MPa)		P_B(MPa)		S	M
	Water	W=0	W=0.08	W=0	W=0.08	W=0	W=0.08	W=0.08	
	0	.26	.26	1.1	1.1	15.3	15.3	0.02	0
Variation of	0.01	.17	.17	1.8	1.8				0.03
Parameters from	0.03								0.08
Base Condition	0.05								
	1.10								

TABLE 7

Effect of Surfactant Addition on the Combustion of the Sprays of No. 4 and No. 6 Oils and Their Emulsions With Water

	No. 4		No. 6	
Emulsion	W = 0.08	W = 0.08	W = 0.08	W = 0.08
Condition	S = 0.00	S = 0.02	S = 0.00	S = 0.02
R_{O_2}	0.031	0.019	0.016	0.010
R_{CO_2}	0.178	0.188	0.141	0.185
NO (PPM)	28.0	17	19	34
T_f (K)	1100	1033	1006	1130
CO (%)	-	-	5.9	0.11

TABLE 8

Effect of Nozzle Opening Pressure on the Combustion of Sprays of No. 4 and No. 6 Oils and Their Emulsions With Water

NO. 4 OIL

	Rated		Decreased	
	W=0.00	W=0.08	W=0.00	W=0.08
R_{O_2}	0.12	0.03	0.01	0.01
R_{CO_2}	0.14	0.17	0.13	0.17
NO(ppm)	36	28	24	19
NO_x(ppm)	39	36	38	40
T_f(K)	1117	1100	995	1012

NO. 6 OIL

	Rated		Decreased	
	W=0.00	W=0.08	W=0.00	W=0.08
R_{O_2}	0.012	0.016	0.01	0.01
R_{CO_2}	0.133	0.14	0.17	0.15
NO(ppm)	31	19	42	34
NO_x(ppm)	45	42	46	45
T_f(K)	1025	1006	1056	1048
CO(%)	8.5	5.9	3.1	2.8

TABLE 9

Values of Parameters Used in the Evaluation of Integral Model for No. 4 Oil-Water Emulsion Drop

K	1.0
L_2	56.7 cal/g
C_{P_1}	1.0 cal/g·K
C_{P_2}	0.65 cal/g·K
T_∞	700 K
T_{do}	323 K
a_o	1 mm
m_{2o}	0.001173 g
h	0.00382 cal/cm^2·s·K

TABLE 10

Values of Parameters Used in the Evaluation of Analytic Solution of the Differential Model (No. 4 Oil-Water Emulsion)

T_∞	700 K
T_o	323 K
T_B	647 K
L	56.7 (cal/g)
m_F	4.33
m_X	1.30
C_P	0.25 (cal/g.K)
C_{P_2}	0.65 (cal/g.K)
C_{P_1}	1.00 (cal/g.K)
H	2,403 (cal/g)
ρ_2	0.88 (g/cm^3)
P	0.483 MPa
Y_{X_∞}	0.23
a_o	0.1 cm

TABLE 11

Values of Parameters Used in the Evaluation of Analytic Solution of the Differential Model (No. 6 Oil-Water Emulsion)

T_∞	1100 K
T_o	300 K
T_B	760 K
L	50 (cal/g)
m_F	4.33
m_χ	1.30
C_p	0.25 (cal/g.K)
C_{p_2}	0.65 (cal/g.K)
C_{p_1}	1.00 (cal/g.K)
H	2,350 (cal/g)
ρ_2	0.94 (g/cm^3)
P	0.1 MPa
a_o	0.1 cm

TABLE 12

Measured Durations of Flame Sheath and Individual Drop Burning of the Sprays of No. 4 and No. 6 Oils and Their Emulsions

	No. 4 Oil		
	W=0	W=0.08	W=0.12
$\tau_{fs(s)}$	0.054	0.051	0.065
$\tau_{id(s)}$	0.081	0.078	0.082
$\tau_{total(s)}$	0.135	0.129	0.147

	No. 6 Oil		
	W=0	W=0.05	W=0.10
$\tau_{fs(s)}$	0.065	0.052	0.073
$\tau_{id(s)}$	0.145	0.117	0.104
$\tau_{total(s)}$	0.215	0.167	0.177

PHOTOGRAPHS

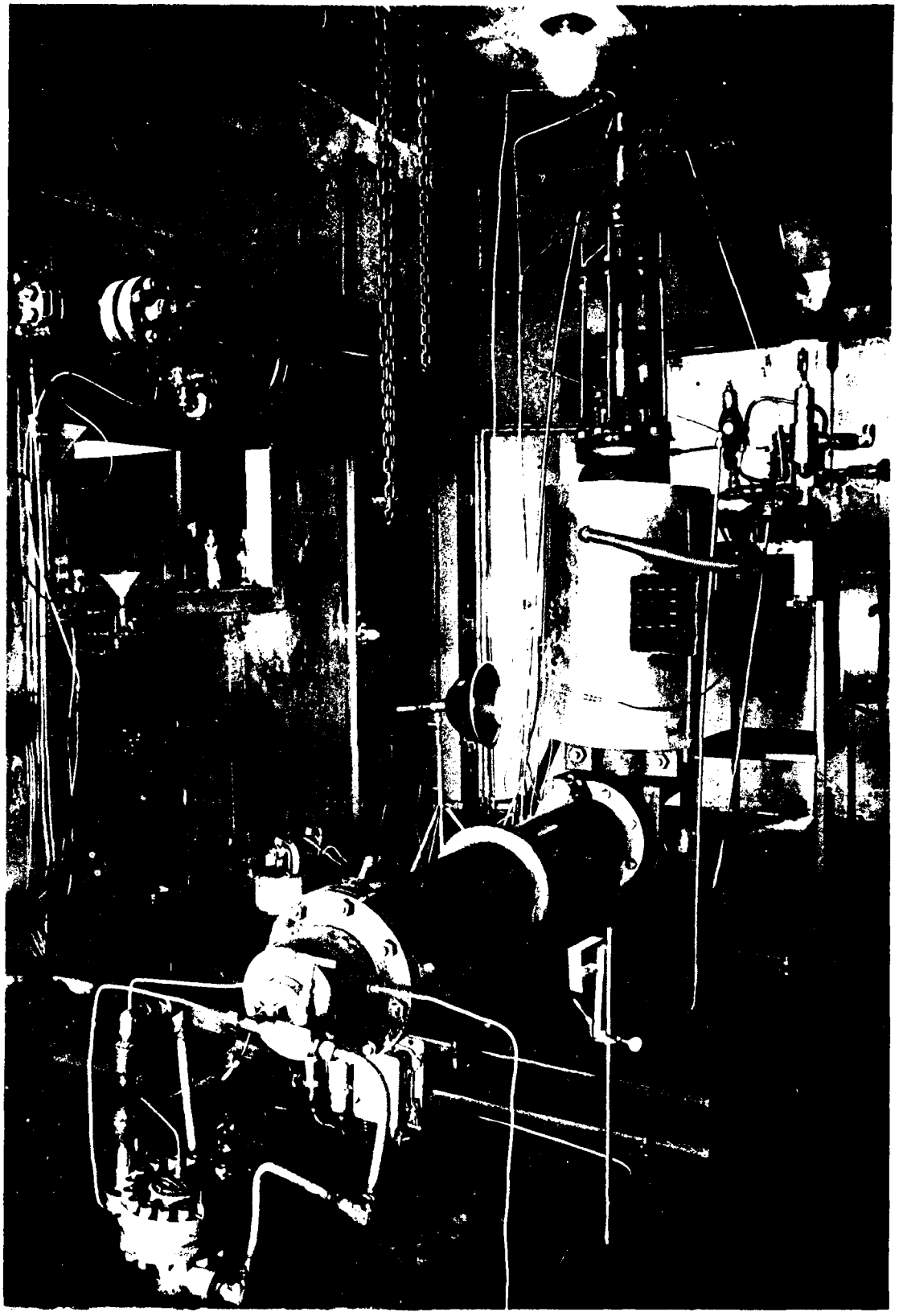

Ph. 1 Overall View of the Experimental Set-Up

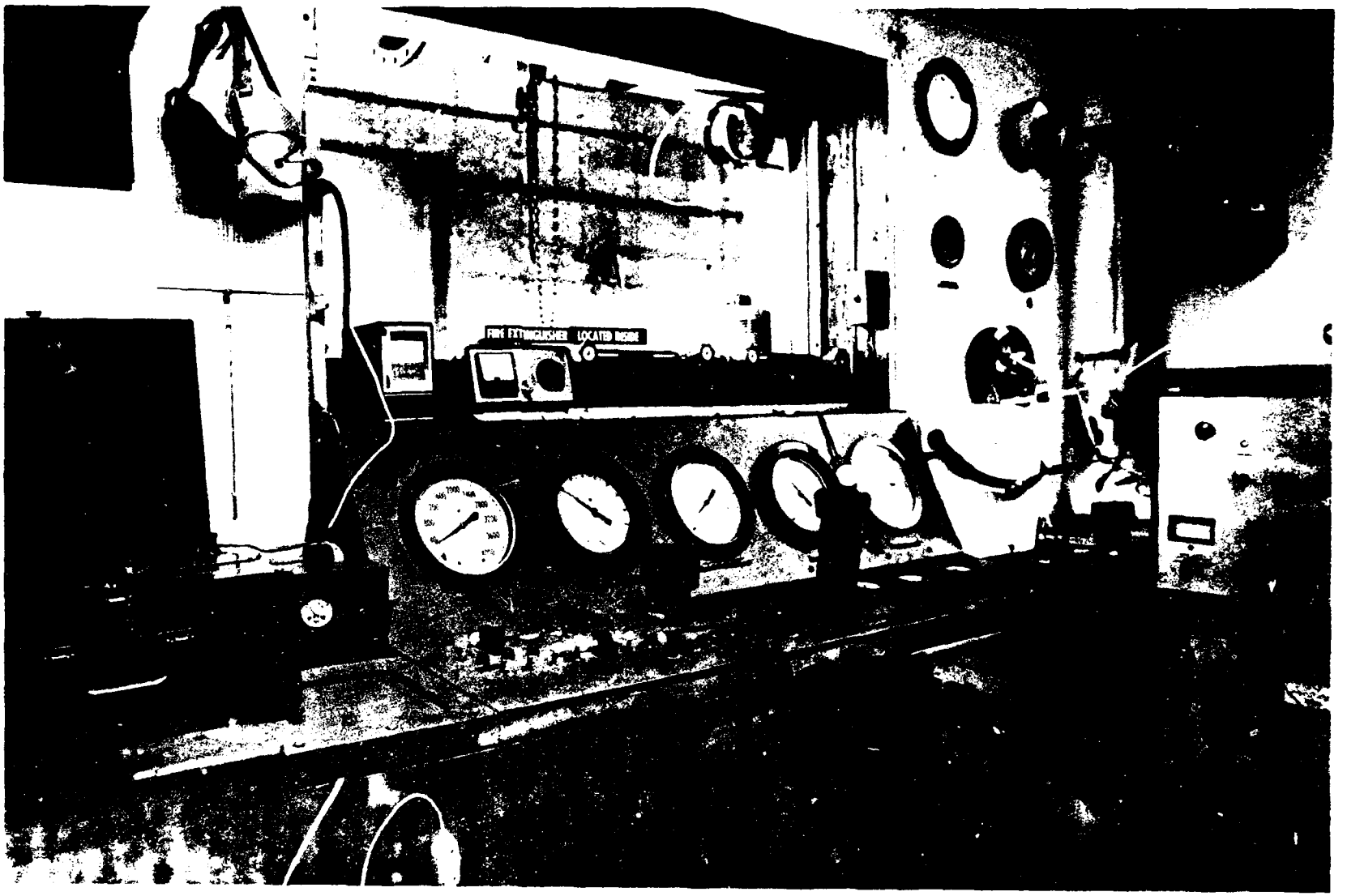

Ph. ' Control Panel

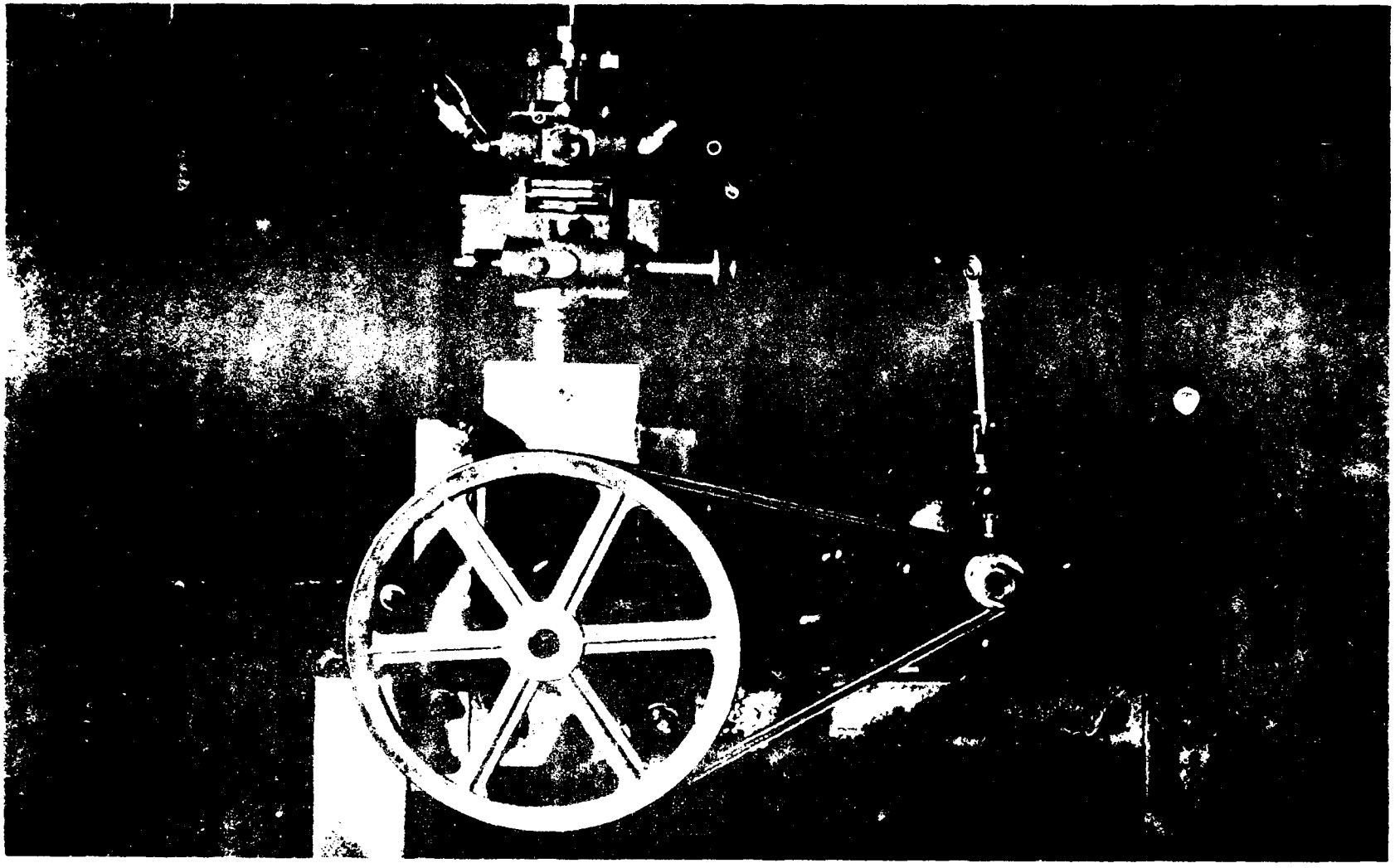

Ph. 3 Modified Fuel Pump Mounting

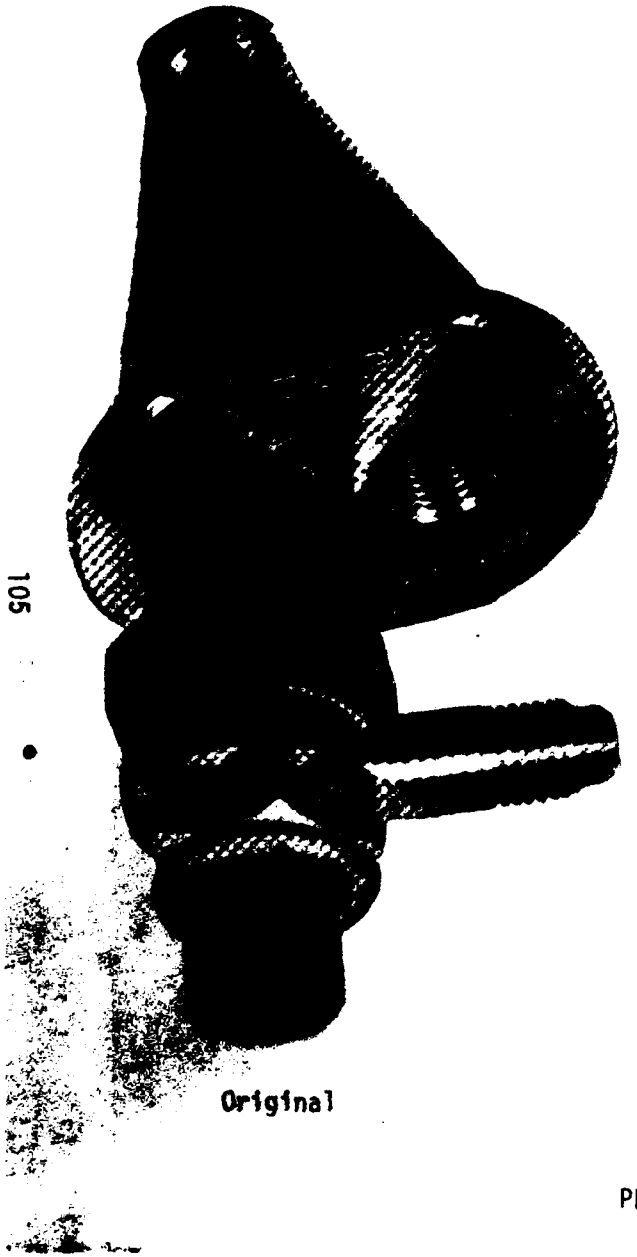

Original

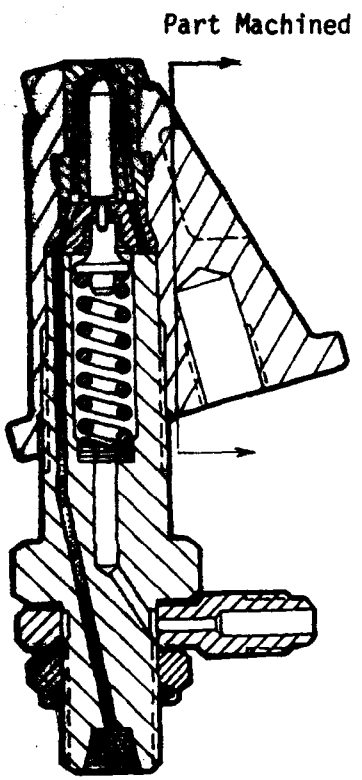

Modification

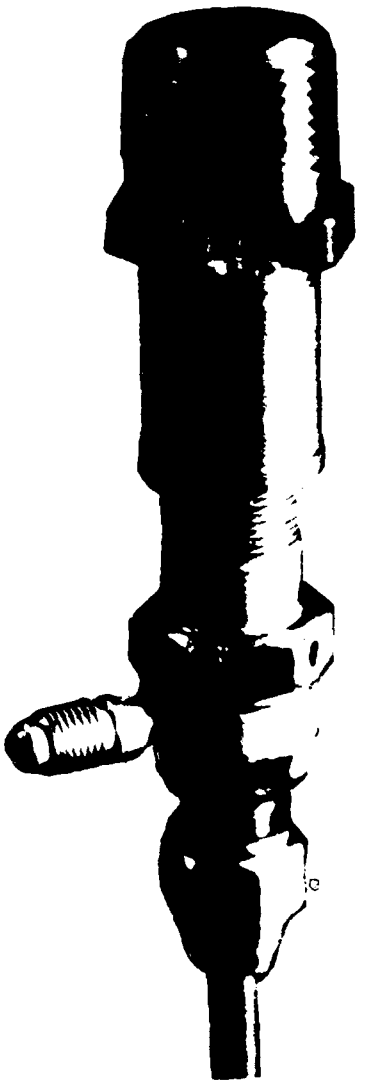

Final Version

Ph. 4 Original and Modified Fuel Nozzles

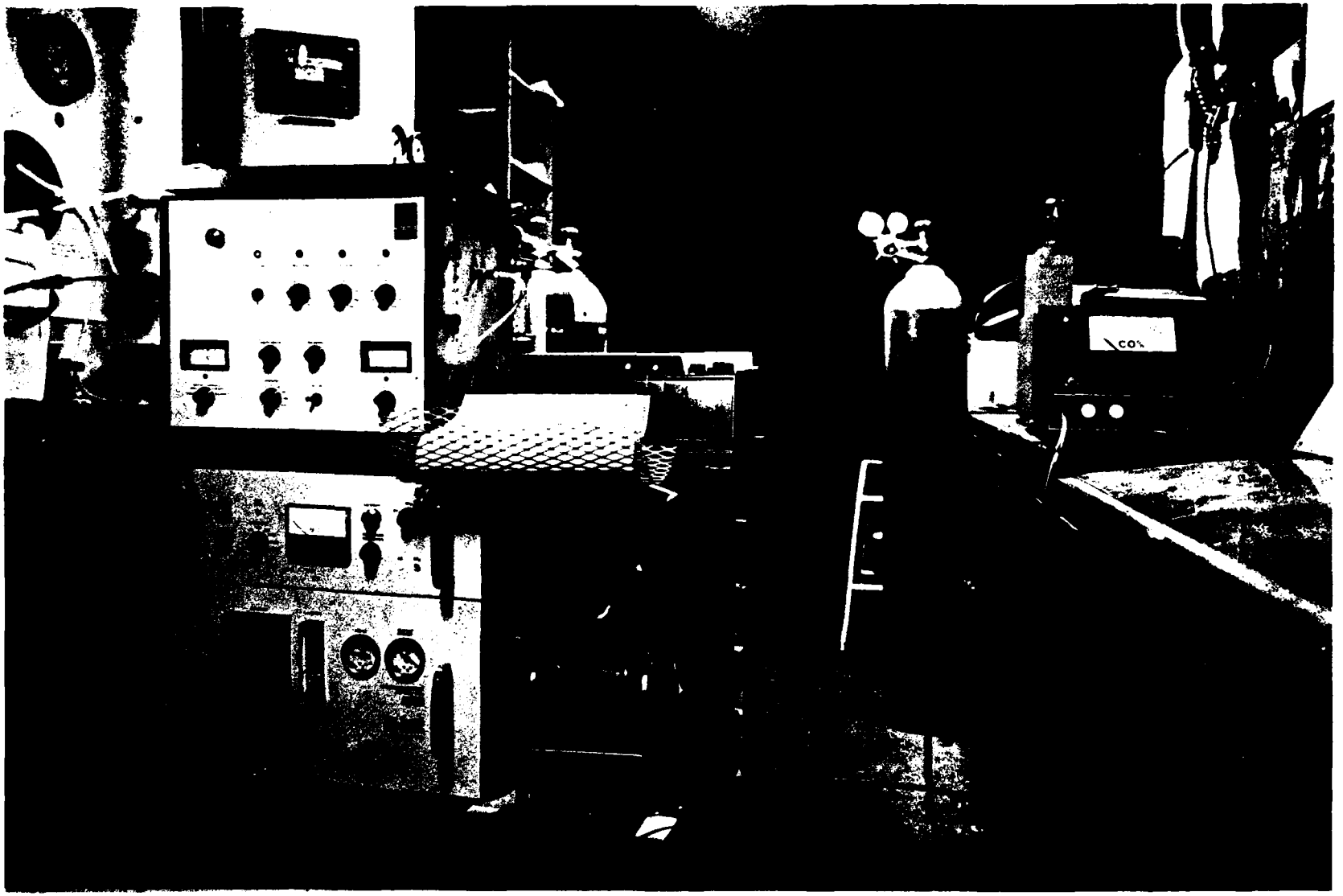

Ph. 5 Gas Analysis Instrumentation

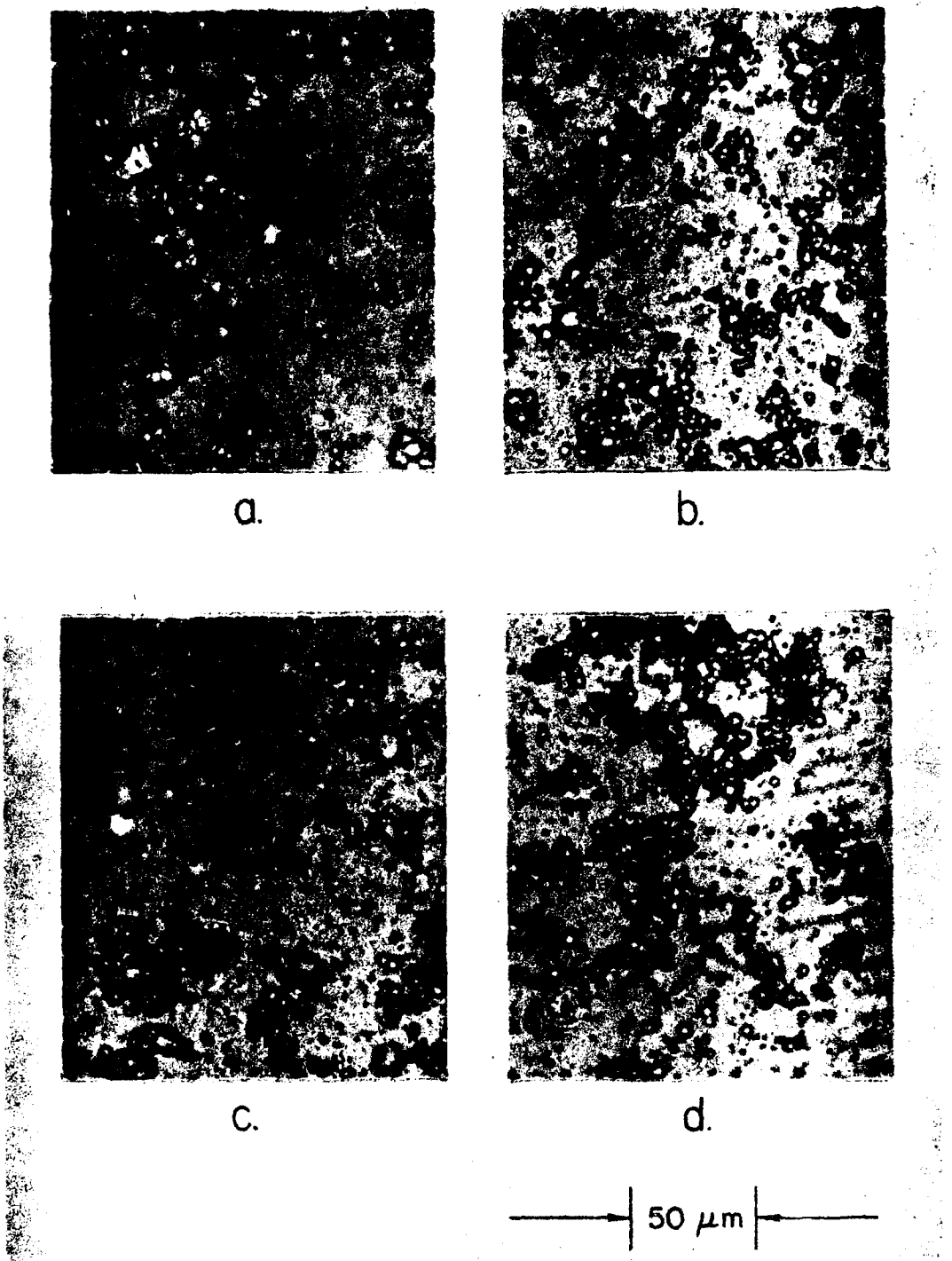

Ph. 6 Effect of Blending Time on the Microstructure of No. 6 Oil-Water Emulsions (CRM); W = 0.08, S = 0
a: t_{bl}=2 min; b: t_{bl}=5 min; c: t_{bl}=10 min; d: t_{bl}=15 min

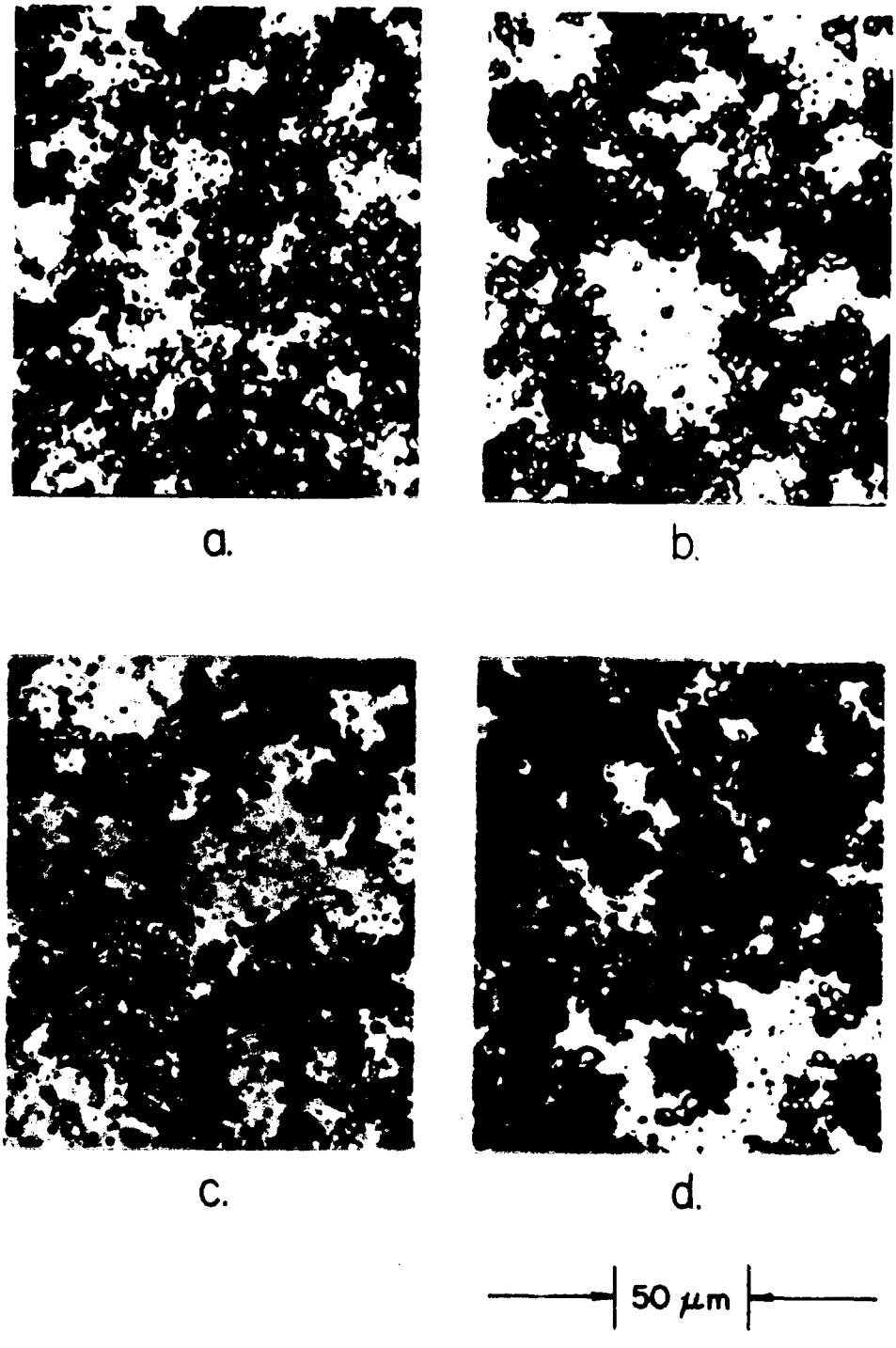

Ph. 7 Effect of Blending Time on the Microstructure of No. 6 Oil-Water Emulsions (CRM), W = 0.15, S = 0
a: 5 min; b: 7.5 min; c: 10 min; d: 15 min

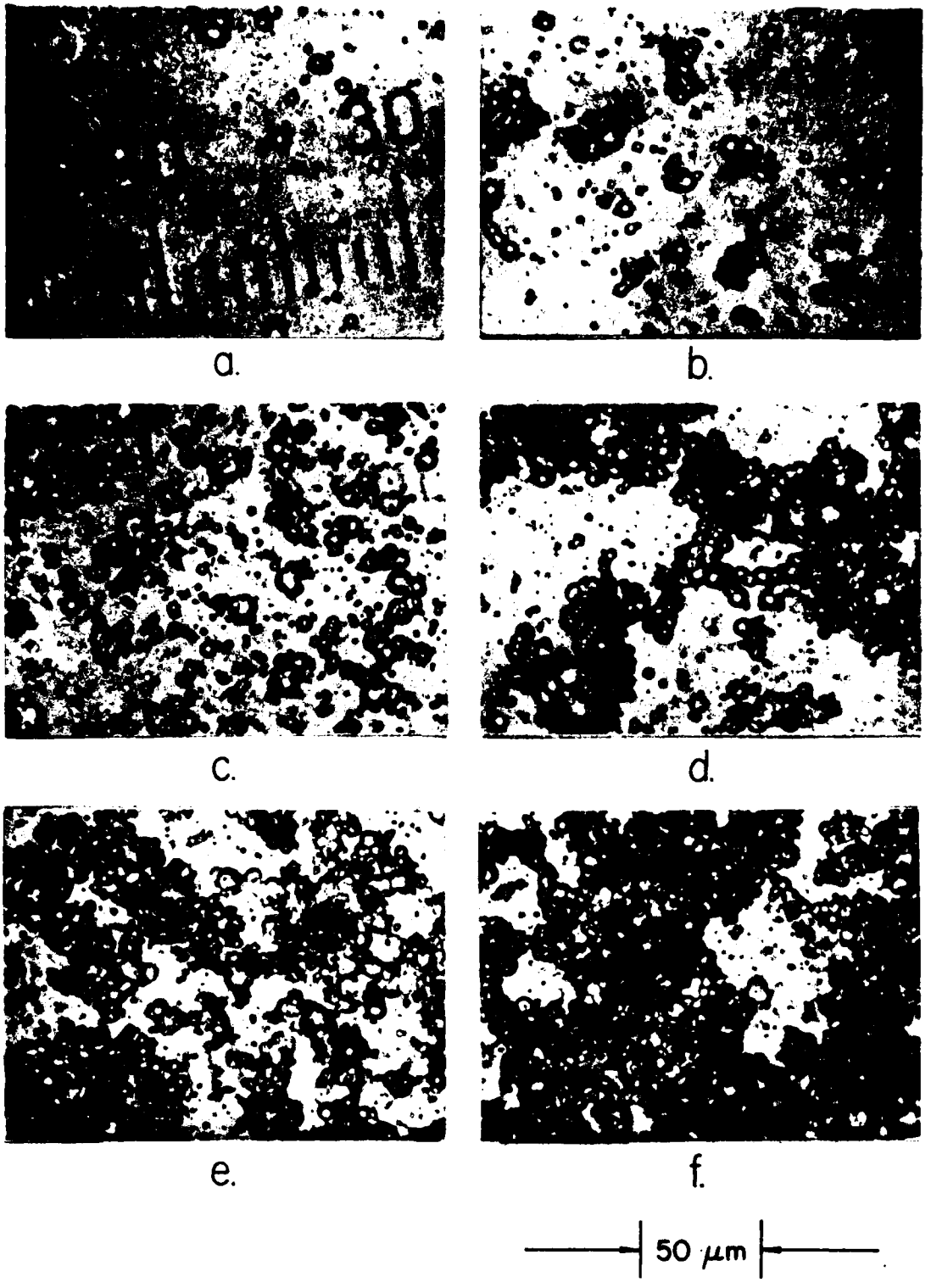

Ph. 8 Effect of Water Content on the Microstructure of No. 6 Oil-Water Emulsions (CRM), t_{bl} = 5 min

a: W=0.01; b: W=0.30; c: W=0.08; d: W=0.12; e: W=0.20; f: W=0.30

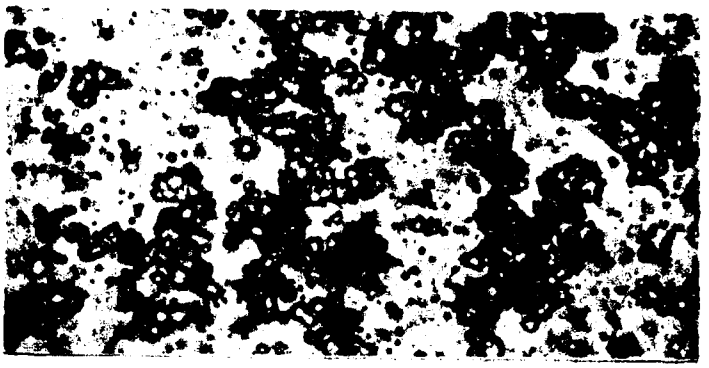

a.

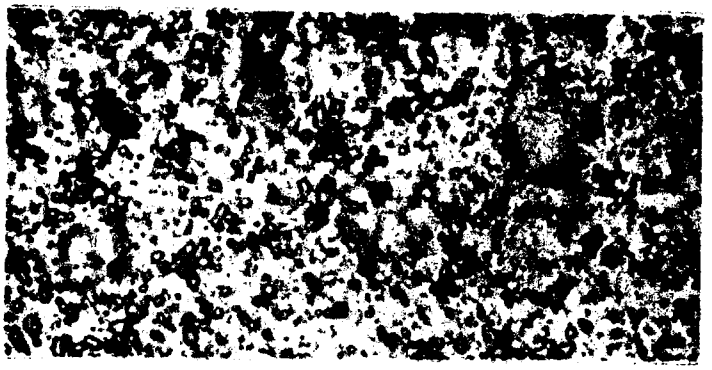

b.

50 μm

Ph. 9 Effect of Surfactant Content on the Microstructure of **No. 6** Oil-Water Emulsions (CRM), W = 0.08, t_{bl} = 10 min

a: S=0; b: S=0.02

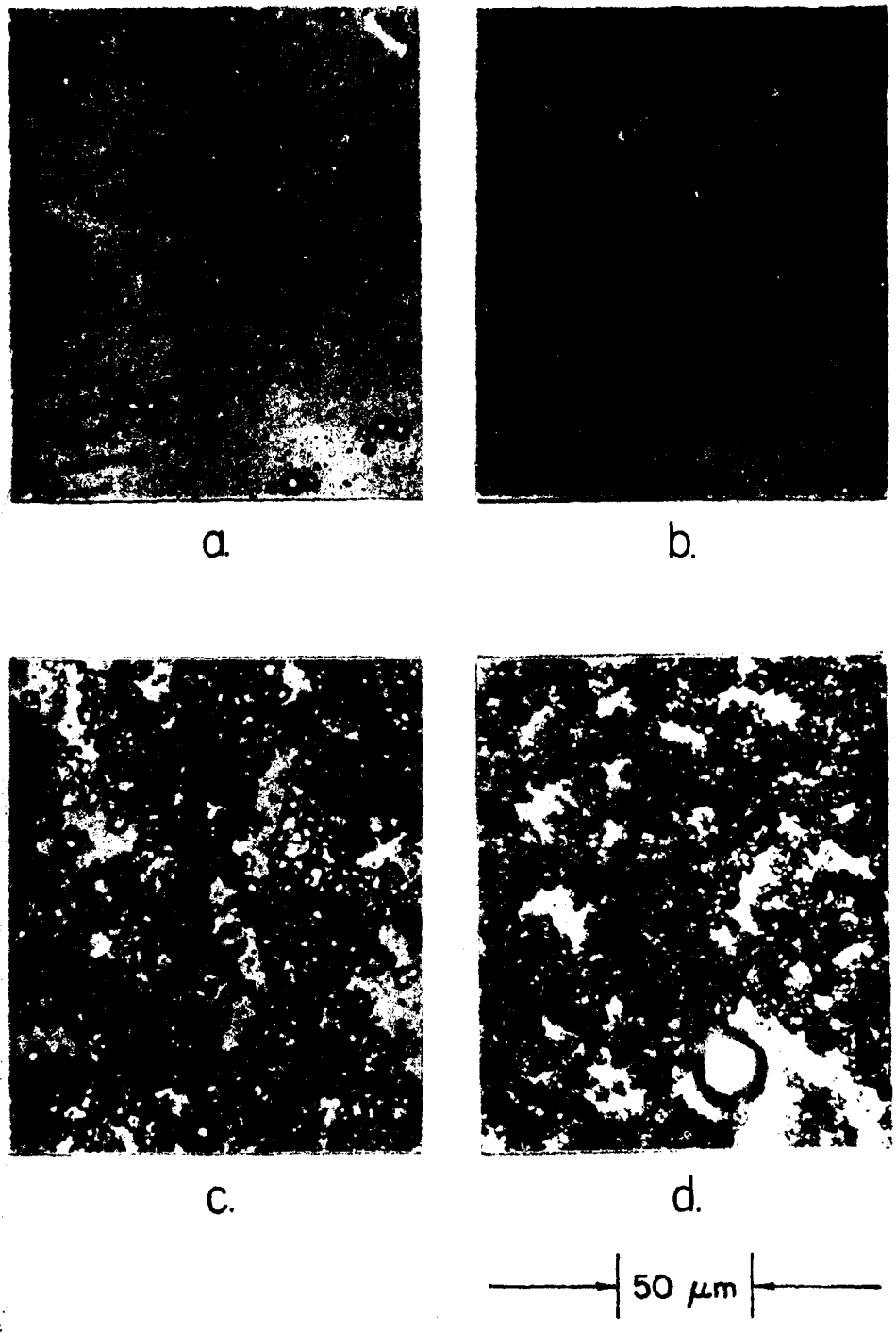

. 10 Difference in the Microstructure of No. 6 Oil-Water Emulsions Prepared Using a High-Speed Blender and a Counter-Rotating Mixer, S = 0
a: W=0.03, CRM, t_{bl}=5 min; b: W=0.03, HSB, t_{bl}=15 min;
c: W=0.30, CRM, t_{bl}=5 min; d: W=0.30, HSB, t_{bl}=15 min

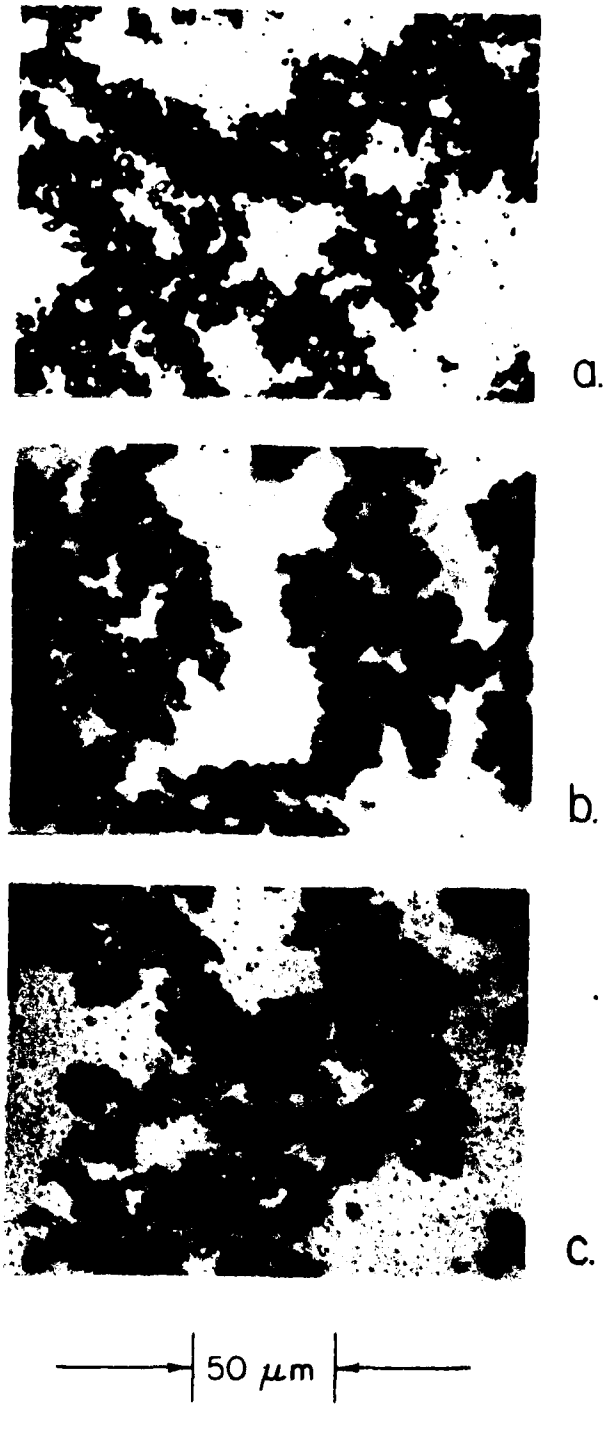

Ph. 11 **Effect of** Blending Time on the Microstructure **of No. 4 Oil-Water Emulsions** (HSB), W = 0.08, S = 0
a: t_{bl}**=2 min;** b: t_{bl}=3 min; c: t_{bl}=5 min

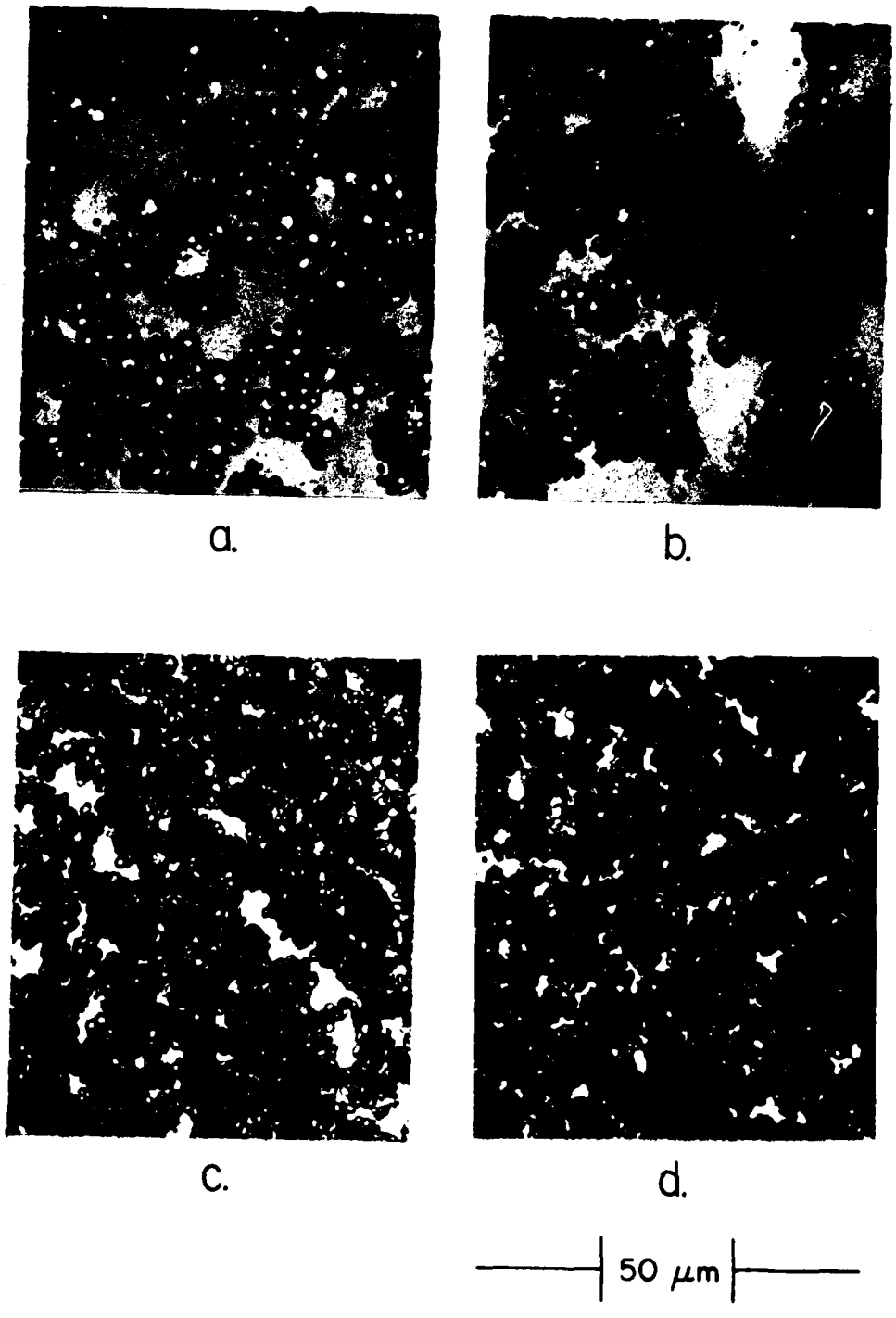

Ph. 12 Effect of Blending Time on the Microstructure of No. 4 Oil-Water Emulsions (HSB), W = 0.15, S = 0
a: t_{bl}=1 min; b: t_{bl}=2 min; c: t_{bl}=2 min; d: t_{bl}=3 min

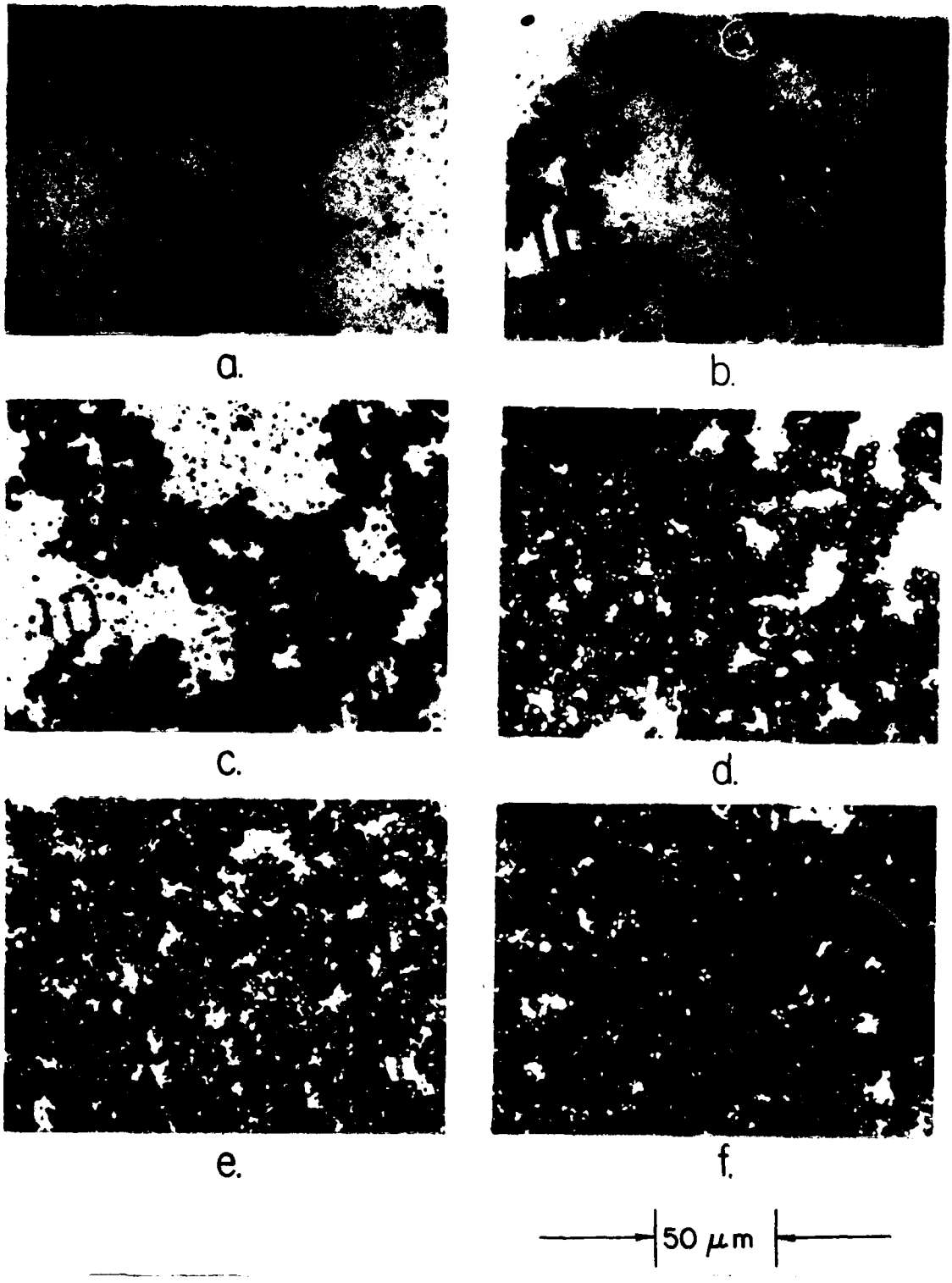

Ph. 13 Effect of Water Content on the Microstructure of No. 4 Oil-Water Emulsions (HSB), t_{bl} = 2 min, S = 0

a: W=0.01; b: W=0.03; c: W=0.08; d: W=0.12; e: W=0.20; f: W=0.30

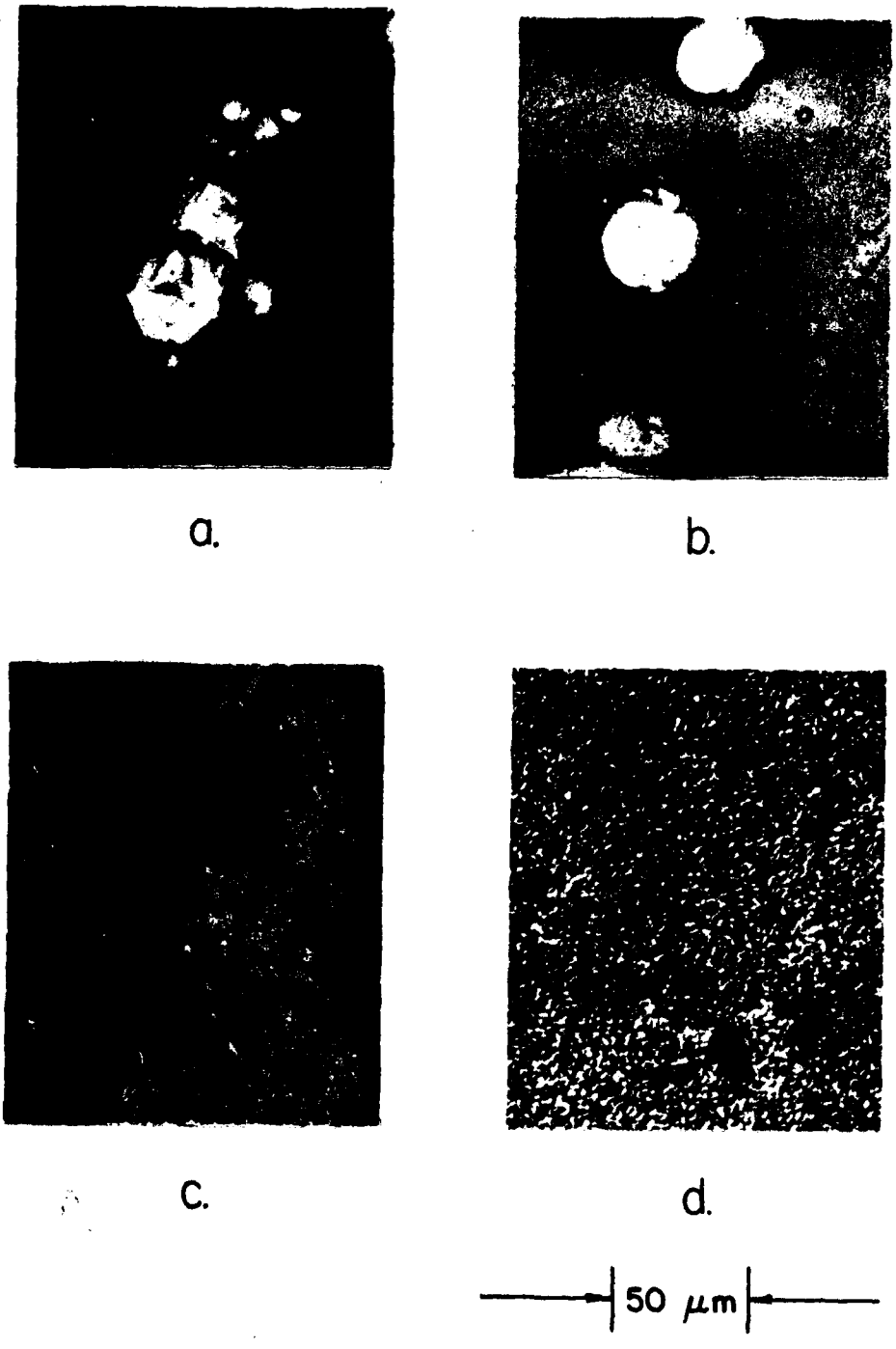

Ph. 14 Effects of the Type of Blender and Surfactant Addition on the Microstructure of No. 4 Oil-Water Emulsions, W = 0.08
a: CRM, t_{bl}=2 min, S=0; b: CRM, t_{bl}=5 min, S=0
c: HSB, t_{bl}=2 min, S=0, d: HSB, t_{bl}=2 min, S=0.02

a.

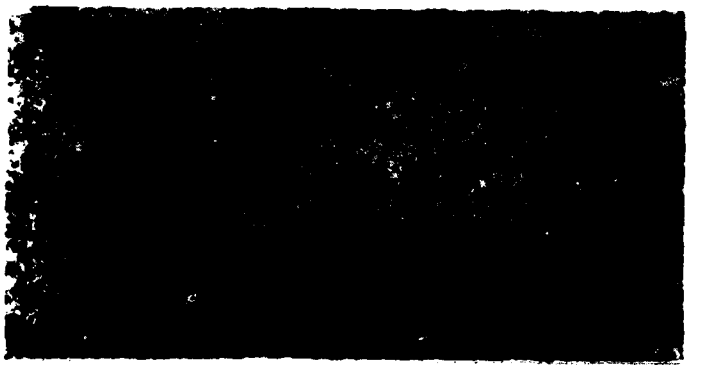

b.

50 μm

Ph. 15 **Effect of Passing the No. 4 Oil-Water (W=0.08) Emulsion Through Injection Hardware**
a: Upstream of Injectors; b: Downstream of Injectors

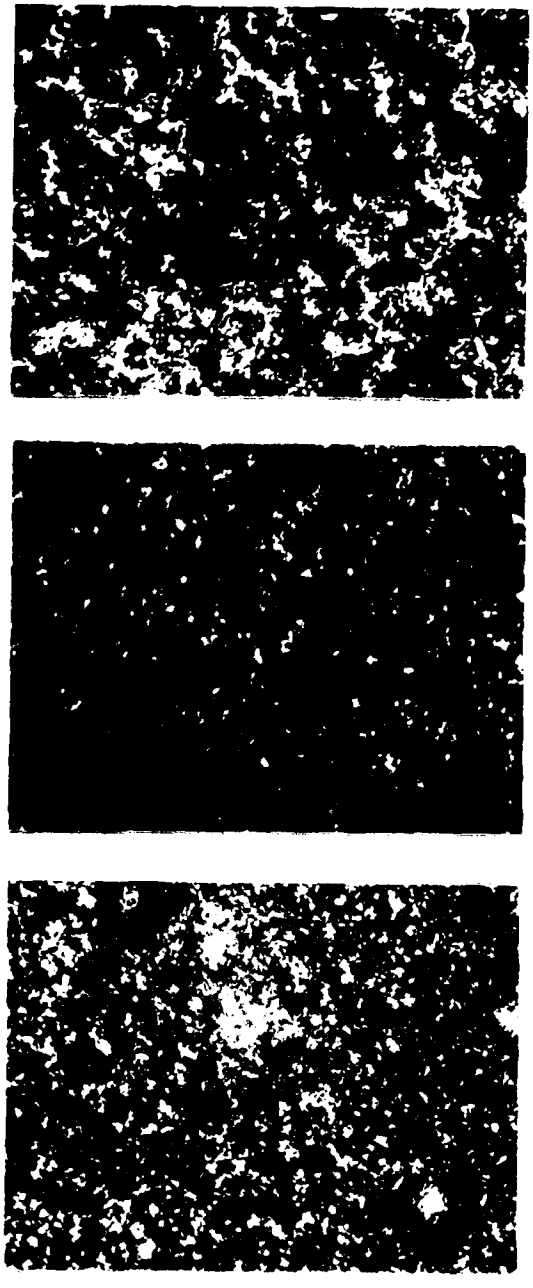

Ph. 16 Effects of Preheating and Passage Through Injection Hardware on the Microstructure of No. 6 Oil-Water Emulsion (W=0.08)
a: Emulsion as Prepared; b: After Preheating to 370 K; c: After Passing Through Injection Hardware at 370 K

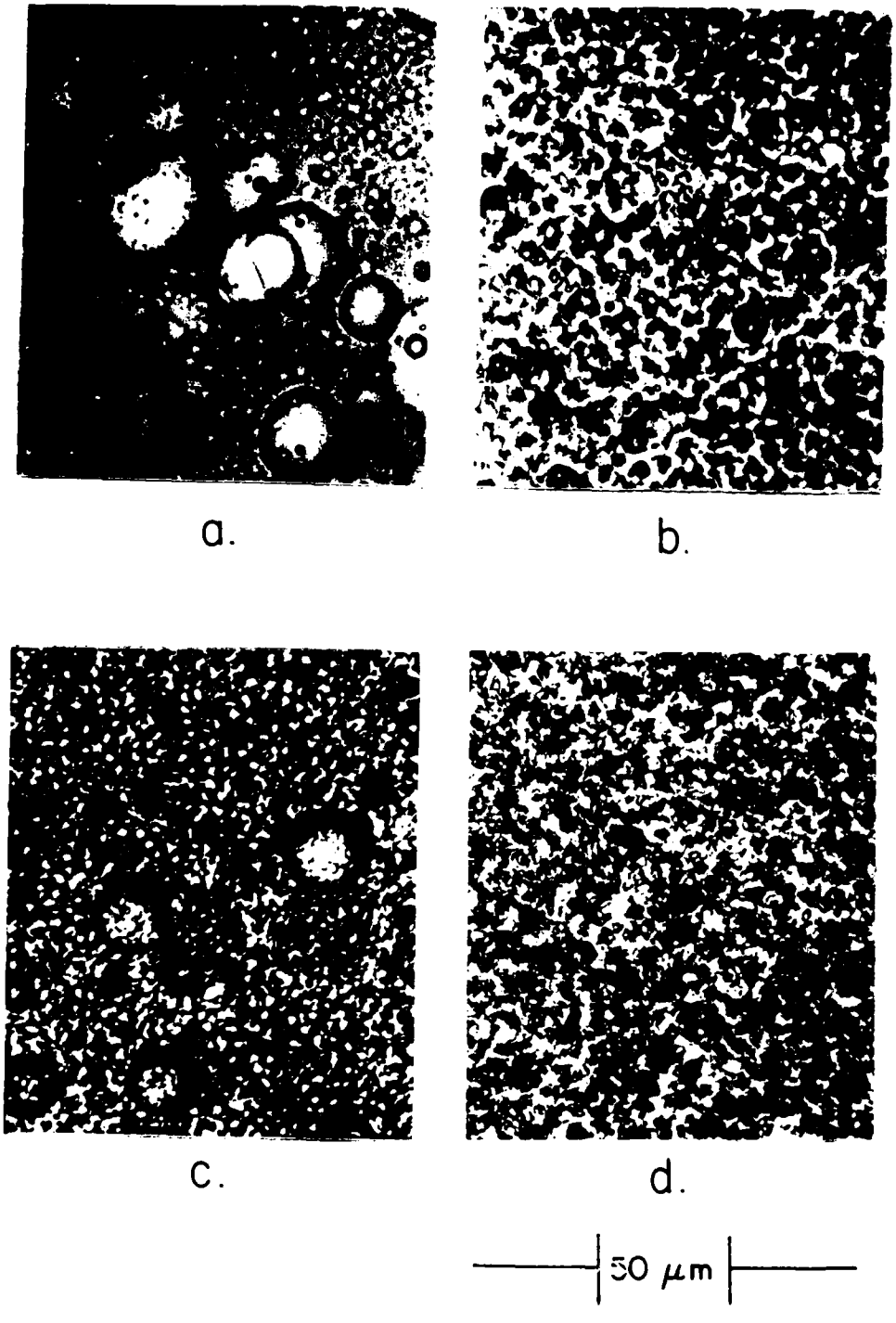

Ph. 17 Microstructure of Emulsions with Methanol as Internal Phase a: No. 4 Oil-Methanol (M=0.08) as Prepared; b: No. 6 Oil-Methanol$_o$(M=0.08) as Prepared: c: No. 6 Oil-Methanol (M=0.08) after Preheating to 370 K; d: No. 6 Oil-Methanol (370 K) Downstream of Injector

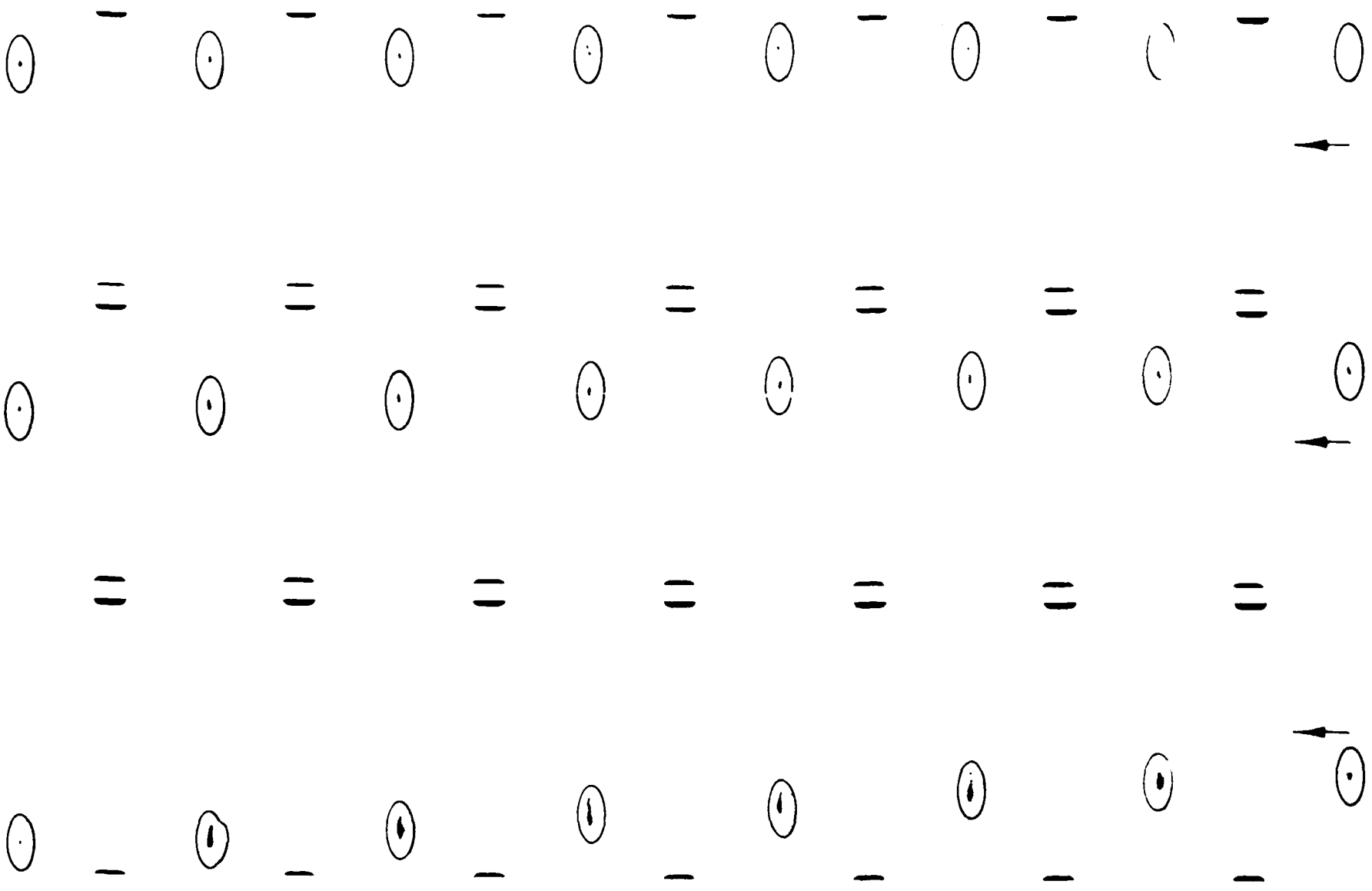

Ph. 18 Cinematography Sequence of a Burning Pure No. 4 Oil Drop (100 pps)

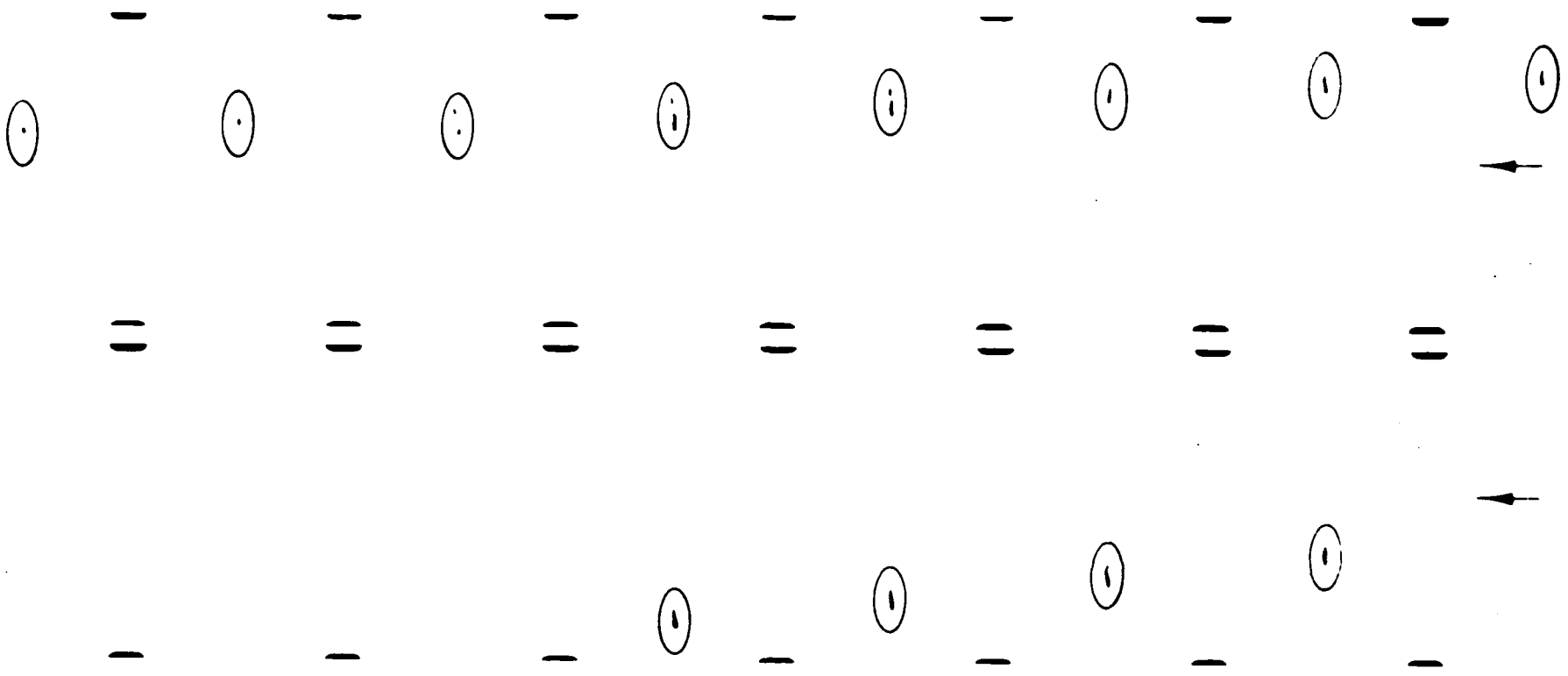

Ph. 19 Cinematography Sequence of a Burning No. 4 Oil-Water (W=0.01) Emulsion Drop (60 pps)

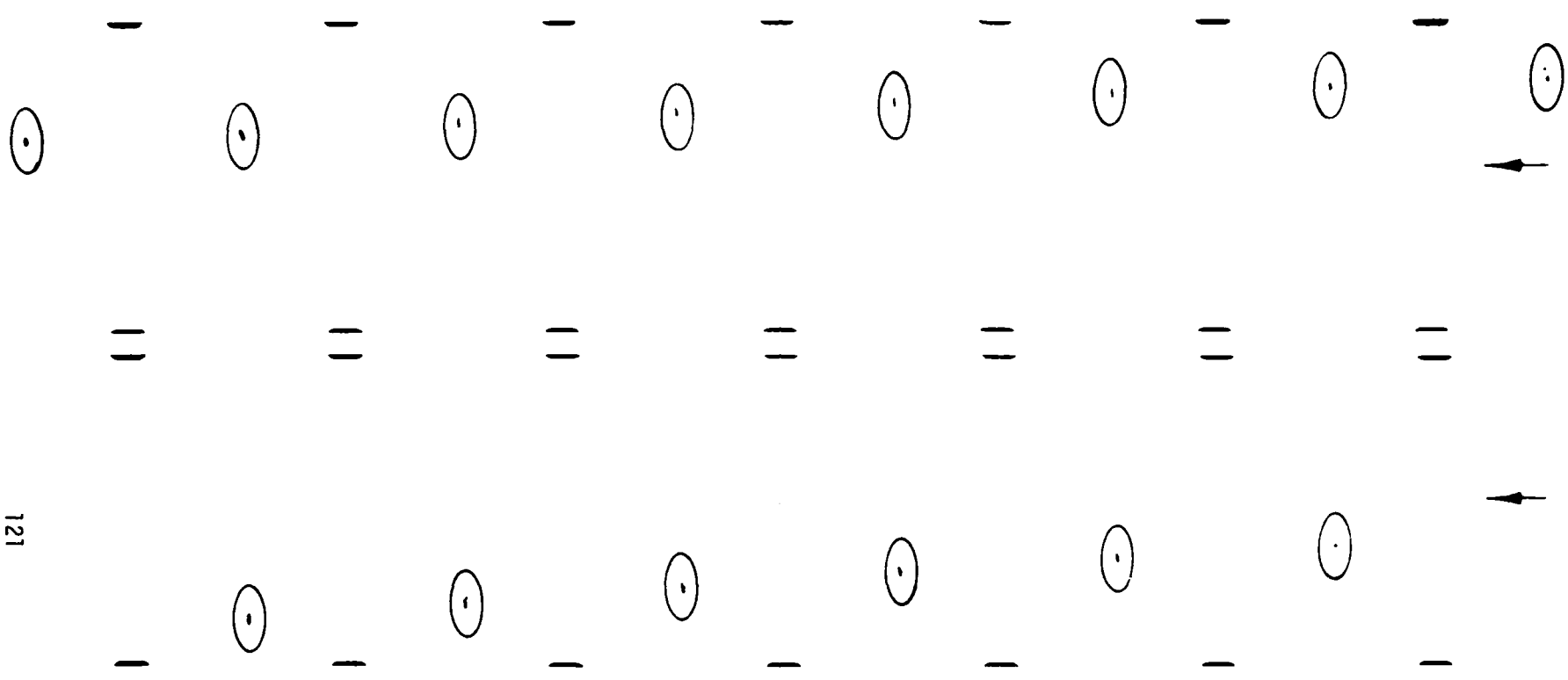

Ph. 20 Cinematography Sequence of a Burning No. 4 Oil-Water (W=0.03) Emulsion Drop (90 pps)

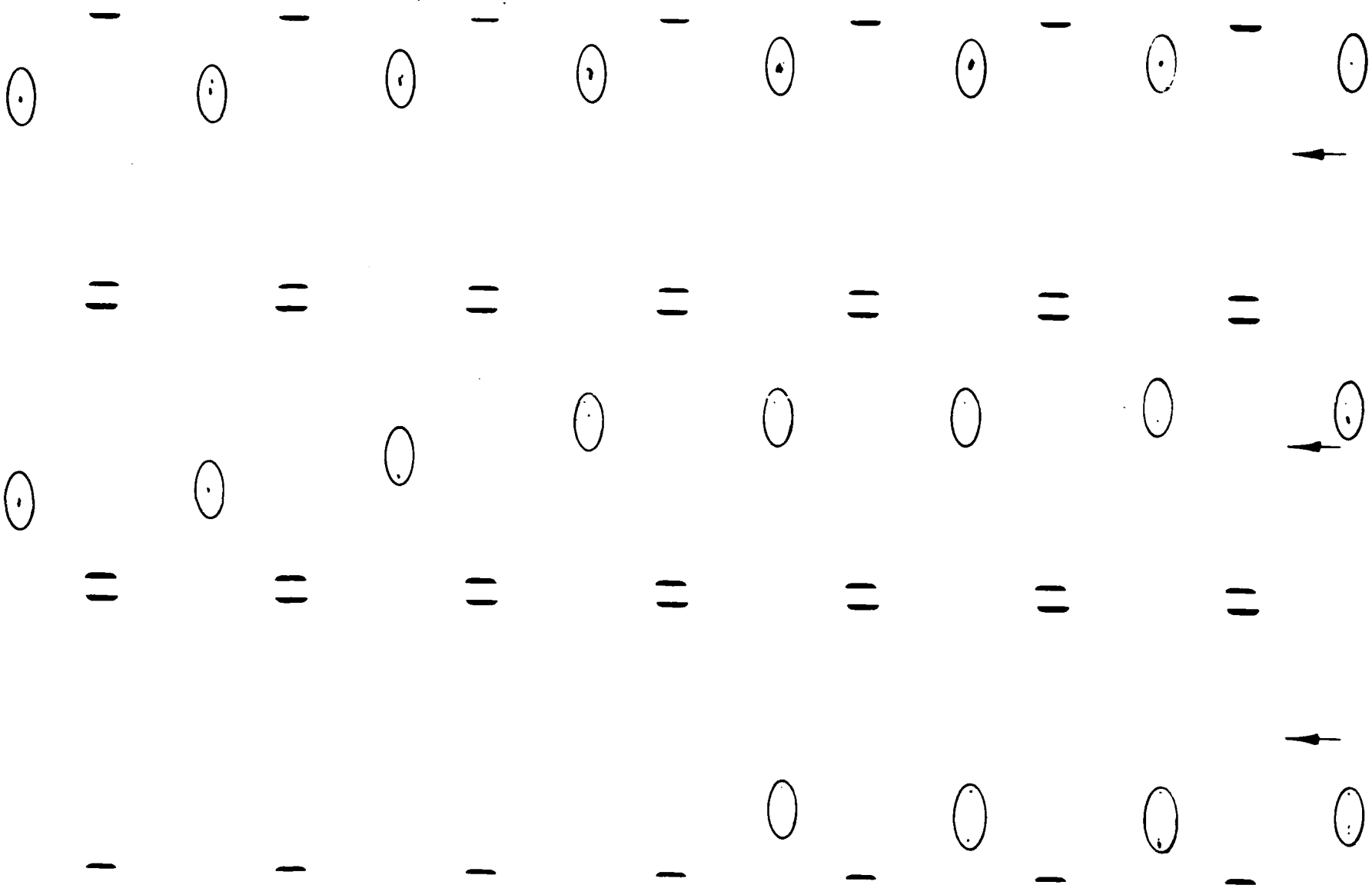

Ph. 21 Cinematography Sequence of a Burning No. 4 Oil-Water (W=0.08) Emulsion Drop (70 pps)

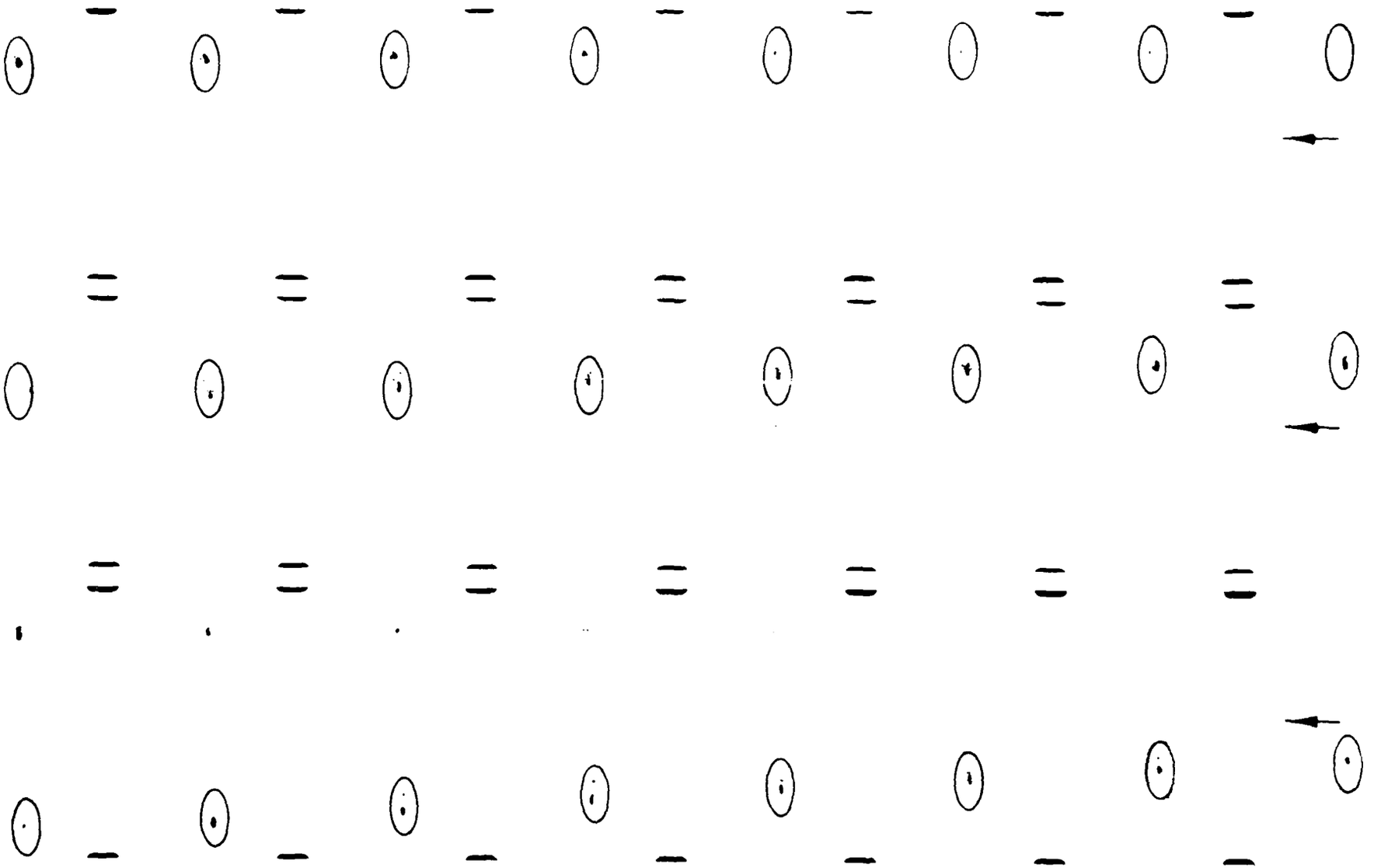

Ph. 22 Cinematography Sequence of a Burning No. 4 Oil-Water (W=0.12) Emulsion Drop (95 pps)

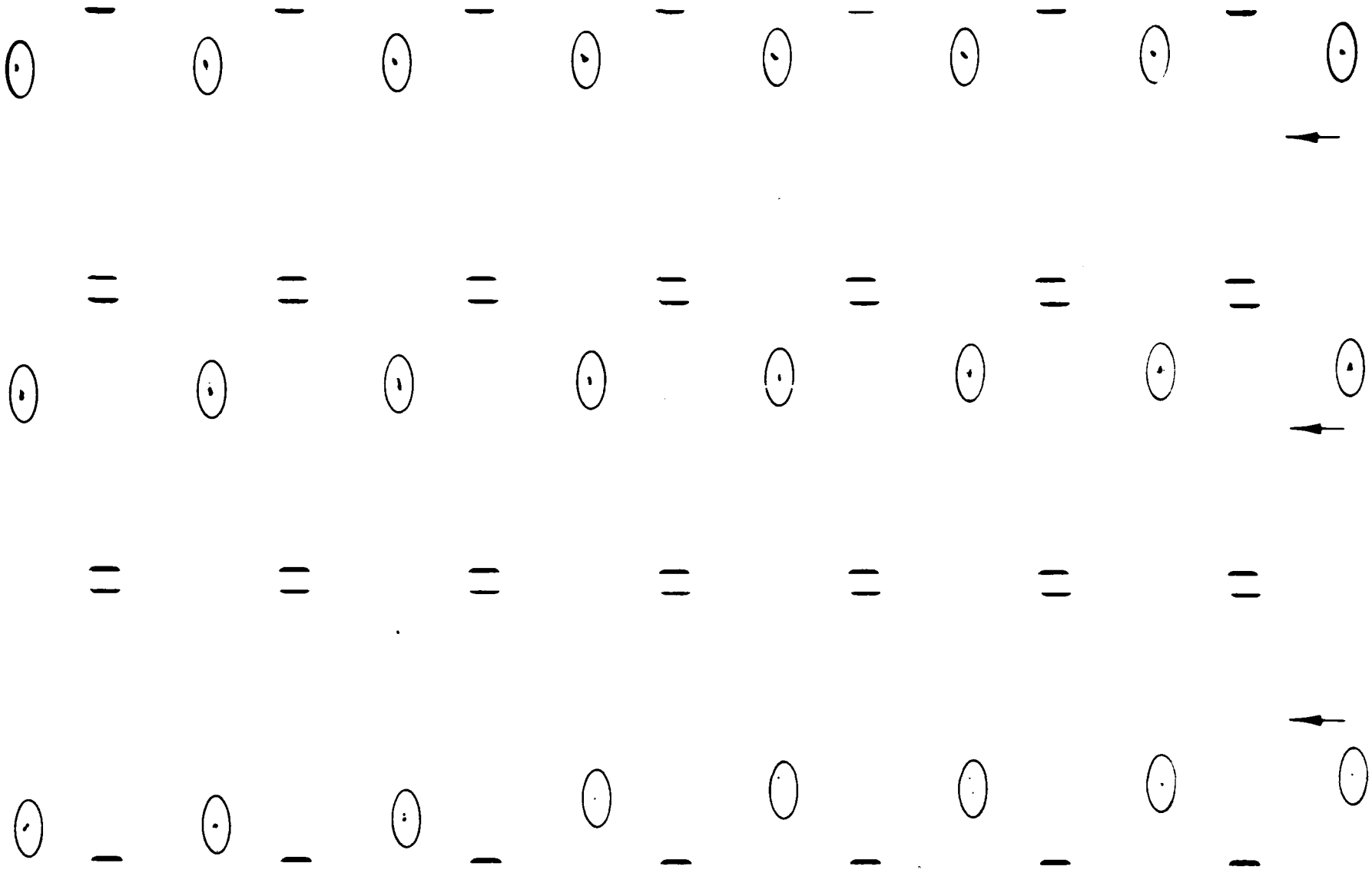

Ph. 23 Cinematography Sequence of a Burning No. 4 Oil-Water (W=0.15) Emulsion Drop (135 pps)

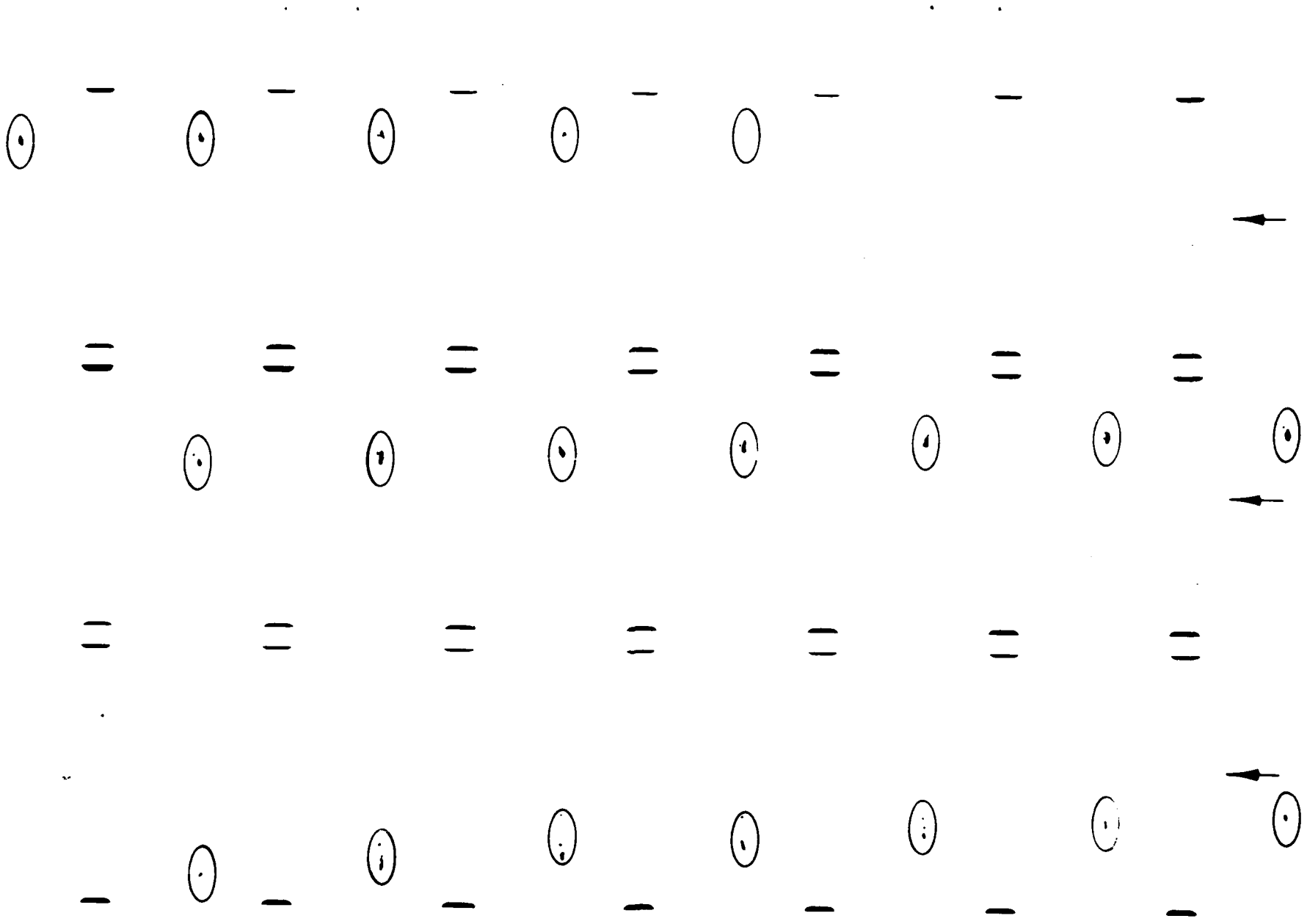

Ph. 24 Cinematography Sequence of a Burning No. 4 Oil-Water (W=0.20) Emulsion Drop (90 pps)

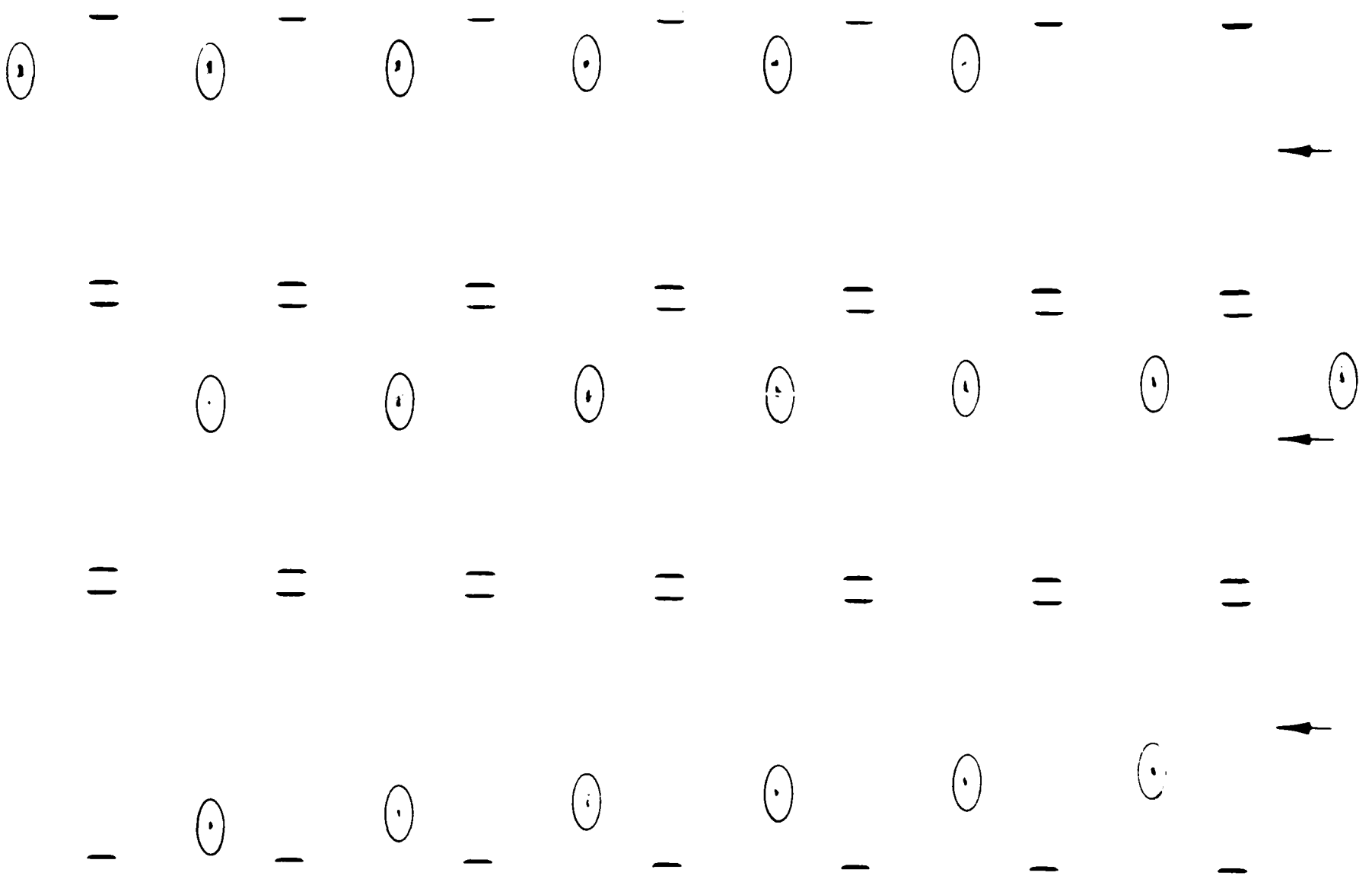

Ph. 25 Cinematography Sequence of a Burning No. 4 Oil-Water (W=0.30) Emulsion Drop (95 pps)

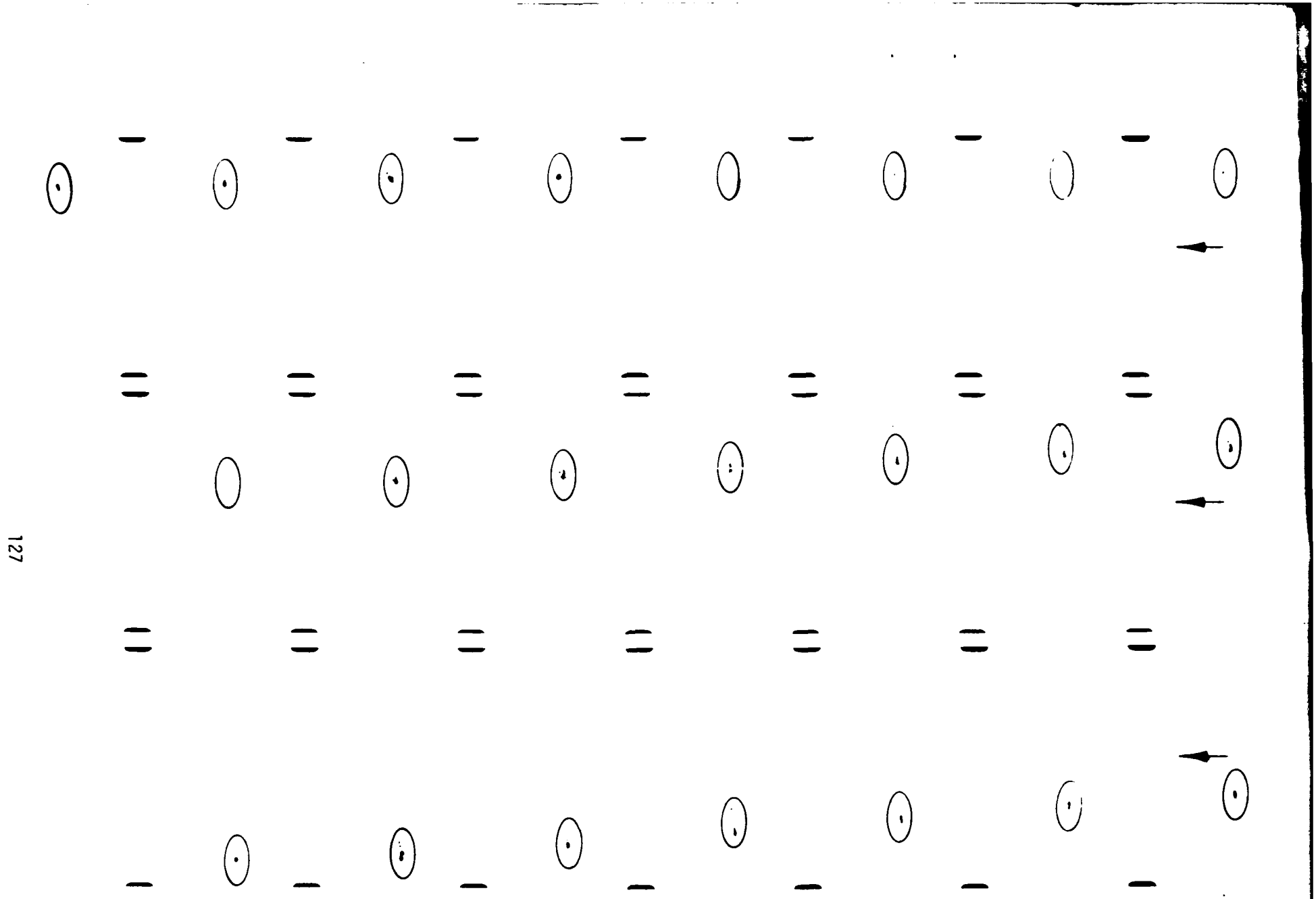

Ph. 26 Cinematography Sequence of a Burning No. 4 Oil-Water (W=0.40) Emulsion Drop (85 pps)

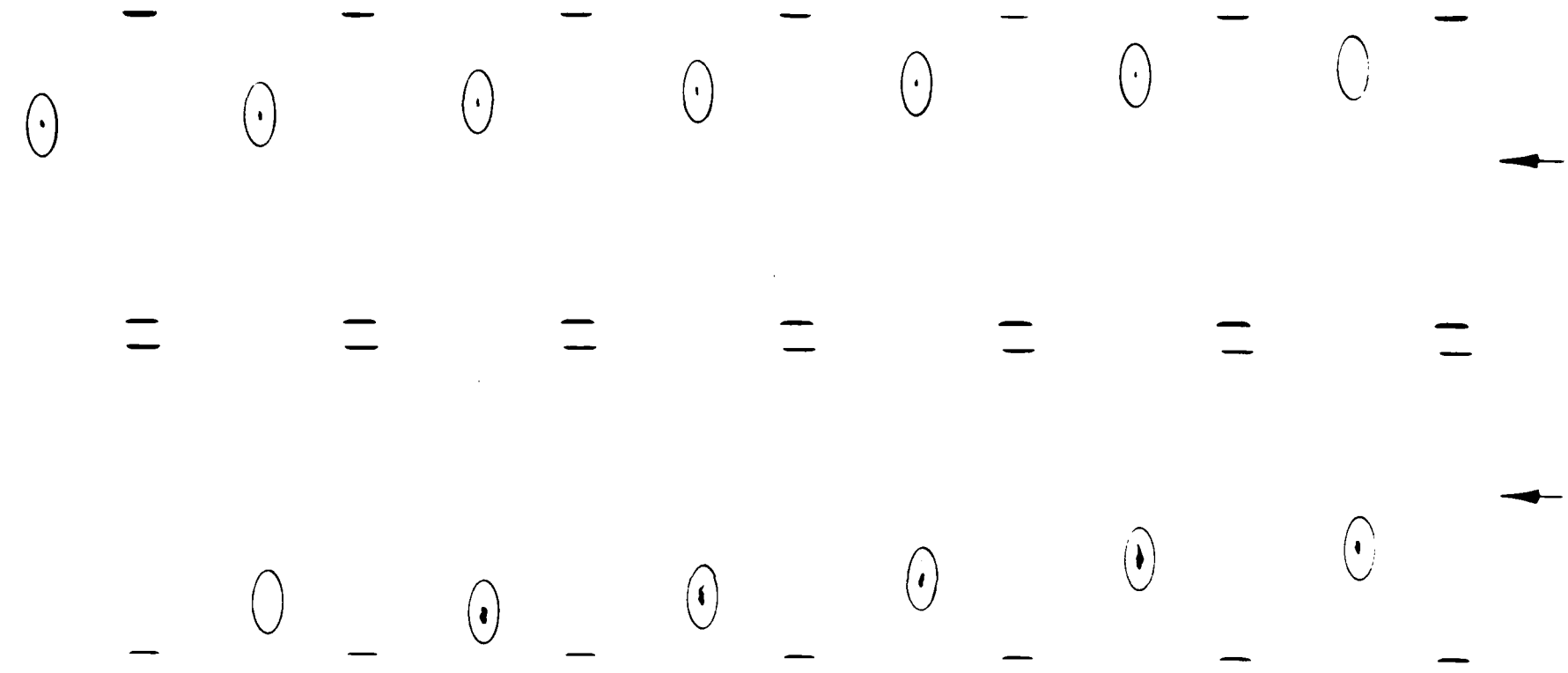

Ph. 27 Cinematography Sequence of a Burning No. 4 Oil-Methanol (M=0.15) Emulsion Drop (70 pps)

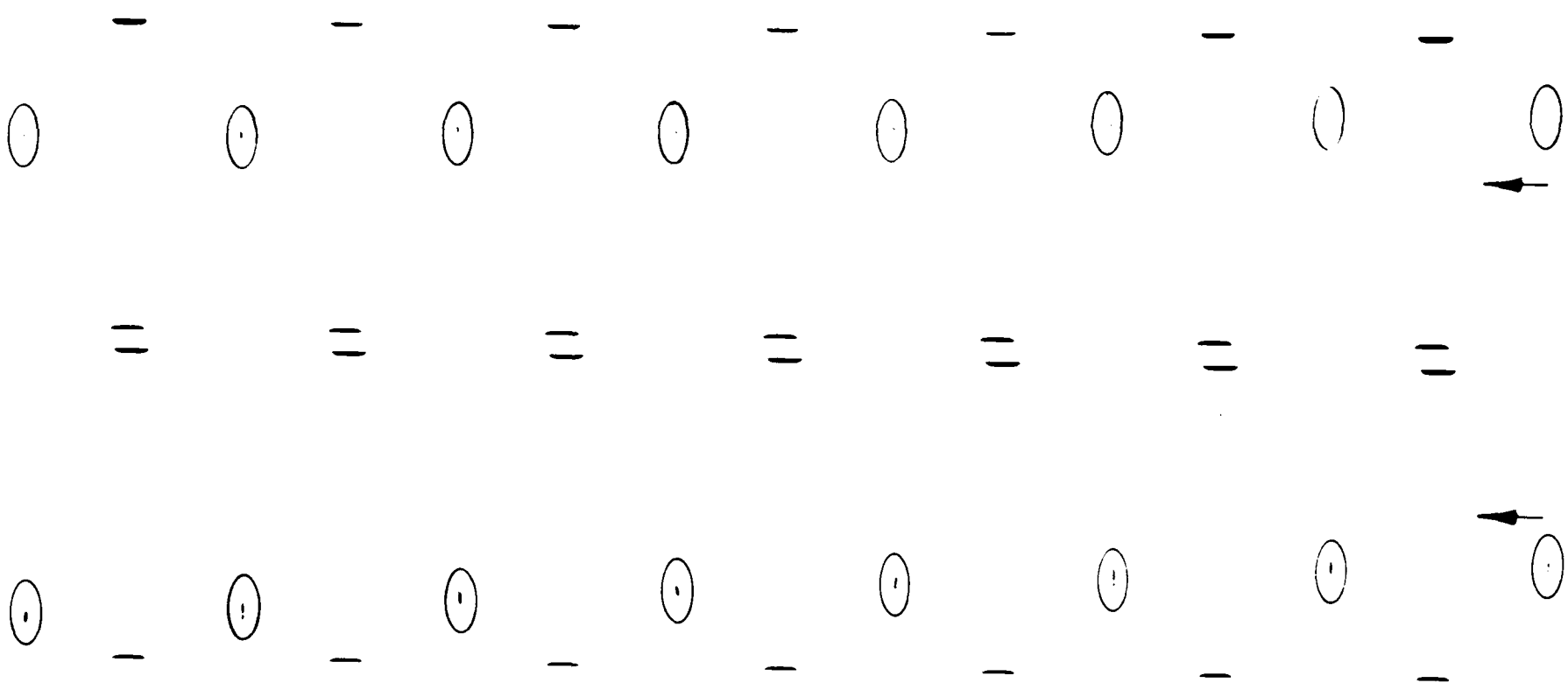

Ph. 28 Cinematography Sequence of a Burning No. 4 Oil-Water (W=0.12) Emulsion Drop at Chamber Temperature of 534 K (125 pps)

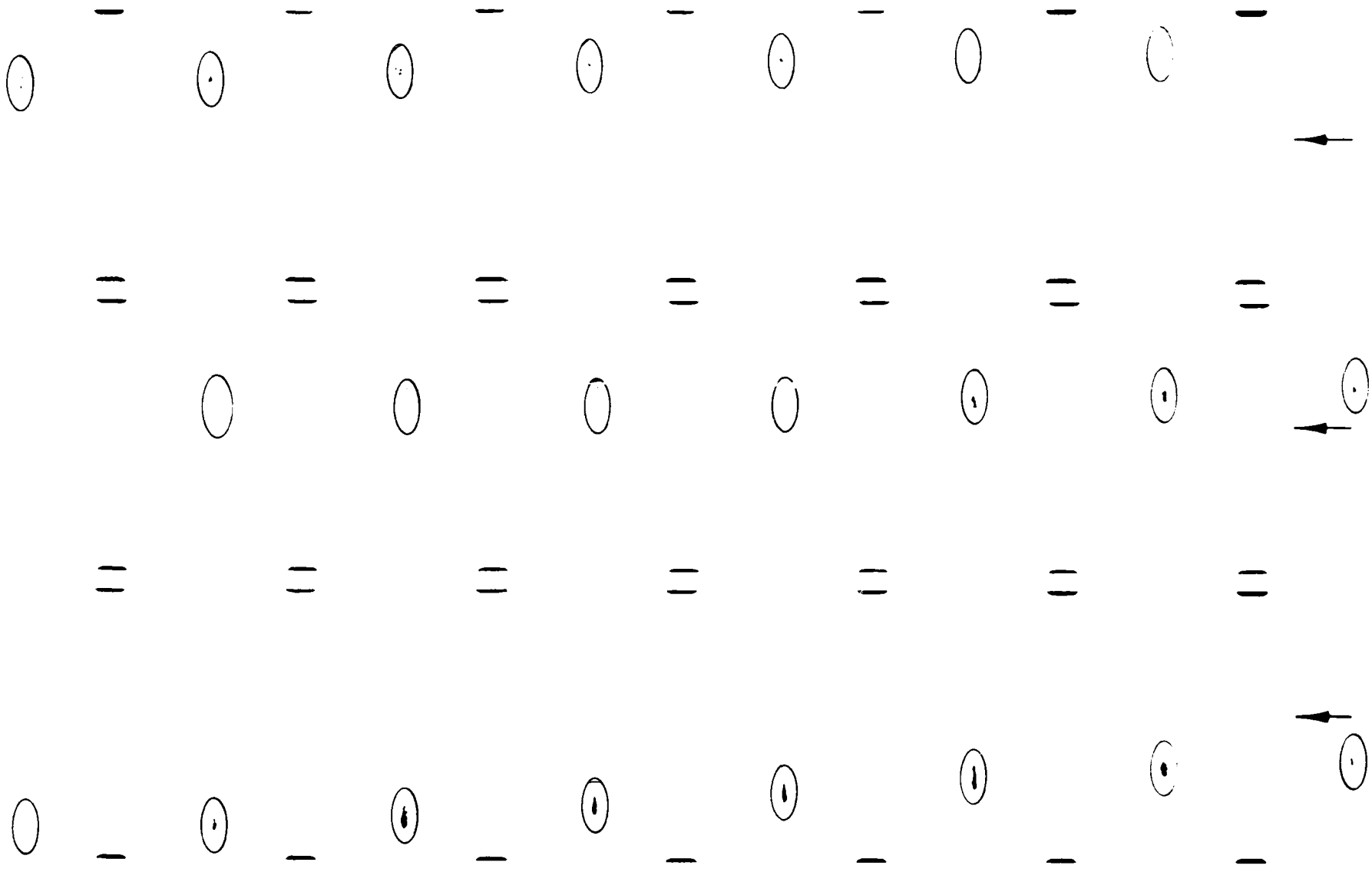

Ph. 29 Cinematography Sequence of a Burning No. 4 Oil-Water (W=0.12) Emulsion Drop at Injection Temperature of 367 K (85 pps)

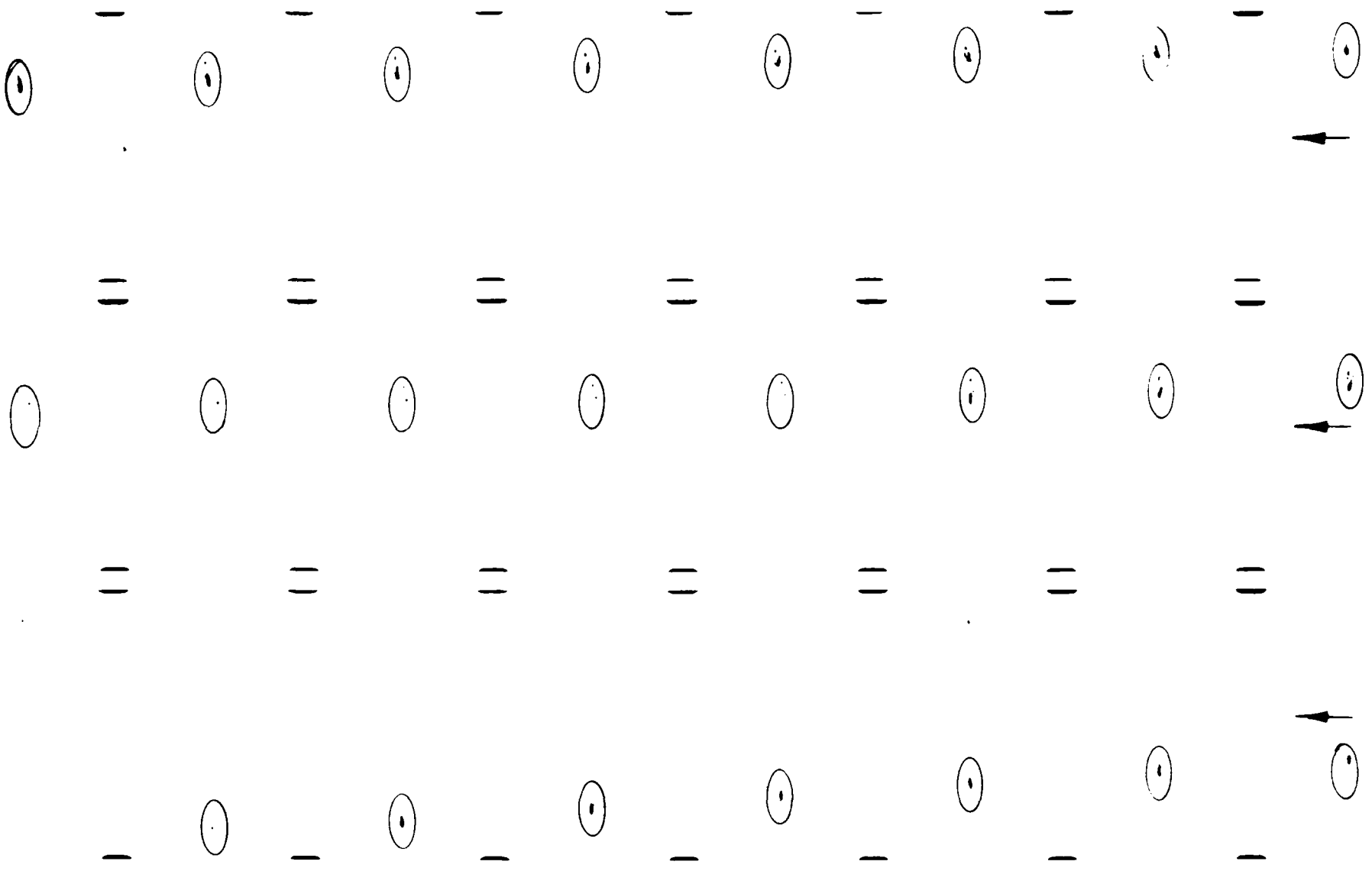

Ph. 30 Cinematography Sequence of a Burning Drop of No. 4 Oil-Water (W=0.12) Emulsion Prepared with Surfactant (S=0.02)(100 pps)

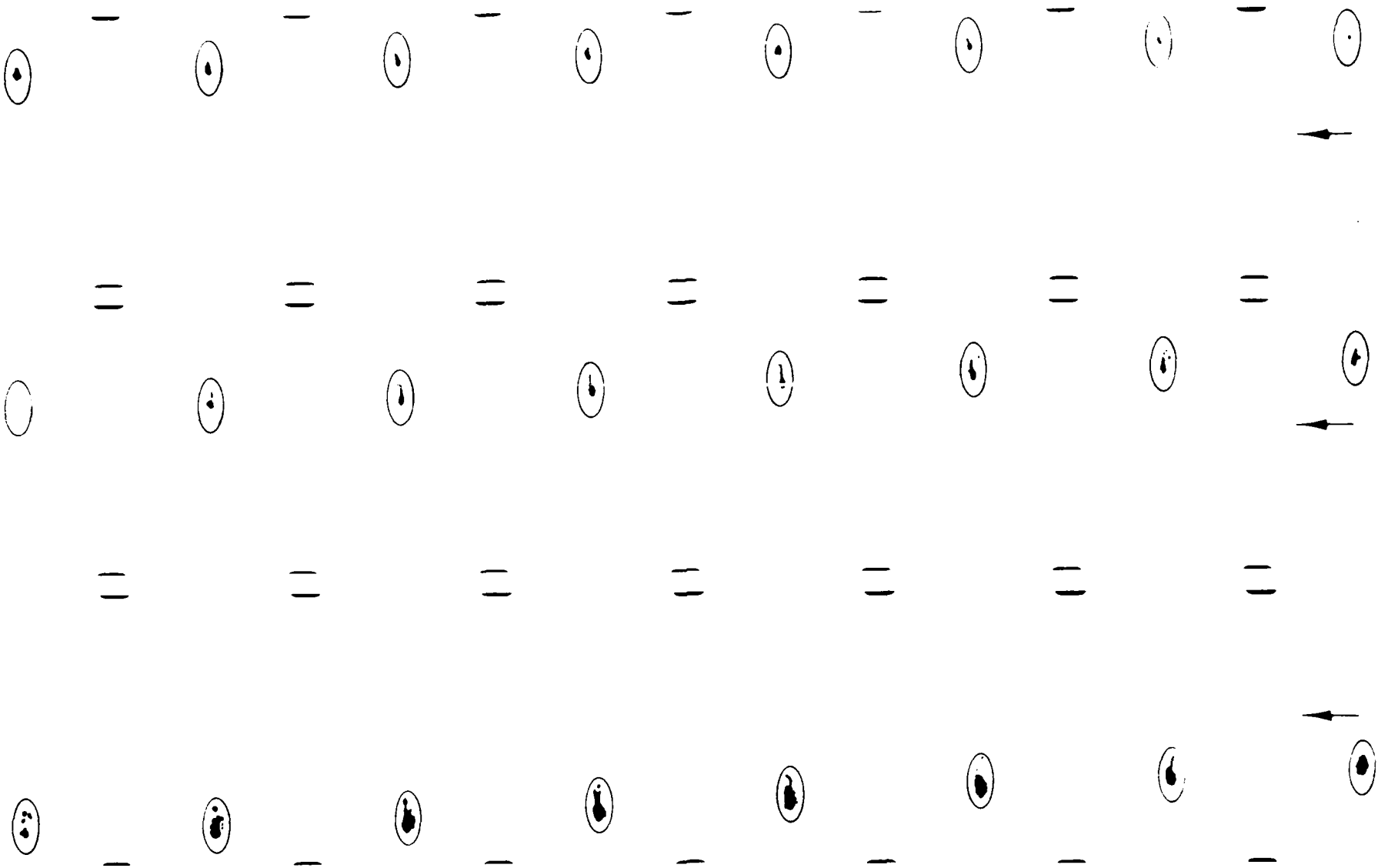

Ph. 31 Cinematography Sequence of a Burning No. 4 Oil-Water (W=0.12) Emulsion Drop in Oxygen Enriched Air (X_{O_2}=0.280)(110 pps)

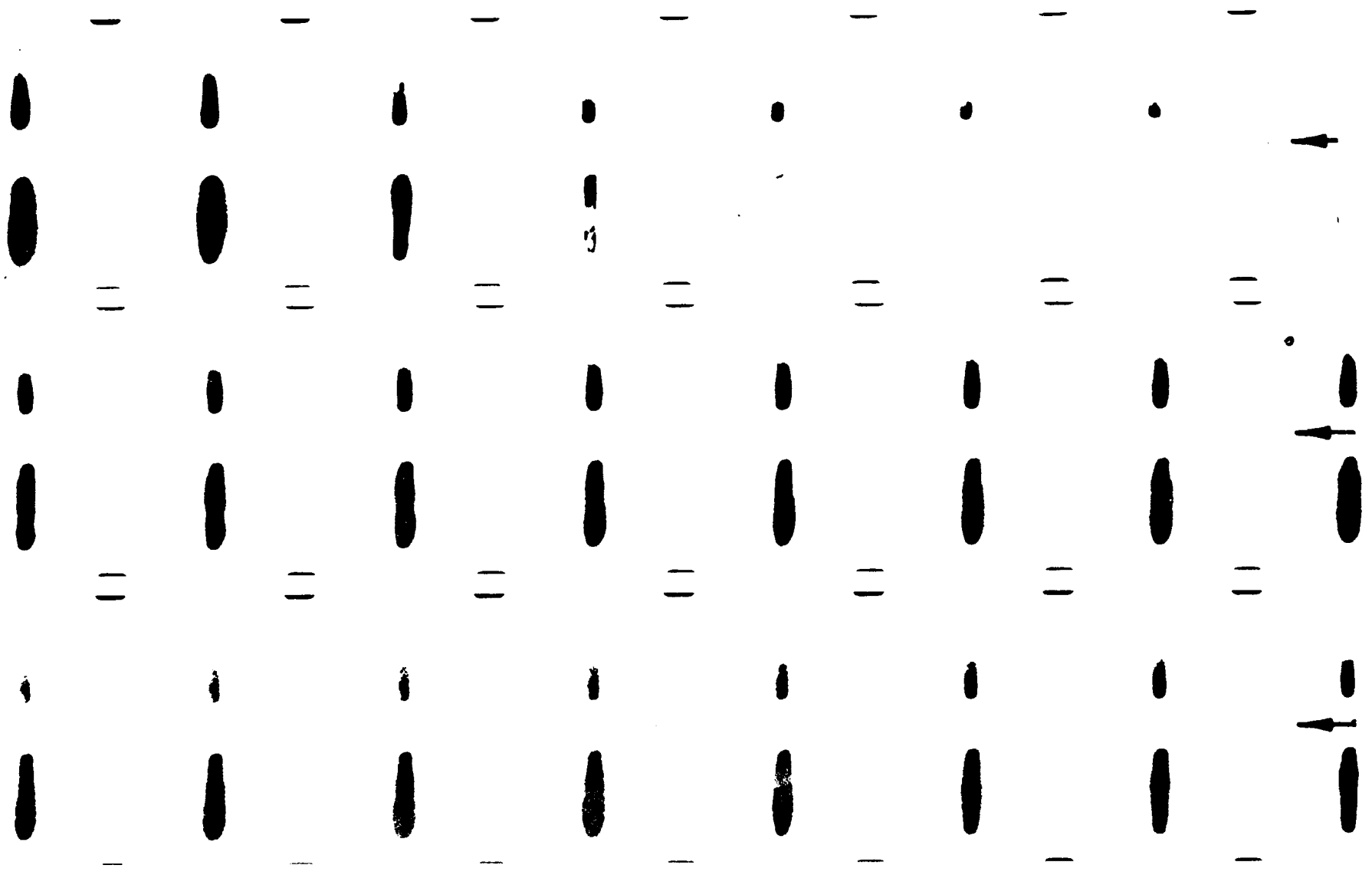

Ph. 2 Cinematography Sequence of a Burning Pure No. 4 Oil Spray

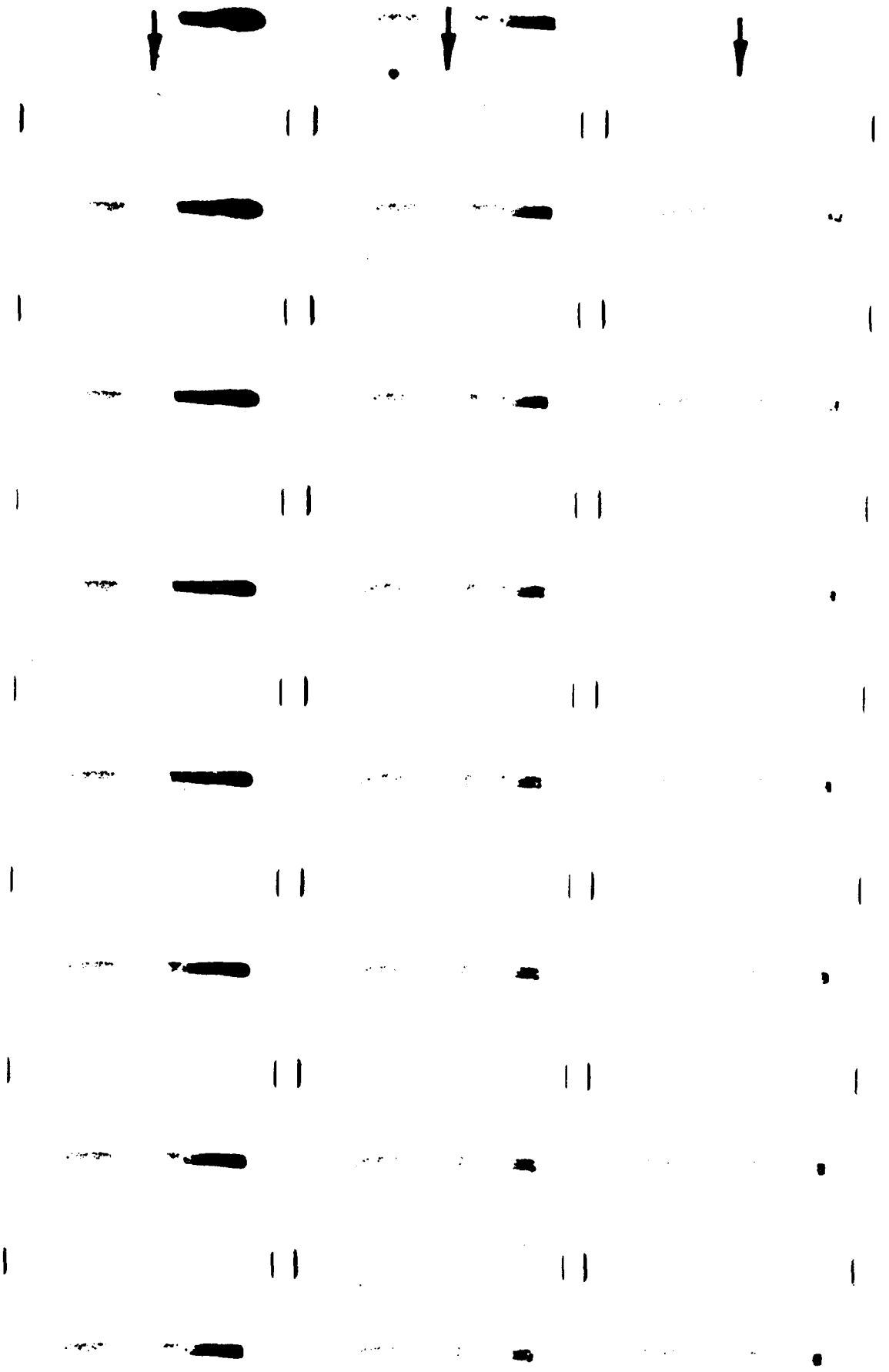

Fig. 38 - Continued

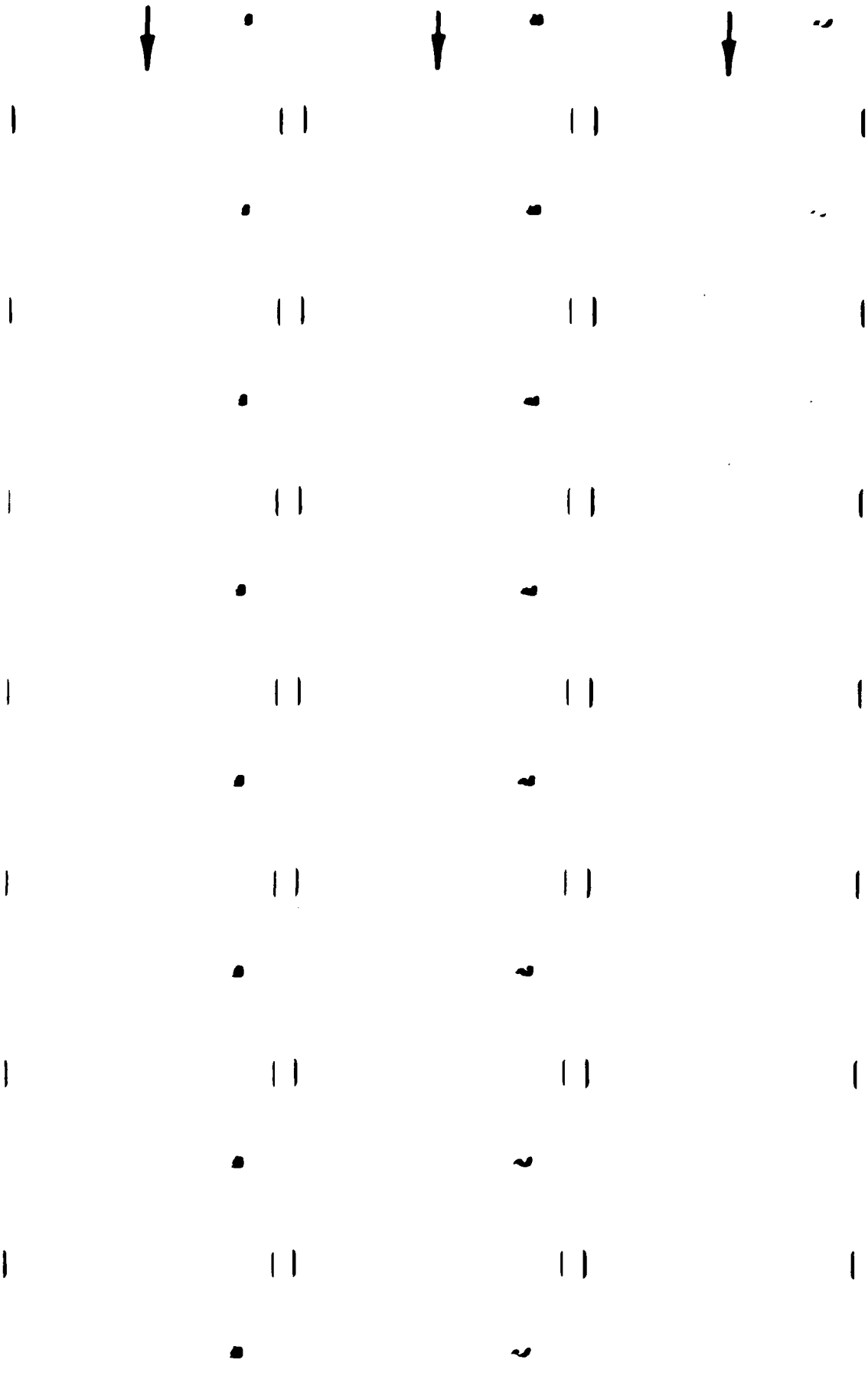

Ph. 32 - Continued

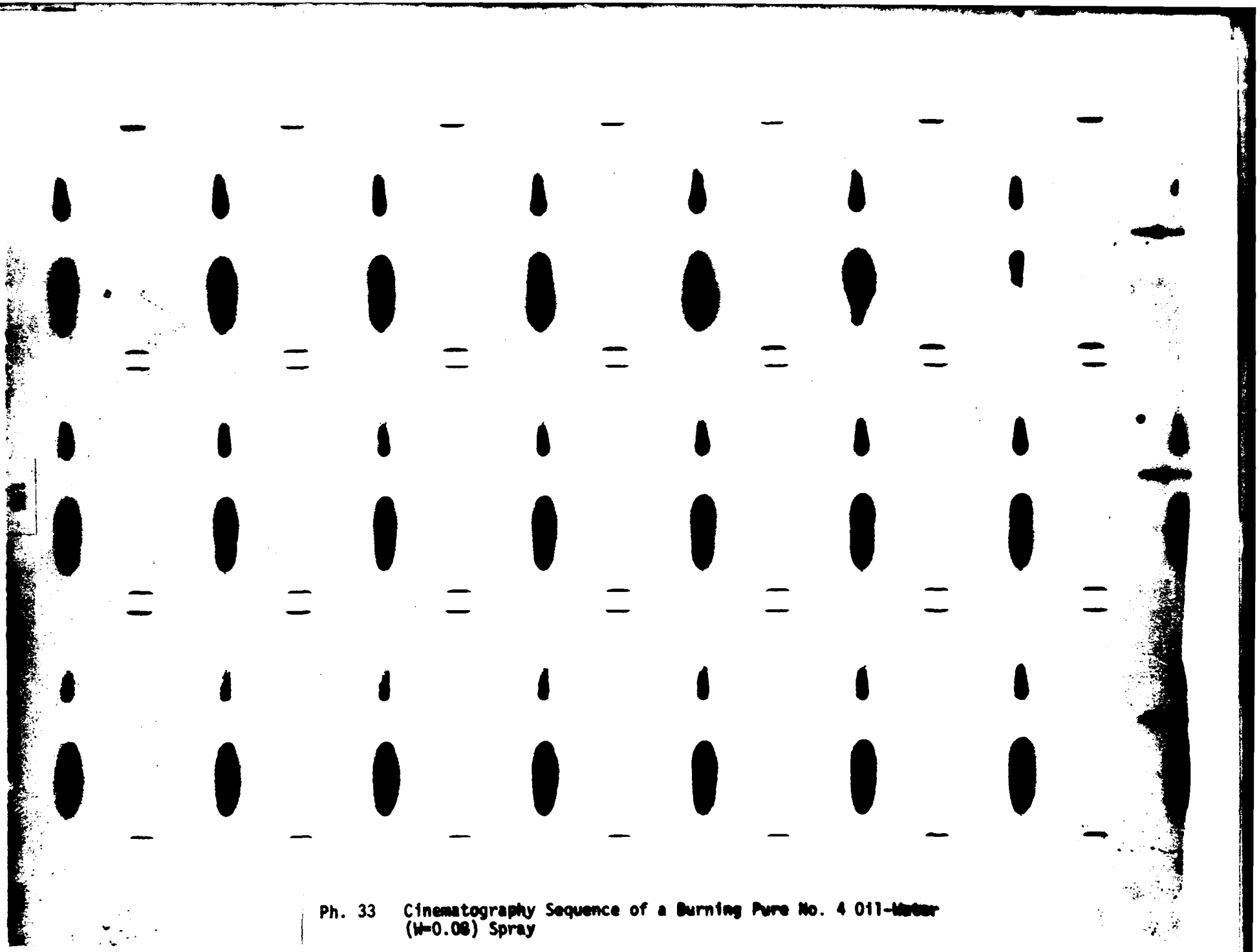

Ph. 33 Cinematography Sequence of a Burning Pure No. 4 Oil-Water (W=0.08) Spray

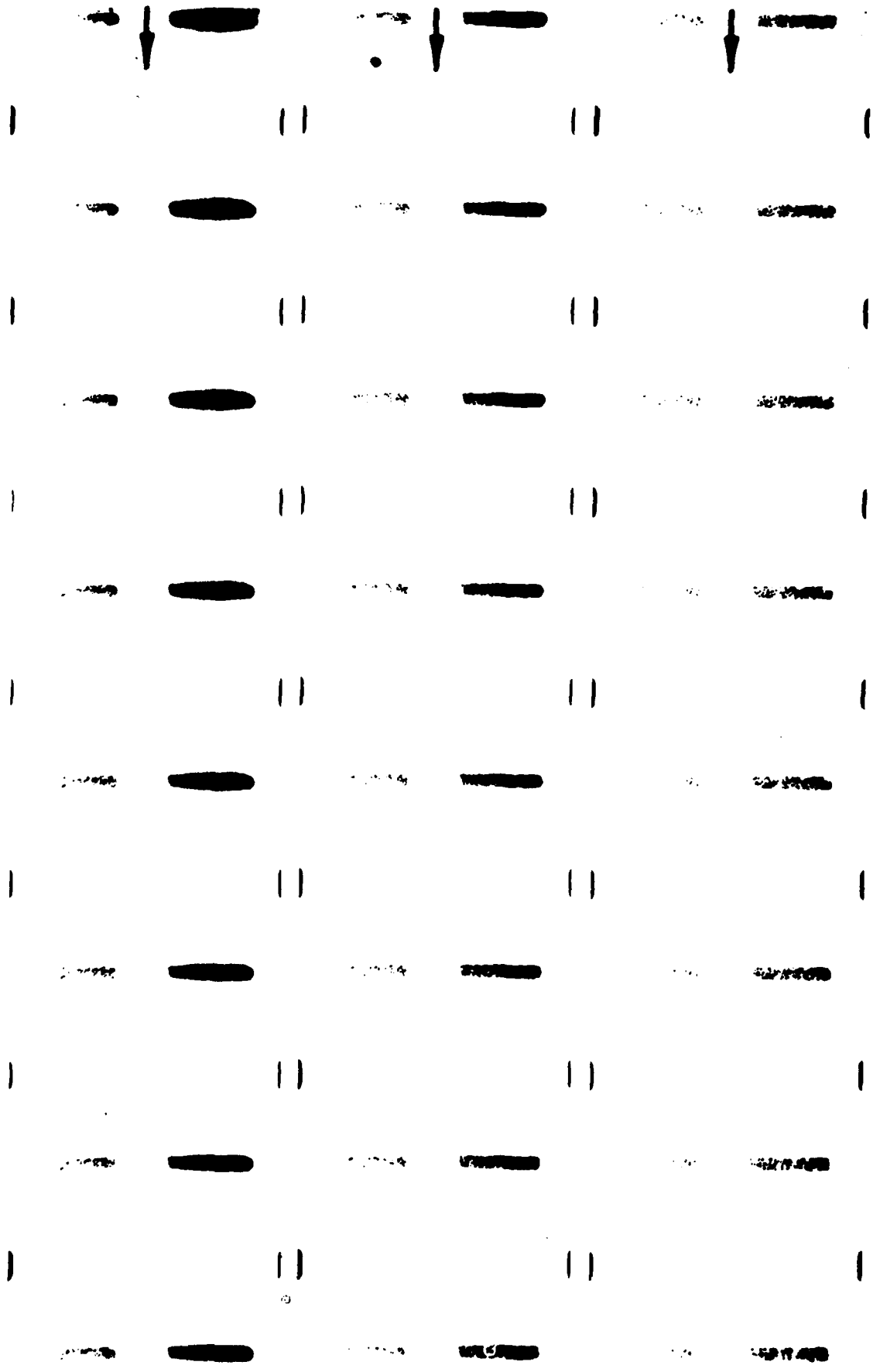

Ph. 33 - Continued

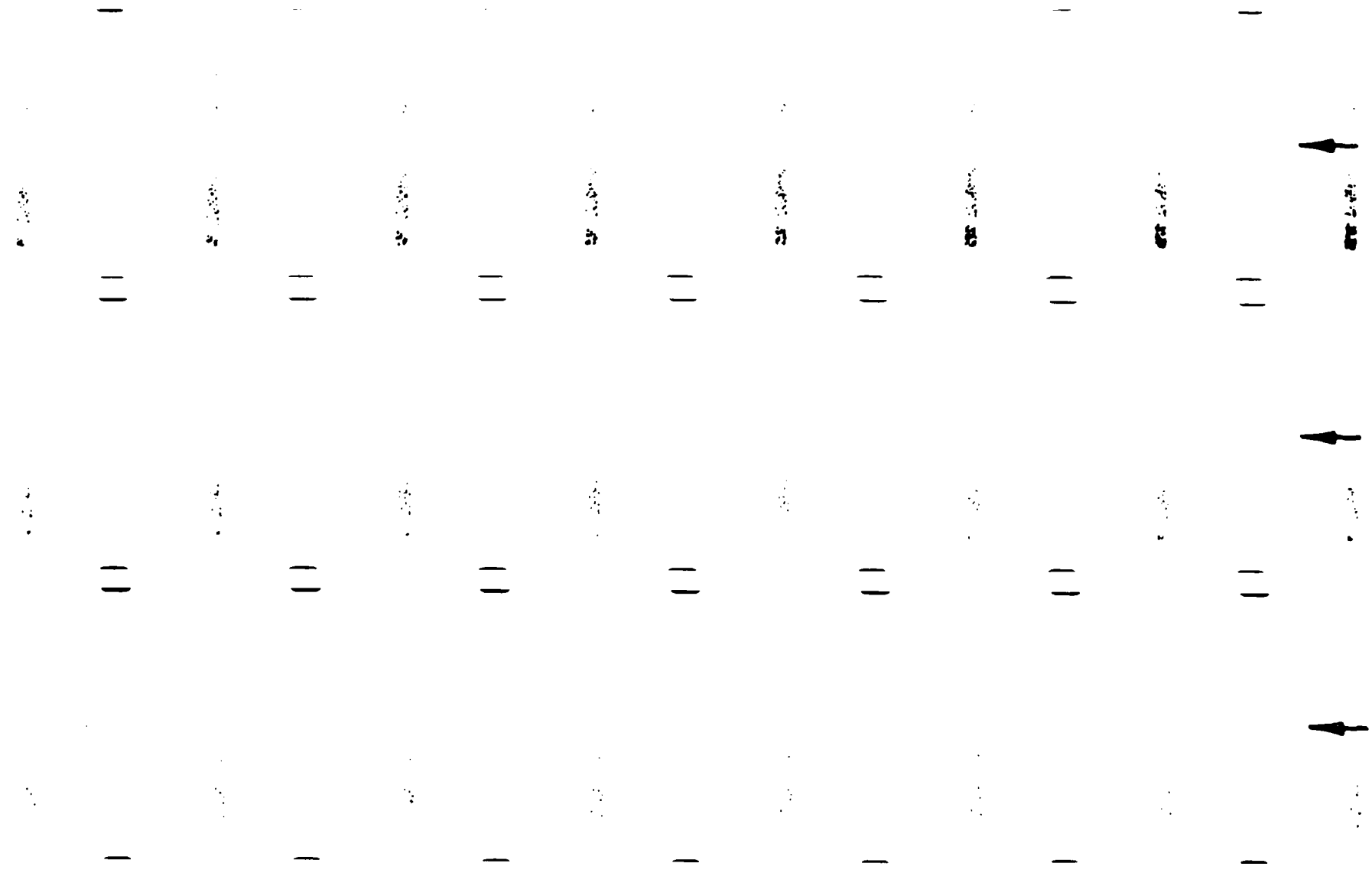

Ph. 33 - Continued

FIGURES

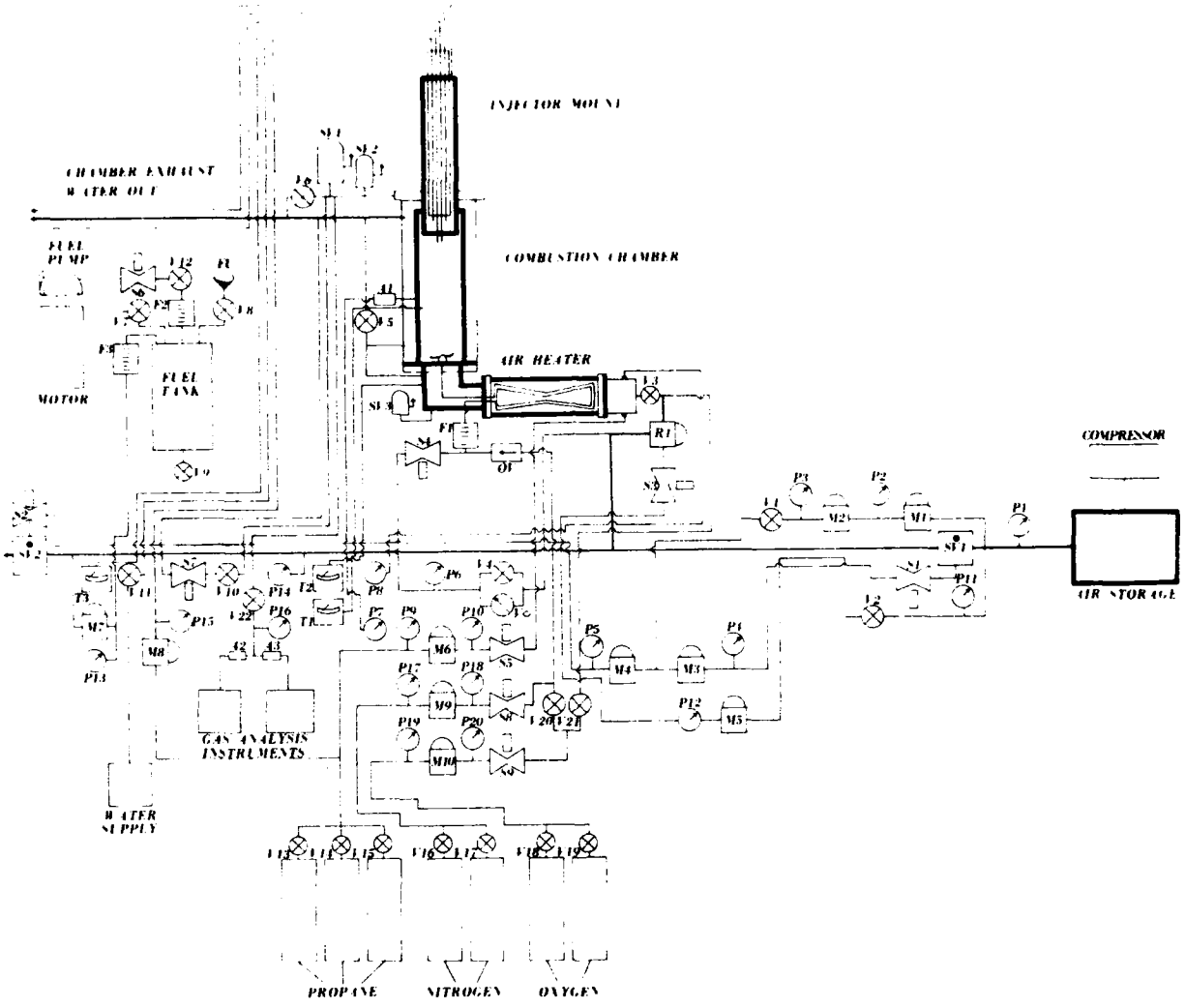

Fig. 1. Schematic Diagram of the Experimental Facility

KEY TO FIGURE 1

P1 - P20:	Pressure gages.
V1 - V22:	Manual valves
S1 - S9:	Solenoid valves
M1 - M10:	Manual pressure regulators
R1:	Two stage servo-regulator
F1 - F3:	Filters
A1 - A3:	Air dryers
OV:	One way valve
V:	Quick open valve
T1 - T3:	Thermocouple read out meters
SV1 - SV3:	Safety valves
FU:	Funnel
SV1 - SV3:	Servo-valves

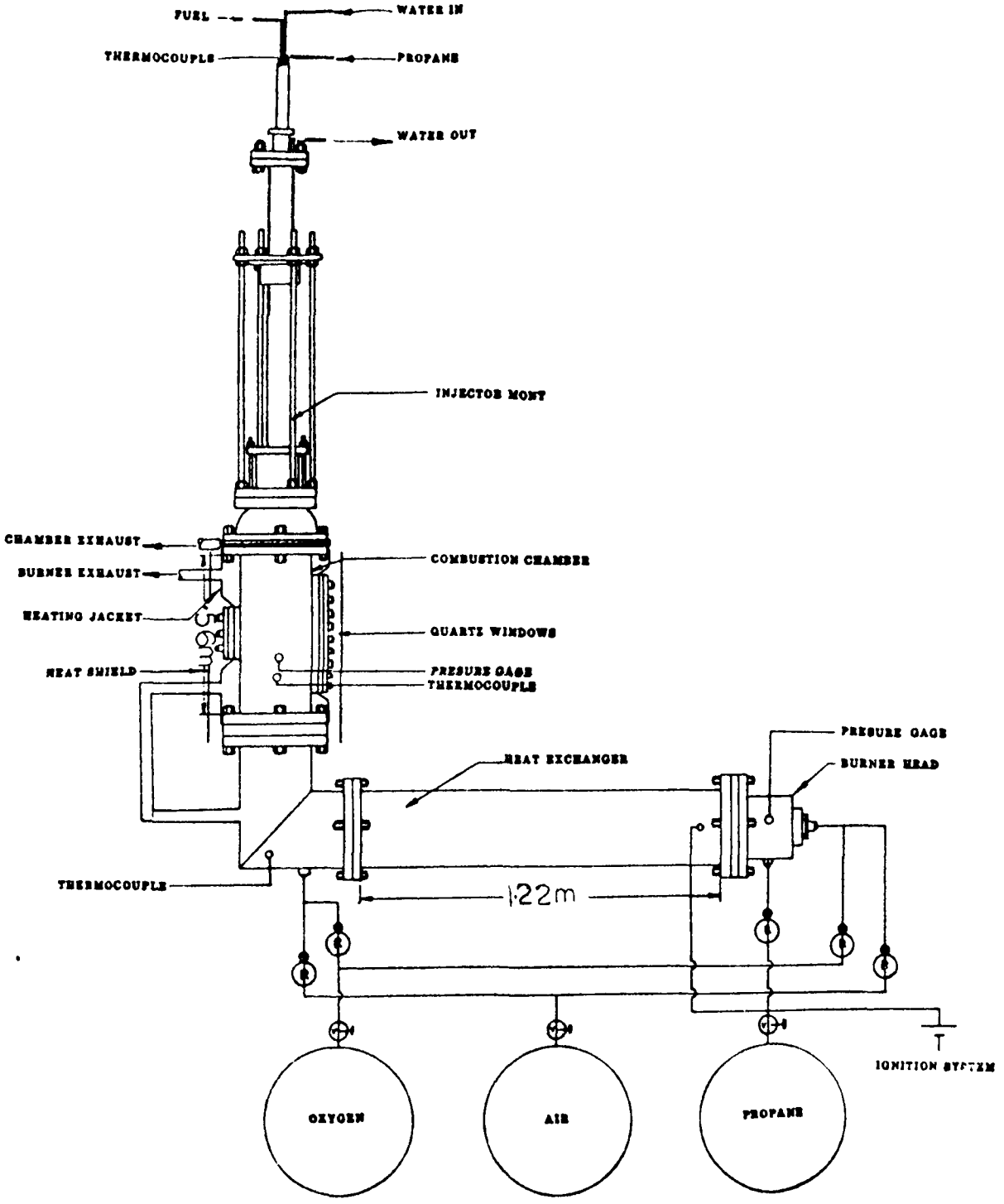

Fig. 2. Arrangement of Air-Heating, Combustion, and Fuel Injection Systems.

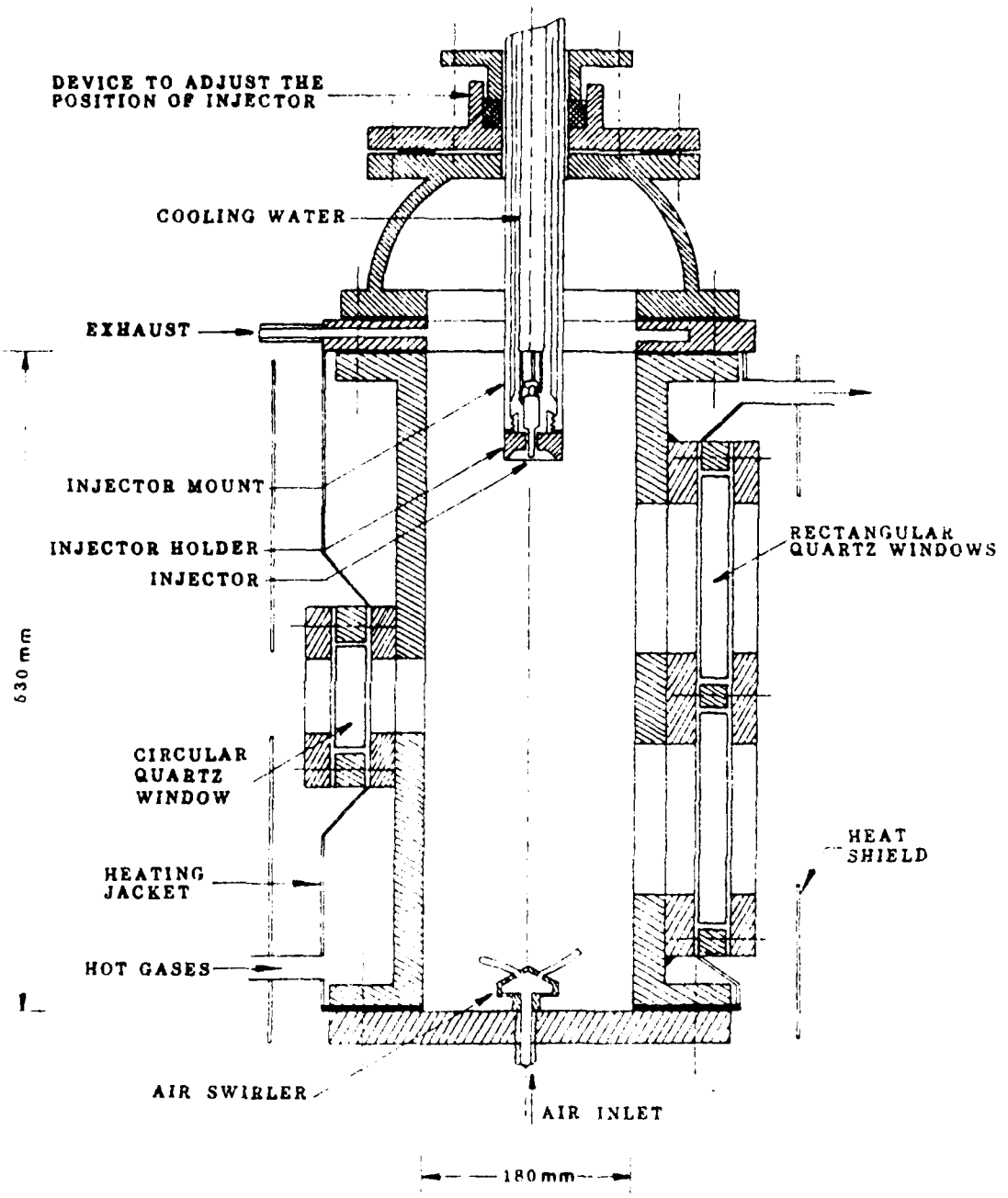

Fig. 3. Cross-Sectional Sketch of the Combustion Chamber

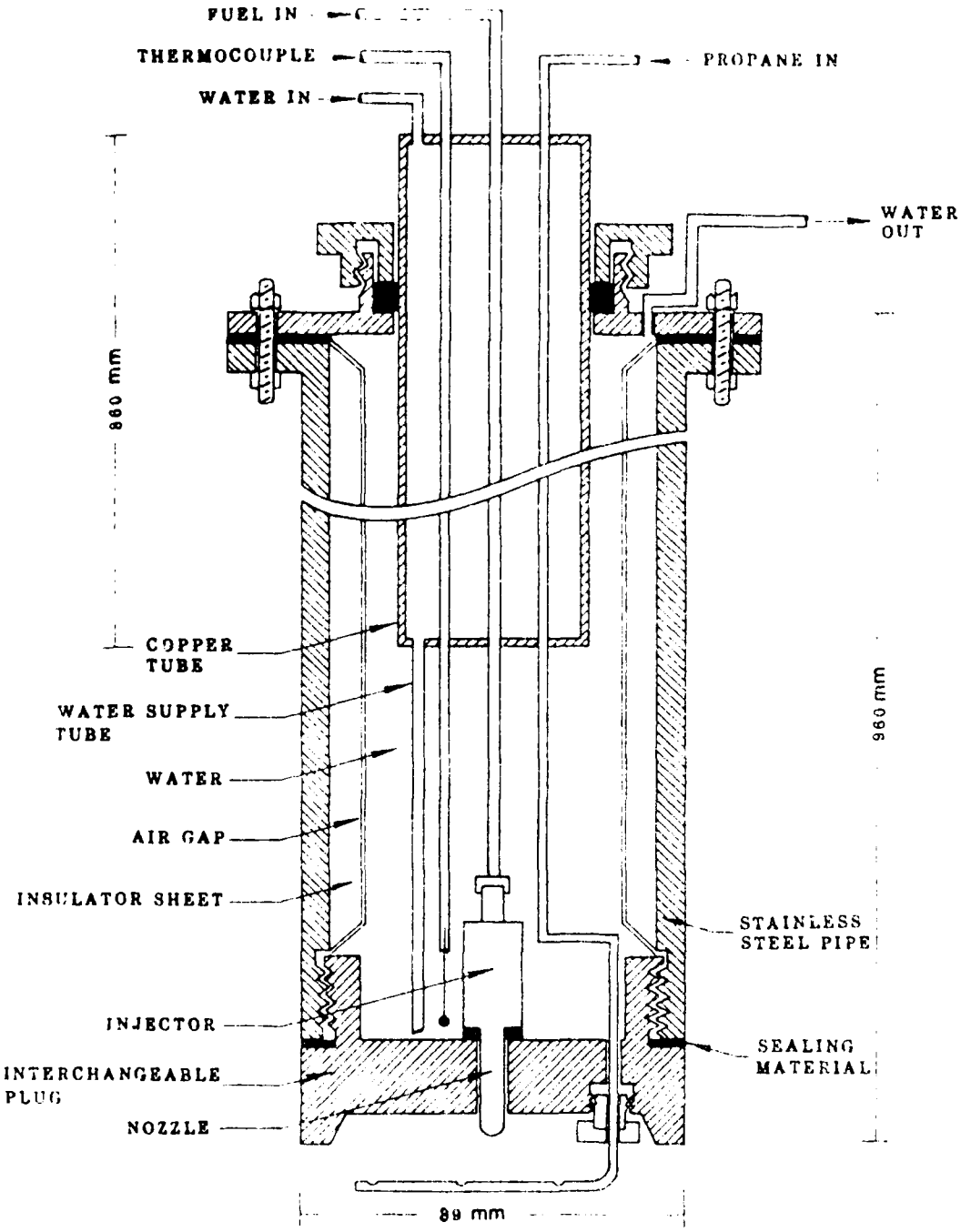

Fig. 4. Details of the Injector Mount

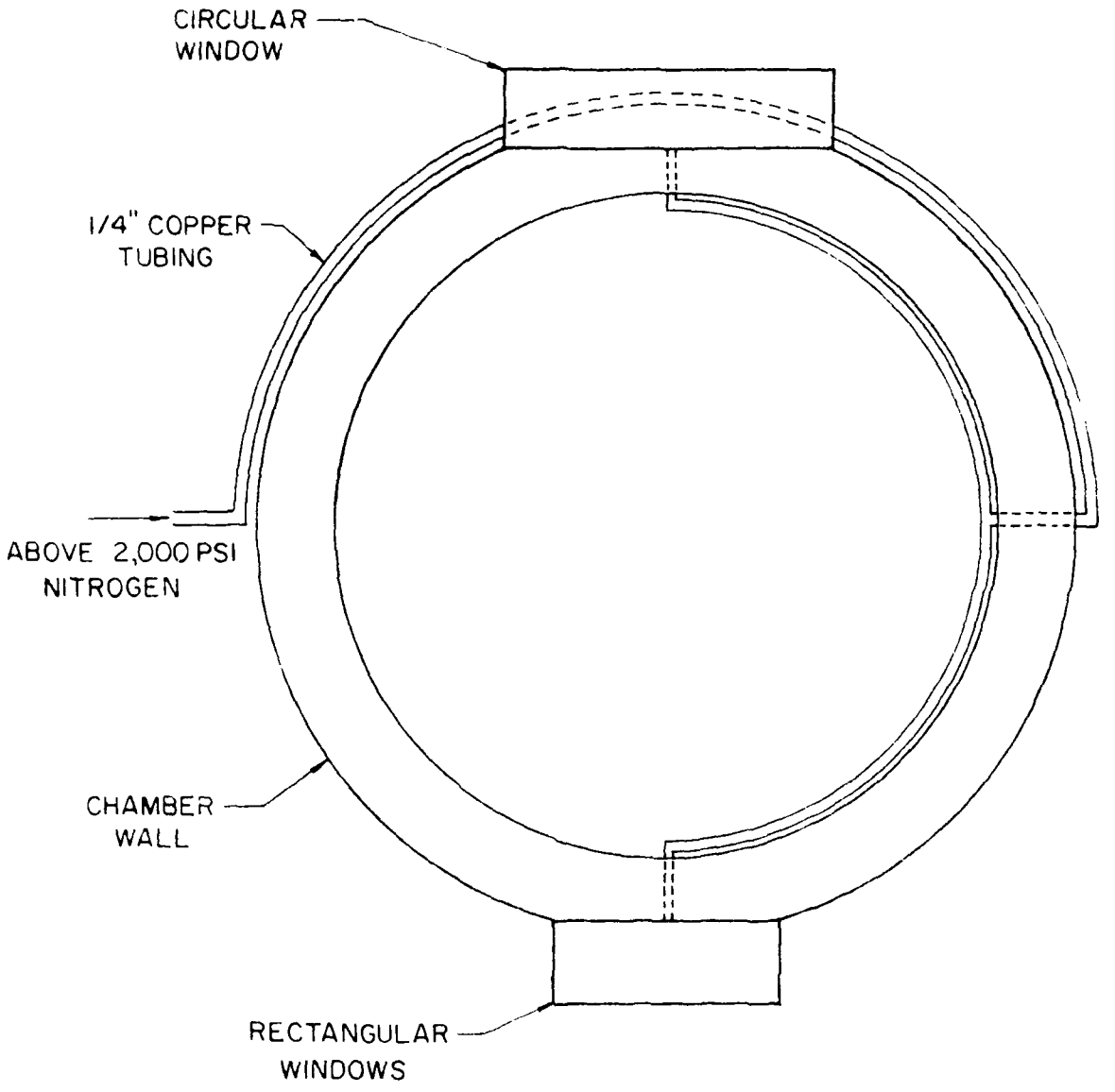

Fig. 5. Arrangement to Remove Soot from Windows

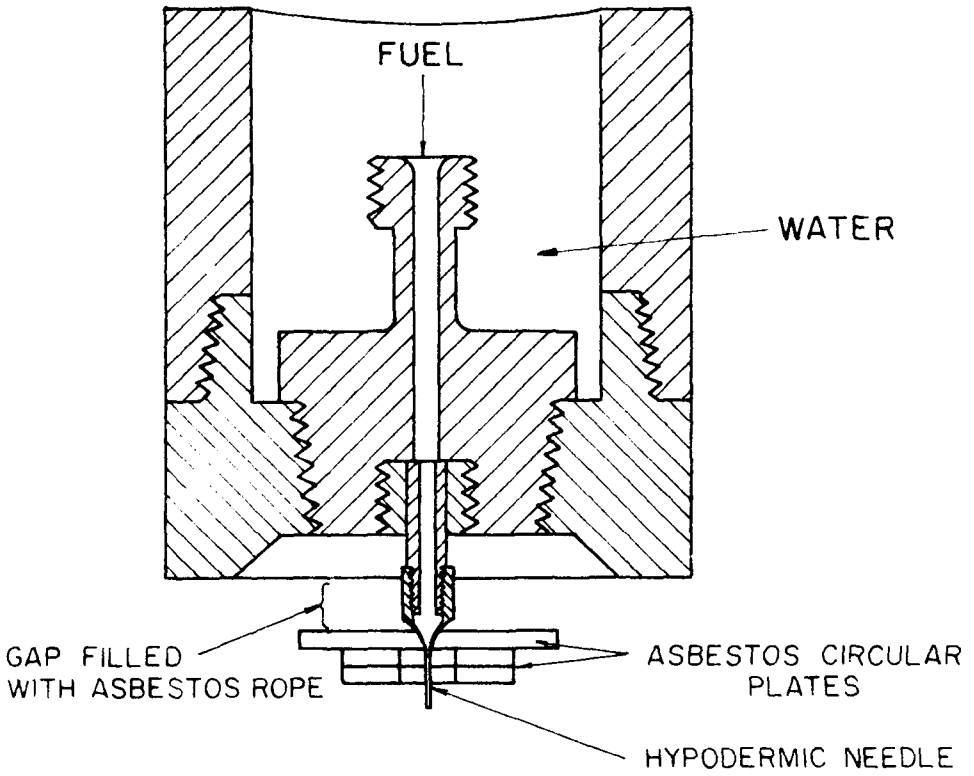

Fig. 6. Modified Injector Plug for Single Drop Studies

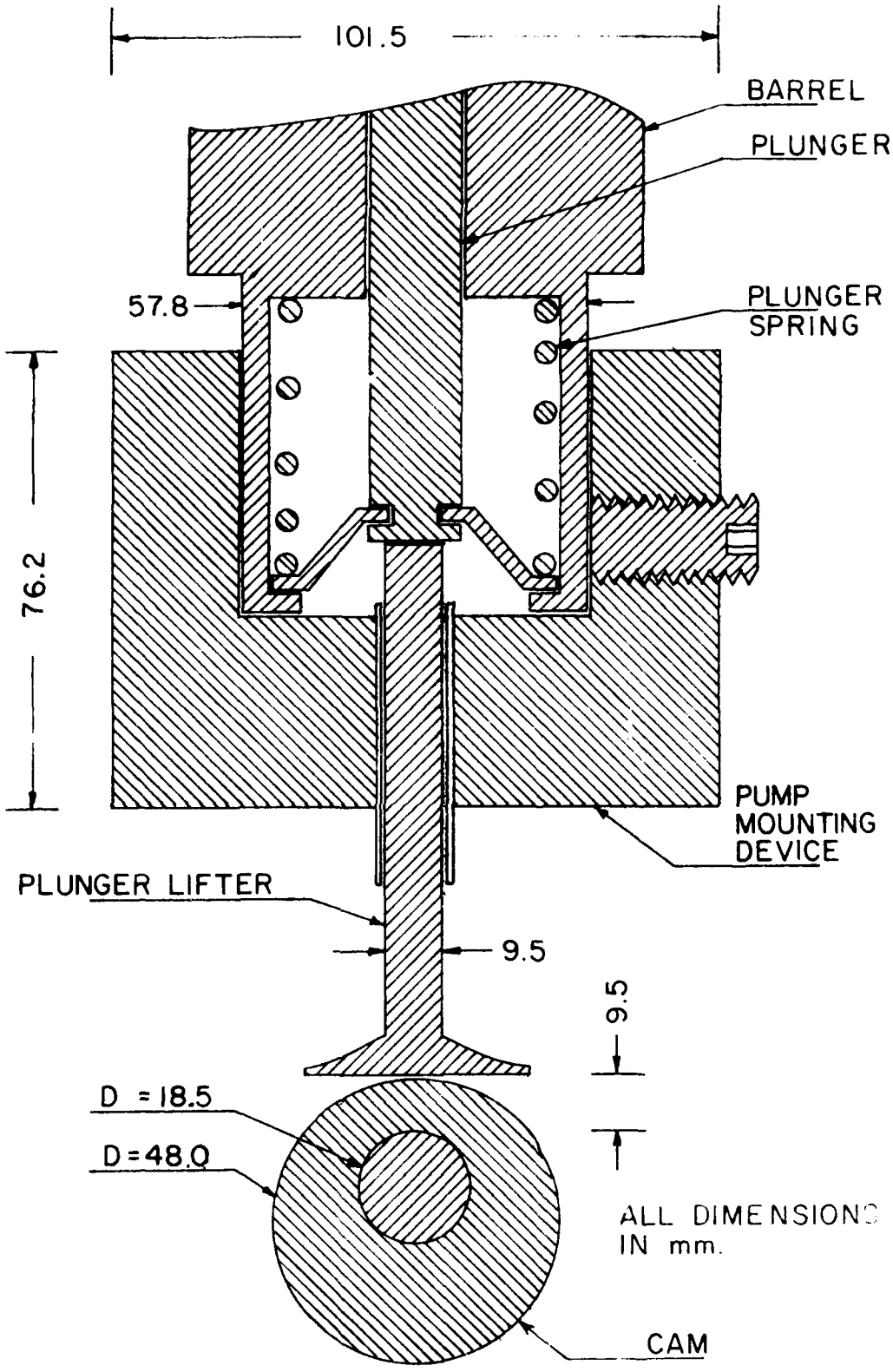

Fig. 7. Sketch of the Fuel-Pump Mount

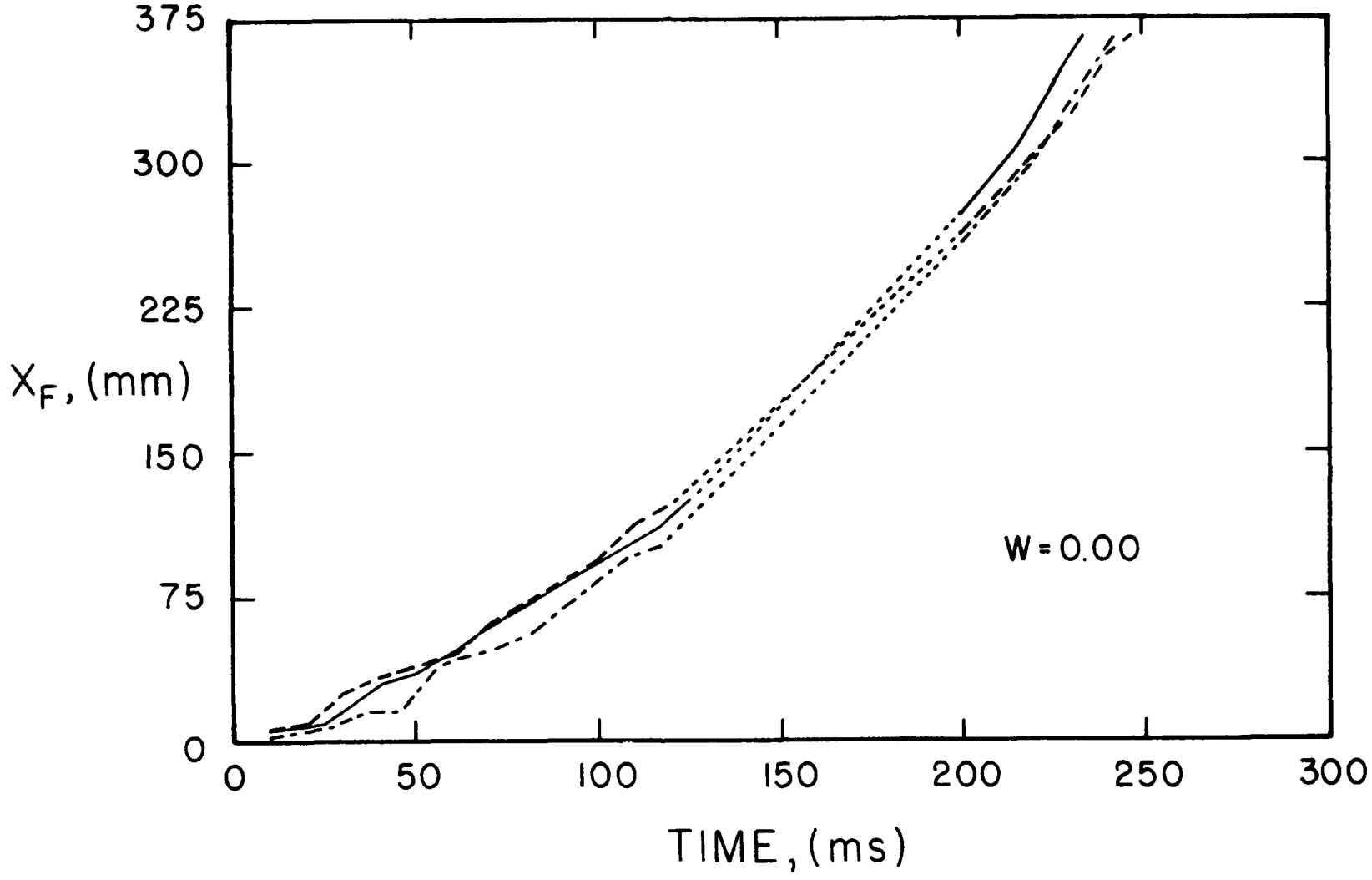

Fig. 8. Variation of the Drop Travel with Time (Pure No. 4 Oil)

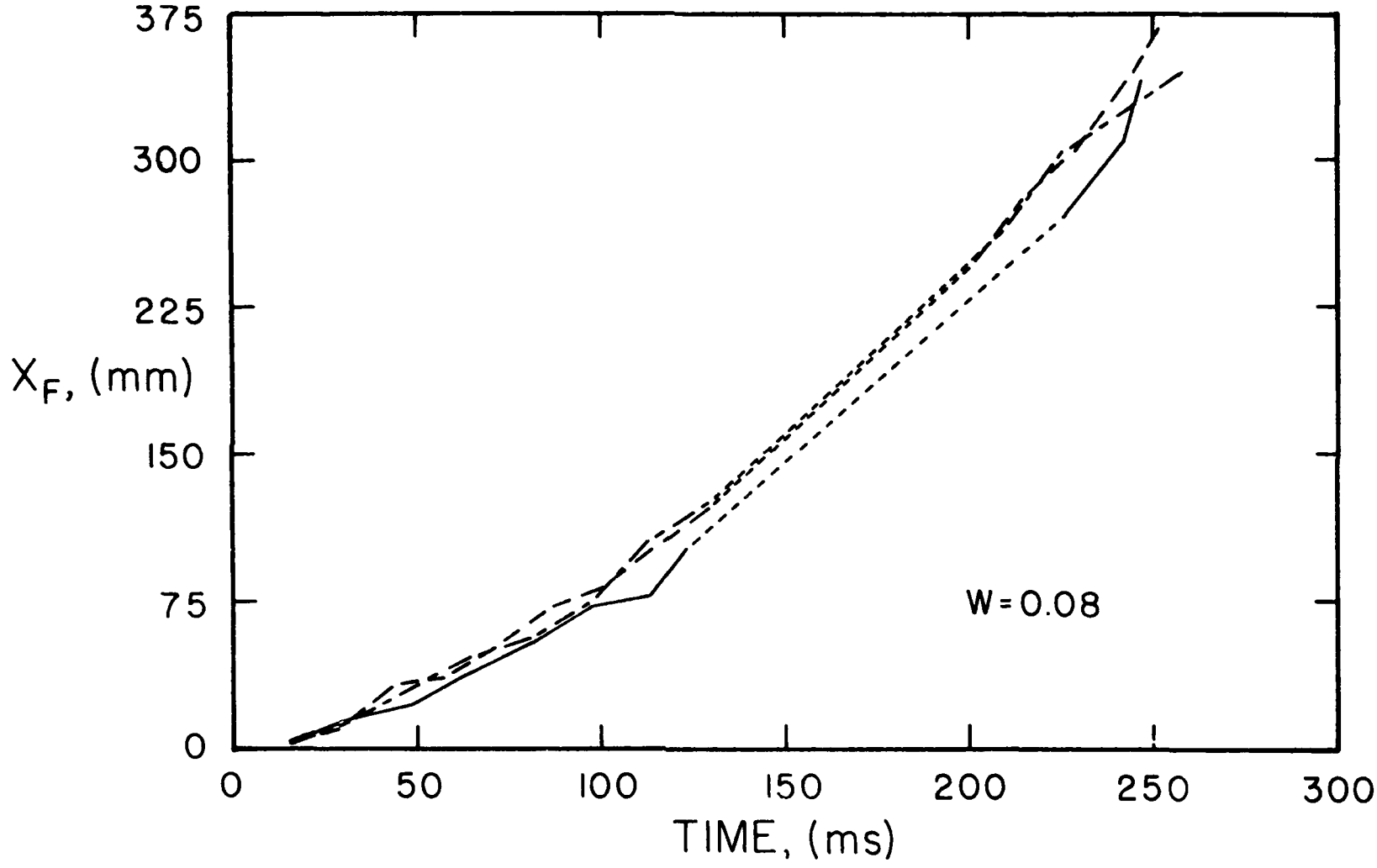

Fig. 9. Variation of the Drop Travel with Time (No. 4 Oil-Water Emulsion, W = 0.08)

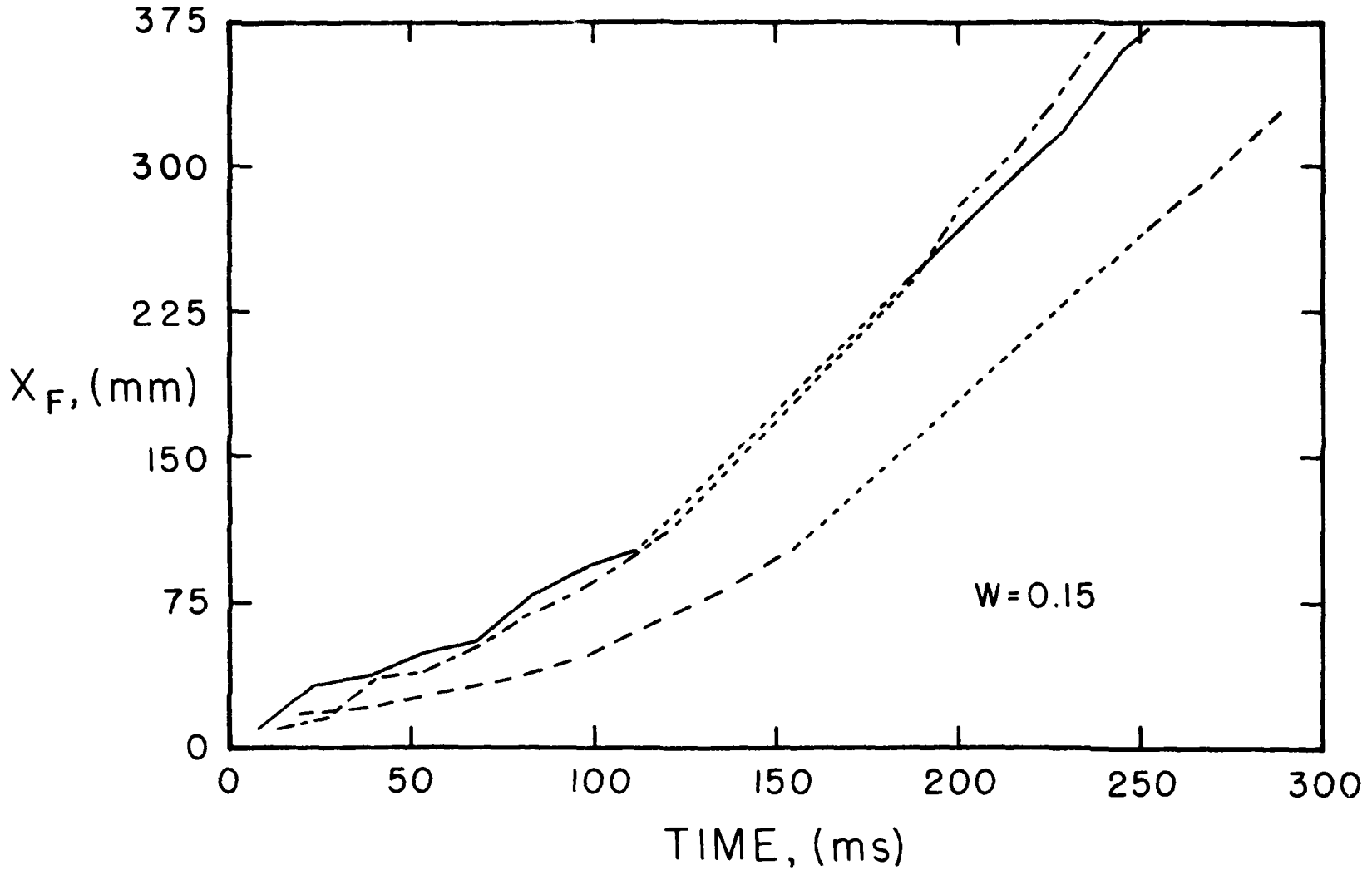

Fig. 10. Variation of the Drop Travel with Time (No. 4 Oil-Water Emulsion, W = 0.15)

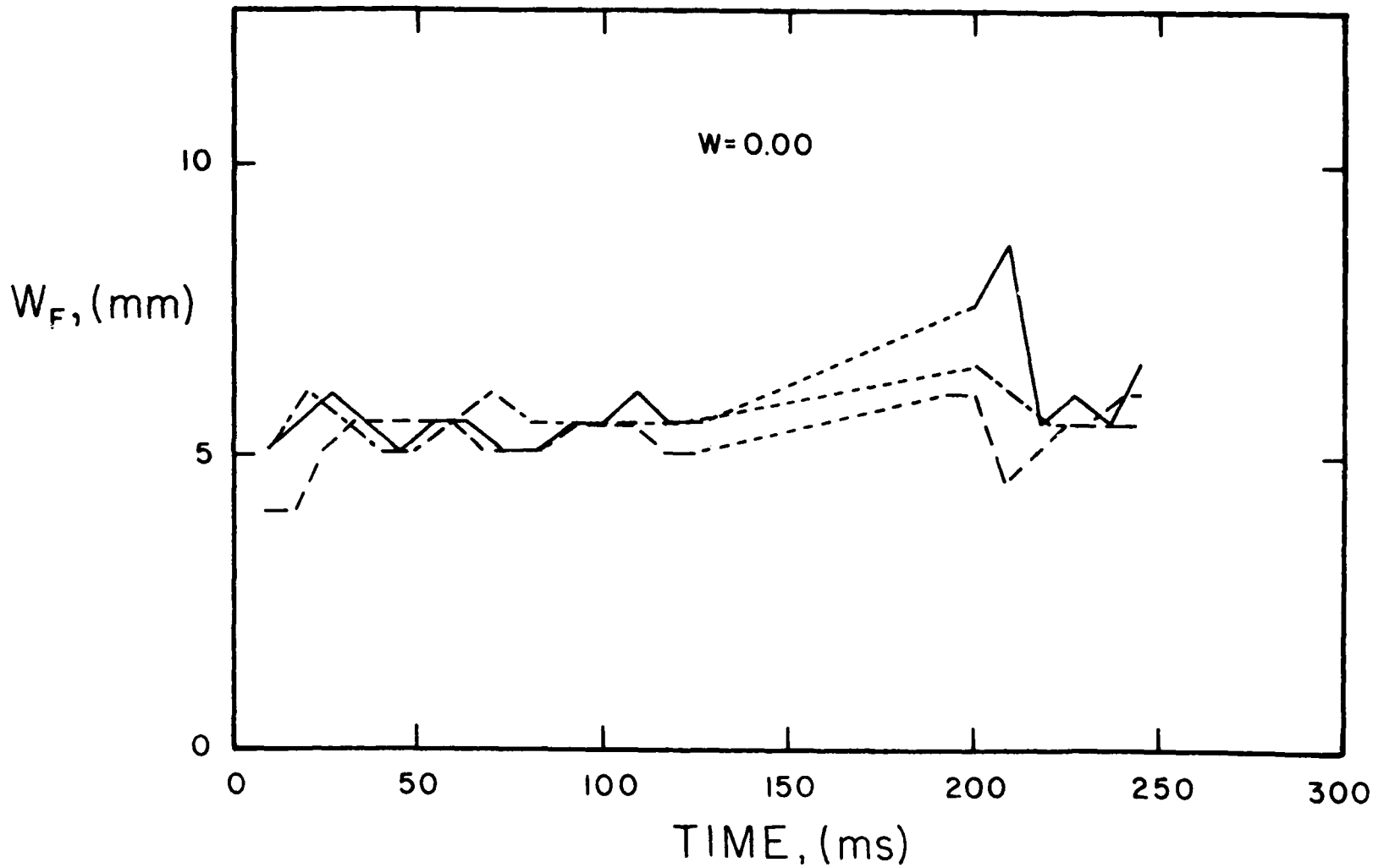

Fig. 11. Variation of the Maximum Flame Width of Drop with Time (Pure No. 4 Oil)

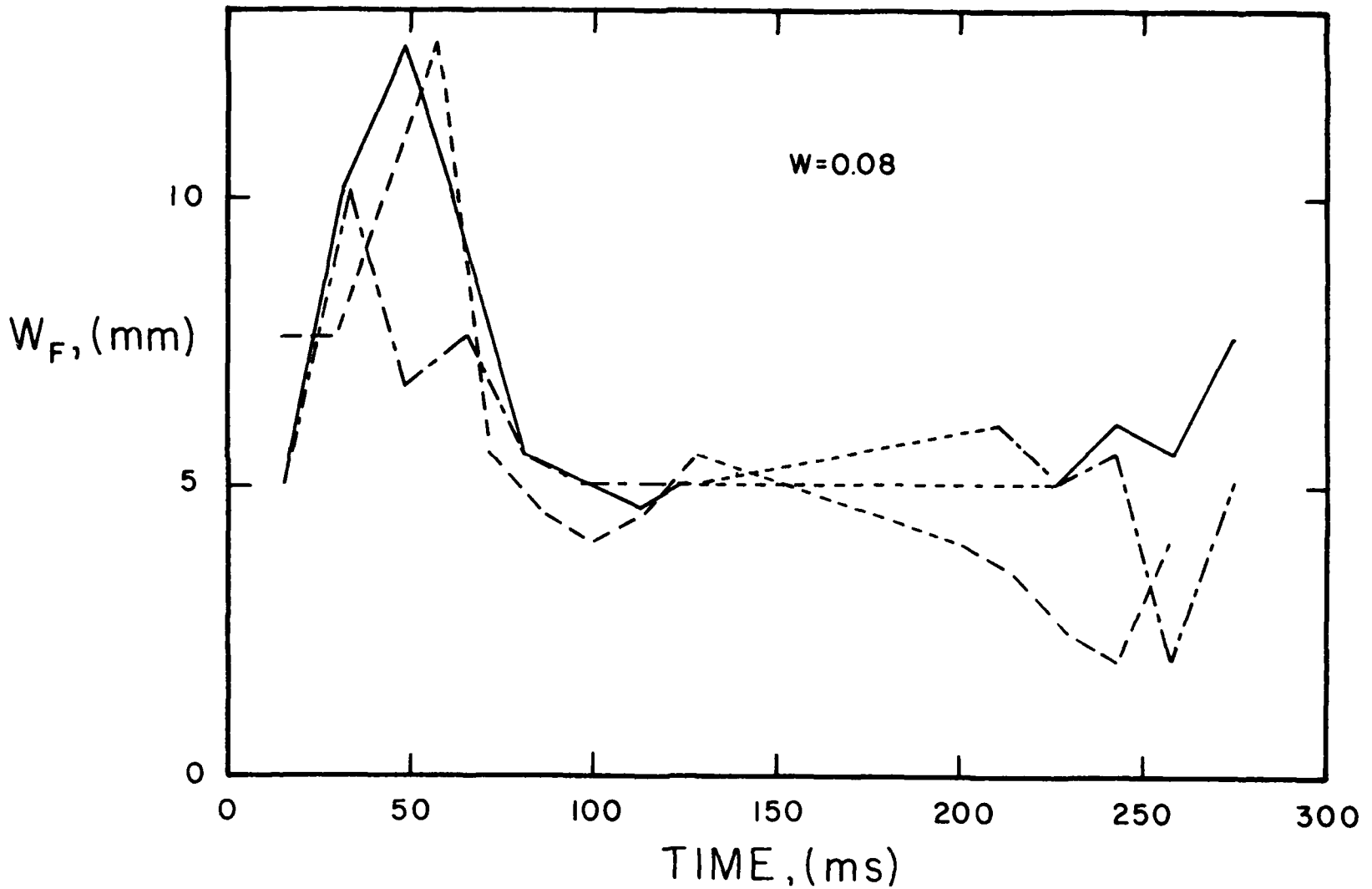

Fig. 12. Variation of the Maximum Flame Width of Drop with Time (No. 4 Oil-Water Emulsion, W = 0.08)

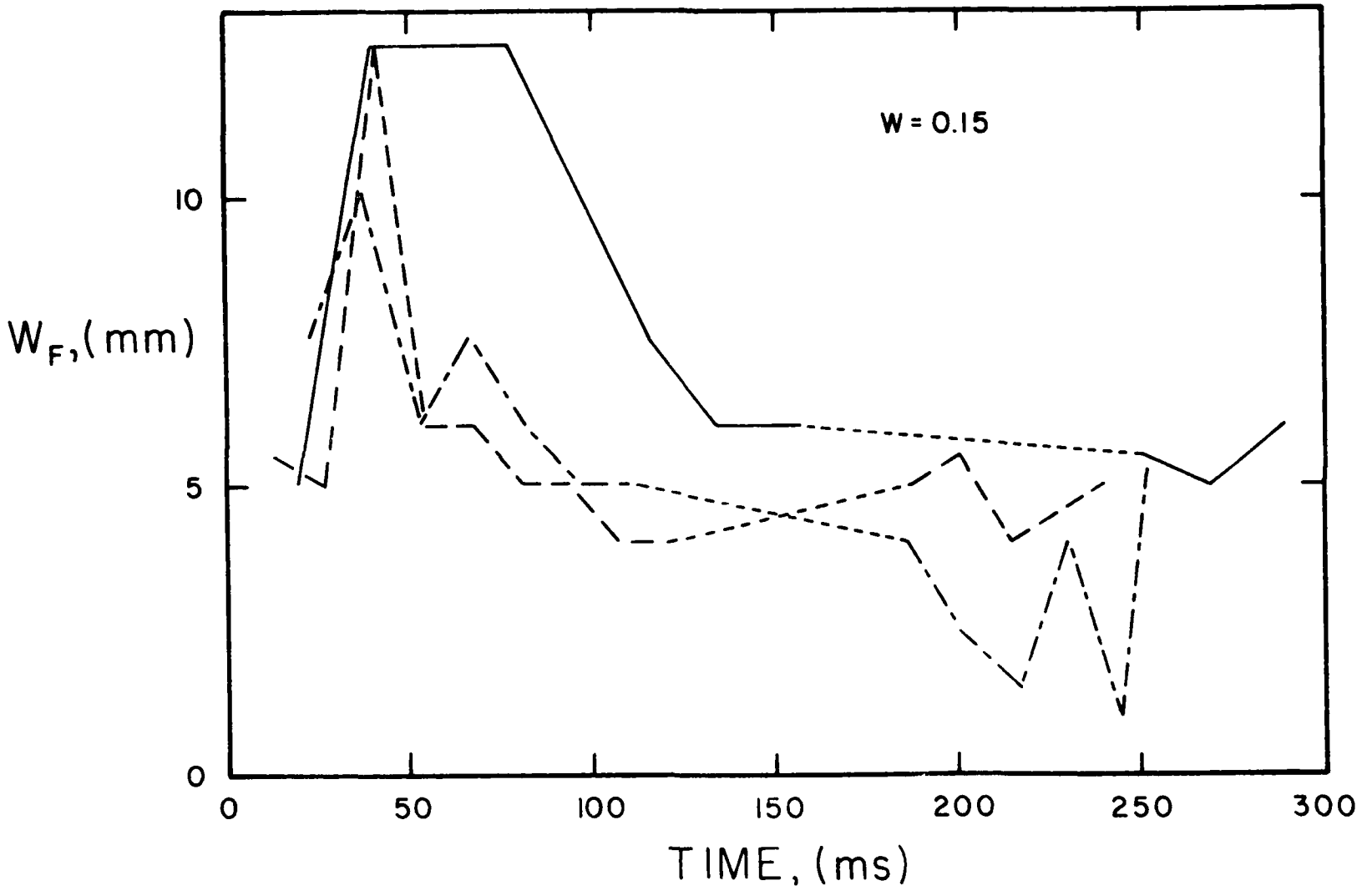

Fig. 13. Variation of the Maximum Flame Width of Drop with Time (No. 4 Oil-Water Emulsion, W = 0.15)

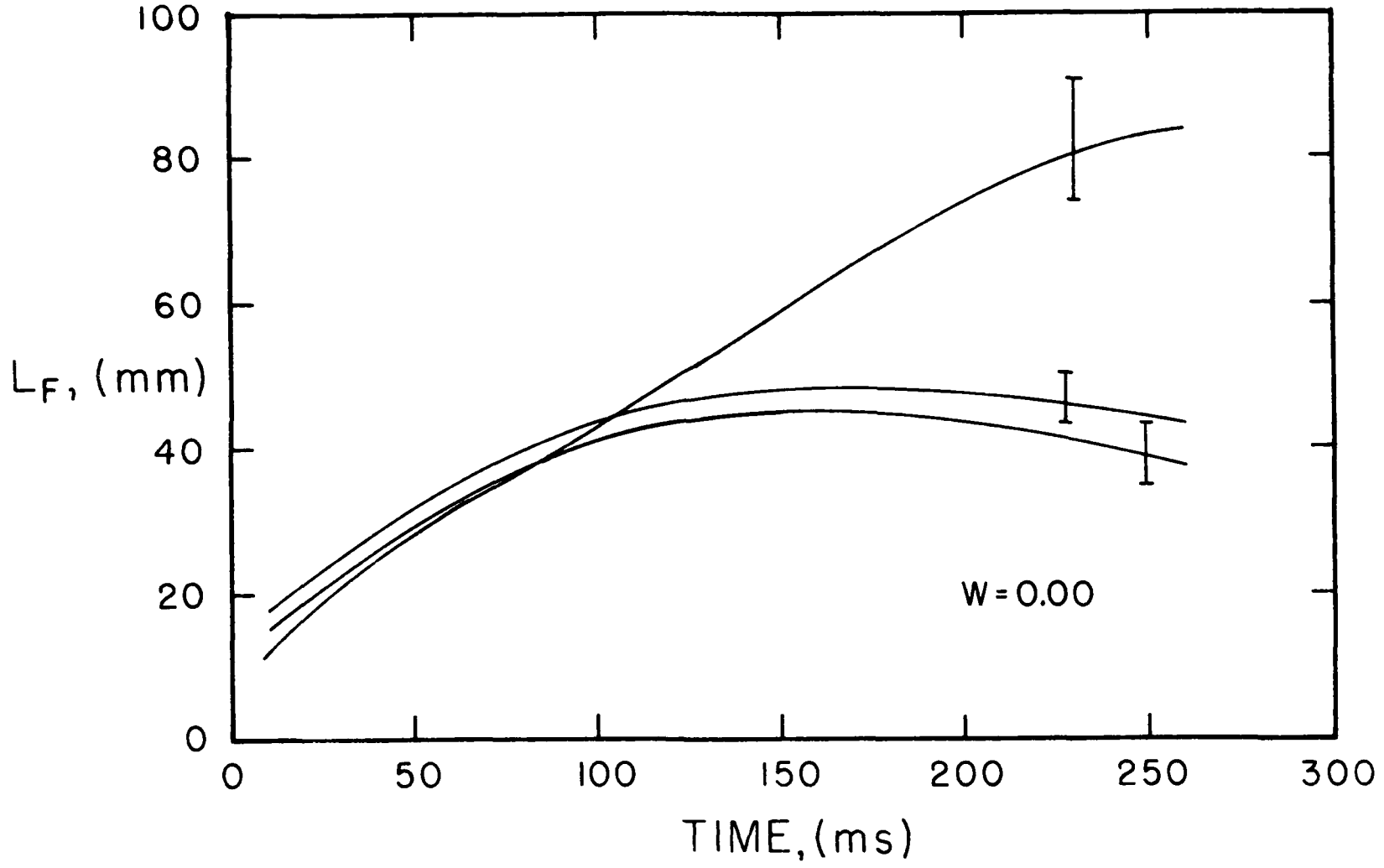

Fig. 14. Variation of the Flame Length of Drop with Time (Pure No. 4 Oil)

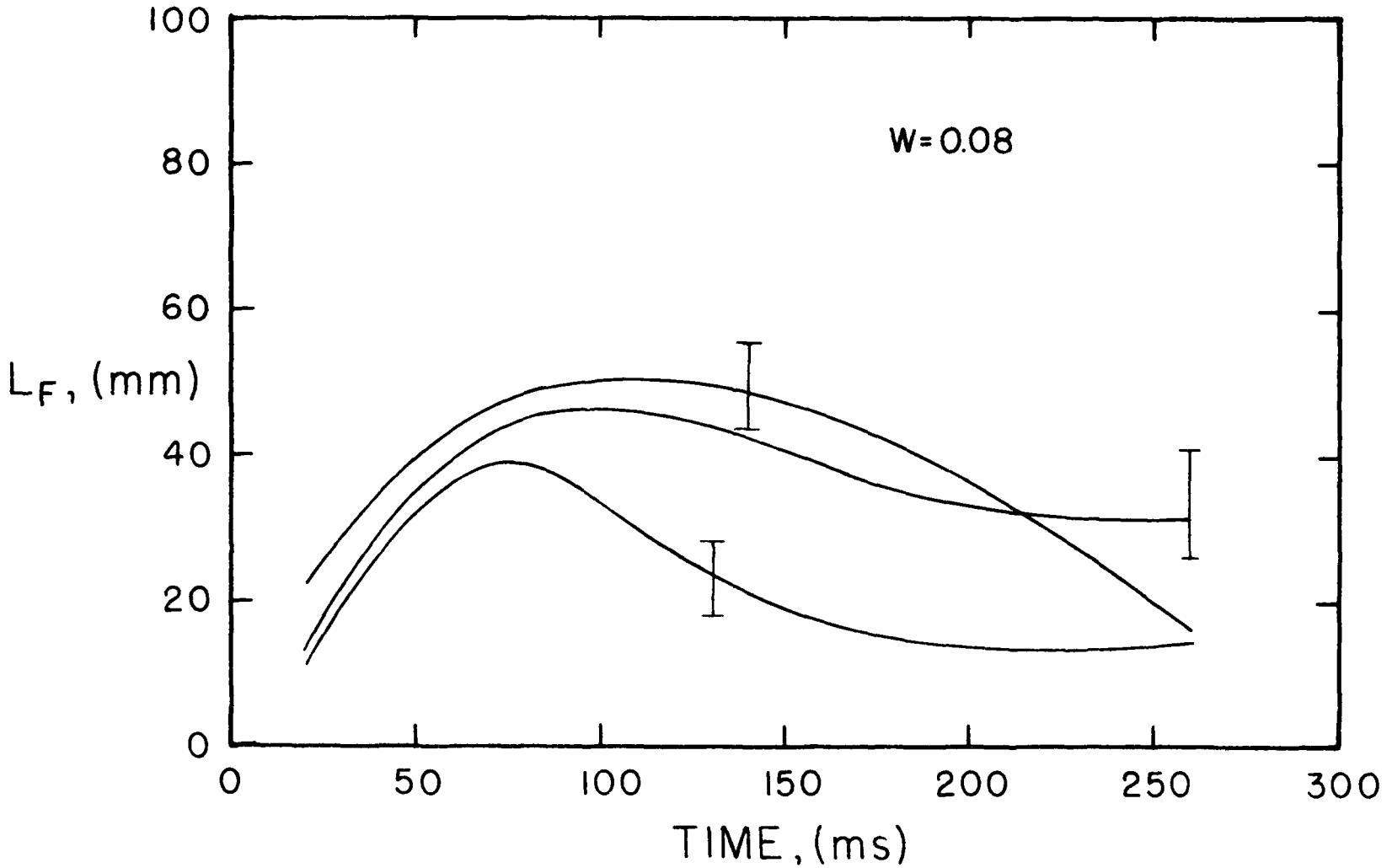

Fig. 15. Variation of the Flame Length of Drop with Time (No. 4 Oil-Water Emulsion, W = 0.08)

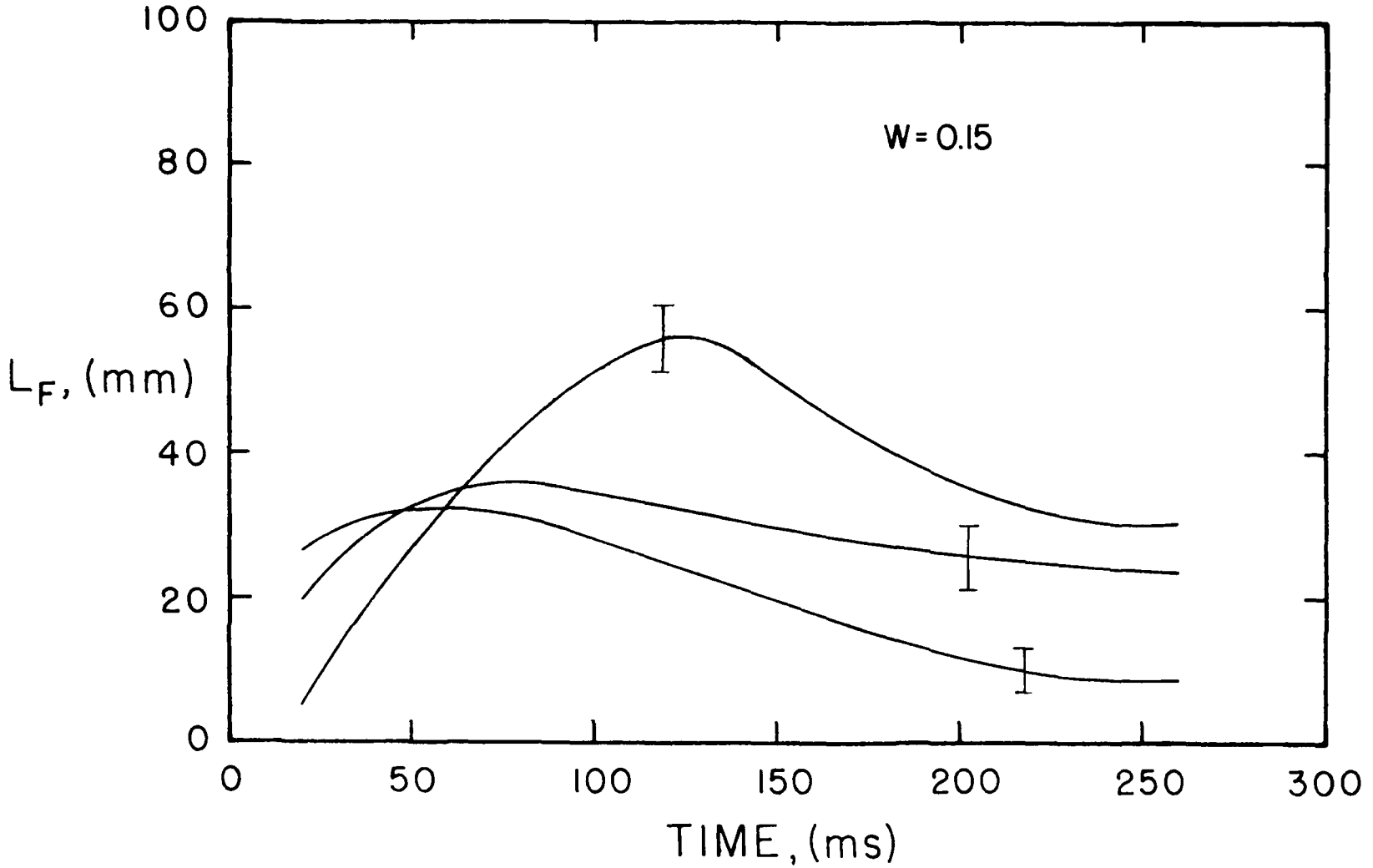

Fig. 16. Variation of the Flame Length of Drop with Time (No. 4 Oil-Water Emulsion, W = 0.15)

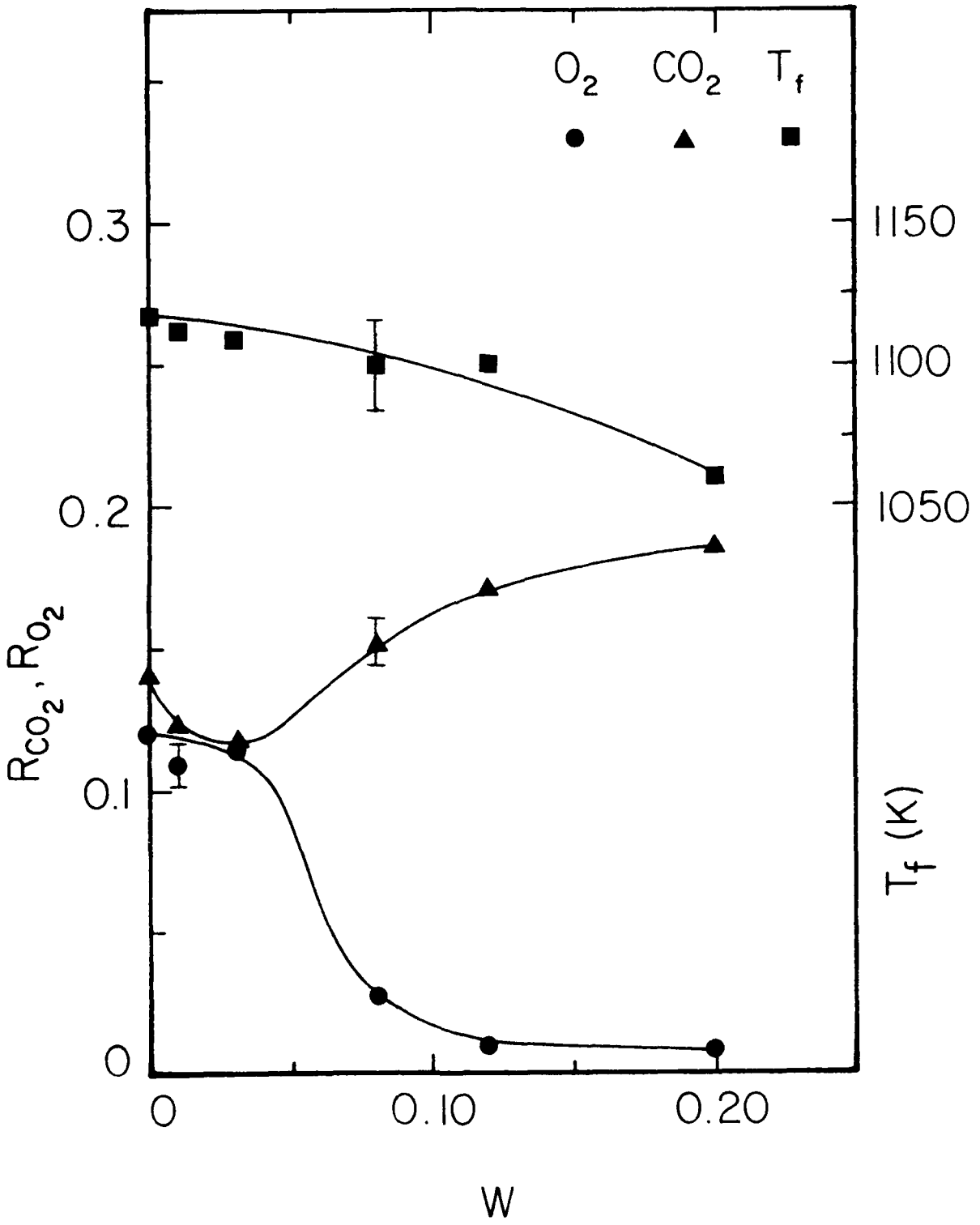

Fig. 17. Effects of Volume Fraction of Water on CO_2 and O_2 in the Exhaust and the Flame Temperature (Burning Sprays of No. 4 Oil-Water Emulsion)

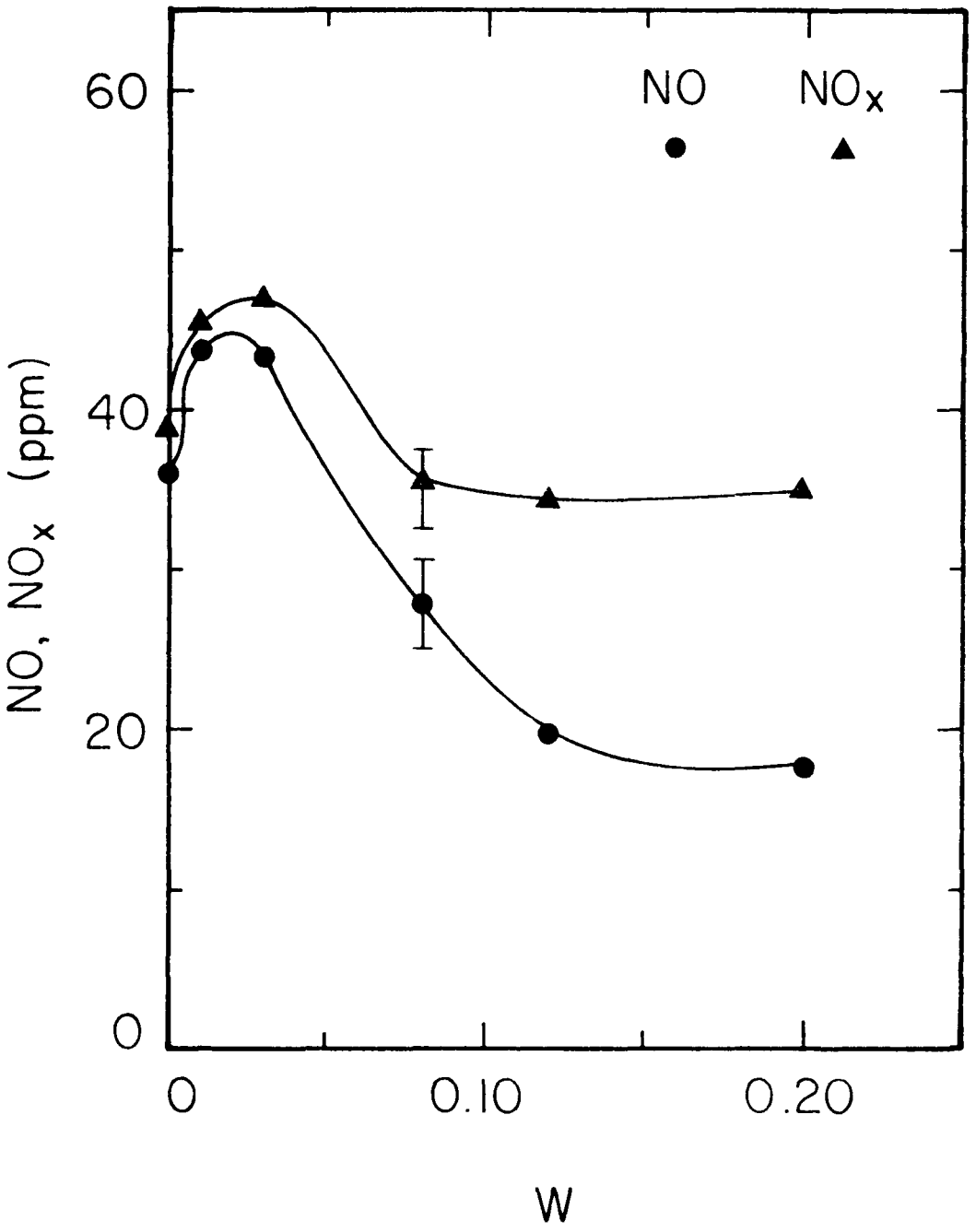

Fig. 18. Effects of Volume Fraction of Water on the Emission of Nitrogen Oxides (Burning Sprays of No. 4 Oil-Water Emulsion)

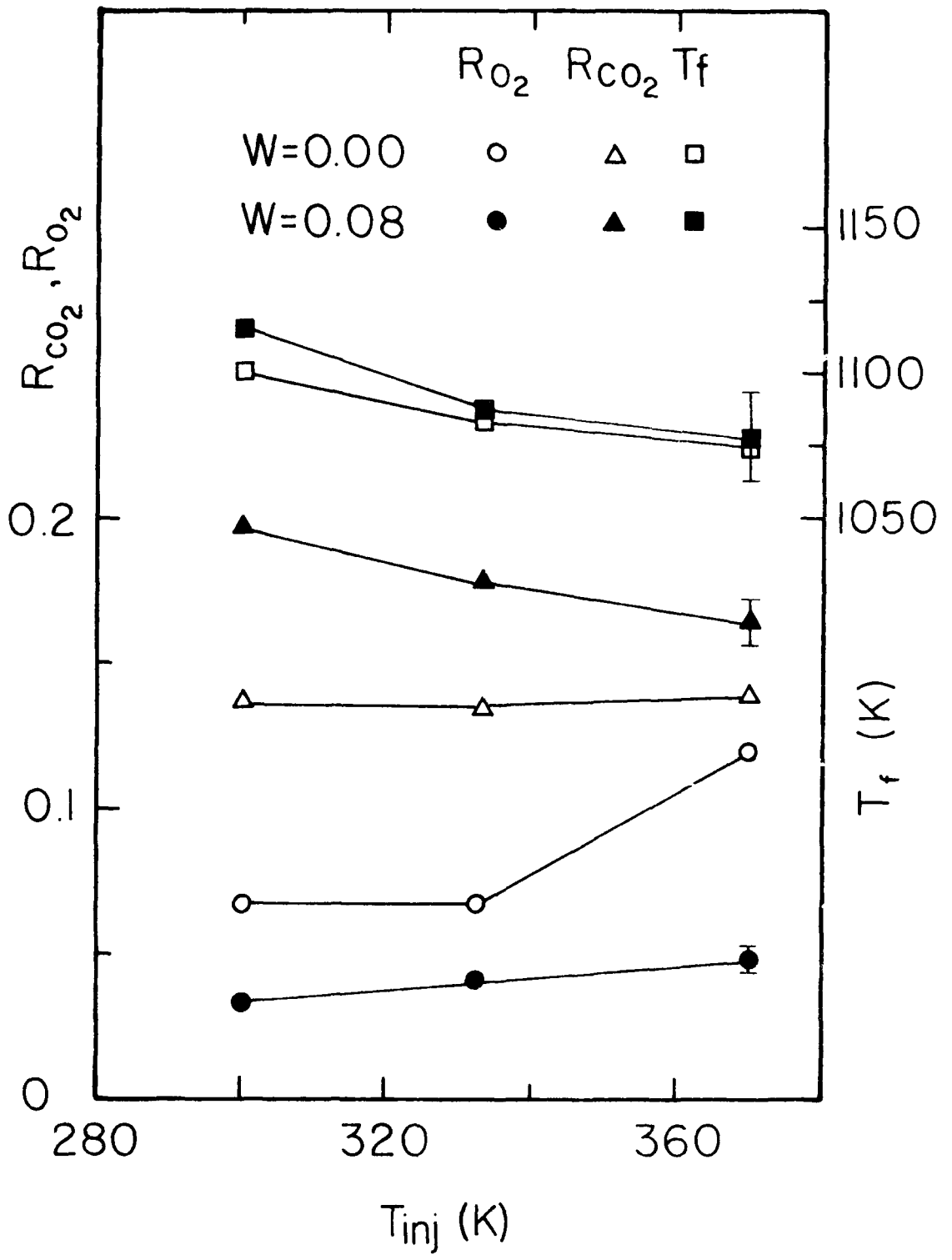

Fig. 19. Effects of Injection Temperature on CO_2 and O_2 in the Exhaust and Flame Temperature (Burning Sprays of No. 4 Oil and its Emulsion with Water)

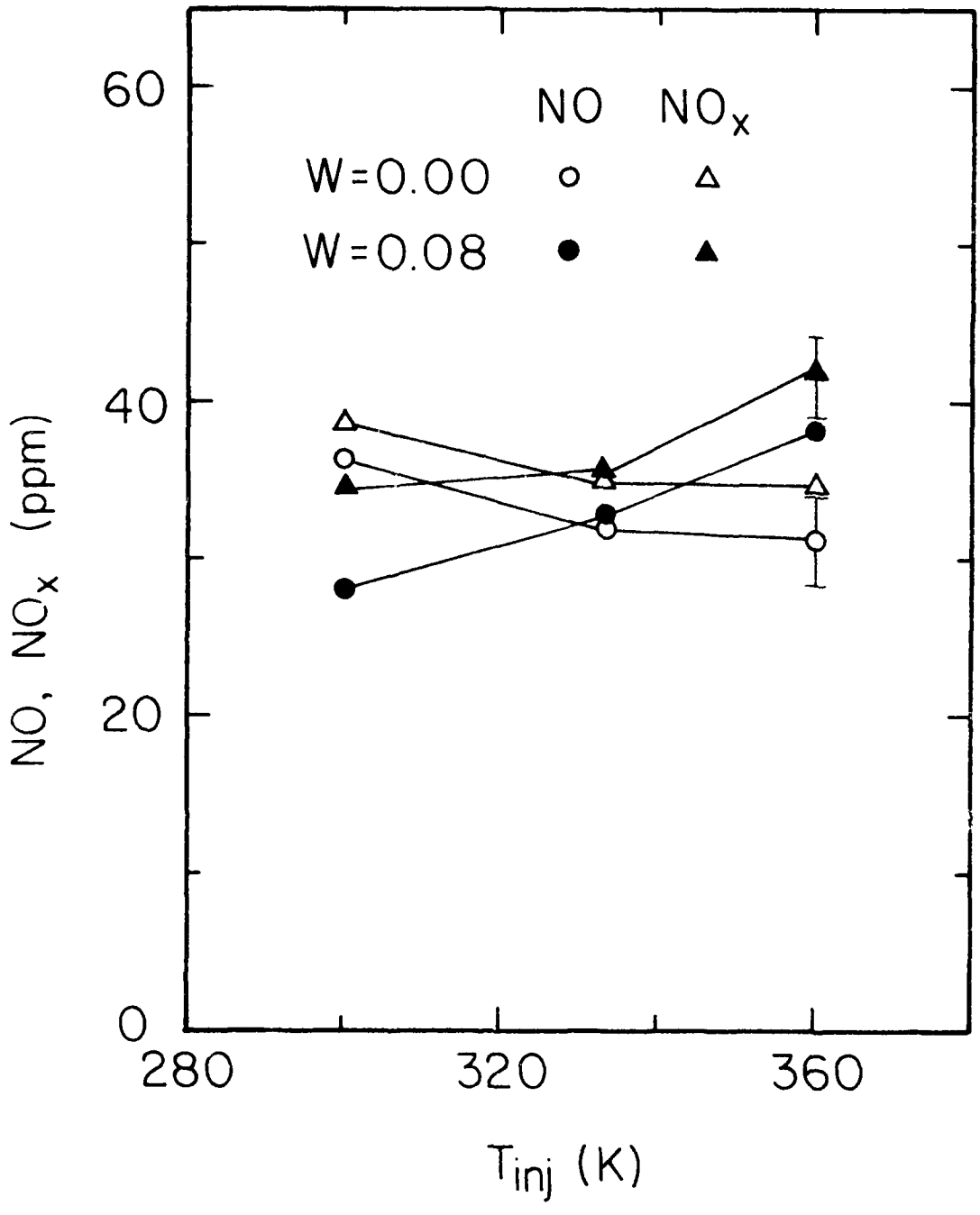

Fig. 20. Effects of Injection Temperature on the Emission of Nitrogen Oxides (Burning Sprays of No. 4 oil and its Emulsion with Water)

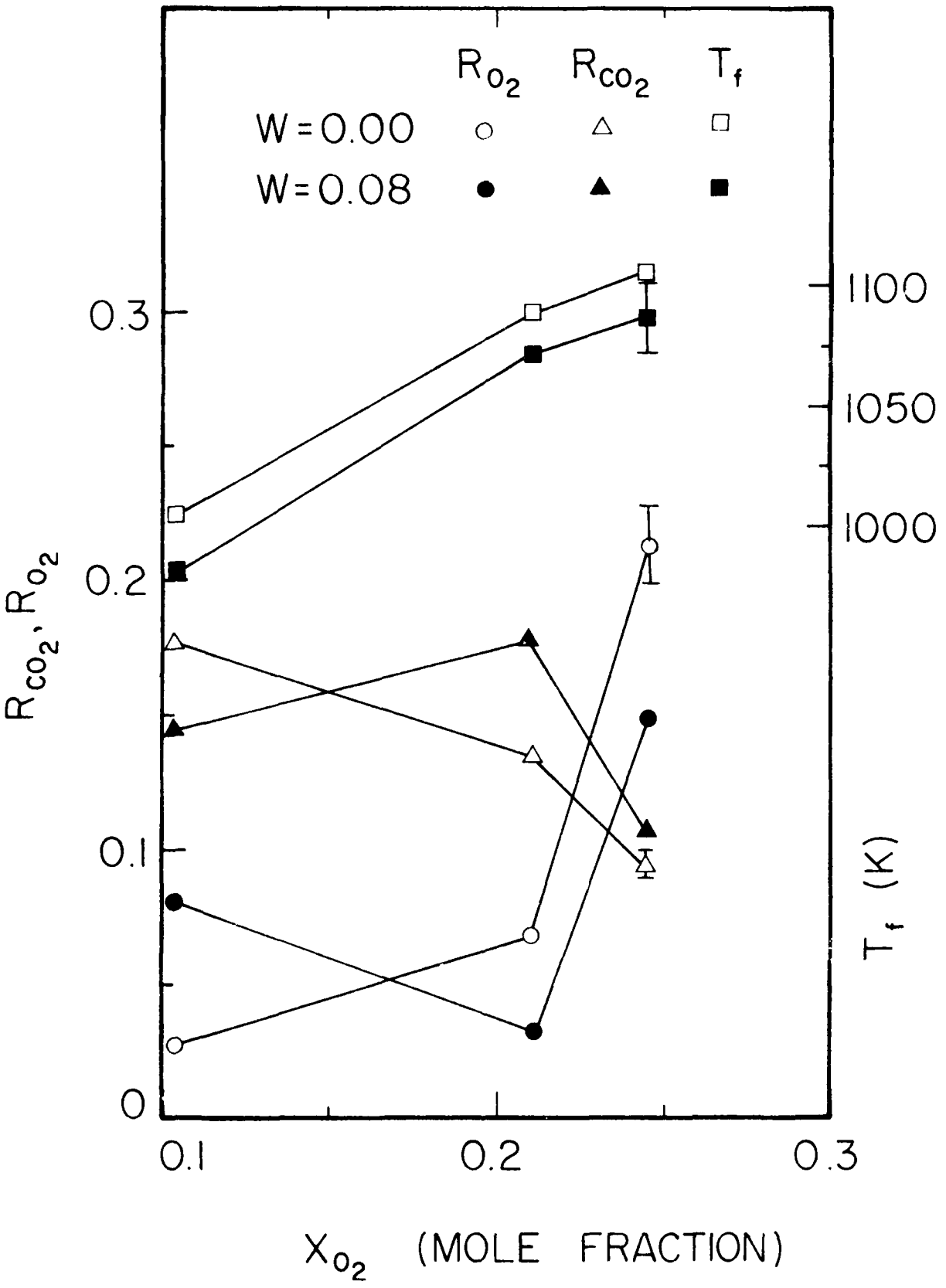

Fig. 21. Effects of Chamber Oxygen Content on CO_2 and O_2 in the Exhaust and the Flame Temperature (Burning Sprays of No. 4 Oil and its Emulsion with Water)

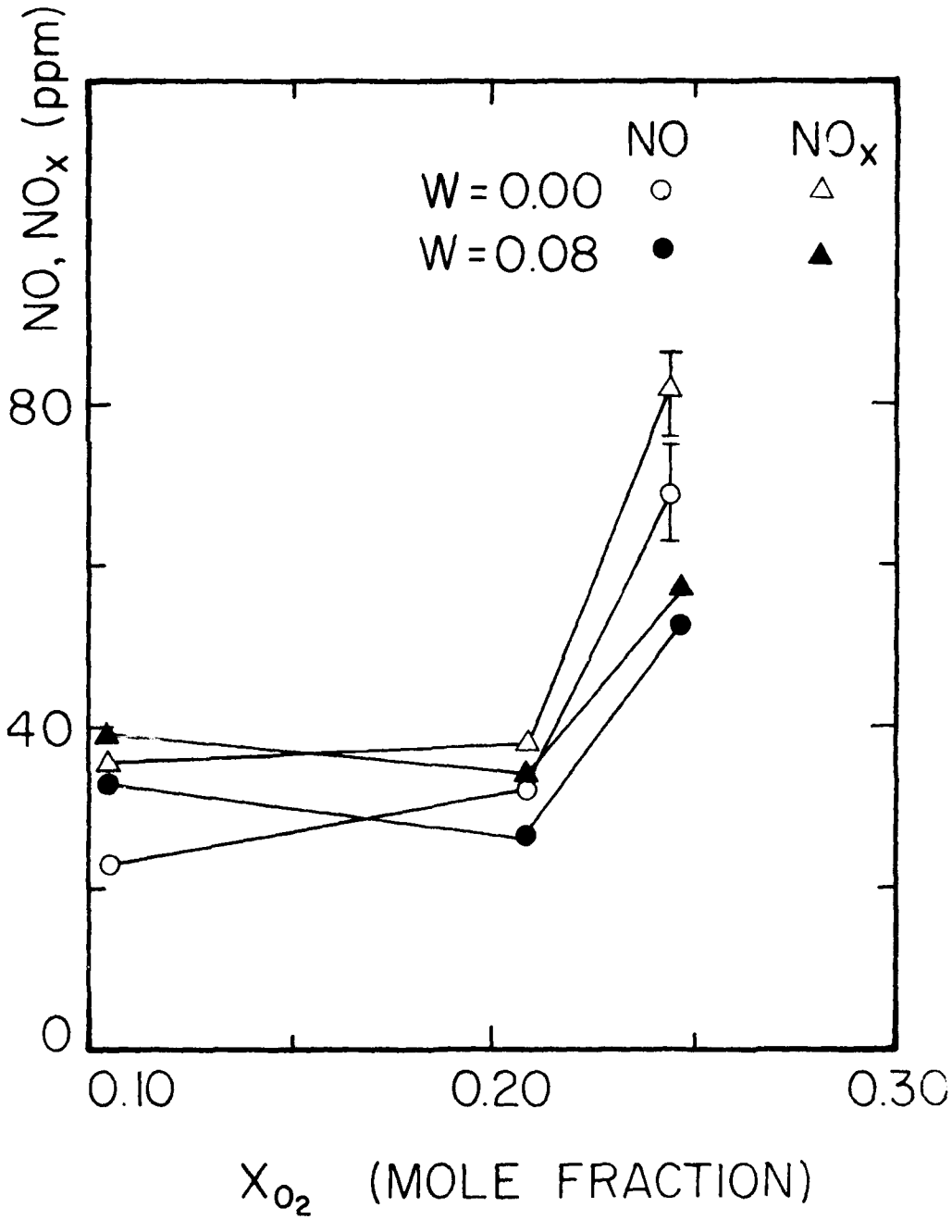

Fig. 22. Effects of Chamber Oxygen Content on the Emission of Oxides of Nitrogen (Burning Sprays of No. 4 Oil and its Emulsion with Water)

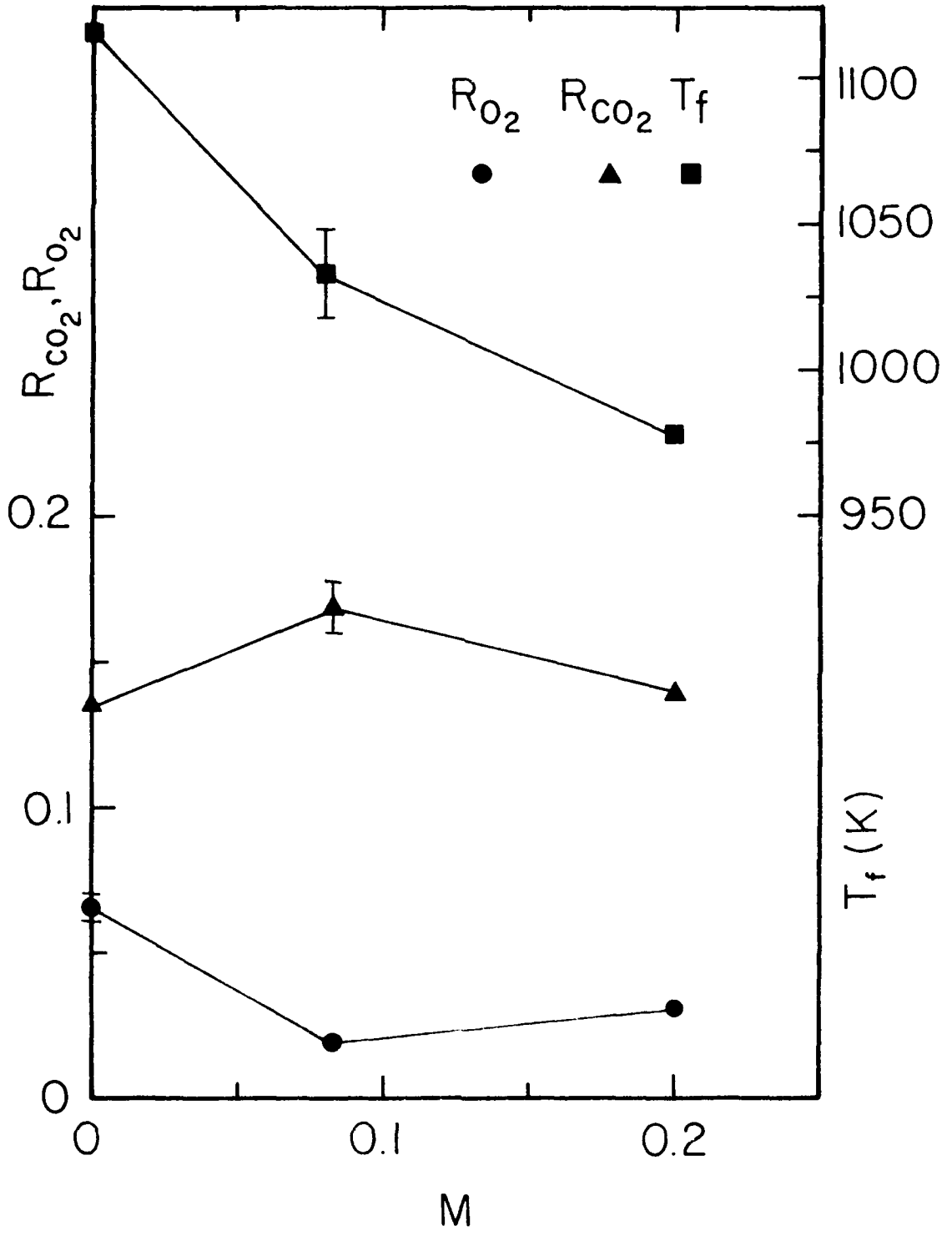

Fig. 25. Effects of Methanol Content on CO_2 and O_2 in the Exhaust and the Flame Temperature (Burning Sprays of No. 4 Oil-Methanol Emulsion)

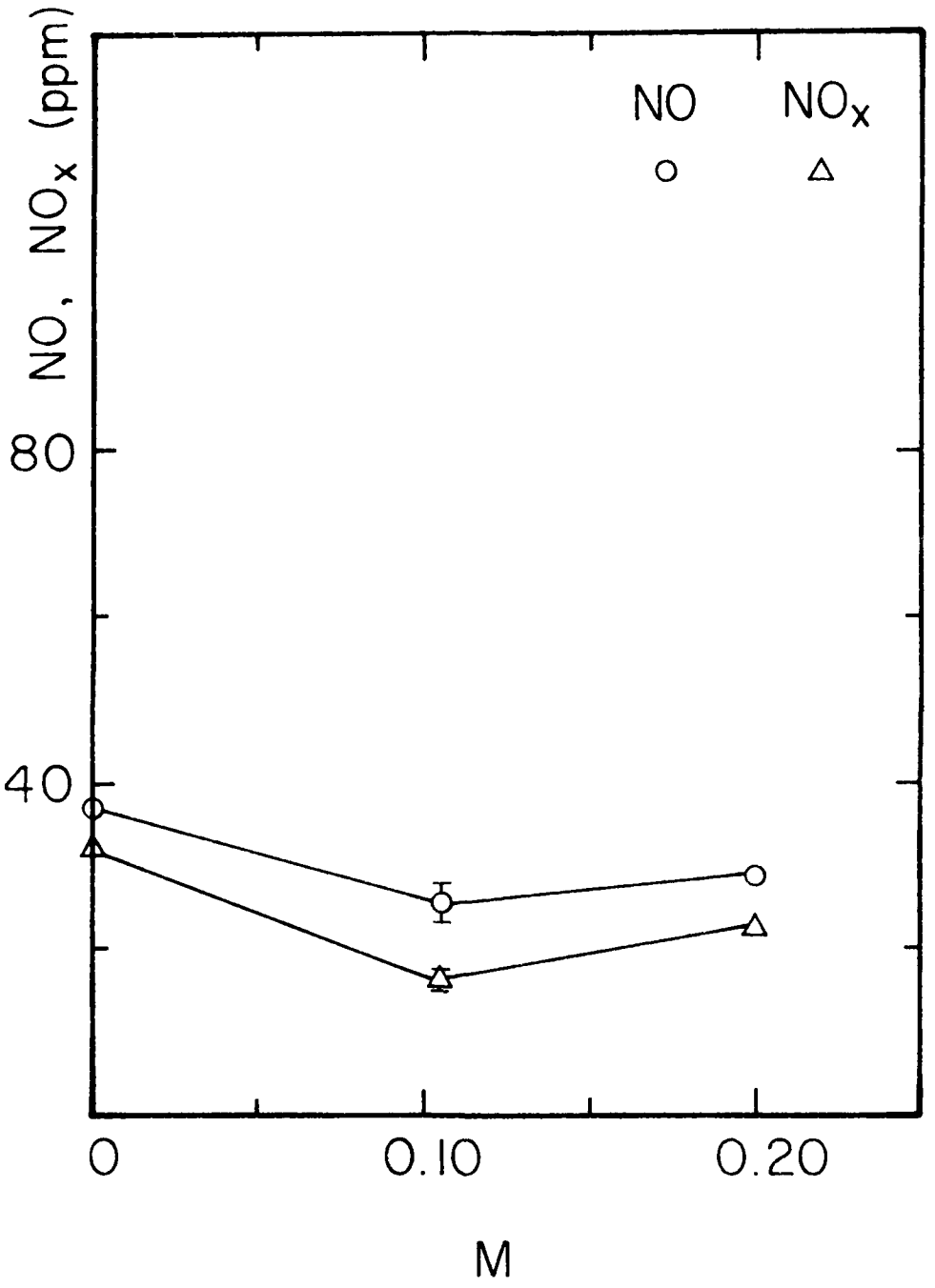

Fig. 24. Effects of Methanol Content on the Emission of the Oxides of Nitrogen (Burning Sprays of No. 4 Oil-Methanol Emulsion)

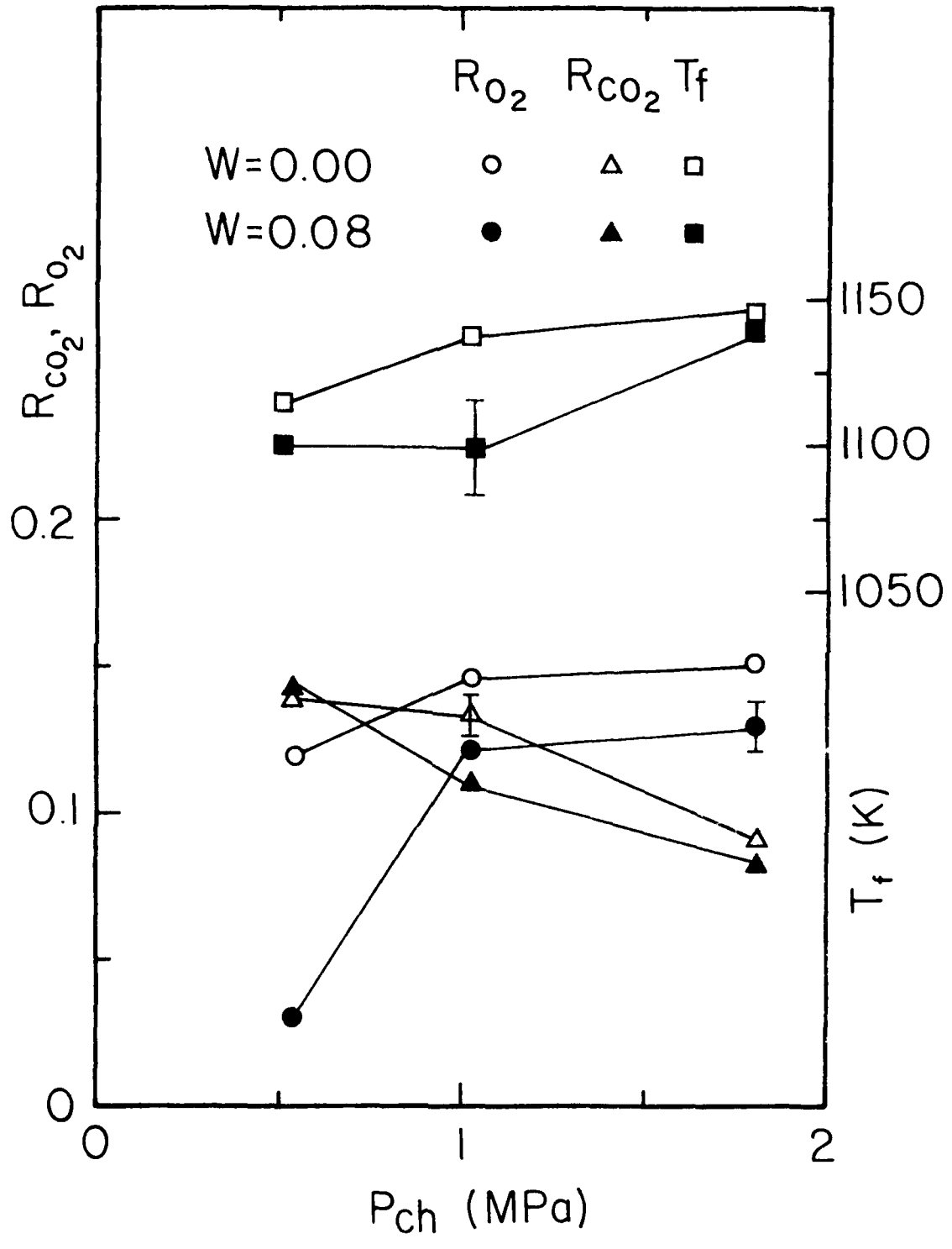

Fig. 25. Effects of Chamber Pressure on CO_2 and O_2 in the Exhaust and Flame Temperature (Burning Sprays of No. 4 Oil and its Emulsion with Water)

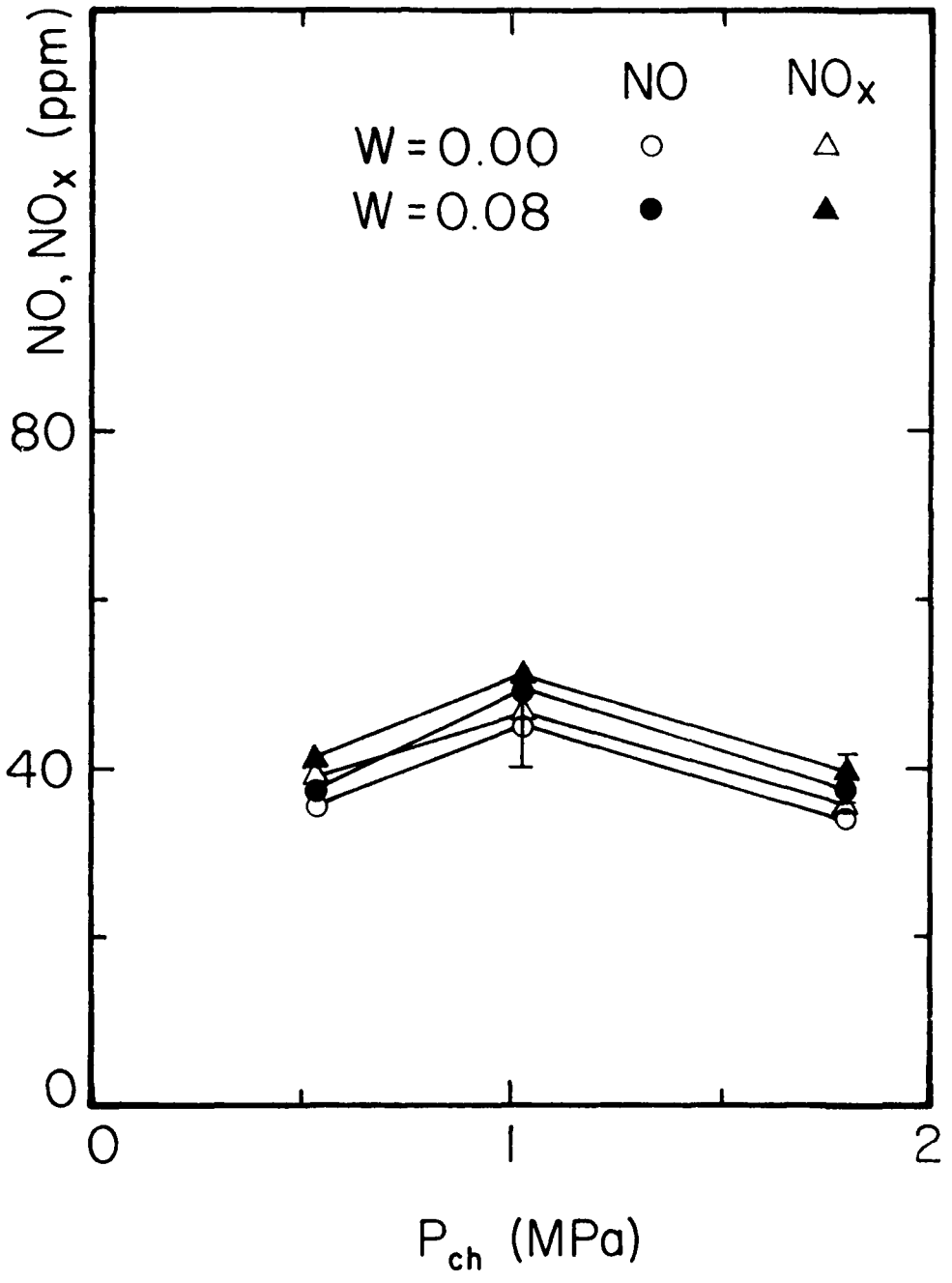

Fig. 26. Effects of Chamber Pressure on the Emission of Oxides of Nitrogen (Burning Sprays of No. 4 Oil and its Emulsion with Water)

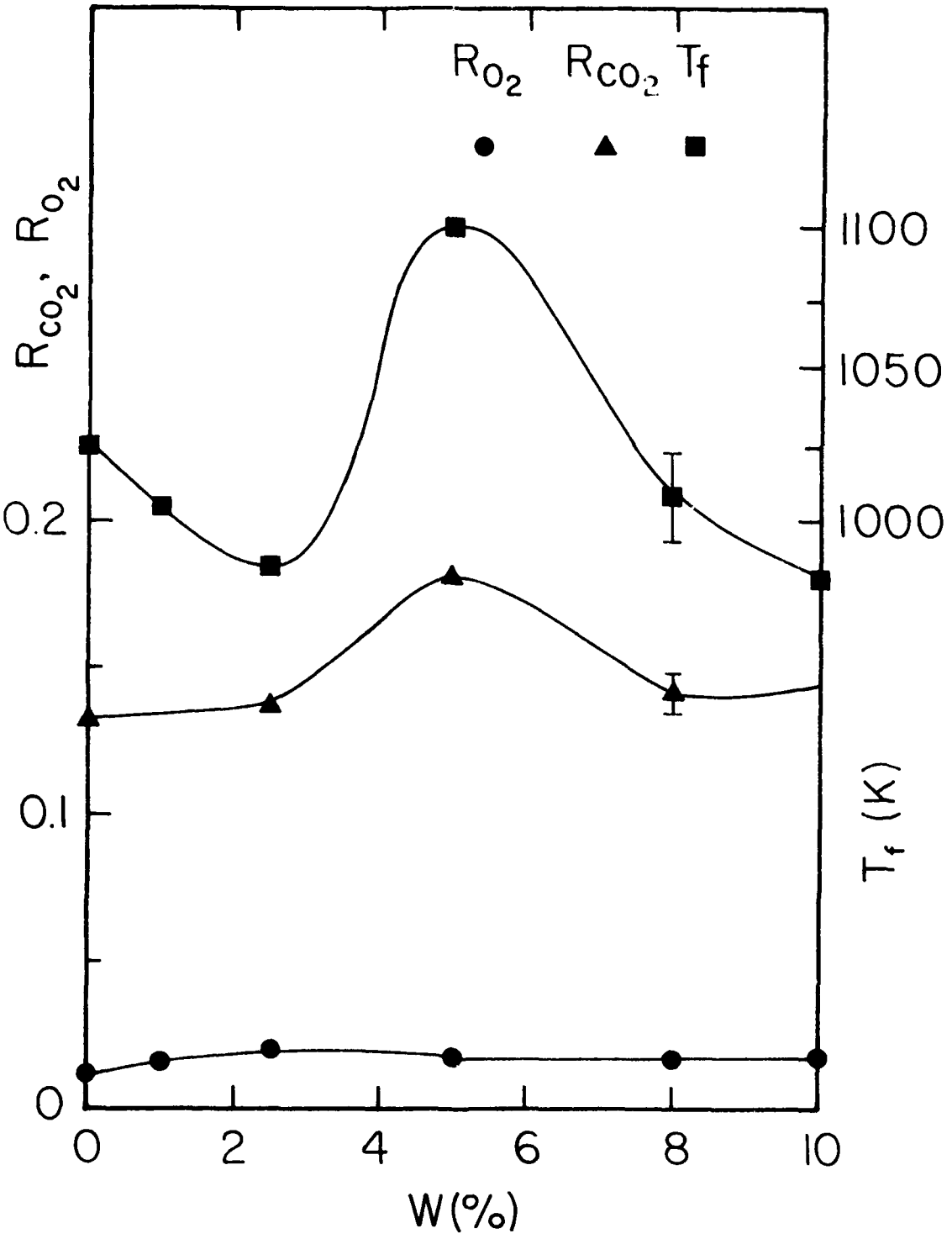

Fig. 27. Effects of Water Content on CO_2 and O_2 in the Exhaust and Flame Temperature (Burning Sprays of No. 6 Oil-Water Emulsion)

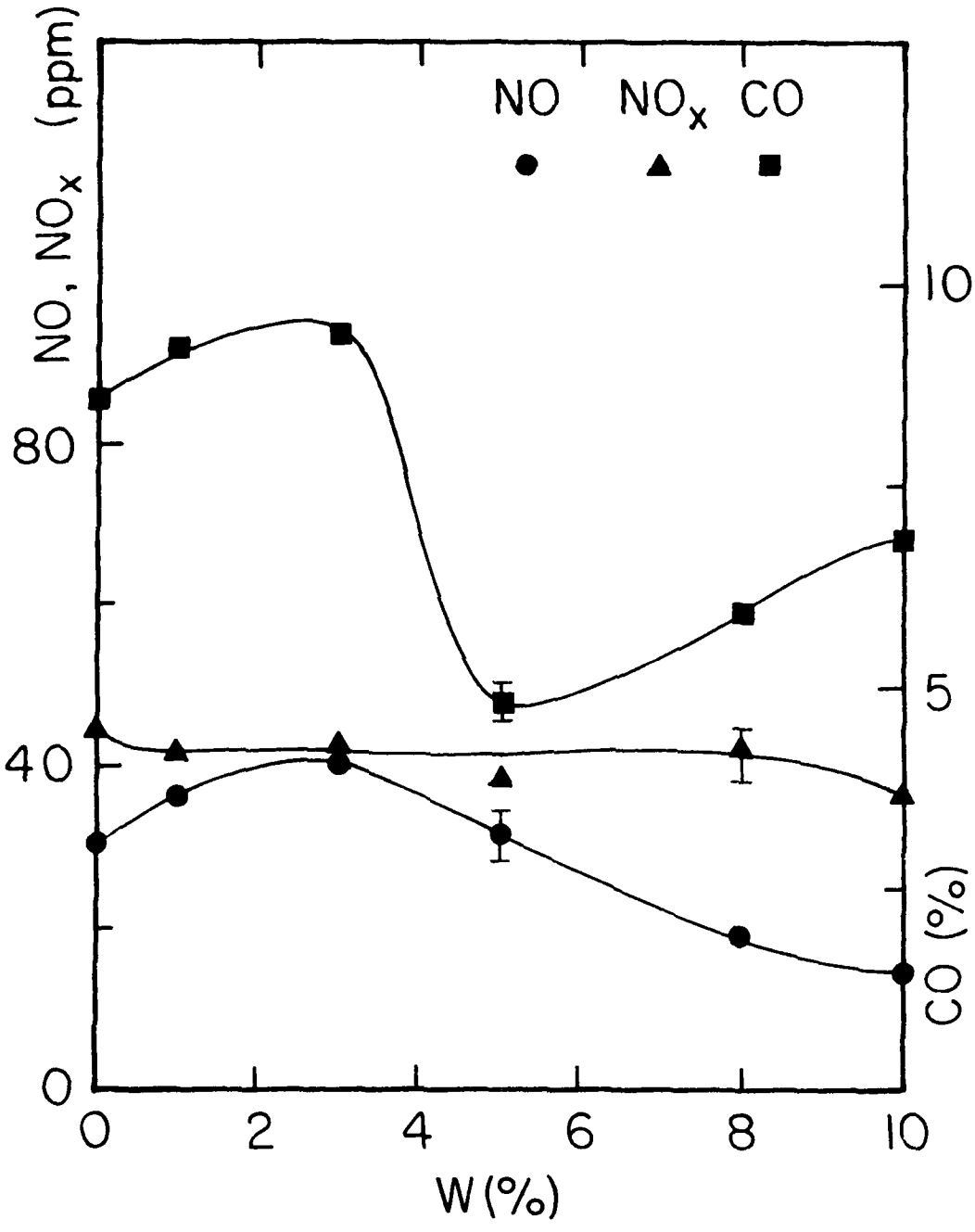

Fig. 28. Effects of Water Content on the Emission of the Oxides of Nitrogen and Carbon Monoxide (Burning Sprays of No. 6 Oil-Water Emulsion)

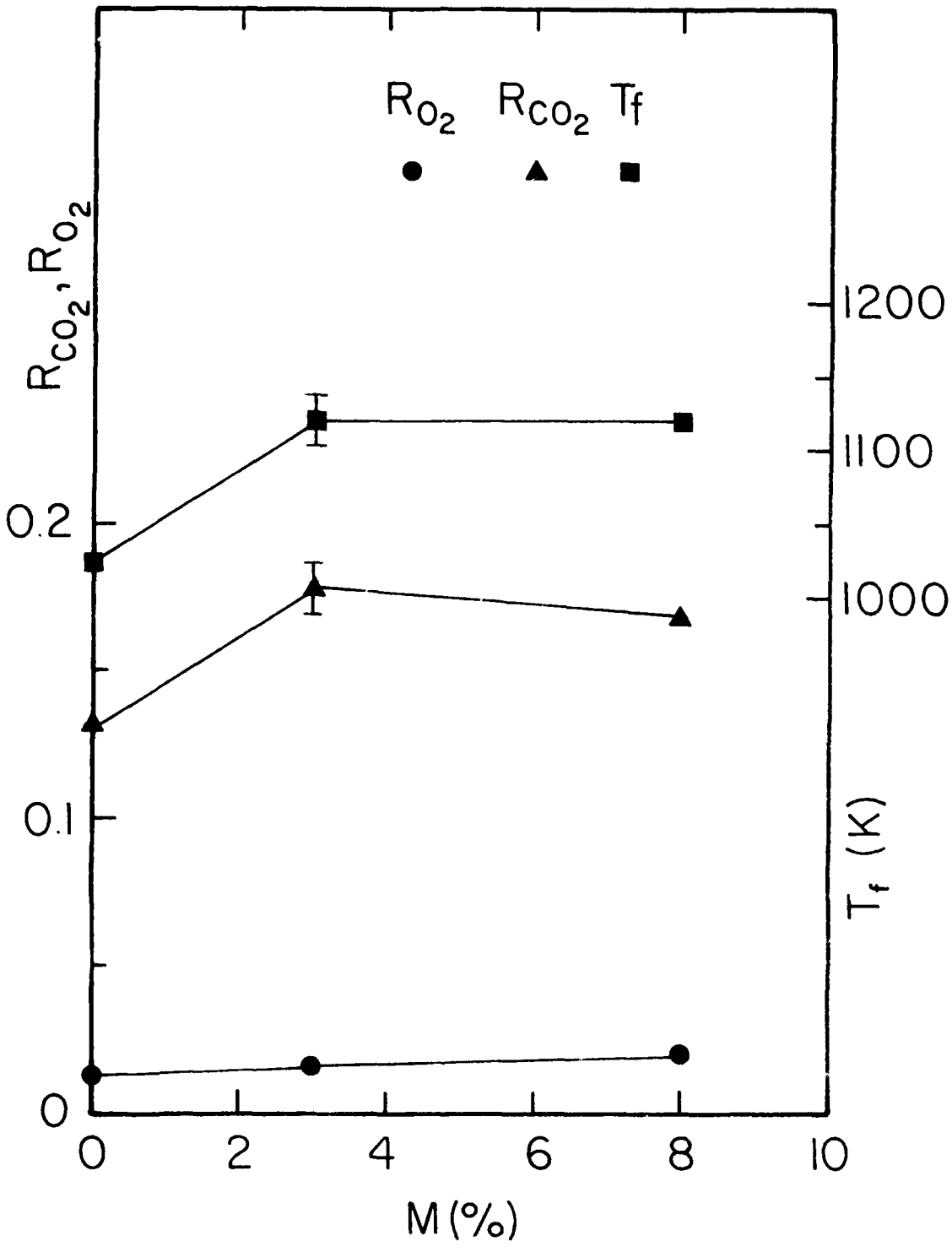

Fig. 29. Effects of Methanol Content on CO_2 and O_2 in the Exhaust and Flame Temperature (Burning Sprays of No. 6 Oil-Methanol Emulsion)

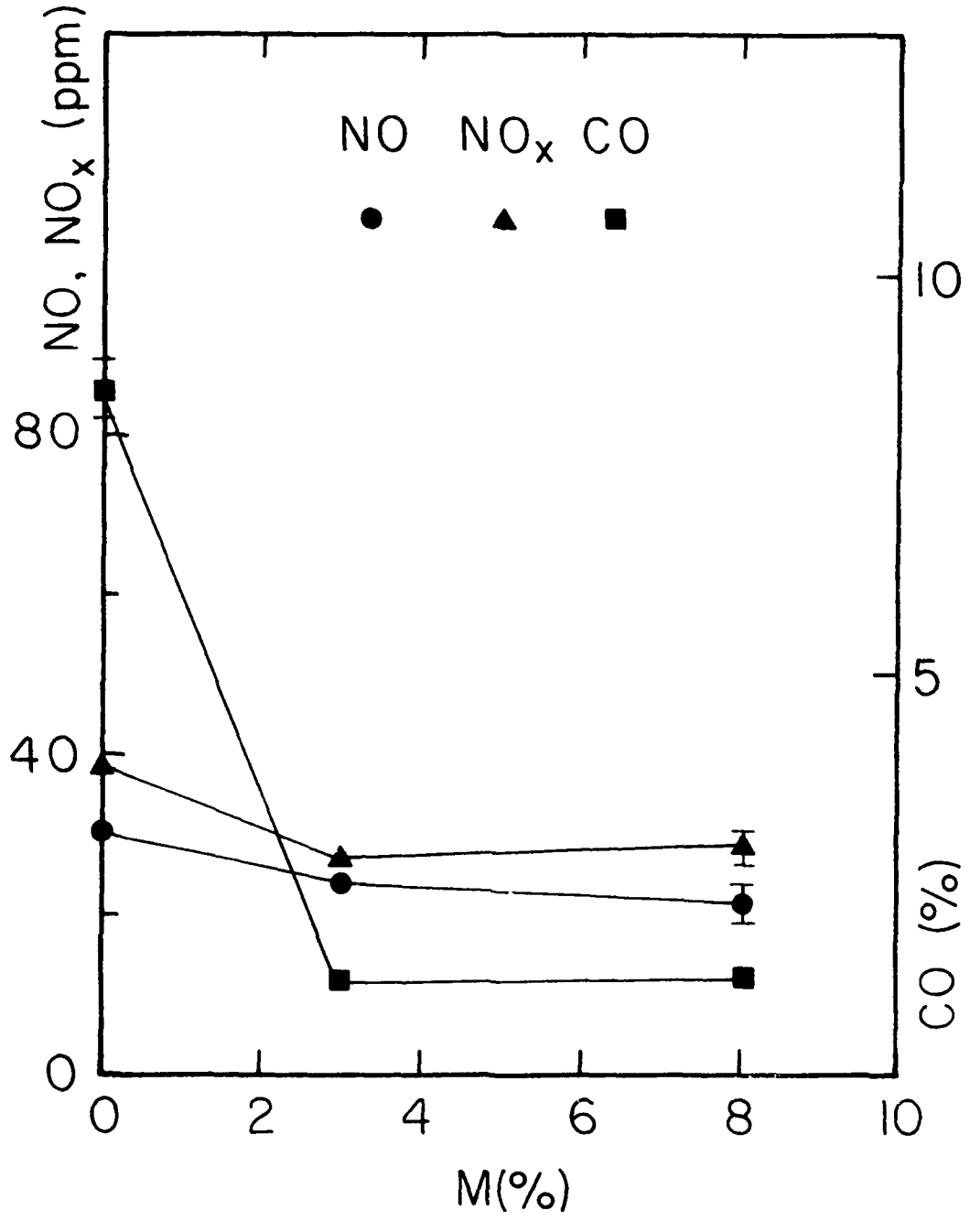

Fig. 30. Effects of Methanol Content on the Emission of the Oxides of Nitrogen and Carbon Monoxide (Burning Sprays of No. 6 Oil-Methanol Emulsion)

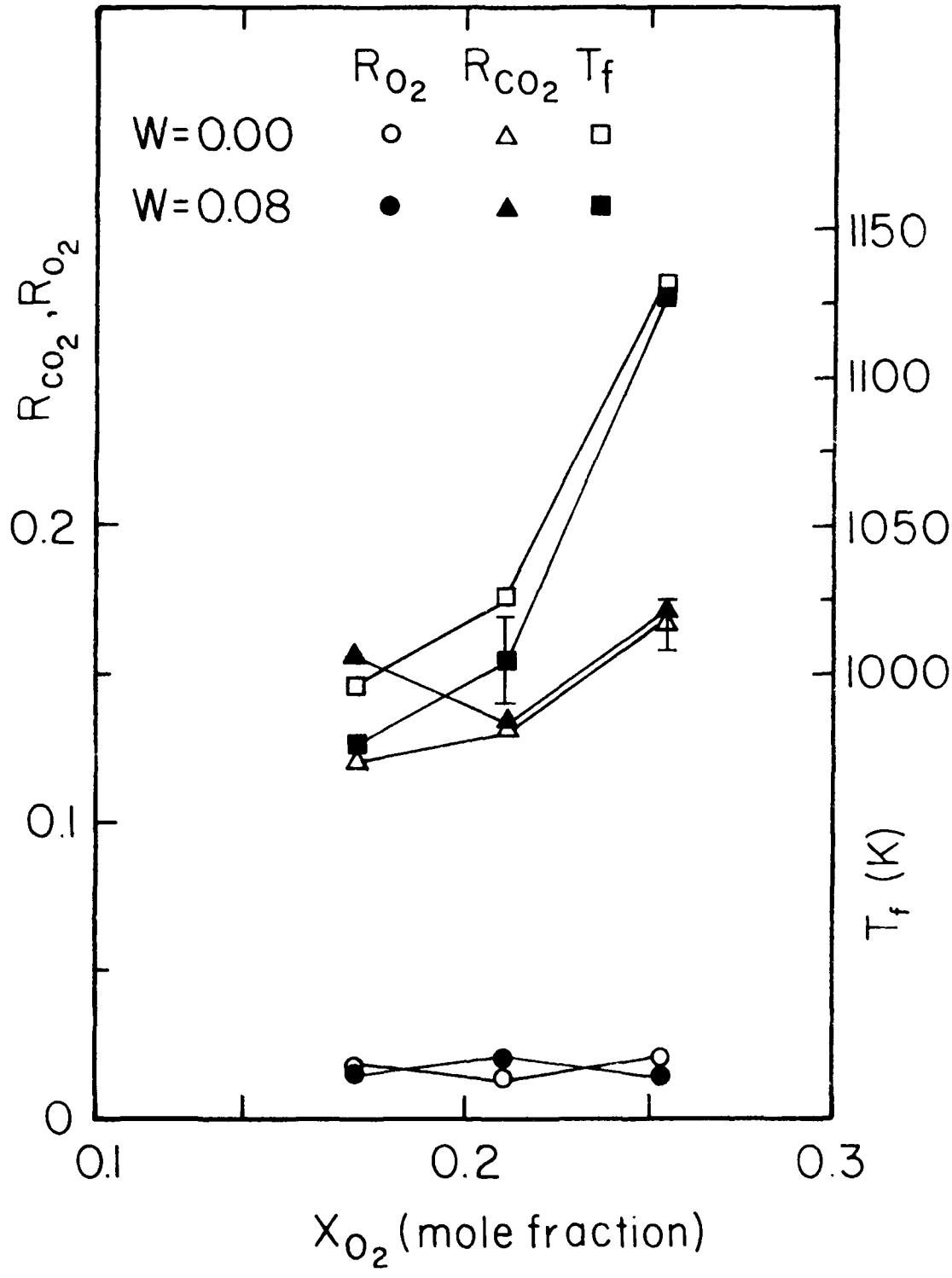

Fig. 31. Effects of Chamber Oxygen Content on CO_2 and O_2 in the Exhaust and Flame Temperature (Burning Sprays of No. 6 Oil and its Emulsion with Water)

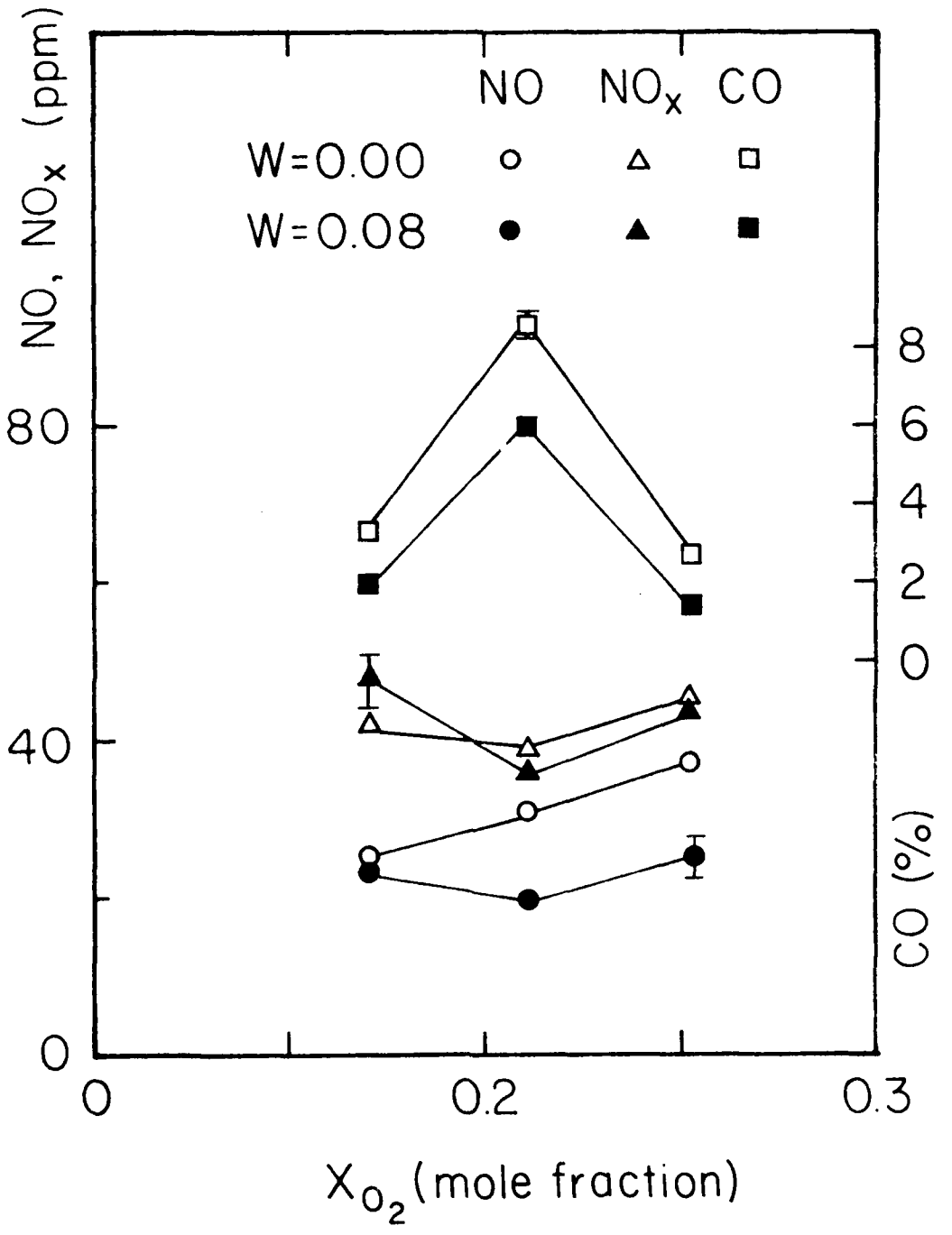

Fig. 32. Effects of Chamber Oxygen Content on the Emission of the Oxides of Nitrogen and Carbon Monoxide (Burning Sprays of No. 6 Oil and its Emulsion with Water)

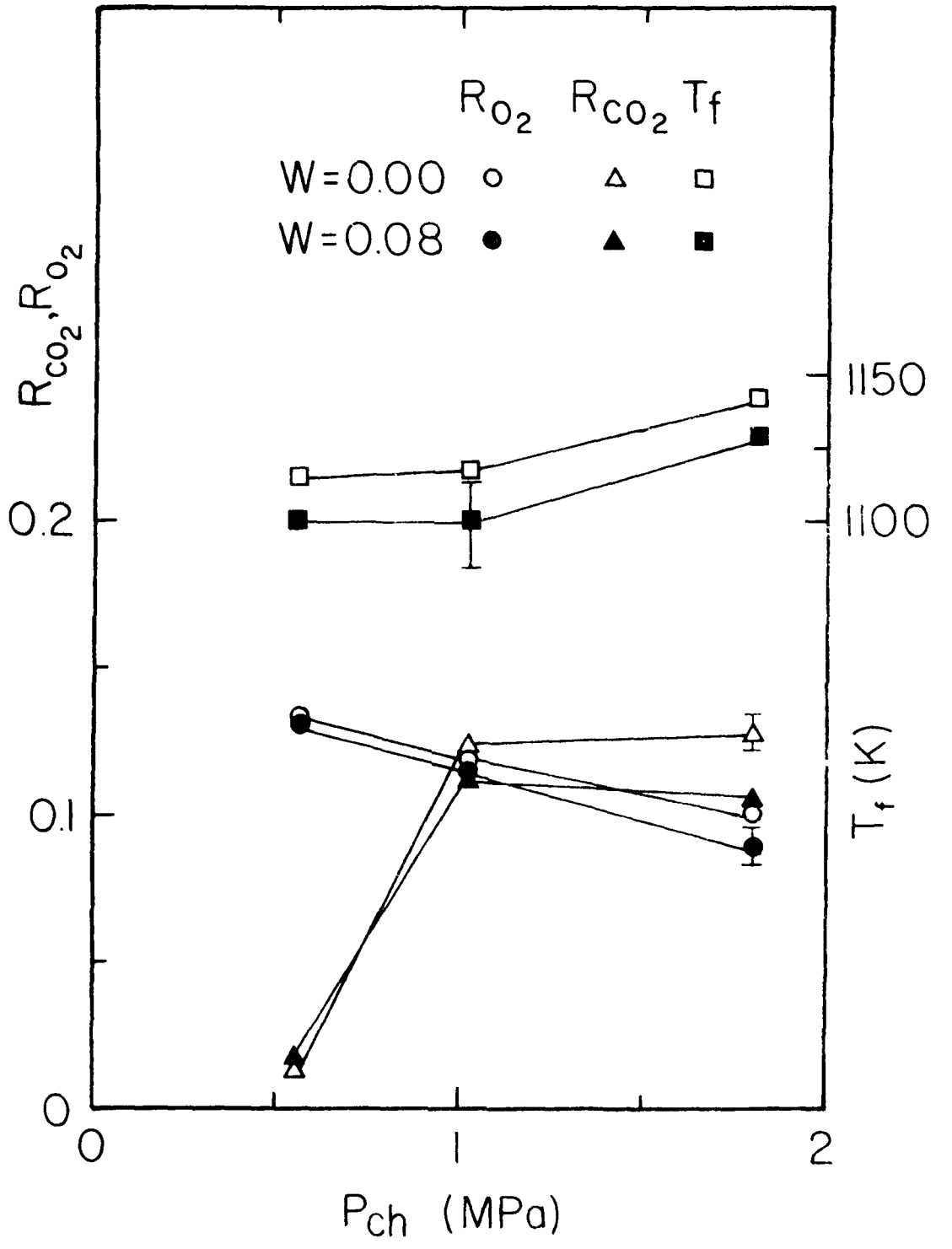

Fig. 33. Effects of Chamber Pressure on R_{O_2} and R_{CO_2} in the Exhaust and Flame Temperature (Burning Sprays of No. 6 Oil and its Emulsion with Water)

AD-A095 612 OKLAHOMA UNIV NORMAN SCHOOL OF AEROSPACE MECHANICAL --ETC F/G 21/2
COMBUSTION OF DROPS AND SPRAYS OF HEAVY FUEL OILS AND THEIR EMU--ETC(U)
DEC 80 S R GOLLAHALLI, M L RASMUSSEN DOT-CG-93621-A
UNCLASSIFIED OU-AMNE-80-19 USCG-D-64-80 NL

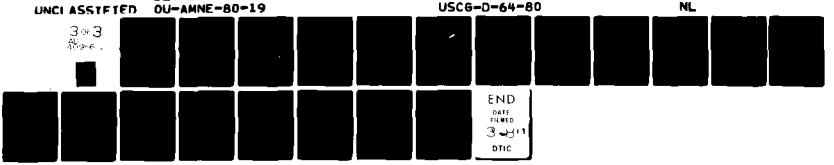

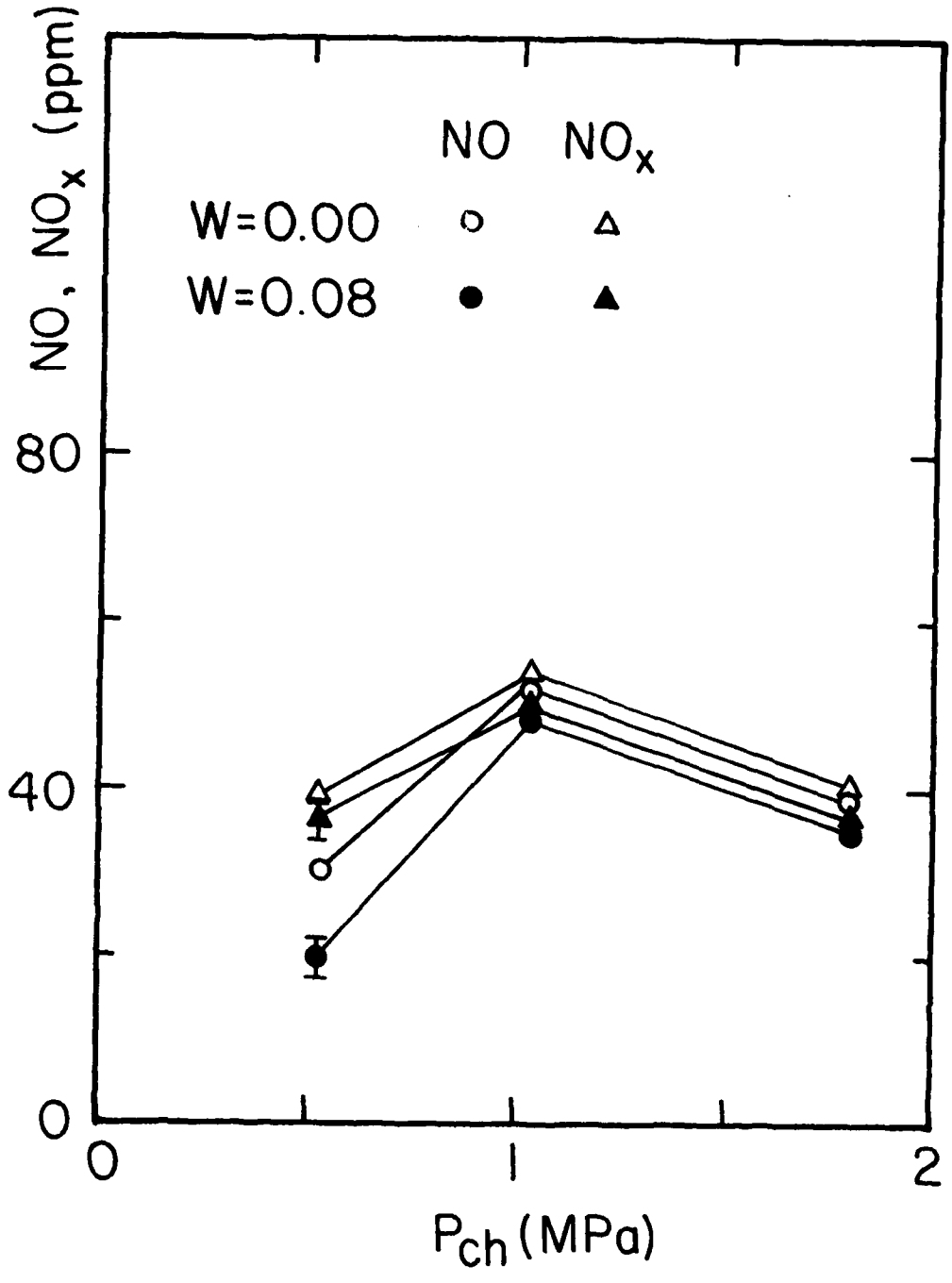

Fig. 34. Effects of Chamber Pressure on the Emission of the Oxides of Nitrogen and Carbon Monoxide (Burning Sprays of No. 6 Oil and its Emulsion with Water)

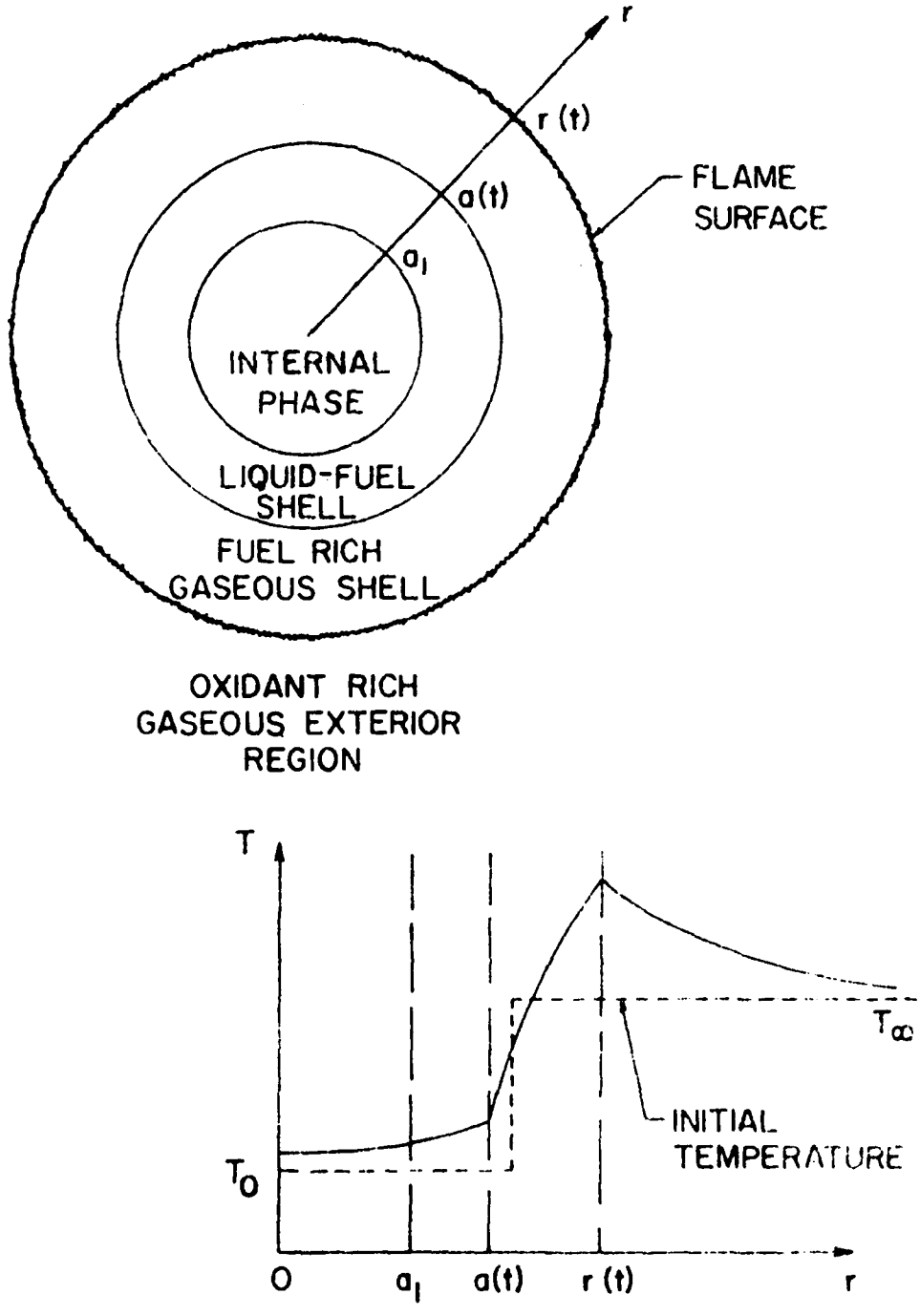

Fig. 35. Schematic Diagram and Temperature Distribution for the Spherical Drop

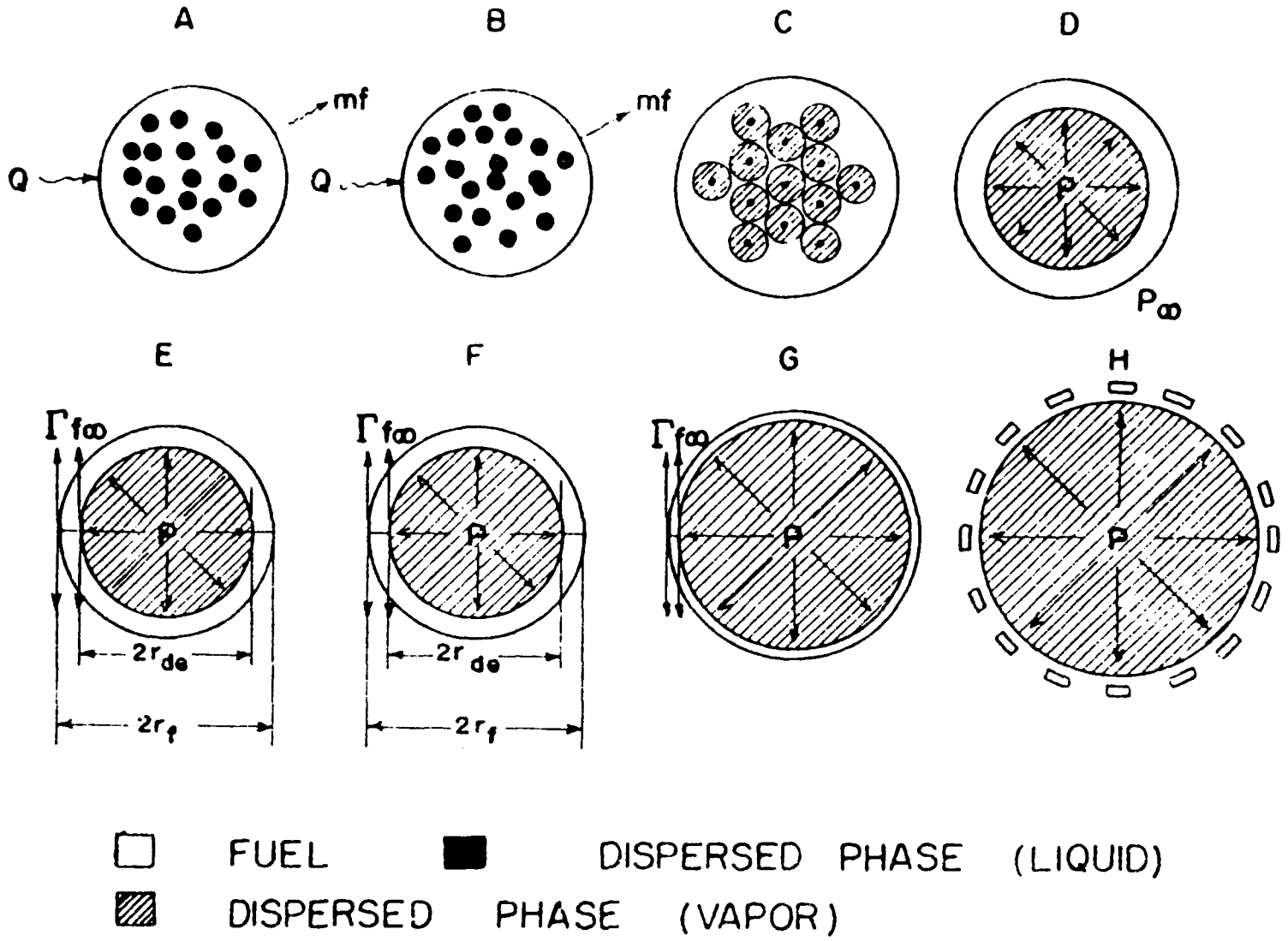

Fig. 36. Model of a Burning Emulsion Drop

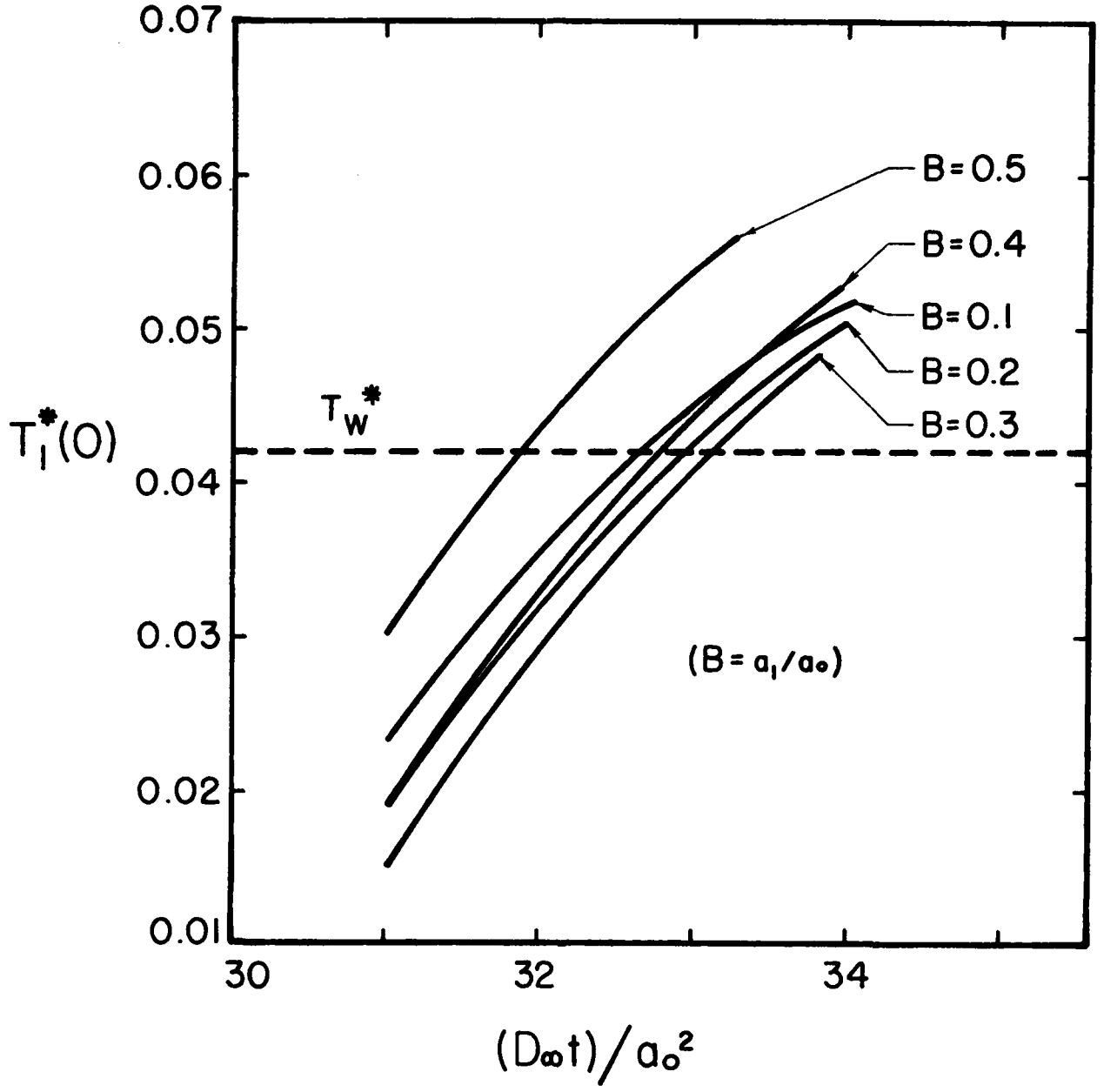

Fig. 37. Variation of the Center Temperature of the Composite Drop with Time for Various Amounts of Internal-Phase Liquid

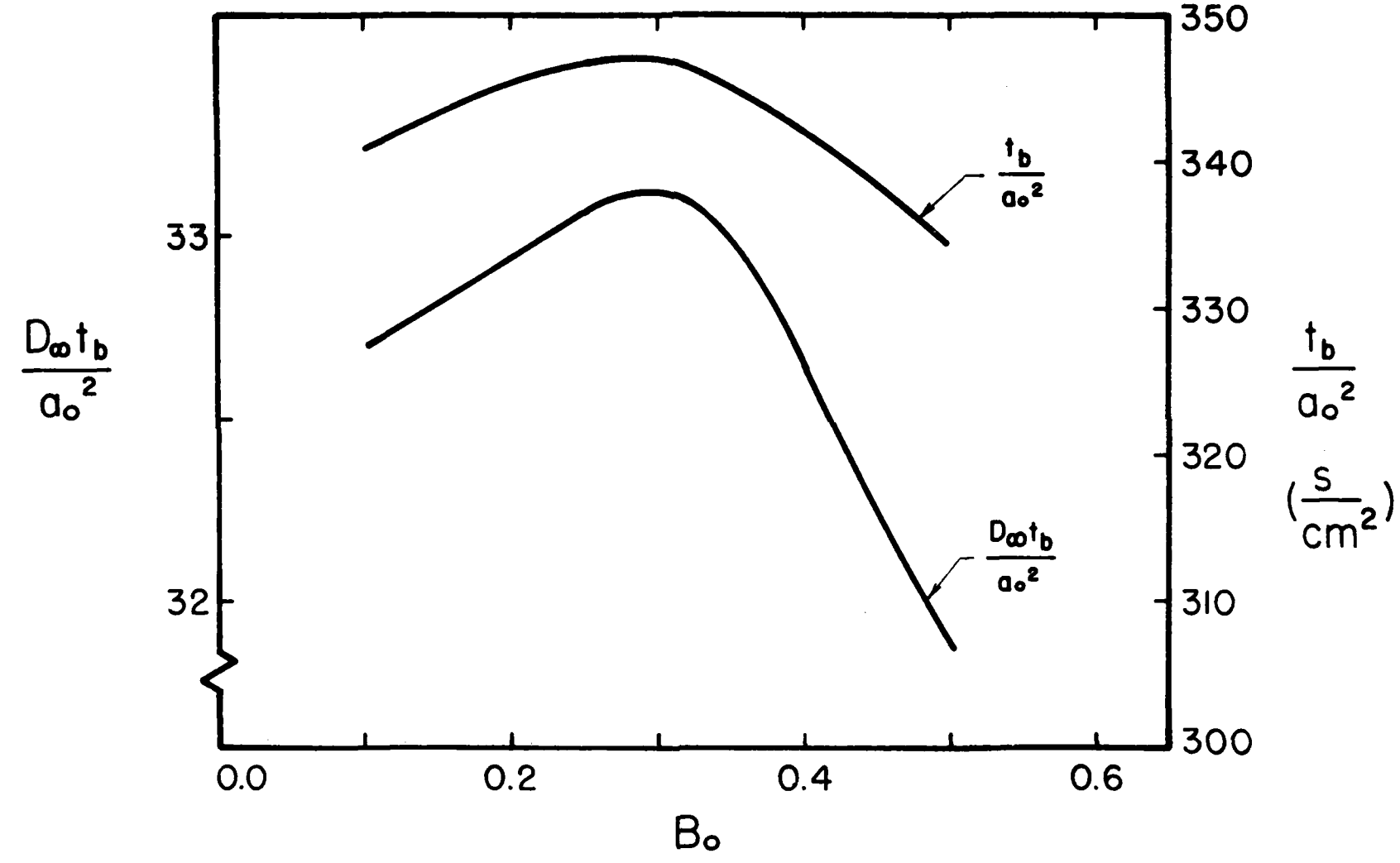

Fig. 38. Variation of Disruption of the Composite Drop Time with Initial Radius Ratio of the Composite Drop

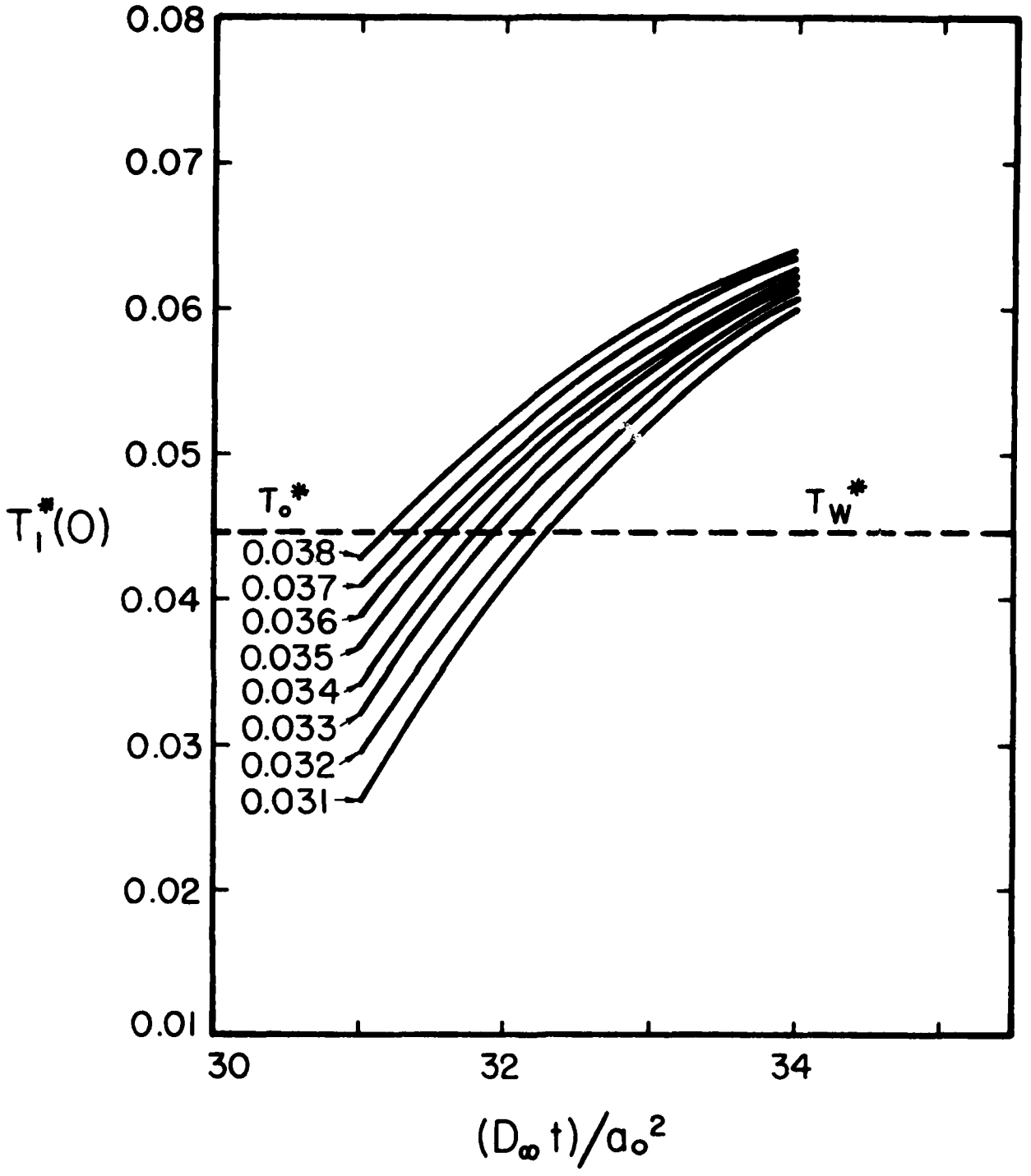

Fig. 39. Variation of the Center Temperature of the Composite Drop with Time for Various Injection Temperature

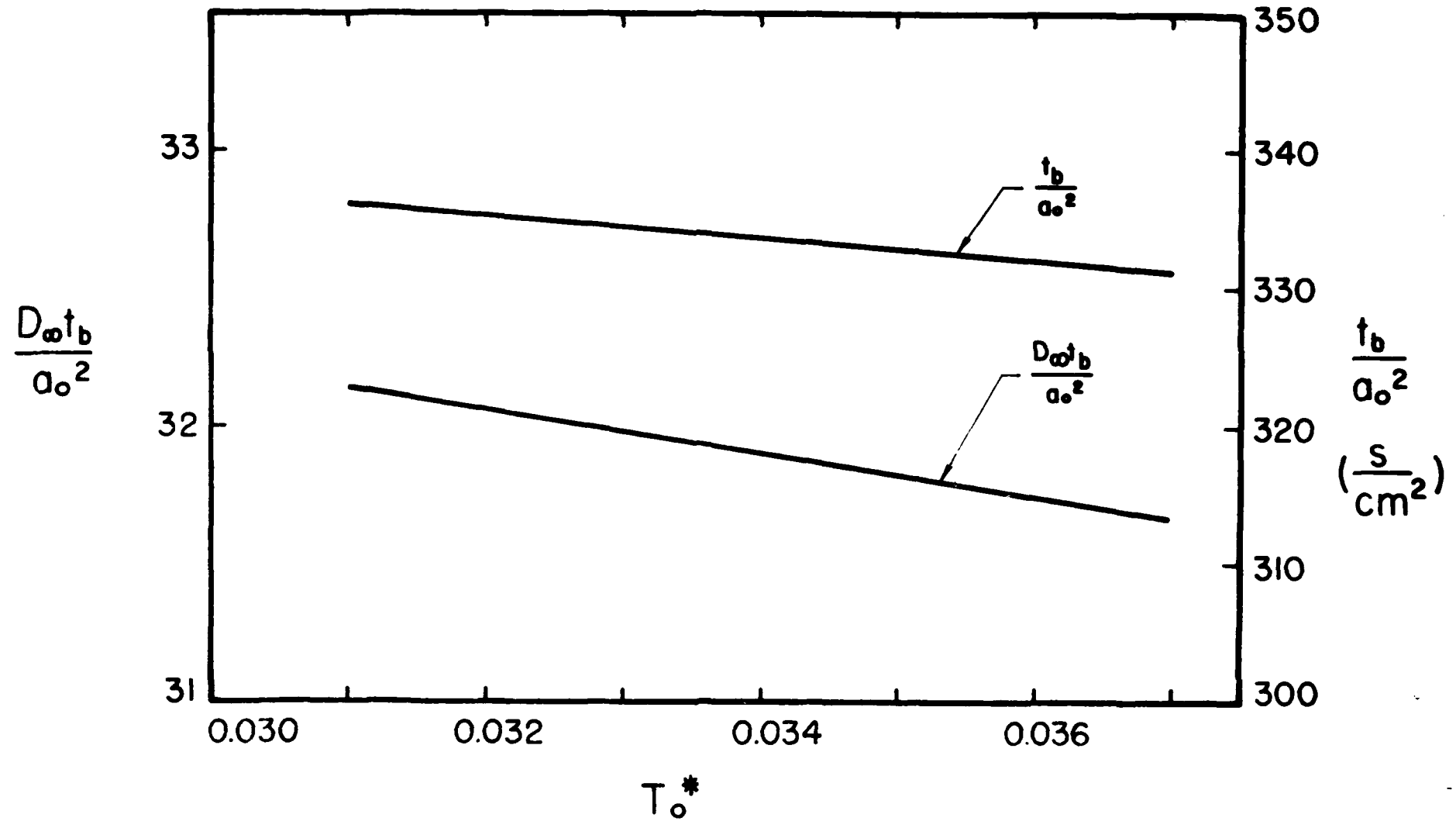

Fig. 40. Variation of Disruption Time of the Composite Drop with Injection Temperature

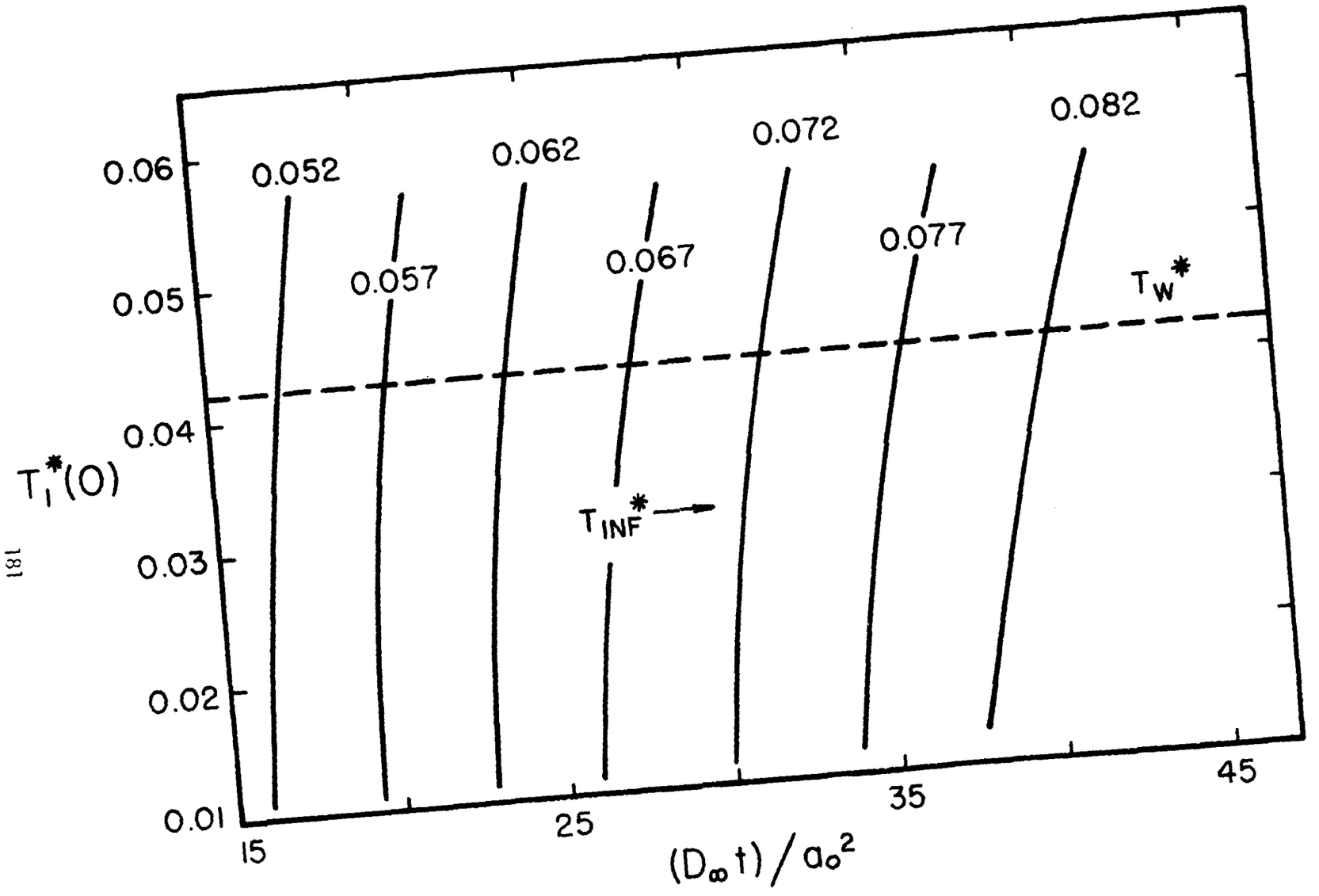

Fig. 41. Variation of the Center Temperature of the Composite Drop with Time for Various Ambient Temperatures

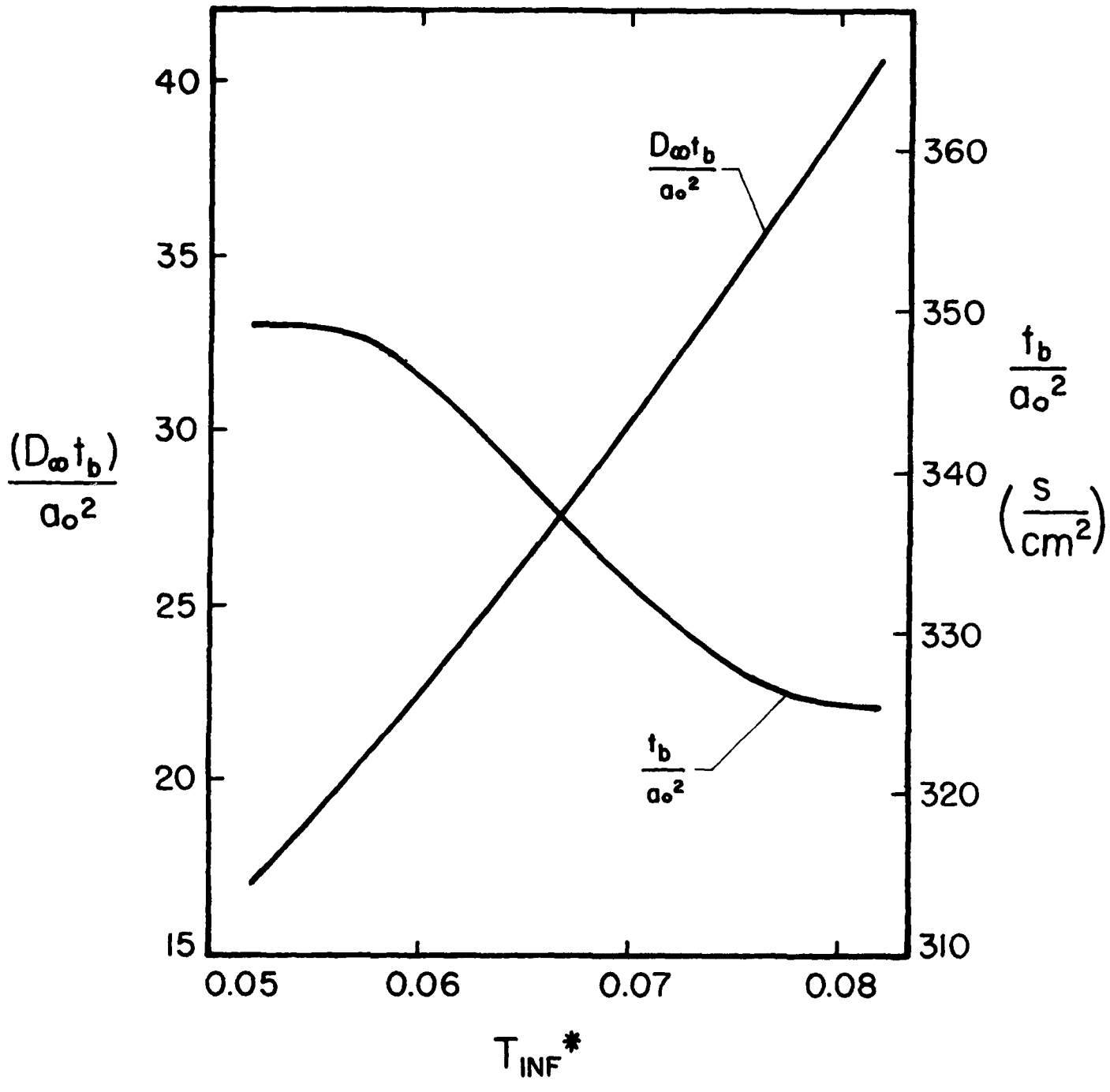

Fig. 42. Variation of the Disruption Time of the Composite Drop with Ambient Temperature

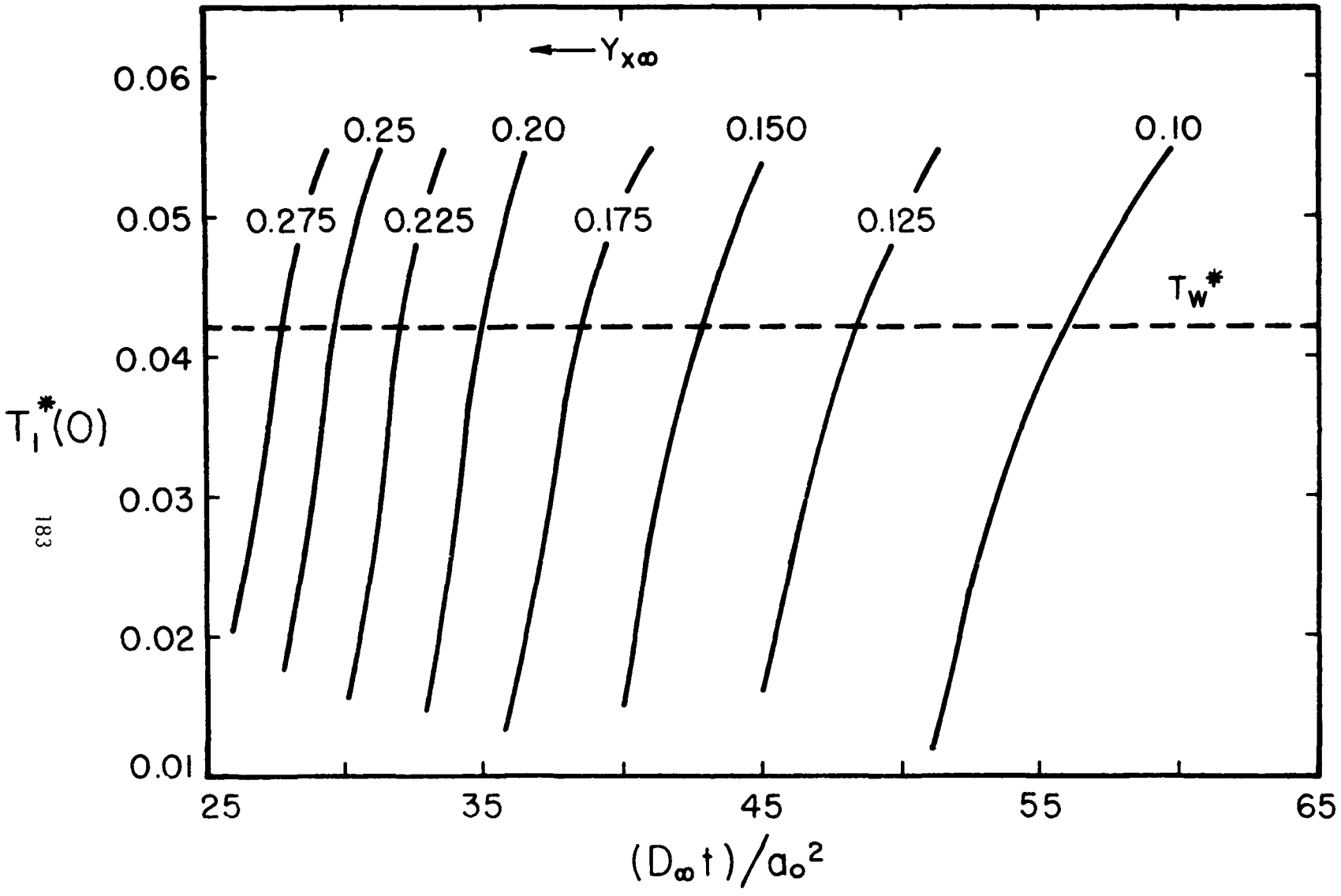

ig. 43. Variation of the Center Temperature of the Composite Drop with Time for Various Ambient Oxygen Concentrations

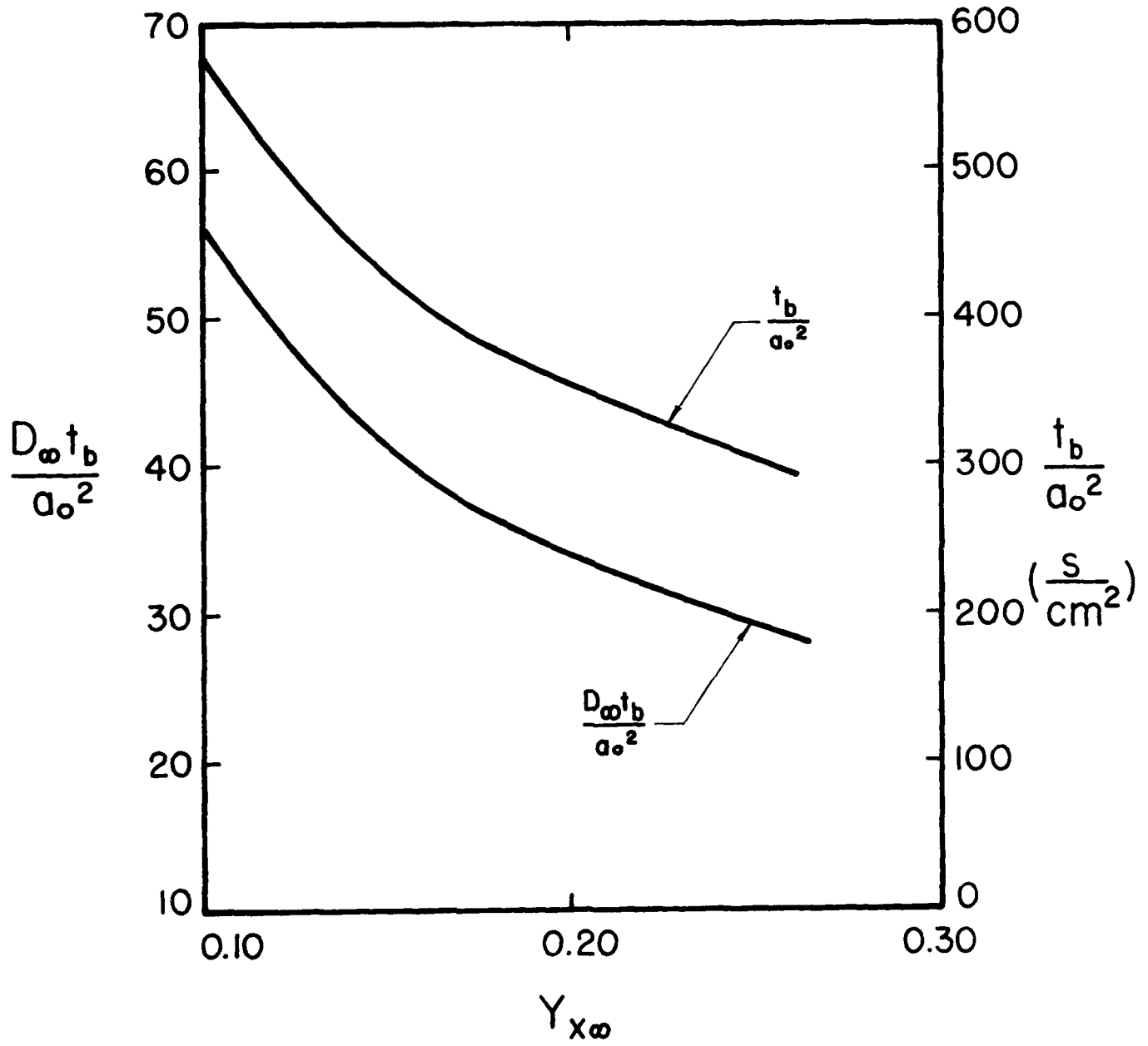

Fig. 44. Variation of the Disruption Time of the Composite Drop *with Ambient Oxygen Concentration*

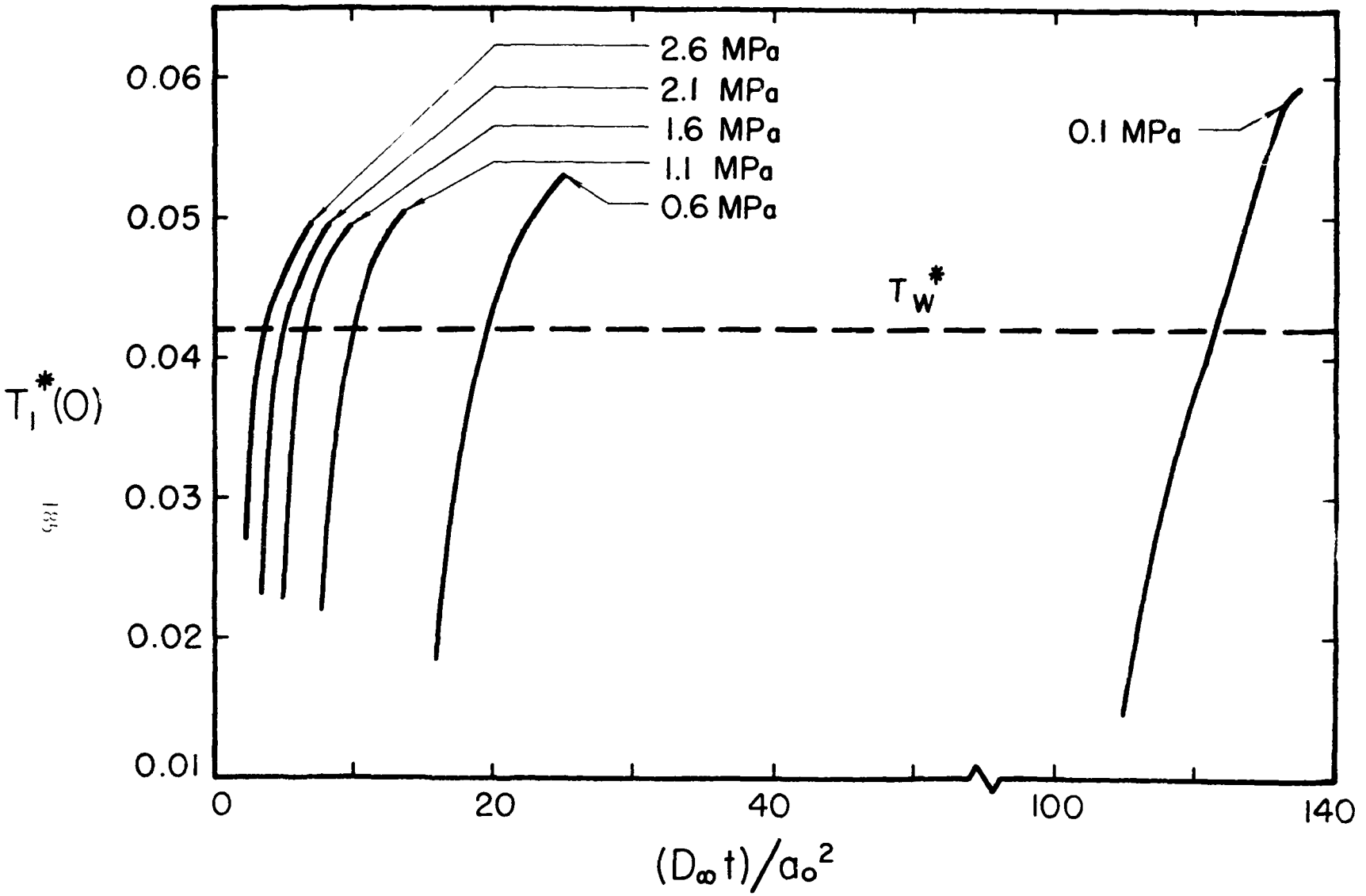

ig. 45. Variation of the Center Temperature of the Composite Drop with Time for Various Ambient Pressures

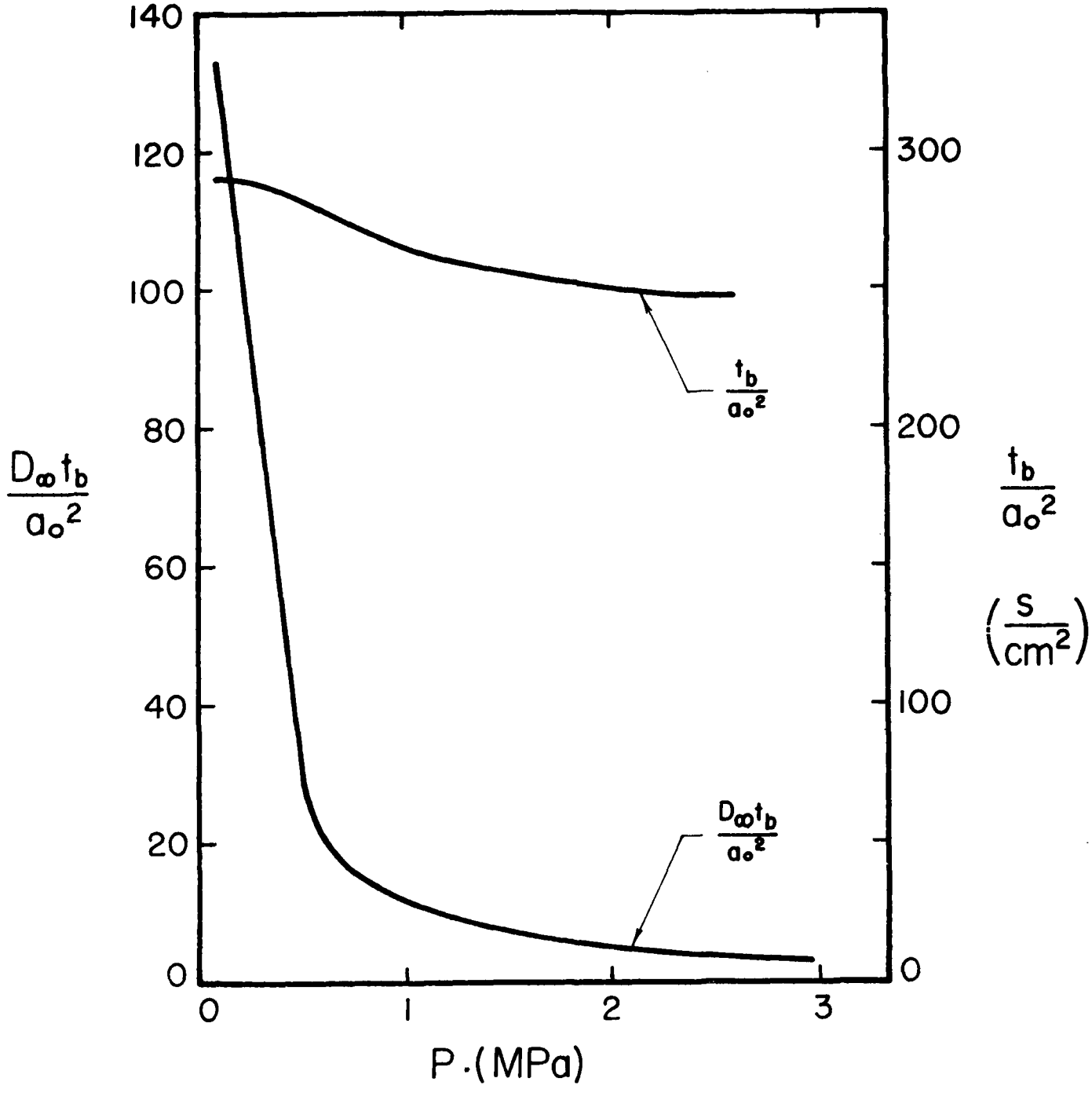

Fig. 46. Variation of the Disruption Time of the Composite Drop with Ambient Pressure

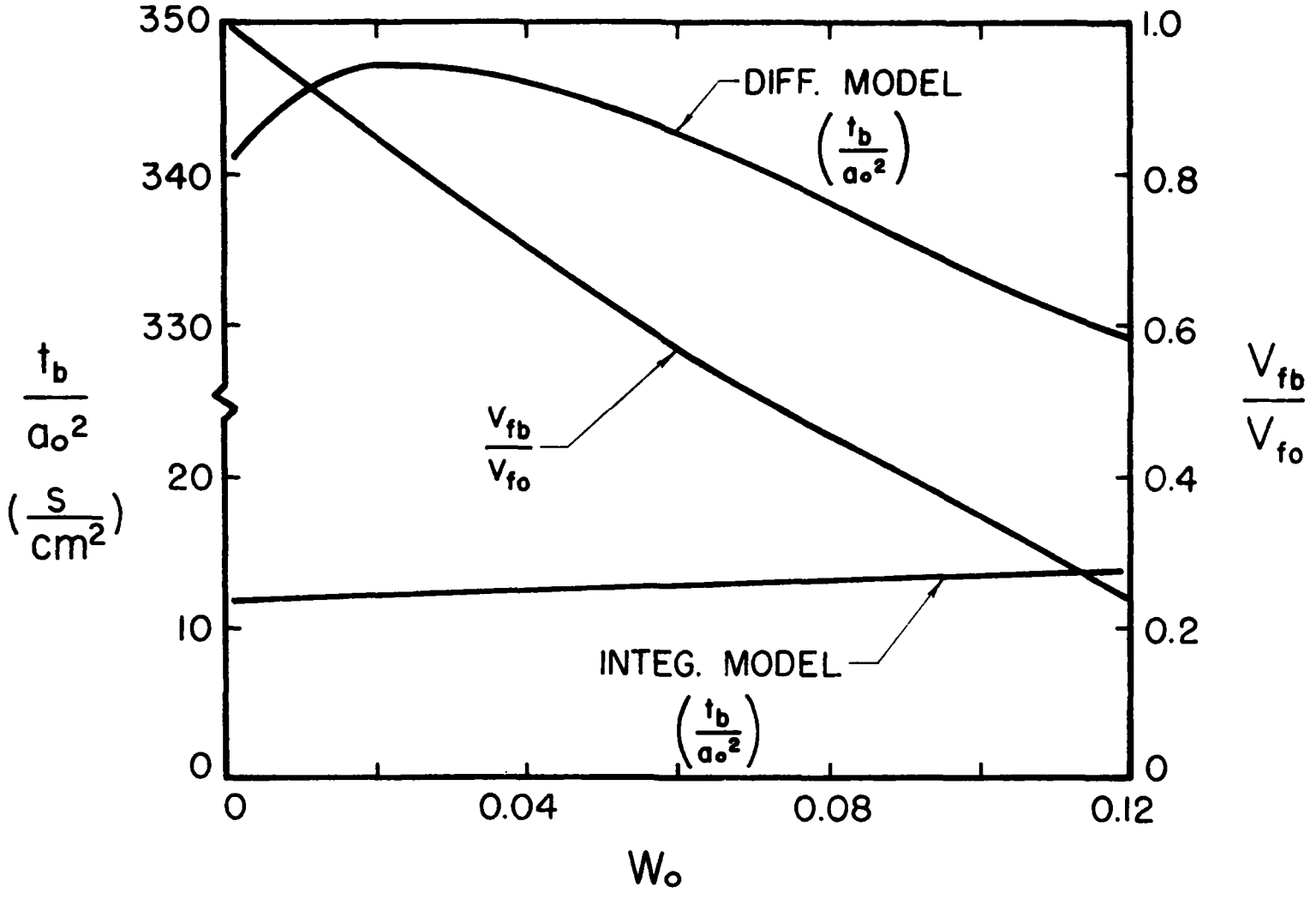

Fig. 47. Comparison of the Integral and Differential Model Predictions with Experimental Disruption Times for Various Water Contents

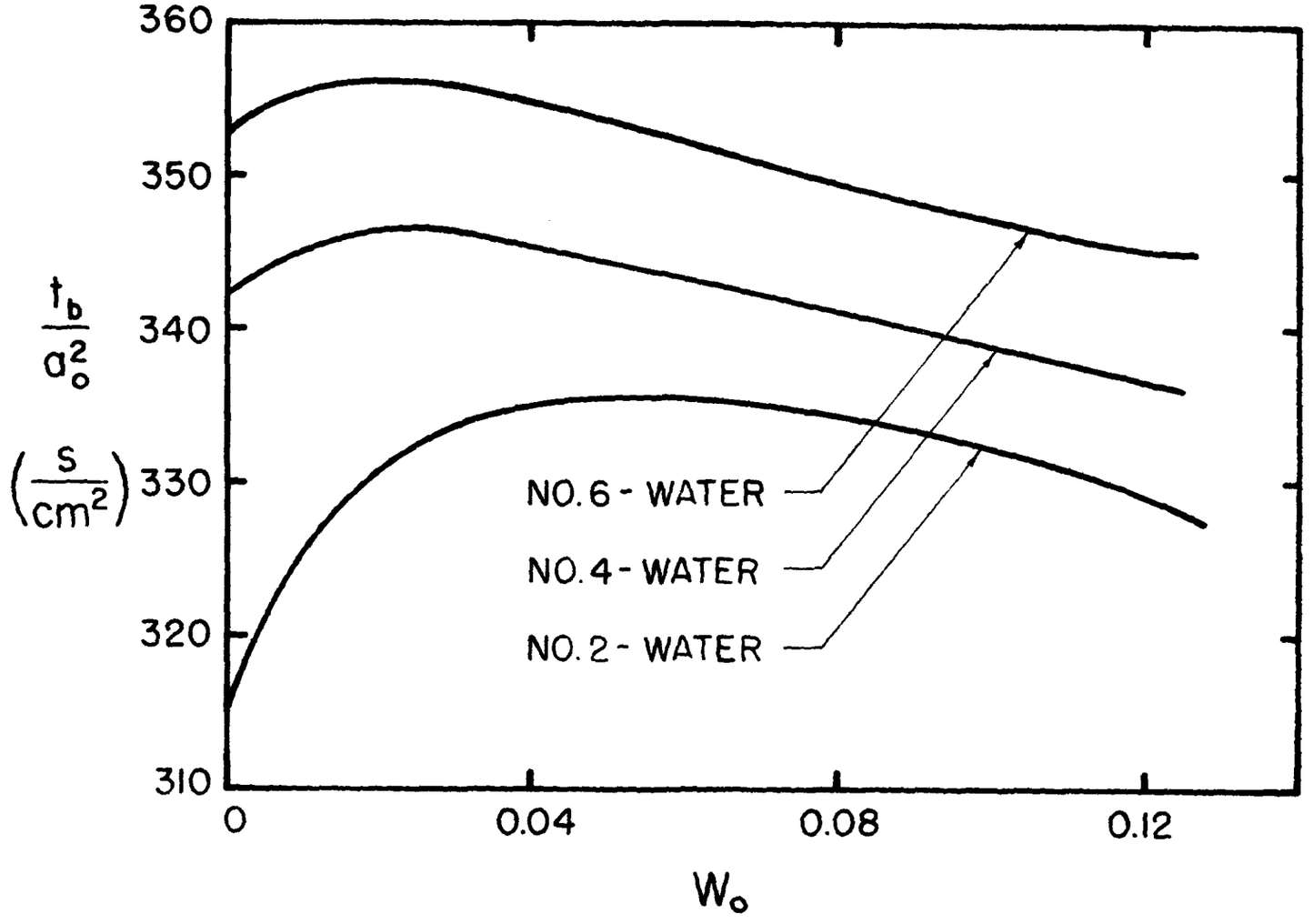

g. 48. Comparison of the Predicted Variation of Disruption Time with Water Content of the Emulsions of No. 2, No. 4, and No. 6 Oils

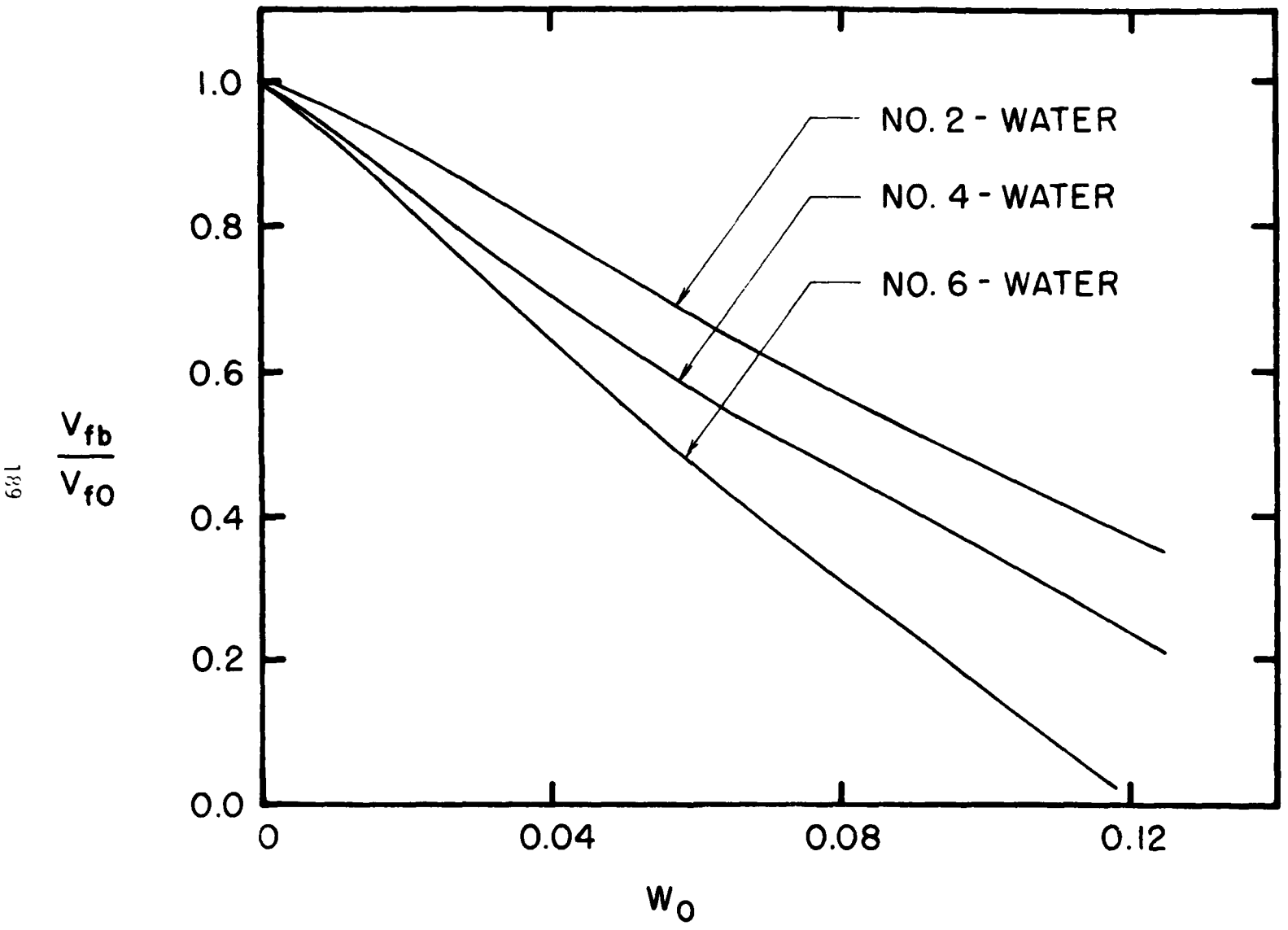

Fig. 49. Comparison of the Variation of the Fraction of the Initial Volume of Oil at the Instant of Disruption with Water Content of the Emulsions of No. 2, No. 4, and No. 6 Oils

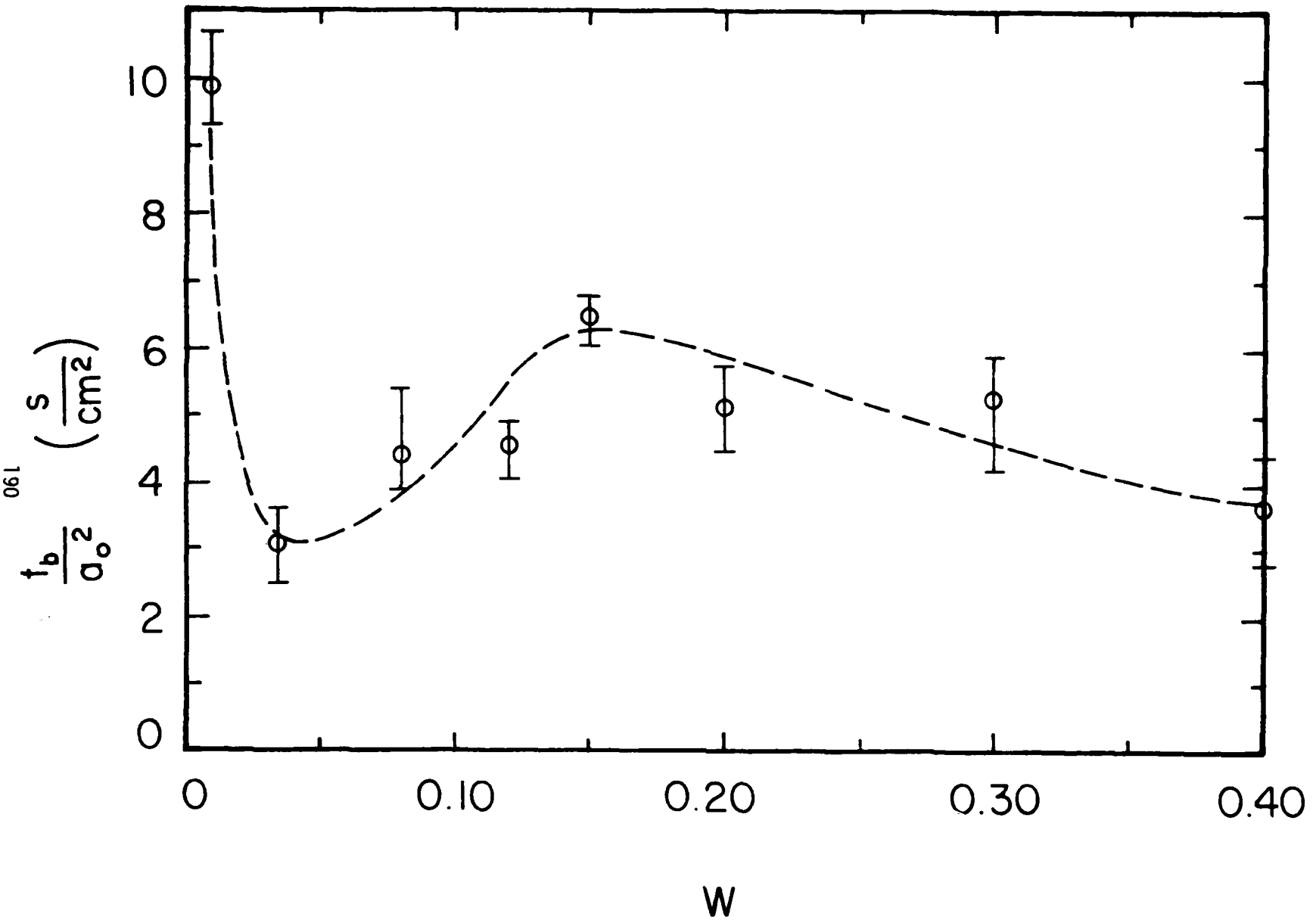

Fig. 50. Variation of Measured Disruption Time of a Burning Emulsion Drop with Water Content (No. 4 Oil)

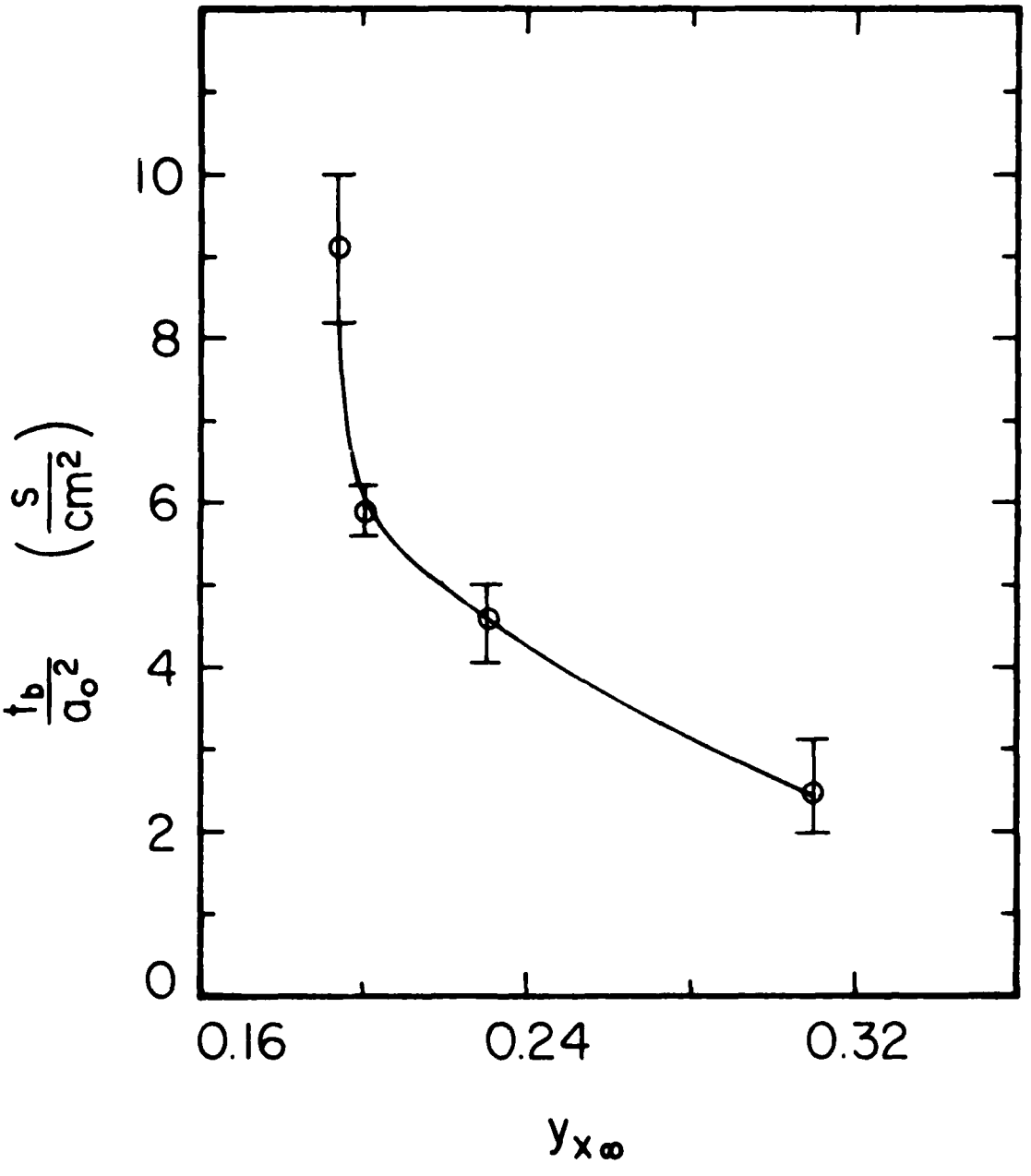

Fig. 51. Variation of Measured Disruption Time of a Burning Emulsion Drop (W = 0.12) with Chamber Oxygen Concentration (No. 4 Oil-Water)

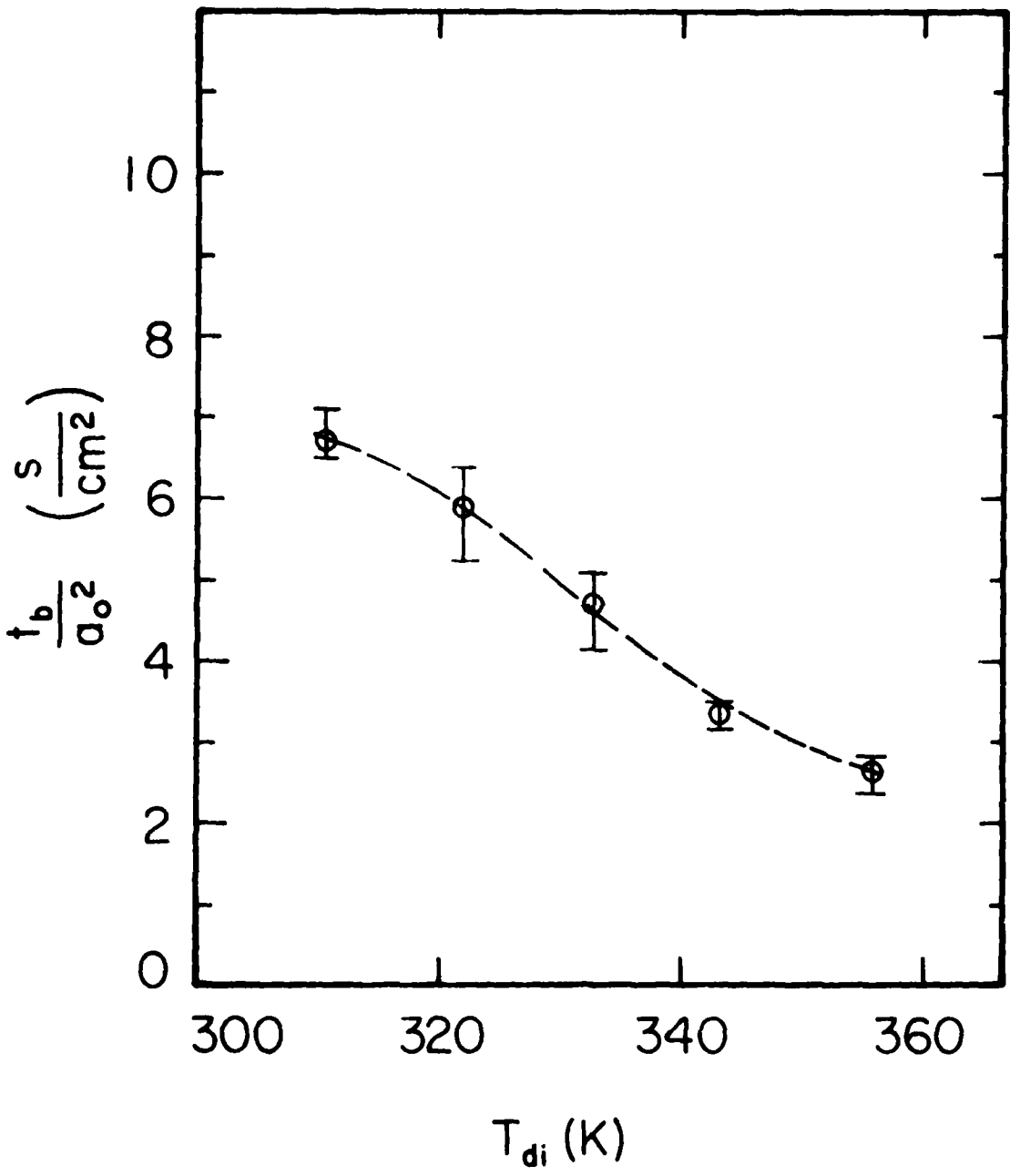

Fig. 52. Variation of Measured Disruption Time of a Burning Emulsion Drop (W = 0.12) with Initial Temperature of the Drop (No. 4 Oil-Water)

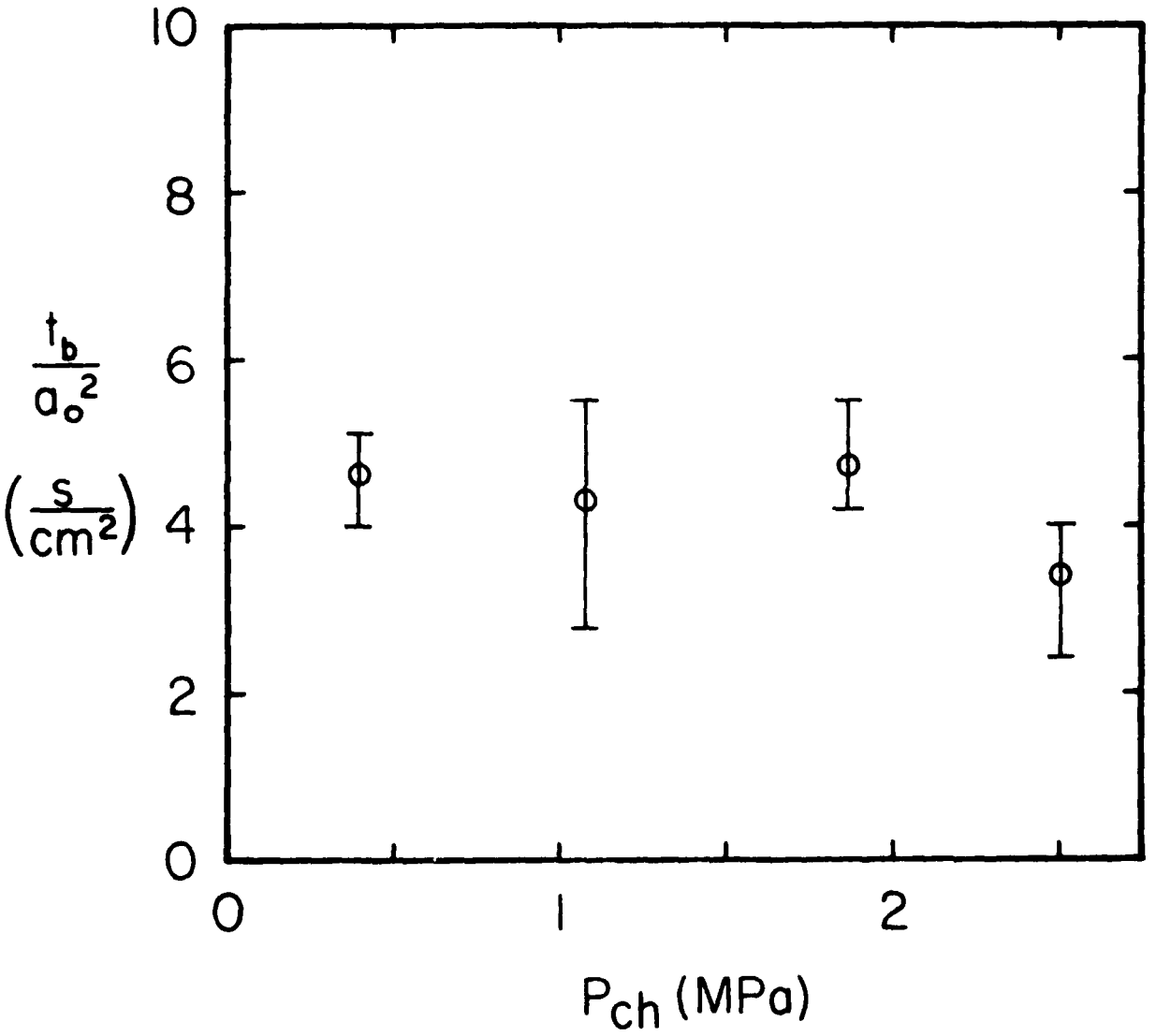

Fig. 53. Variation of Measured Disruption Time of a Burning Emulsion Drop (W = 0.12) with Chamber Pressure (No. 4 Oil-Water)

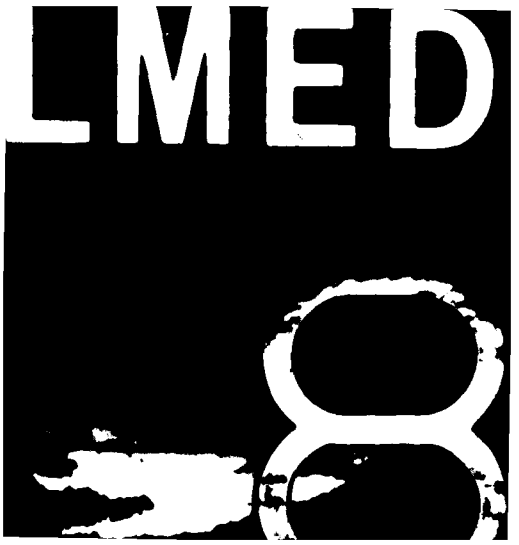
LMED